



8-2008

Development Of A Slide-Rolling Contact Fatigue Tester

Gregory T. Dvorak

Follow this and additional works at: <https://commons.und.edu/theses>

 Part of the [Mechanical Engineering Commons](#)

Recommended Citation

Dvorak, Gregory T., "Development Of A Slide-Rolling Contact Fatigue Tester" (2008). *Theses and Dissertations*. 740.
<https://commons.und.edu/theses/740>

This Thesis is brought to you for free and open access by the Theses, Dissertations, and Senior Projects at UND Scholarly Commons. It has been accepted for inclusion in Theses and Dissertations by an authorized administrator of UND Scholarly Commons. For more information, please contact zeinebyousif@library.und.edu.

DEVELOPMENT OF A SLIDING-ROLLING CONTACT FATIGUE TESTER

by

Gregory T. Dvorak
Bachelor of Science, University of North Dakota, 2007

A Thesis

Submitted to the Graduate Faculty

of the

University of North Dakota

In partial fulfillment of the requirements

For the degree of

Master of Science

Grand Forks, North Dakota

August

2008

This thesis, submitted by Gregory T. Dvorak in partial fulfillment of the requirements for the Degree of Master of Science from the University of North Dakota, has been read by the Faculty Advisory Committee under whom the work has been done and is hereby approved.

Yonah Palus
Chairperson

Bryce M.
Mathewson

This thesis meets the standards for appearance, conforms to the style and format requirements of the Graduate School of the University of North Dakota, and is hereby approved.

Joseph D. Benoit
Dean of Graduate School

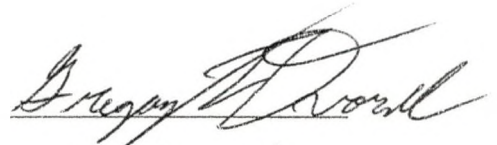
August 1, 2008
Date

PERMISSION

Title Development of a Sliding-Rolling Contact Fatigue Tester
Department Mechanical Engineering
Degree Master of Science

In presenting this thesis in partial fulfillment of the requirements for a graduate degree from the University of North Dakota, I agree that the library of this University shall make it freely available for inspection. I further agree that permission for extensive copying for scholarly purposes may be granted by the professor who supervised my thesis work or, in his absence, by the chairperson of the department or the dean of the Graduate School. It is understood that any copying or publication or other use of this thesis or part thereof for financial gain shall not be allowed without my written permission. It is also understood that due recognition shall be given to me and to the University of North Dakota in any scholarly use which may be made of any material in my thesis.

Signature



Date

7-16-08

TABLE OF CONTENTS

LIST OF FIGURES	vii
LIST OF TABLES	xi
ACKNOWLEDGEMENTS	xii
ABSTRACT	xiii
CHAPTER	
I. INTRODUCTION	1
Background	2
Known Factors Affecting Contact Fatigue Life	4
Failure Types and Modes of Contact Fatigue	8
Contact Fatigue Testers	11
II. S-RCF DESIGN	18
Design Requirements	19
Main Structure	25
Base Structure	27
Internal Structure	28
Driving Mechanism	32
Loading Mechanism	34
Lubrication System	39
Failure Detection System	41

Nondestructive Inspection (NDI) Methods.....	41
Eddy Current Inspection and Parameters.....	43
Data Manipulation System.....	48
Data Storage.....	48
Data Analysis.....	58
Summary of S-RCF Tester Abilities and Controls	65
III. TESTING PROCEDURE AND CONDITIONS.....	67
Test Setup Procedure	67
Test Disassembly Procedure	77
Testing Conditions and Failure Criteria.....	79
IV. RESULTS AND DISCUSSION	84
Verification of Part Specifications.....	84
S-RCF Tester Performance	89
S-RCF Specimen Test Results	95
Sample Specimen.....	95
Specimen 11	100
Specimen 2.....	101
V. CONCLUSIONS AND RECOMMENDATIONS.....	105
APPENDICES	110
APPENDIX A.....	111
Supplemental Test Data	111
Roughness Measurements of AISI 8620.....	111
Microstructure Pictures and Composition Analysis	112

Sample Specimen.....	117
Specimen 1.....	136
Specimen 2.....	152
APPENDIX B.....	157
Mathcad® Files.....	157
Matlab® Files.....	161
APPENDIX C.....	182
S-RCF Tester Supplemental Information.....	182
APPENDIX D.....	189
Specimen and Roller Drawings.....	189
Heat Treatment for 8620.....	192
APPENDIX E.....	194
Outline for S-RCF Test Setup Procedure.....	194
Outline for S-RCF Test Disassembly Procedure.....	202
Replacement Parts.....	205
BIBLIOGRAPHY.....	211

LIST OF FIGURES

Figure	Page
1. General Hertzian Stress Distribution for Contacting Cylinders	5
2. Dimensional Difference between a Macropit and a Micropit [8]	9
3. Photograph of Subcase Fatigue Failure [9]	10
4. Hertzian Stress Distribution for Different Contact Fatigue Failure Modes	11
5. NASA Glenn Research Center's Gear Test Apparatus (a) Cutaway View (b) Schematic View [10]	12
6. Pennsylvania State's Gear Research Institute (GRI) Rolling/Sliding Contact Fatigue Tester a.) Schematic b.) Roller and Specimen [12]	14
7. High Pressure Twin Disc (HPTD) Test Device Loading Frame [6]	15
8. Backup-Roller-Type Two-Roller (BRT2R) Fatigue Test Rig (a) Schematic View (b) BRT2R Test Rig [7]	16
9. ZF-RCF Tester [13]	17
10. S-RCF Tester	19
11. Testing Time Required for a Number of Load Cycles Using a Three Contact Point Testing Machine	20
12. Hertzian Stress Variables and Distribution for Contacting Cylinders	22
13. Required Motor Power for Various Applied Loadings under Dry Rolling Conditions	24
14. Required Motor Power for Various Applied Loadings under Dry and Thin Film Sliding Conditions	24
15. Pro-E® Model of the Main Structure of the S-RCF Tester	26
16. Main Structure of the S-RCF Tester	26
17. Pro-E® Model of the Base Structure of the S-RCF Tester	27

18. Specimen and Roller for S-RCF Tester	28
19. Top Roller and Specimen Assembly.....	29
20. Pro-E® Model of the Internal Components of S-RCF Tester	30
21. Types of Collars Used in the S-RCF Tester's Internal Structure	31
22. Tightening Disk on Top Roller Assembly	31
23. Diagram of Symmetrical Spacing (120° apart) of the Rollers Around the Specimen and the Applied and Reaction Forces under Loading	32
24. S-RCF Tester Roller Motor and Gearing.....	33
25. S-RCF Tester Specimen Motor.....	33
26. Power Flex Controllers for the S-RCF Tester Motors.....	34
27. View of the Back Side of the S-RCF Tester's Loading Structure	35
28. Pneumatic Schematic for S-RCF Tester	37
29. Pro-E® Model of Rollers and Specimen in Contact with One Inner Wall Removed	38
30. Hertzian Pressure Conversion to Applied Pressure of the S-RCF Tester for AISI 8620.....	39
31. Lubrication System for S-RCF Tester (Oil Flow Shown in Yellow)	39
32. S-RCF Tester's Lubrication Flow Controls to Specimen and Gears.....	40
33. Schematic of the S-RCF Tester's Lubrication System	41
34. Basic Eddy Current Magnetic Field Description [20]	43
35. Foerster® Defectomat EZ 2.828 Eddy Current Detection Device	45
36. Eddy Current Depth of Penetration [20].....	46
37. Calibration Results for the S-RCF Pressure Transducer.....	49
38. Calibration Results for the S-RCF Temperature Thermistor Probe.....	50
39. LX Navi Program Window.....	51
40. LX-Navi New File Window.....	52

41. LX-Navi System Window System Tab Menu	53
42. LX-Navi System Window Slot1 (PA-8) Tab.....	54
43. LX-Navi Trigger Window	55
44. Number of Load Cycles Represented by Each File for Various Specimen Motor Speeds	56
45. Recording Time Needed to Store a Given Number of Load Cycles per File for Various Specimen Motor Speeds	57
46. Flowchart Description of the Failure Detection Stage.....	61
47. Example of Figures Stored during the Failure Detection Stage	63
48. Example of Figures Generated during Screening Stage	64
49. Example of Figures Generated during Analysis Stage	65
50. LX-Navi Digital Readout Windows	75
51. Eddy Current Calibration Device (ECCD)	83
52. Defects at the Edge of the Rollers.....	84
53. Defect Across the Face of the Roller	84
54. Specimen Testing Surface (Untested).....	86
55. Decarburized Layer of AISI 8620 Test Cylinder at a Magnification of 500	87
56. Decarburized Layer of AISI 8620 Test Cylinder at a Magnification of 1000.....	87
57. Microstructure Analysis 20 Microns from the Edge.....	88
58. Hardness Measurements for Verifying the Case Depth.....	89
59. Keyway Damage to the Top Roller Shaft	91
60. S-RCF Tester Eddy Current Probe Holders: Old (left) and New (right)	92
61. Broken Bottom Roller Shaft	94
62. Screening Figure 1 for Sample Specimen (Testing Time 18 - 27.8 hrs)	97
63. Screening Figure 1 for Sample Specimen (Testing Time 27.8 - 40 hrs)	98

64. Pitting on S-RCF Sample Specimen	99
65. SEM 35x Photograph of the Sample Specimen	99
66. S-RCF Specimen 11 Test Surface Wear Track.....	100
67. Comparison between an Untested S-RCF Specimen Test Surface (left) and the Tested Test Surface of Specimen (right).....	101
68. Screening Figures 1 and 2 for Specimen 2 (Testing Time: 0 to 33 hrs)	102
69. S-RCF Specimen 2 Photograph of Tested Surface	103
70. S-RCF Specimen 2 Optical Microscope Photograph Tested Surface.....	104

LIST OF TABLES

Table	Page
1. Mechanical Failure Modes of Metals [1].....	2
2. Lubrication Regime Values and Description [5]	6
3. ZF-RCF Results for Various Materials [13]	20
4. Coefficient of Friction Values for Steel-on-Steel Contact under Different Lubrication and Sliding Conditions [14]	23
5. Basic Characteristics of Common NDI Methods [19]	42
6. Channel Descriptions for the TEAC LX-10 Recording Unit.....	48
7. LX Navi Setup Parameters and Description	58
8. Description of Inputs for <i>TestingParametersValues</i> Matlab® File	60
9. Tools Needed to Set Up the S-RCF Tester	68
10. Heat Treatment and Surface Finish Specifications for AISI 8620	80
11. Summary of S-RCF Testing Conditions for AISI 8620 Specimens	81
12. Roughness Measurements of Randomly Chosen Specimens and Rollers.....	85
13. AISI 8620 S-RCF Specimen Test Results	95
14. Summary of Eddy Current Voltage Changes for Sample Specimen.....	99

ACKNOWLEDGEMENTS

I would like to express my appreciation to the University of North Dakota's Engineered Surfaces Center for providing me with this project. A special thanks to Karen Harrie, Doug Larson and Bryce Mitton for all their help, both financial and otherwise. I would also like to thank the Damian Wilmot and Jared Schell, members of Alion Science and Technology, for their continued assistance on this project.

I would also like to thank the Mechanical Engineering Department at the University of North Dakota for all their assistance, especially Dr. Marcellin Zahui for all his guidance and wisdom over the past years and also Dr. Matthew Cavalli for serving on my thesis committee.

I would like to personally thank Gary Dubuque and Jay Evenstad for their help in the shop, Cathy Jones, Kay Olesen and Cadence Youngberg for getting me through the paperwork and the other group members of Penta-X who designed, analyzed and assembled this project. The members of Penta-X included Christopher Beddoe, Brenton Clyne, David Dunham and Lance Willer. A special thanks to Donovan Voeller and Brandon Weltikol for their assistance assembling the tester.

Finally, I would like to thank Martina M. Wolf for calmly listening to my complex problems, correcting me in the rare cases that I am wrong and for believing in me.

ABSTRACT

Contact fatigue failure is a common problem experienced in many applications such as bearings, gears and railway tracks. In recent years, research companies have developed finishing processes which aim to improve a component's contact fatigue life. One such process has been patented by REM Chemicals in Texas. Preliminary contact fatigue tests have shown that this superfinishing process could potentially improve a component's contact fatigue life by 300%. Before this technology can move from the laboratory to an industrial platform, more tests are needed to verify the claim. To the best of the author's knowledge, no standard process or test machine exists to assess the fatigue endurance of superfinished contacting surfaces.

The objective of this thesis is to discuss the completion and verification of a sliding-rolling contact fatigue (S-RCF) test rig. A majority of the development and fabrication was performed by a group of students at the University of North Dakota before May 2007. After this, completion of the tester was finished by the graduate student of this thesis. Unlike other contact fatigue testers built for specific purposes, the proposed tester allows for more flexible testing parameters such as any combination of slide-roll ratio between the surfaces, any operating speed and dry or lubricated testing. For failure detection, the proposed tester is equipped with a state-of-the-art eddy current crack detection system. However, it can be easily modified to use ultrasonic or vibration based crack detection devices. The eddy current crack detection system can also be used to

monitor and investigate crack growth for different materials, levels of superfinish and operating conditions.

Three preliminary tests on a common gear material (AISI 8620 steel) were performed mechanical limits as well as the software performance of the tester. Two of the 8620 specimens exhibited signs of failure during testing, while one specimen was suspended after running for several days. While the last specimen was being tested, a shaft broke and further testing could not be performed. The tester failure was caused due to poor manufacturing of the shafts and a slight misalignment of the rollers.

During the three tests, the various systems of the S-RCF tester were left running for several days and only minor problems were found. These problems were either inconsequential or fixed. Several Matlab® scripts were developed and modified to control the tester and analyze the data online and offline.

The S-RCF tester has a few components that need to be fixed before further testing can be performed. Two options exist to continue testing. The first option is to repair the current S-RCF tester and continue testing. The second option is to design a second generation machine with several upgrades and improvements. Either option will provide the University of North Dakota's Engineered Surfaces Center the ability to test and compare the fatigue endurance for different surface finishes.

CHAPTER 1

INTRODUCTION

The University of North Dakota's Engineered Surfaces Center (ESC) funded the development of a sliding-rolling contact fatigue (S-RCF) test machine to simulate gear contact. The machine's purpose is to test gear materials with various surface finishing processes under sliding and rolling contact fatigue conditions in a controlled and timely manner. The ESC will use the tester to determine the performance of a new superfinishing process for gears.

Development of the tester began in the summer of 2006, with Dr. Marcellin Zahui and two undergraduate students. In September of 2006, the tester was a project for the senior design class at the University of North Dakota and three more undergraduates were added to the team. The team's name was Penta-X. The overall design and drawings for the S-RCF tester were completed in December of 2006 and the majority of the assembly was completed by May of 2007. After graduation, one team member remained to complete the construction of the tester and perform the first preliminary contact fatigue tests.

This paper presents a short background of contact fatigue testing and documents the results of the preliminary fatigue tests performed with the S-RCF tester. These test results are used to assess the overall design quality and fatigue testing capability of the S-RCF tester.

Background

In any mechanical system, failure happens eventually. Depending on the mechanics of the failure mode, failure can occur suddenly or gradually over a short or long period of time. If unexpected, the results could be significant financial losses, damage to the machine and/or severe injuries. In any design, planning for and predicting failure can help save time, money and lives.

For metals, many failure modes exist. A description of these failure modes can be seen in Table 1. Since most devices are designed to work in the elastic region, the most studied failure mode is excessive deformation or yielding [1]. However, the most common type of failure is fatigue, which has been reported to account for 50 to 90 percent of all mechanical failures; most of these unexpected [1].

Table 1 Mechanical Failure Modes of Metals [1]

Failure Mode	Description
Excessive Deformation	Elastic, yielding, or the onset of plasticity
Ductile Fracture	Substantial plasticity and high-energy absorption
Brittle Fracture	Little plasticity and low-energy absorption
Impact or Dynamic Loading	Excessive deformation or fracture
Creep	Excessive deformation or fracture
Relaxation	Loss of residual stress or external loading
Thermal Shock	Cracking and/or fracture
Wear	Many possible failure mechanisms
Buckling	Elastic or plastic
Corrosion	
Stress Corrosion Cracking	Environmental-assisted cracking
Aesthetic Failure	
Fatigue	Repeated loading

The focus of this thesis is fatigue failure as defined by ASTM as follows [2]:

The process of progressive localized permanent structural change occurring in a material subjected to conditions that produce fluctuating stresses and strains at some point or points and that may culminate in cracks or complete fracture after a sufficient number of fluctuations.

From this definition, several key aspects of fatigue are defined. The word “progressive” states that fatigue damage occurs over a period of time. “Localized” implies that the damage occurs in a small section rather than the entire part. Since fatigue is irreversible, it is described as “permanent”. Finally, the word “fluctuating” describes the dynamic type of loading that is experienced during fatigue failure.

Even with the above definition, many different types of fatigue failure exist. These various fatigue failures can be described by the loading type applied. Examples of different loadings include bending, uniaxial, multi-axial, torsion, rolling and/or sliding contact or a combination of each. Since fatigue failure occurs over time, the load history can also affect the fatigue life of a part.

In this thesis, rolling contact fatigue is defined as follows: [3]:

...the mechanism of crack propagation caused by the near-surface alternating stress field within the rolling-contact bodies, which eventually leads to material removal.

Although this definition is for rolling situations, it applies to sliding conditions as well. Two key points are made in the definition. First, the stress that causes failure is “near-surface alternating stress”. Secondly, the failure results in “material removal”, meaning pieces of material can cause further damage if not removed.

Contact fatigue issues can be traced back to the railway industry in the 1840s [1]. Other than the railways, gears and bearings are other components commonly studied for contact fatigue strength. These three parts affect many major industries, including automotive, manufacturing and aerospace. Therefore, improving the RCF life of these components can create a safer, longer-lasting device.

Known Factors Affecting Contact Fatigue Life

Contact fatigue is the gradual wear that results from two surfaces directly contacting each other. For gears, contact fatigue is experienced when teeth mesh. In bearings and railways, contact fatigue occurs when the balls or wheels move inside or along a surface.

A material's contact fatigue strength is affected by numerous factors. For a given material, these factors can be separated into two classifications. The first class describes the various operational and environmental conditions the material is expected to experience. The second class of factors describes the process-induced characteristics of the material.

The environmental factors that are part of the first class include the contacting force, sliding ratio between the two surfaces, lubrication type, lubrication regime and surface temperature.

The most obvious environmental factor affecting a material's contact fatigue life is the contact force. The magnitude of the force determines the intensity of the stress field at the point of contact. The higher applied force, the higher the Hertzian compressive and shear stresses. Hertzian stress is the stress that results from two curved surfaces in contact. The general parabolic shape for a Hertzian stress field can be seen in Figure 1.

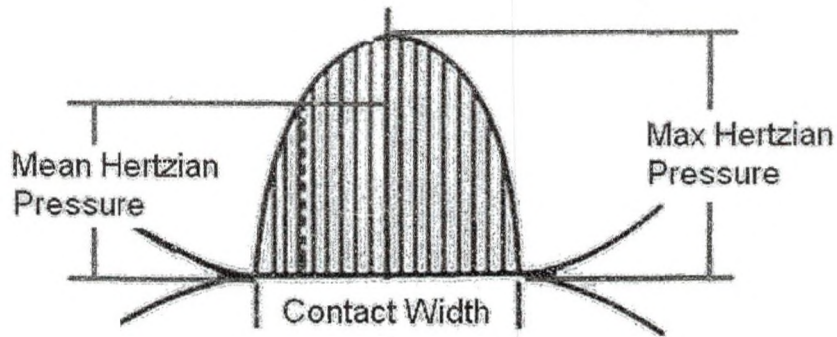


Figure 1 General Hertzian Stress Distribution for Contacting Cylinders

The effect of the contact force has been studied extensively in uniaxial and bending fatigue tests. For uniaxial and bending testing, stress fatigue life (S-N) curves are developed to show the trend of a material's fatigue life for different stress values. Similar curves can be generated for materials in sliding/rolling contact fatigue conditions [4]. The biggest difference between the testing types is uniaxial and bending produce tensile stresses; whereas, contact fatigue creates multi-axial compressive stresses [4]. Since cracks do not grow in compressive stresses, tensile stresses are present in the material [4].

Another important environmental factor is the slide ratio (also known as slip ratio) between the two surfaces. The slide ratio (SR) is simply the ratio of the velocities of the two surfaces. This is an important factor when simulating gear teeth meshing. As gear teeth mesh, sliding occurs between the teeth. Equation 1 is used to define the slide ratio between the surfaces. The variables v_r and v_s are the surface velocities of the roller and specimen, respectively. Rolling occurs when the two surface velocities are equal or when the SR value is zero. For the S-RCF tester, positive SR values will be used since the roller motor is three times slower during a rolling condition.

$$SR = \frac{v_r - v_s}{v_s} \quad \text{Eq. 1}$$

Since different applications require different lubricants, the type of lubricant is an environmental factor. These lubricants vary in properties as well as form (grease or oil). The S-RCF tester allows for dry or lubricated testing. Therefore, lubricants can be tested against a dry baseline sample to determine which performs the best.

Another environmental factor affected by the lubrication is the amount of lubrication supplied to the part. The amount of lubrication present can be classified into one of three lubrication regimes. The lubrication regime describes the elasto-hydrodynamic lubrication (EHL) present during testing. EHL is used to describe the lubrication for rolling or sliding conditions under extreme pressures which cause the surfaces to deform. Regime 1 is essentially metal on metal contact. Regime 2 is partial metal-to-metal contact with a thin oil film. Regime 3 has an oil film thick enough to prevent metal-on-metal contact [5]. The lubrication regime can be determined by using Equation 2, where h_{\min} is the minimum film thickness and $R_{q,i}$ is the surface roughness RMS (root mean square) values of the individual contacting surfaces [6]. Table 2 provides the range of values for each regime.

$$\Lambda = \frac{h_{\min}}{\sqrt{R_{q,1}^2 + R_{q,2}^2}} \quad \text{Eq. 2 [6]}$$

Table 2 Lubrication Regime Values and Description [5]

Regime	Λ	Description
1	<.3	No Appreciable Oil Film
2	.3-3.0	Mixed Lubrication (Thin Film)
3	>3.0	Complete Separation and Full EHL Contact

The final environmental factor is the surface temperature. The surface temperature is a hard variable to control since it is influenced by the contacting force, geometry of the contact area, slide ratio, surface roughness and the lubrication conditions [7]. Deng et al. examined the effect of surface temperature on surface strength and recommended that it be included in surface strength evaluation for high temperature environments.

The second class of factors affecting the contact fatigue strength of a material is the process-induced factors. These factors include the surface roughness, microstructure purity, heat treatment and the residual stresses in the material.

The most studied processing factor is the surface roughness. The surface roughness is the small-scale variations in height on a material's surface. While a rough surface can prevent surfaces from welding together, it can have several negative effects for a material's contact fatigue life. A high surface roughness causes variations in the distribution of the contact pressure, resulting in localized plastic deformation and crack initiation [4]. If the lubricant becomes trapped, a region of high hydrostatic pressure will form [4]. Therefore, many gears, bearings and railways have low surface roughness values. These low values are accomplished by finishing processes.

The microstructure purity and the heat treatment of the material both affect the contact fatigue strength of a material. Impurities, such as inclusions and soft spots, can act as crack nucleation sites. As the microstructure becomes purer, the failure mode moves closer to the surface [4]. The type and quality of heat treatment will affect the amount of impurities as well as the case depth and hardness of the part. A poor heat treatment can result in an insufficient case depth causing a subcase failure.

The final-process induced factor is the residual stresses present in the material. Compressive stresses are induced into the surface of a component in several ways such as shot-peening or case-hardening. Compressive stresses are considered beneficial to improving a materials contact fatigue life [1]. Since cracks form in areas of tension, compressive regions will hinder crack propagation and growth. However, due to the complex changes in the stress field during contact fatigue conditions, areas of tension exist in the area of contact [4].

Even though contact fatigue testing has been performed since the begin of the railway system, the effect and importance of each factor has not been assessed [4]. Therefore, contact fatigue standards have not been set. The S-RCF tester discussed in this report is a tester with the ability to systematically test these parameters. A design of experiments approach can be used to identify key factors and assess their effect on a material's contact fatigue strength.

Failure Types and Modes of Contact Fatigue

Due to the lack of knowledge and information about the basic mechanisms of contact fatigue failures, different industries use different terminologies to describe the same failure mode. In this thesis, the definitions and terminology used will be as defined by ASM International. ASM International states that the various terminologies can be categorized into two failure types and two contact fatigue failure modes [3].

The failure types for contact fatigue are macropits (large pits) and micropits (small pits). The scale used to determine what is large and what is small is the asperity height. The asperity height is the roughness height of the part in question. Macropits are

much larger in size than the asperity height; whereas, micropits are much closer to the asperity height. Figure 2 shows the size difference between a macropit and a micropit.

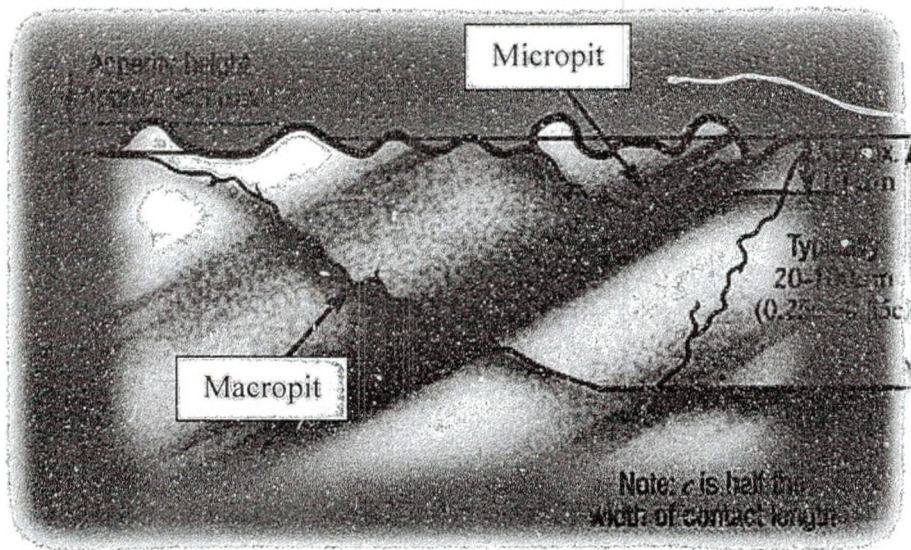


Figure 2 Dimensional Difference between a Macropit and a Micropit [8]

The failure modes for contact fatigue are subsurface-origin (SS-O) failure and surface-origin (S-O) failure. SS-O failure modes form macropits and can be separated into two classes. The two classes are inclusion originated (IO) and subcase fatigue. IO macropits develop in random locations where a defect in the bulk material is present, such as an inclusion or microstructure alteration [3]. Subcase fatigue macropits originate at the interface of the case/core interface where the case hardness is lower than the Hertzian shear stress field [3]. A photograph of subcase fatigue failure is shown in Figure 3.

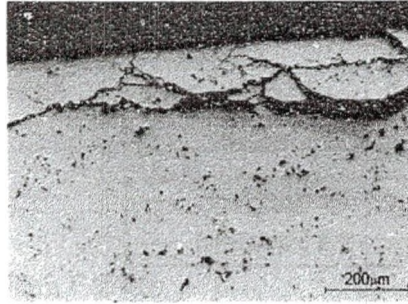


Figure 3 Photograph of Subcase Fatigue Failure [9]

Surface-origin (S-O) pits result from asperity (surface roughness changes) and tractive (pulling) forces acting on defects or surface discontinuities on the surface or in the immediate subsurface [3]. The three classes of S-O failure modes are point-surface origin (PSO), geometric stress concentration (GSC) and micropitting. PSO failure forms random macropits like IO macropits; however, the PSO macropits originate on the surface and have no inclusion as an initiation site [3]. GSC macropits result from misalignments, deflections under loading and contact geometries which increase the Hertzian shear stress field at the surface [3]. Micropitting is the only failure mode which creates micropits. Micropitting occurs at low operating speeds when a low viscosity lubricant is used and a thin elasto-hydrodynamic lubrication (EHL) layer is present [3]. The onset of micropitting is a glazed surface due to plastic deformation that contains microscopic cracks. If severe enough, micropitting can lead to macropitting.

The failure modes occur when the Hertzian stress field is greater than the material's strength. Since the significant stress in contact fatigue is the alternating shear stress, the shear strength of the material is important [3]. In a pure rolling condition, the plane of maximum shear stress is slightly below the surface [3]. In a sliding condition, the frictional forces and temperature change increase the magnitude and distribution of

the shear stress field [3]. Figure 4 shows how different locations where the Hertzian stress field is larger than the material's strength results in different failure modes.

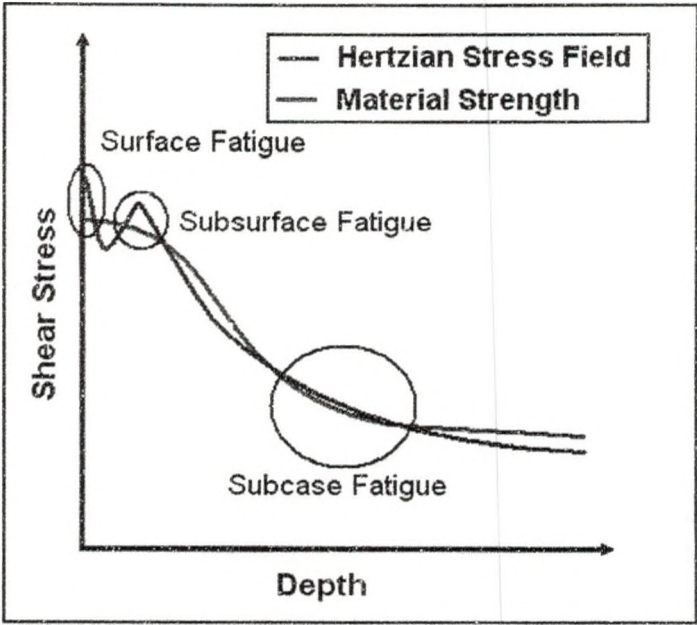


Figure 4 Hertzian Stress Distribution for Different Contact Fatigue Failure Modes

Contact Fatigue Testers

Several contact fatigue testing devices are available in the world today. Since no standard method exists for designing a contact fatigue test machine, each tester is developed for a specific application. Therefore, the parameters controlled and investigated vary for each machine. A summary of the many different types of RCF testing methods and a brief description of their capabilities can be found in reference [3]. A few of the available testers are presented here in more detail.

Figure 5 is the picture of the gear test apparatus located at the Glenn Research Center.

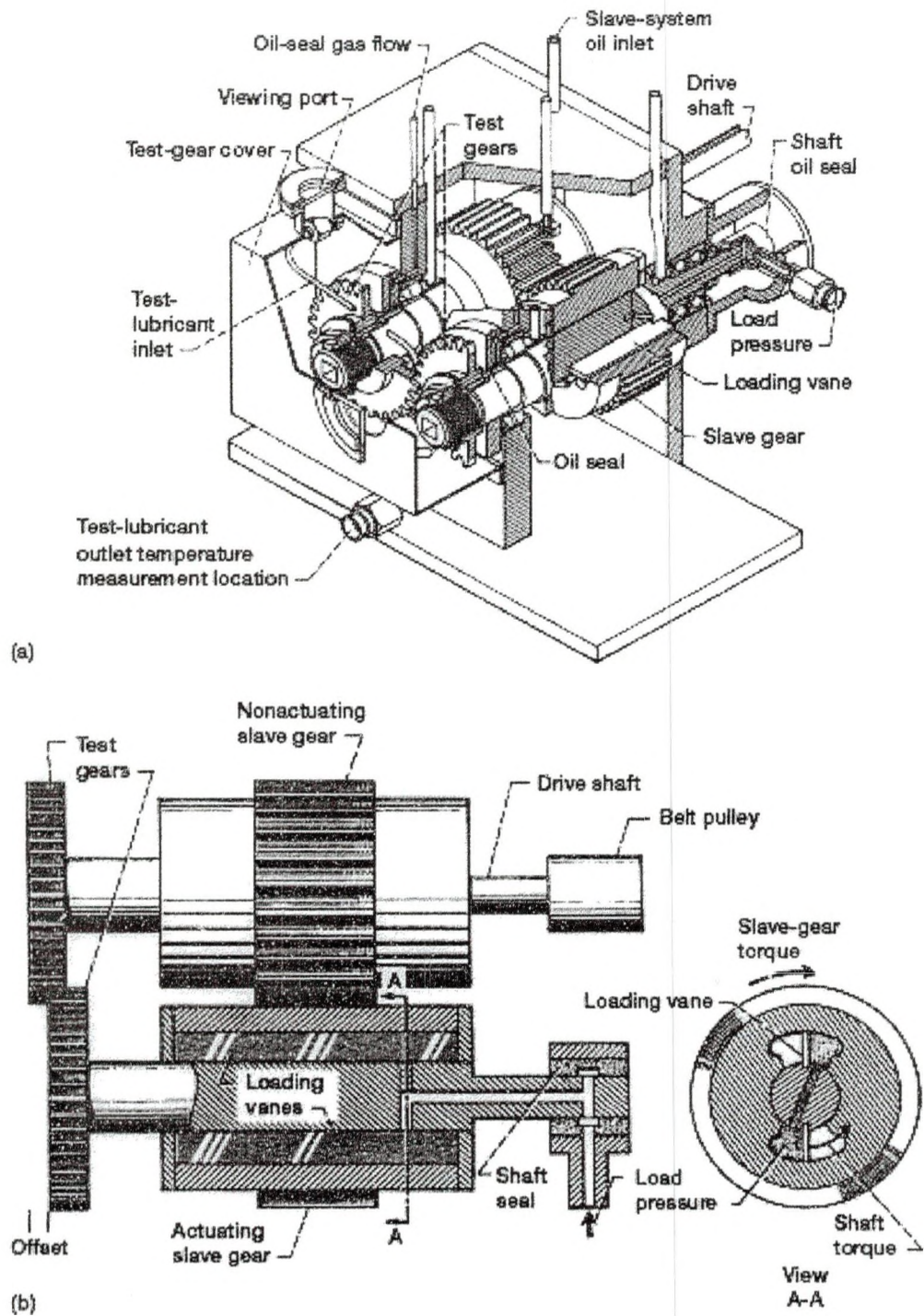
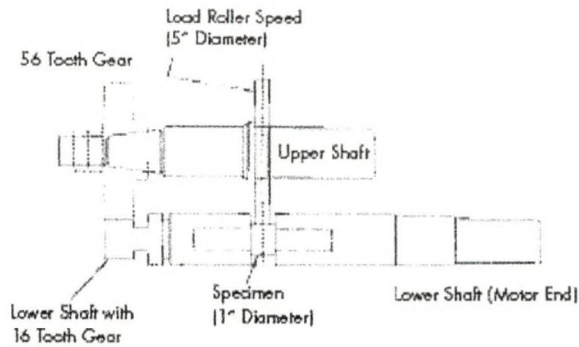


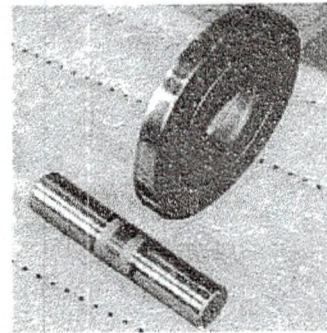
Figure 5 NASA Glenn Research Center's Gear Test Apparatus (a) Cutaway View (b) Schematic View [10]

The NASA tester uses a gear as the test specimen. Therefore, a gear must be manufactured for each test. The test gears are offset to allow four sets of fatigue tests to be performed on each set of gears [10]. Since gears are being used, the sliding ratio cannot be varied or controlled. Loading is applied gradually and controlled by adjusting the hydraulic pressure which applies a breaking torque to one of the shafts of the meshing gears [10]. Separate lubrication systems are used to lubricate the test gears and the slave gears, allowing dry testing to be performed on the gears. Testing is typically run continuously at a speed of 10,000 rpm [10]. Crack detection is accomplished visually and/or by using a vibration monitoring system. In one study, the gears were inspected after every 50 million cycles and continued to run until the vibration detection transducer broadband RMS magnitude increased over a preset threshold [11]. In the same study, surface fatigue failure was defined as one or more pits covering 50 percent or more of the contact width [11].

Instead of using NASA's tester, one study used the rolling/sliding contact fatigue (R/SCF) tester at Pennsylvania State as a screening test [12]. Since the R/SCF tester uses a round cylinder, specimens could be tested at a cheaper cost. The screening experiment spun the R/SCF specimen at a speed of 1330 rpm with the load being applied hydraulically on the roller [12]. The slide ratio between the roller and the specimen can be varied by changing the gears on each of the shafts. No information in the literature was found as to how failure was defined or detected. Figure 6 shows the schematic view of the R/SCF tester along with a picture of the actual testing specimen and roller.



a.) Schematic of R/SCF Tester



b.) R/SCF Roller and Specimen

Figure 6 Pennsylvania State's Gear Research Institute (GRI) Rolling/Sliding Contact Fatigue Tester a.) Schematic b.) Roller and Specimen [12]

In Tampere, Finland, a high pressure twin disc (HPTD) test device was developed to simulate gear contact [6]. Loading is applied by pushing on one disc while the other is held in place. The maximum load that can be applied is 11,000 N (2,473 lbf) [6]. The maximum speed is 6,000 rpm and the slip can be controlled since each disc is controlled by a separate motor [6]. The lubrication system has two filters on it along with a heater and cooler to control the oil temperature [6]. The failure detection method and criteria were not mentioned because reference [6] dealt with determining the friction coefficients at different slip ratios. Figure 7 shows the HPTD loading frame and testing specimens.

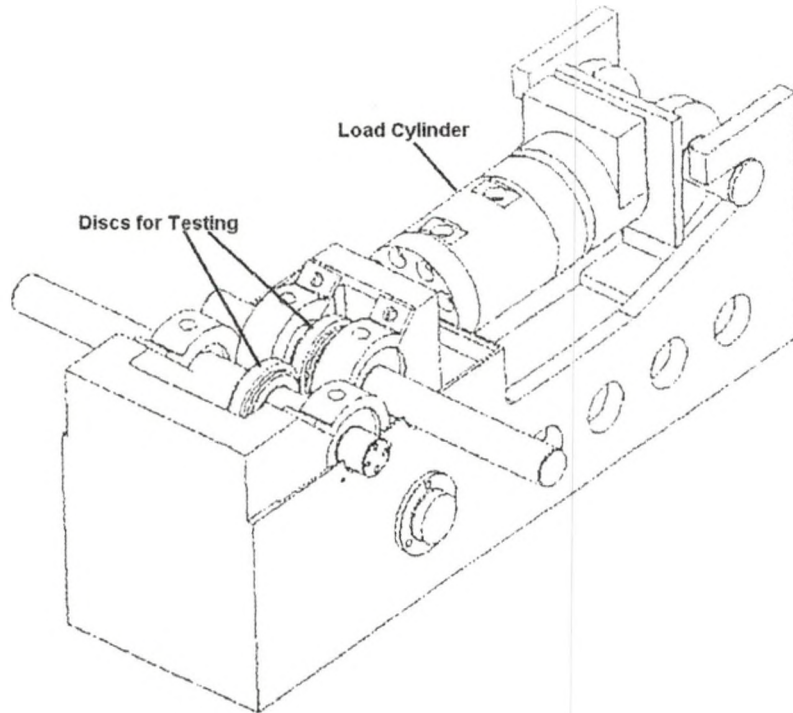
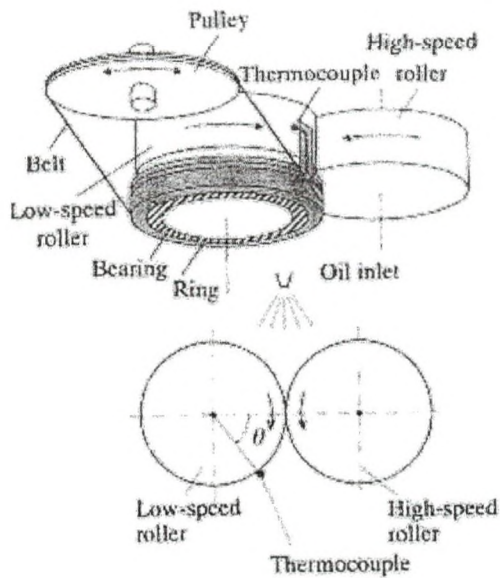
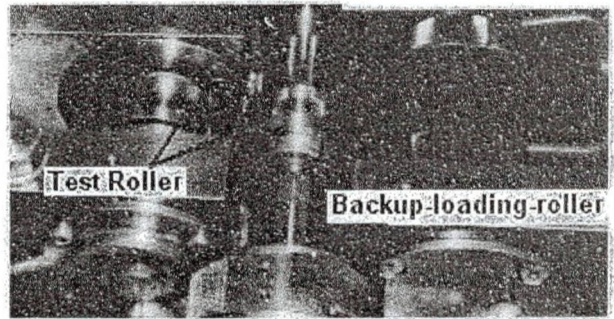


Figure 7 High Pressure Twin Disc (HPTD) Test Device Loading Frame [6]

In Japan, a study was conducted using a backup-roller-type two-roller (BRT2R) fatigue test rig on the effect of surface temperature on a material's fatigue strength [7]. The BRT2R tester uses two disks of similar material, one as the roller and the other as a specimen. The specimen is slightly smaller in diameter than the roller, thus creating slip between the surfaces. Since the specimen is smaller, it has been labeled as the high-speed roller; whereas, the other roller was labeled as the low-speed roller. The shafts are turned using a belt and pulley at a speed of 2000 rpm [7]. Figure 8 shows the Japanese tester, with the specimen and roller both labeled at test rollers. The backup-loading-roller loads the tester, but it is unclear as to how this load is applied.



(a) Schematic View



(b) Backup-roller-type two-roller fatigue test rig

Figure 8 Backup-Roller-Type Two-Roller (BRT2R) Fatigue Test Rig (a) Schematic View (b) BRT2R Test Rig [7]

The last tester is the entitled the ZF-RCF tester. The first ZF-RCF tester was developed in Germany and a second has been created at V-Tech International in West Bend, Wisconsin. The ZF-RCF tester uses three rollers to contact one specimen. Each revolution of the specimen results in three load cycles, thereby decreasing testing time. The ZF-RCF can turn the specimen at a maximum speed of 3600 rpm [5]. Loading is applied by pressurizing the oil, meaning the specimen is submerged in oil and the compartment must be sealed tight [5]. The oil pressure is controlled by a servo-hydraulic valve, allowing variable loading to be applied during a test [5]. Since gears are used to turn the roller shafts, different gearing will create different slip ratios between the rollers and specimen. The detection method used for the ZF-RCF is a non-destructive eddy current method. Failure is defined as an increase in the output voltage from the eddy current device [5]. When calibrated correctly, a certain voltage increase will correspond

to a crack length or size. In this way, crack growth can be monitored with the eddy current system. The ZF-RCF also incorporates a vibration sensor to allow for testing to catastrophic failure [4]. The specimen is a cylinder with tapered ends. A photograph of the ZF-RCF can be seen in Figure 9.

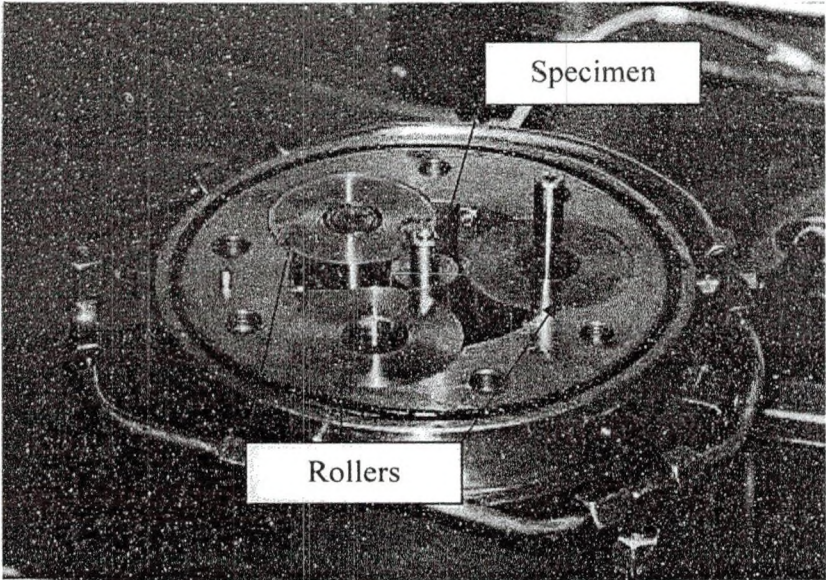


Figure 9 ZF-RCF Tester [13]

Several other contact fatigue tester and test methods are available that have not been mentioned in this paper. The machines discussed were primarily designed for the purpose of simulating gear contact. Other testing devices exist to simulate bearing and railway conditions. Some testers are designed to simulate contact fatigue in the most general conditions.

CHAPTER 2

S-RCF DESIGN

The S-RCF tester was designed, analyzed and assembled primarily during August 2006 to May 2007 by the University of North Dakota's senior design group Penta-X. After this, one student remained to improve the tester and perform the first tests with the machine.

In Chapter 1, several known factors affecting a material's contact fatigue strength were discussed. The quality of a contact fatigue tester depends upon its ability to accurately control and monitor the operational conditions. These factors include the contacting force, the slide ratio, the lubrication type, lubrication regime and the surface temperature. A design that controls and monitors each factor efficiently will be a more robust tester.

The S-RCF tester can be divided into three major components. These components are the main structure, lubrication system and failure detection system. The main structure can be divided into smaller subsections consisting of the base structure, internal structure, speed mechanism and the loading mechanism. These components and systems were designed to allow the testing of as many factors as possible. Figure 10 shows a picture of the S-RCF tester.

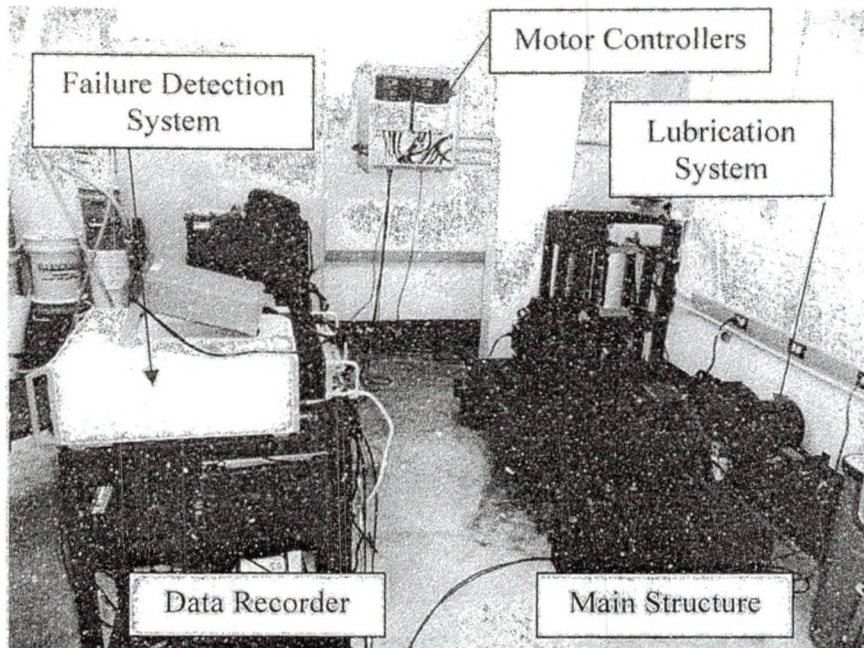


Figure 10 S-RCF Tester

Design Requirements

Two major design requirements were used to design the S-RCF tester. The first requirement stated that testing be completed in a reasonable amount of time. The second requirement was that loading capability be similar or comparable to other testers.

The first requirement of test time depends upon the rotational speed of the specimen and the number of contact points. The faster the specimen is turned, the less time is needed to complete a given number of cycles. The more contact points on the surface will result in more loads per revolution. Since there are many factors affecting a material's contact fatigue strength, testing time can vary significantly. The longest testing time is expected to occur in a well-lubricated condition. In a study using the ZF-RCF tester, several materials were tested in rolling contact fatigue under full EHL conditions [13]. The results of the study are presented in Table 3. The largest value is 20.7 million load cycles.

Table 3 ZF-RCF Results for Various Materials [13]

Material	Load Cycles to First Crack (10 ⁶)	Load Cycles to Final Failure (10 ⁶)
AISI 5120	12.1	14.0
AISI 8620	15.5	20.7
AISI 1060	4.3	6.2
AISI 4150	6.7	7.5

Due to the large number of cycles needed, Penta-X designed the S-RCF to have three contact points on the specimen. In this way, three load cycles can be completed for every one revolution of the specimen. Figure 11 shows the relation between specimen rotation speed, load cycles completed and the required testing time for the S-RCF tester. Penta-X decided that the S-RCF tester should be able to complete 30 million load cycles in under forty-eight hours. In Figure 11, the design requirement line shows that the specimen motor speed should be approximately 3500 rpm.

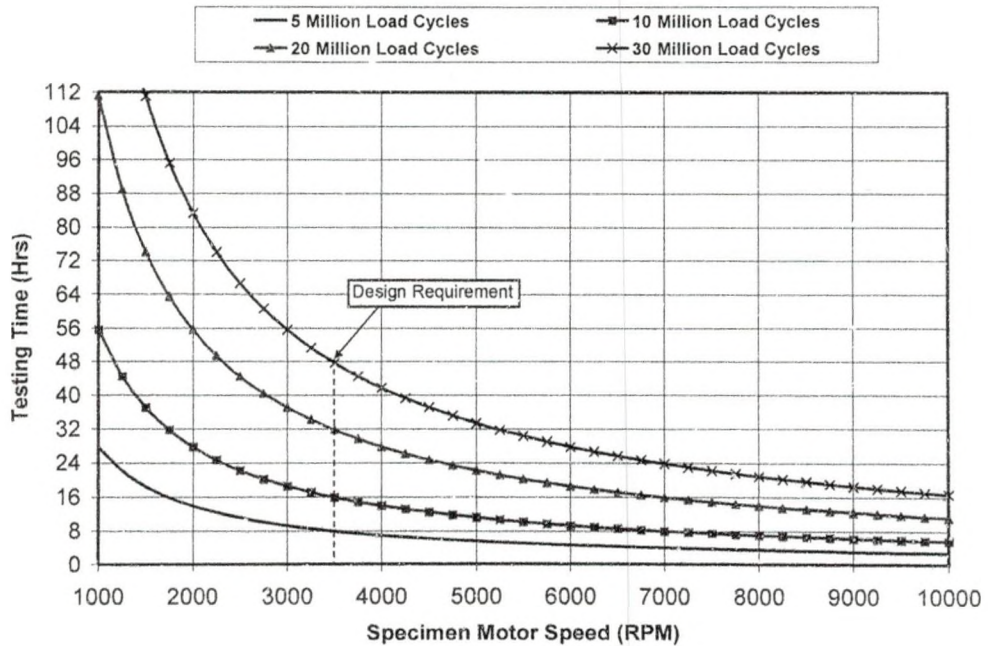


Figure 11 Testing Time Required for a Number of Load Cycles Using a Three Contact Point Testing Machine

The second requirement concerning the loading capability depends on the loading applied and the speed of the specimen. The loading values reported by other testers were given in Hertzian pressure values. Hertzian stress is the localized stress which develops from two curved surfaces contacting each other. The maximum value for the Hertzian contact stress found for the ZF-RCF was 2100 MPa (305 ksi) [13]. This Hertzian contact stress can be converted into a radial and tangential force. The tangential force is the force needed by the motors to turn the specimen. The radial force is the force applied by the loading mechanism.

During the preliminary design phase, it was decided that the S-RCF tester would apply loading directly. Thus, the radial force (F_r) is a user defined variable and can be converted into a maximum Hertzian stress (PHz) using Equation 3. The variable L is the contact length of the contacting surfaces (5 mm for the S-RCF tester).

$$P_{Hz} = \frac{4 \cdot F_r}{L \cdot \pi \cdot B} \quad \text{Eq. 3 [9]}$$

The only unknown variable in equation 3 is the contact width (B). Since the contact width is the amount of deformation that occurs, it is dependent upon the individual size and stiffness of the two contacting surfaces. The effective radius (R) accounts for the size difference and can be calculated using Equation 4, where r_1 and r_2 are the radii of the two surfaces.

$$R = \frac{r_1 \cdot r_2}{r_1 + r_2} \quad \text{Eq. 4 [9]}$$

The stiffness correction requires the Young's moduli (E_1 , E_2) and Poisson's ratios (ν_1 , ν_2) of the two respective surfaces. Equation 5 shows how to calculate the

stiffness correction (K_i) for a surface. With the correction factors now calculated, the contact width (B) can be calculated using Equation 6.

$$K_i = \frac{1 - \nu_i^2}{\pi \cdot E} \quad \text{Eq. 5 [9]}$$

$$B = \sqrt{\frac{16 \cdot F_r \cdot (K_1 + K_2) \cdot R}{L}} \quad \text{Eq. 6 [9]}$$

Figure 12 is a drawing of two cylinders contacting and the resulting Hertzian stress distribution. Some variables used in calculating the Hertzian stress are labeled.

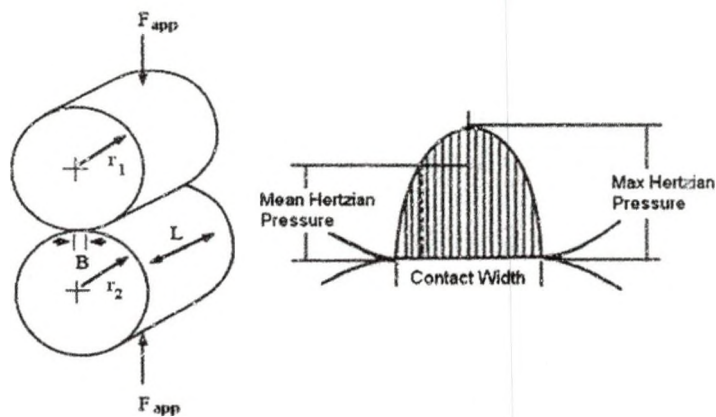


Figure 12 Hertzian Stress Variables and Distribution for Contacting Cylinders

Using the information provided about the ZF-RCF tester, it was determined that testing AISI 8620 material would require a radial force of approximately 9,055 N (2,036 lbf) to achieve a stress of 2.1 GPa [13].

The tangential force can be determined if the coefficient of friction is known. This value depends upon the slide ratio and lubrication regime. A slide ratio of zero would be the two surfaces rolling on each other; whereas, any other value would be a sliding situation. The lubrication regime can be dry, a thin film, or a full EHL layer. Table 4 provides estimates of the coefficient of friction values for steel on steel contact in various conditions.

Table 4 Coefficient of Friction Values for Steel-on-Steel Contact under Different Lubrication and Sliding Conditions [14]

Sliding Condition	Lubrication	Coefficient of Friction
Rolling	Dry	~0.0005 m
Sliding	Dry	0.20 - 0.78
Sliding	Thin Film	0.02 - 0.14
Sliding	Full EHL Layer	0.0002 - 0.007

The coefficient of friction of two steel disks rolling is represented by the variable f . For sliding conditions, the coefficient of friction will be the variable μ_k . Equation 7 shows how to calculate the tangential force for rolling conditions. Equation 8 calculates the force for sliding conditions. The variable r is the radius of the surface in question.

$$F_t = F_r \cdot \frac{f}{r} \quad \text{Eq. 7 [14]}$$

$$F_t = F_r \cdot \mu_k \quad \text{Eq. 8 [14]}$$

After the tangential force is calculated, the motor torque needed can be calculated using Equation 9.

$$T = F_t \cdot r \quad \text{Eq. 9 [14]}$$

The power needed by the motor for a given specimen speed (ω) can be calculated using Equation 10. The variable C_p is the number of contact points on the testing surface (3 for the S-RCF and ZF-RCF testers).

$$P = C_p \cdot T \cdot \omega \quad \text{Eq. 10 [14]}$$

Figure 13 demonstrates how different combinations of motor speeds and applied loadings change the power needed from the motor under dry rolling conditions. Figure 14 shows the same relation for sliding under different lubrication conditions. The dashed vertical line in each figure is the specimen motor speed from the first requirement (3600 rpm).

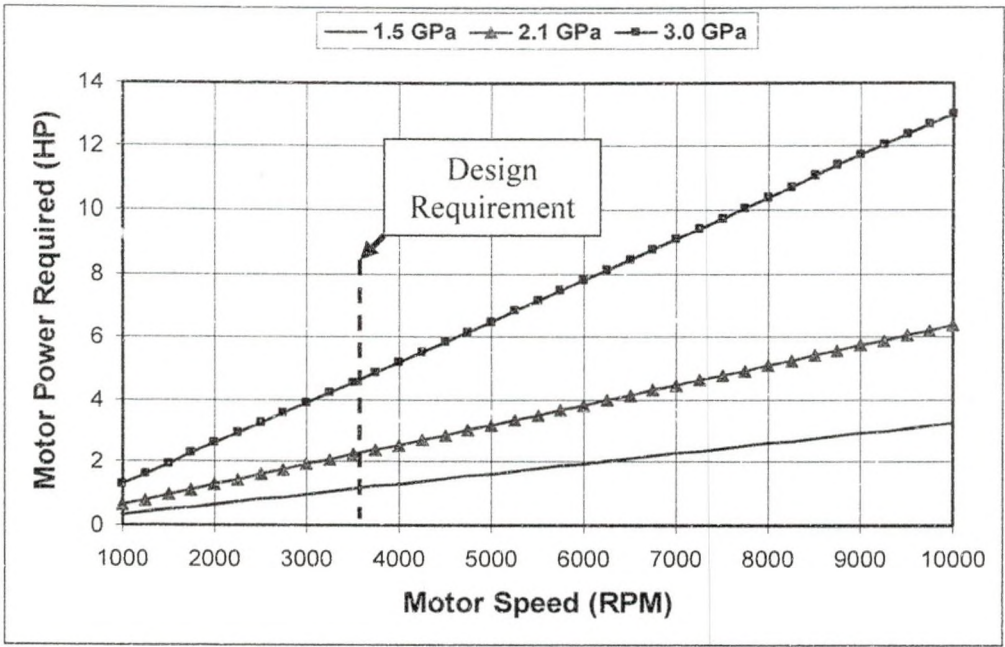


Figure 13 Required Motor Power for Various Applied Loadings under Dry Rolling Conditions

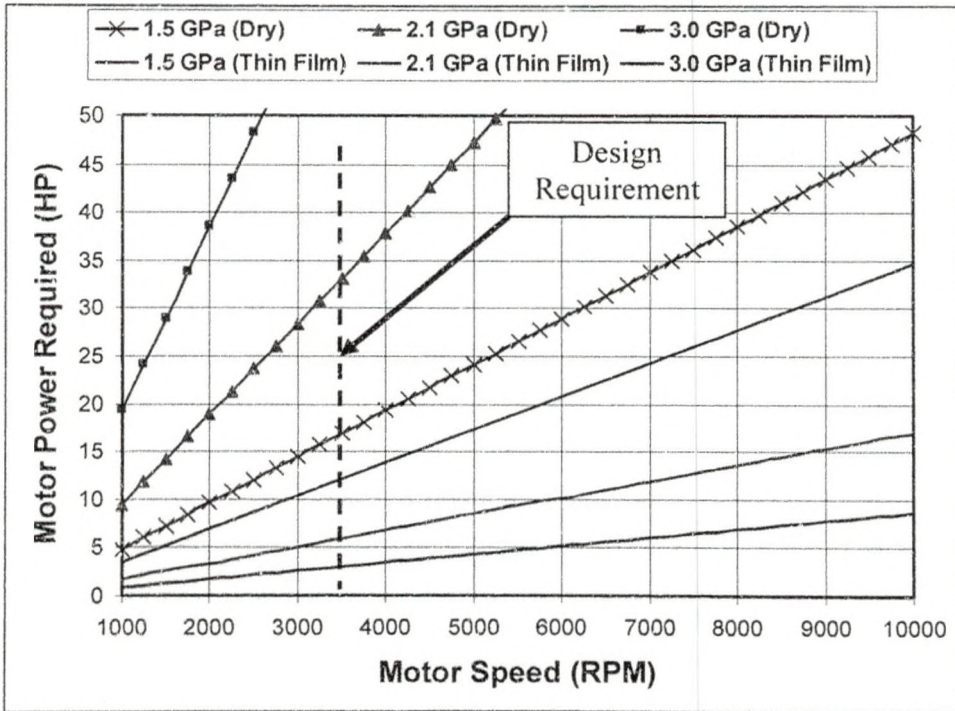


Figure 14 Required Motor Power for Various Applied Loadings under Dry and Thin Film Sliding Conditions

Using the information from Figure 13 and Figure 14, Penta-X decided to use a ten horsepower motor to run the S-RCF tester. In a rolling situation, testing can be performed at max speed of approximately 8000 rpm, well above the requirement of 3600 rpm. In a sliding, thin film condition, testing can be performed at 3.0 GPa Hertzian pressure at a speed of approximately 3000 rpm. Although this is slightly lower than the 3600 rpm requirement, the number of cycles needed for failure will be less than rolling conditions. In a dry sliding condition, the max load that can be applied is 2.1 GPa Hertzian pressure at a speed of 1000 rpm. In dry conditions, the number of cycles until failure should be much less than any lubricated situation. The motors selected for the S-RCF tester will be discussed in this chapter in the Driving Mechanism section.

Main Structure

The main structure is the central component of the S-RCF tester. It can be broken down into four subsections: the base structure, the internal structure, the driving mechanism and the loading mechanism. Several pictures of the S-RCF tester are taken from the Pro-E® model to demonstrate concepts more clearly. Other pictures are photographs of the actual S-RCF tester since this will give a better sense of what is being described. Figure 15 shows the Pro-E® model of the main structure and Figure 16 is a photograph of the S-RCF tester main structure.

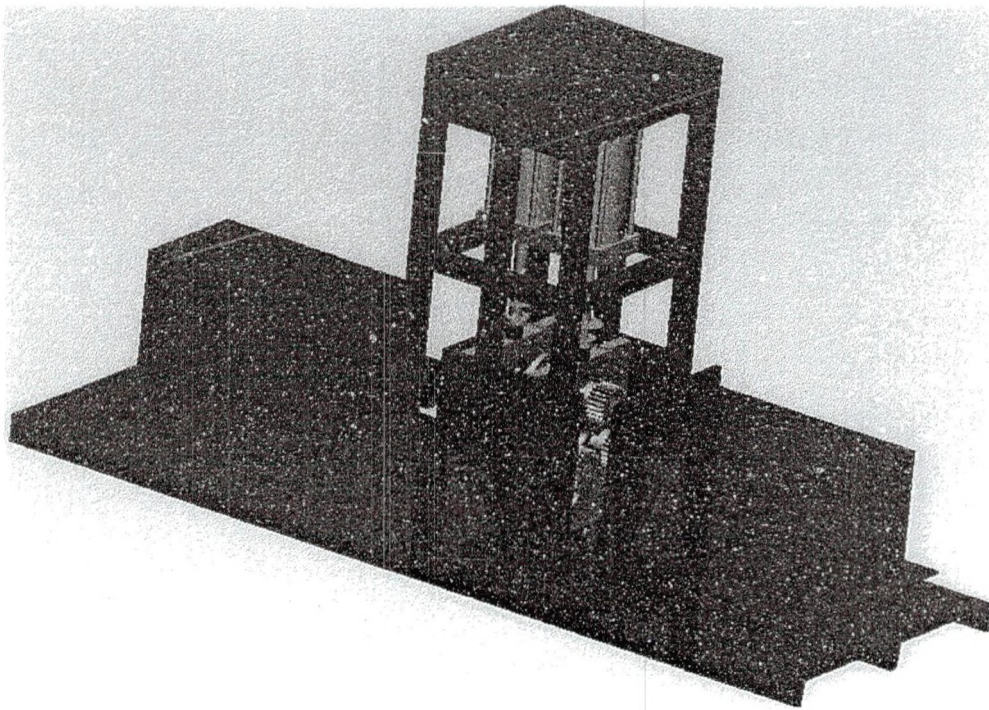


Figure 15 Pro-E® Model of the Main Structure of the S-RCF Tester

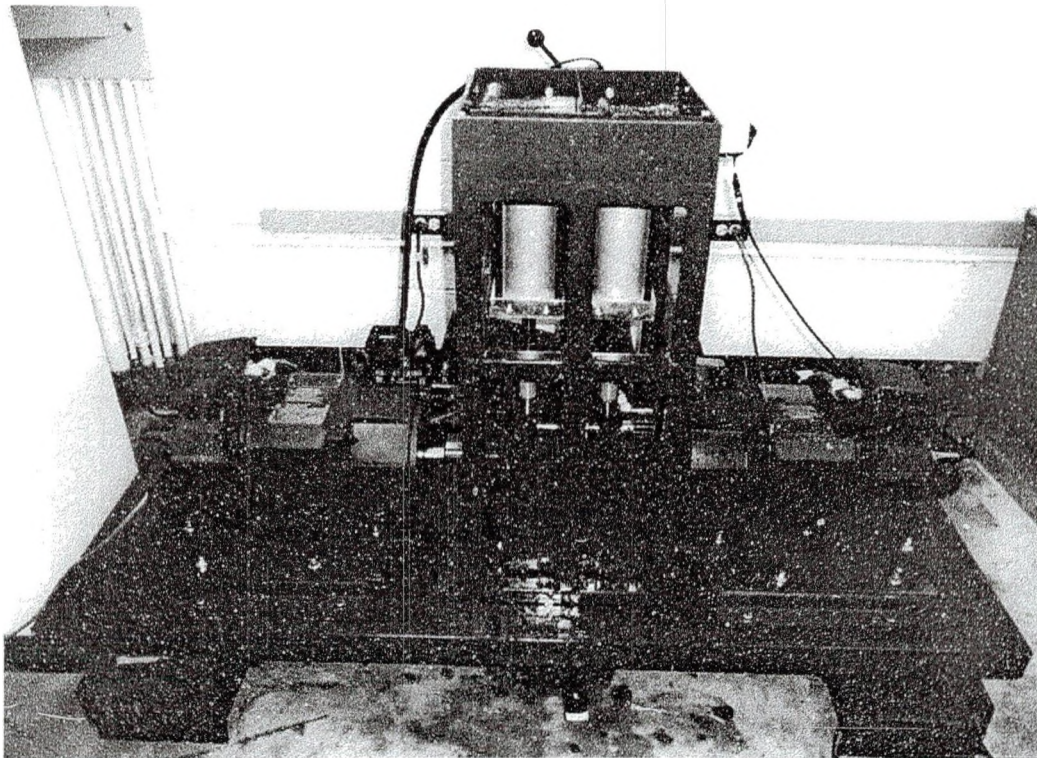


Figure 16 Main Structure of the S-RCF Tester

Base Structure

The base structure is where most of the other parts attach. The four major parts of the base structure are the base, the inner walls, the bearings and the side oil walls. The parts can be seen in Figure 17 which is the Pro-E® version of the base structure.

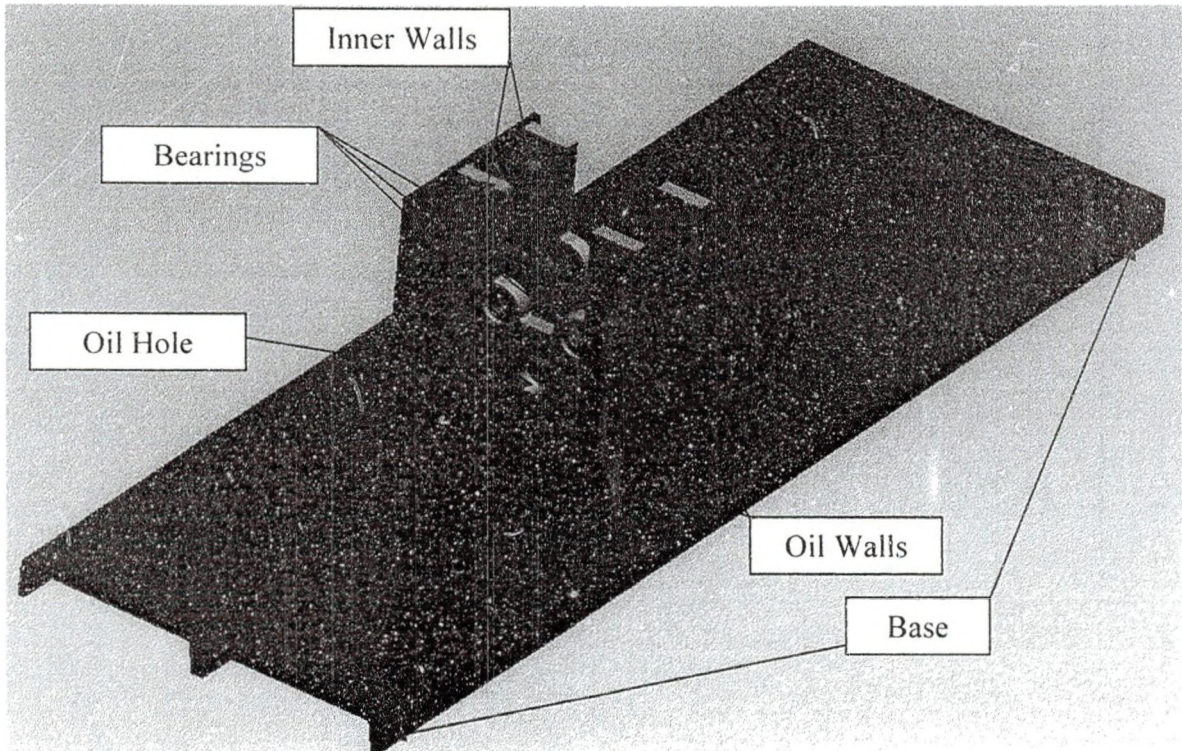


Figure 17 Pro-E® Model of the Base Structure of the S-RCF Tester

The base was constructed by welding two twelve inch channel irons to each other. The inner walls were precision machined at Northern Valley Machining in Grand Forks, ND. The inner walls and side oil walls are attached to the base with screws. The inner walls are attached to the side oil walls in the same way. The bearings were press fit into the inner walls. The inner walls also have an oil hole to allow for better flow of the lubricant.

Internal Structure

The core of the S-RCF tester is the internal structure. This is the part of the machine where the actual testing takes place. The part with the surface that is being tested is called the specimen. The parts with a surface in contact with the specimen are called the rollers. Figure 18 shows a picture of the specimen and rollers used in the S-RCF tester.

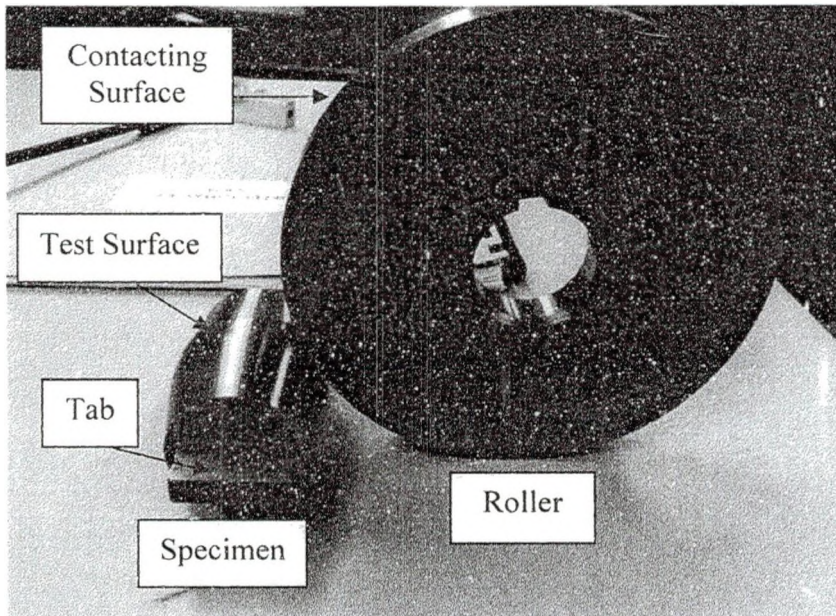


Figure 18 Specimen and Roller for S-RCF Tester

It can be seen in Figure 18 that the specimen is a tapered cylinder with tabs. This taper serves two functions. First, it limits the contact width between the rollers and specimen. The test surface is only 5mm (0.197 in.) wide. This size was chosen because the failure detection system of the S-RCF tester uses a probe with a scanning width of 5mm. Secondly, the taper acts as a crack initiation site. If a cylinder specimen was used, the tester would be measuring the compressive strength of the material being studied rather than the improvement of the surface finish.

The roller diameter is three times larger than the diameter of the test surface on the specimen. The size difference ensures that the rollers do not fail before the specimen. Since the rollers are three times larger, the circumference is three times larger. Under rolling conditions, one revolution of the roller is three revolutions of the specimen. Since three rollers contact the specimen, one revolution of the specimen equal three loadings. Therefore, for one roller revolution, the roller has only been loaded once while the, the specimen has been loaded nine times.

The internal structure is comprised of three assemblies: the top roller assembly, the specimen assembly and the bottom roller assembly. The top roller assembly and the specimen assembly slide vertically into the inner walls. These two assemblies are shown in Figure 19. The bottom roller assemblies are fixed in the inner walls. Figure 20 shows the Pro-E® model of the internal structure with the base attached and one inner wall.

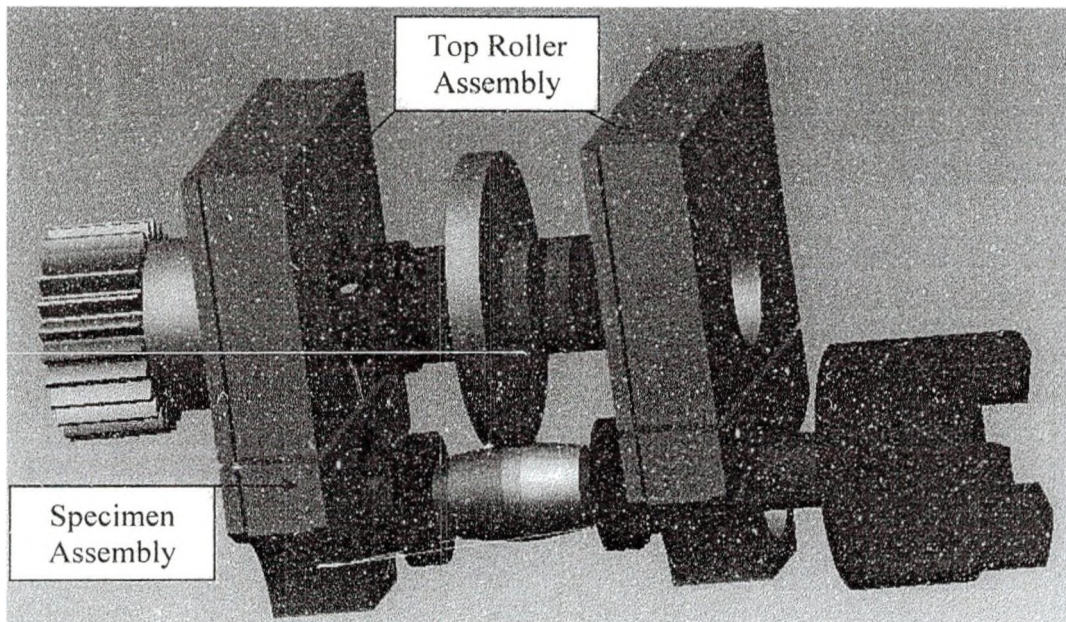


Figure 19 Top Roller and Specimen Assembly

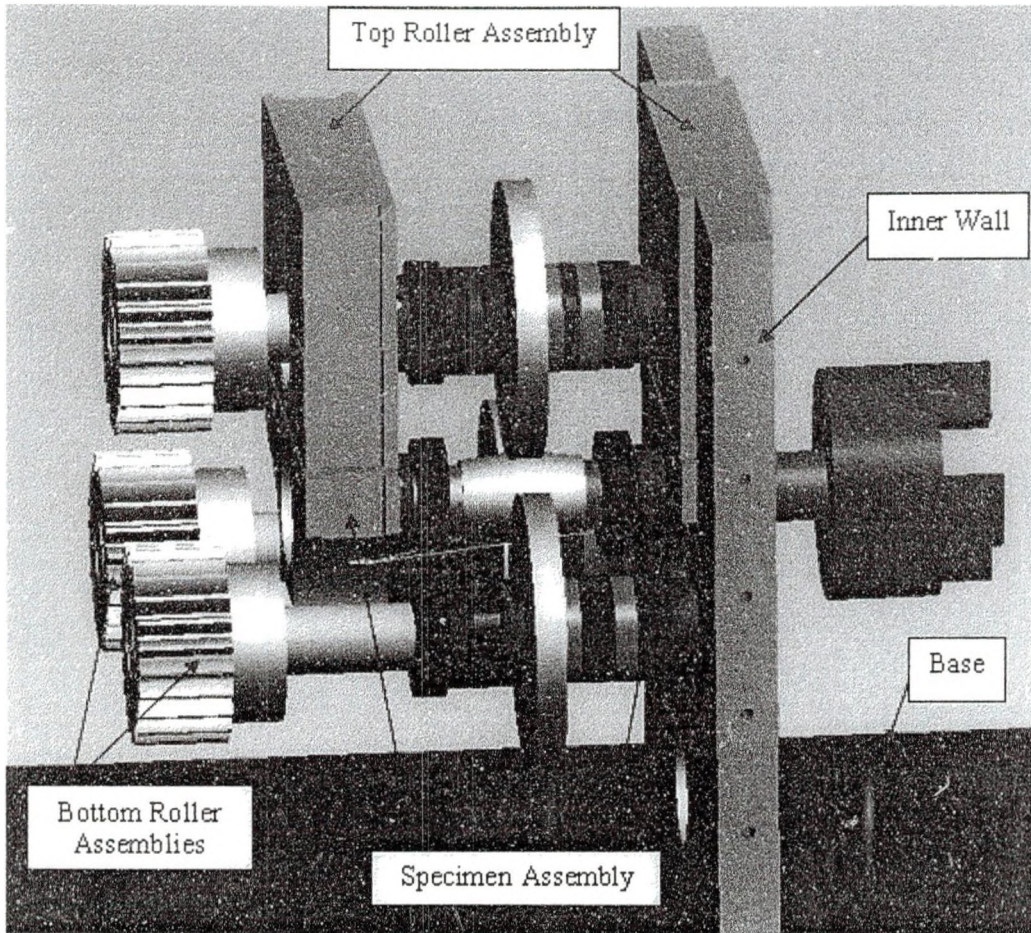


Figure 20 Pro-E® Model of the Internal Components of S-RCF Tester

All of the assemblies have metal collars on them. There are three types of collars used in the S-RCF tester: a hinged collar, a regular collar and a keyed collar. The hinged collars are used on stepped portions in the shafts of each assembly to prevent axial motion. The regular collars and keyed collars are used to hold the rollers in place. The keyed collars have keyways in them to allow the shafts to be pulled out when lined up correctly. The keyed collars and regular collars have roman numerals engraved into their outer surface. Roman numerals I and II are engraved on the collars for the bottom roller assemblies and Roman Numeral III is engraved on the collars for the top roller assembly. Figure 21 shows each type of collar used in the S-RCF tester.

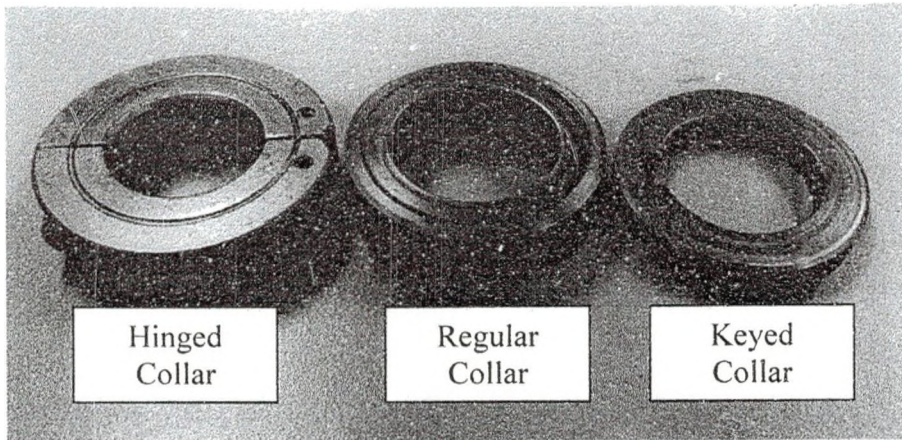


Figure 21 Types of Collars Used in the S-RCF Tester's Internal Structure

The free end of each shaft in each assembly has a 1/4-20 UNC tapped hole. This allows a small flat disk (called the tightening disk) to be screwed onto the end of the shaft. The tightening disk is large enough to set over top of the bearings in the inner wall. The tightening disk removes any gaps between the collars. Figure 22 shows the tightening disk on the top roller assembly.

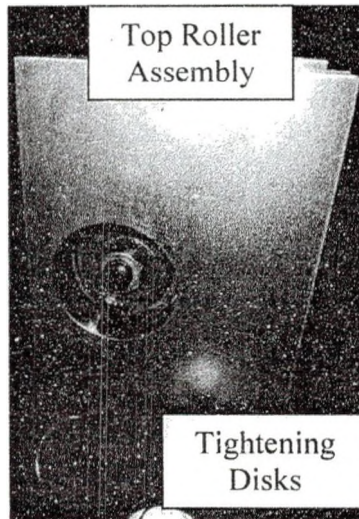


Figure 22 Tightening Disk on Top Roller Assembly

Under loading, the only significant contact point for the top roller assembly is between the top roller and the specimen. This ensures that the load applied to the top

roller is completely transferred to the specimen. In the same way, the only significant contact point for the specimen assembly is with the rollers. The rollers are spaced symmetrically (120°) around the specimen. Neglecting the weight of the top roller and specimen, the bottom rollers return the same magnitude of force applied to the top roller.

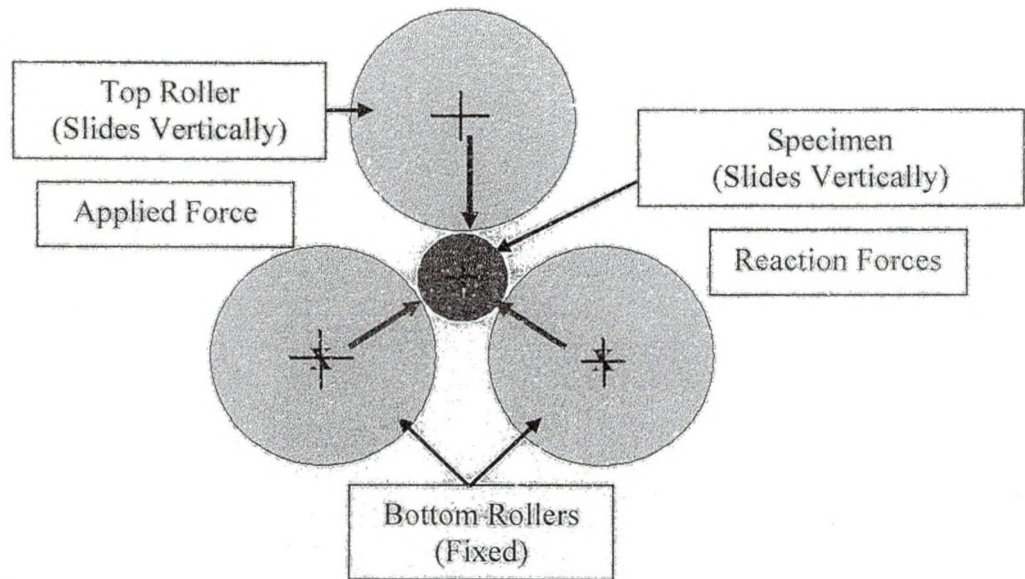


Figure 23 Diagram of Symmetrical Spacing (120° apart) of the Rollers Around the Specimen and the Applied and Reaction Forces under Loading

Driving Mechanism

Using the criteria developed in the Design Requirements, two motors were selected to drive the S-RCF tester. Both motors are Allen-Bradley® CM203-NV01035AXZHA-547 which operates on 230V or 460V three phase AC power. An encoder is attached to each motor for precision control of the speed. The maximum speed that can be maintained at 10 HP is 3550 rpm. The maximum speed is 4150 rpm. Larger and faster motors were available but were considerably more expensive.

The motors enter into the end oil walls through an oil seal. These oil seals allow for submerged testing to be performed. The roller motor drives the rollers shafts through

a series of spur gears. The spur gears have a three inch pitch diameter, a pressure angle of 20° and twelve teeth. Under loading, the gears are spaced so they mesh correctly.

Figure 24 shows the gearing for the S-RCF tester.

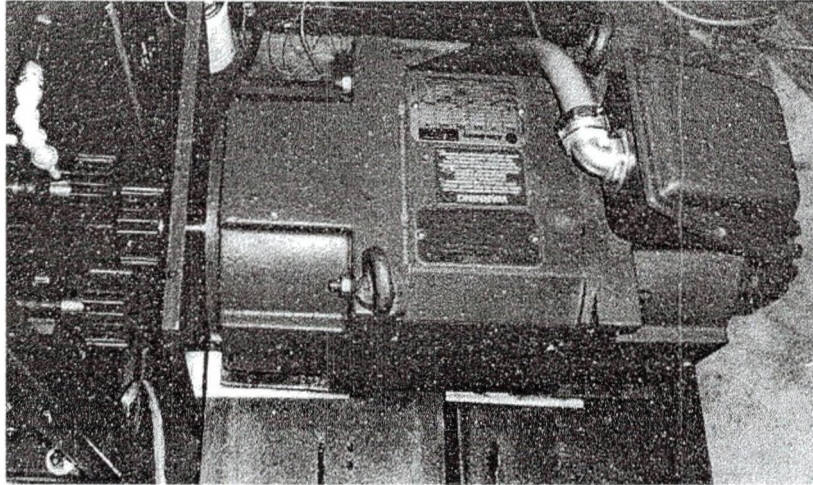


Figure 24 S-RCF Tester Roller Motor and Gearing

The specimen motor connects to the specimen shaft by a spider couples. The spider couple allows for an angular misalignment of 1° and a parallel misalignment of .015 inches. Figure 25 is a picture of the specimen motor.

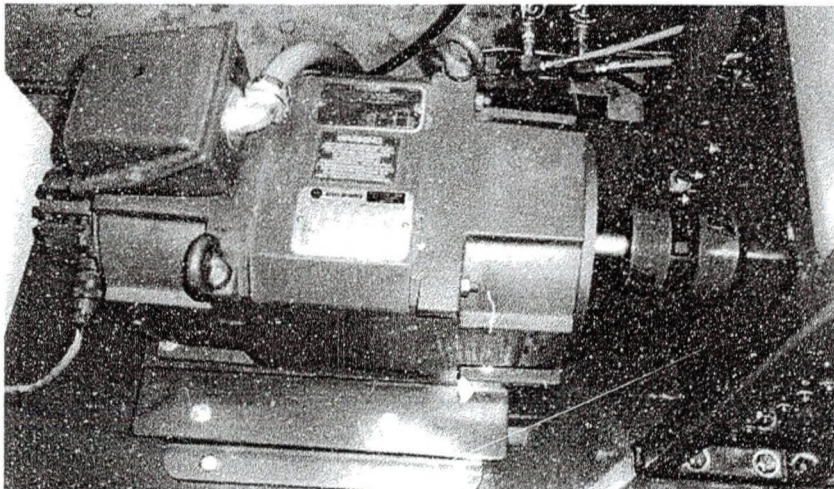


Figure 25 S-RCF Tester Specimen Motor

The motors are controlled by two different controllers in a master-slave setup. The specimen motor is connected to the master controller. The master controller is the Power Flex 70. The motor that drives the rollers is connected to the Power Flex 700S, the slave controller. Figure 26 shows a picture of the controllers.

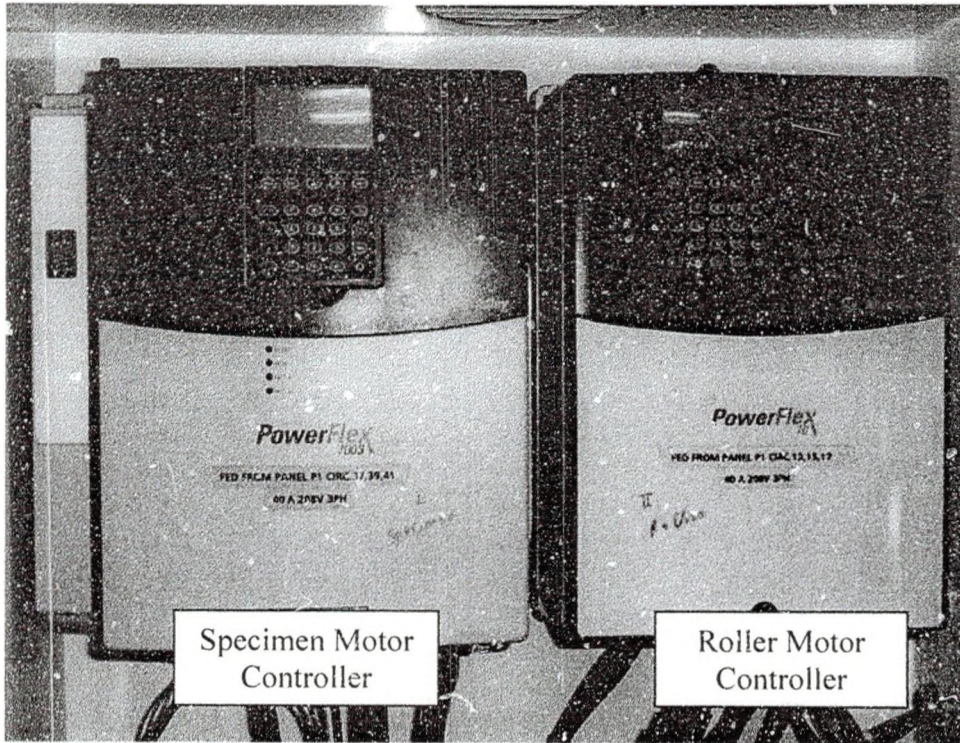


Figure 26 Power Flex Controllers for the S-RCF Tester Motors

Loading Mechanism

The S-RCF tester uses two pneumatic cylinders to apply the desired loading. The cylinders are aluminum tie rod cylinders, each with a bore of 4 ½ inches and a stroke length of approximately 8 inches. The maximum allowable pressure in each cylinder is 250 psi [15]. These cylinders are located in the loading structure. Figure 27 shows the loading structure with several smaller parts labeled.

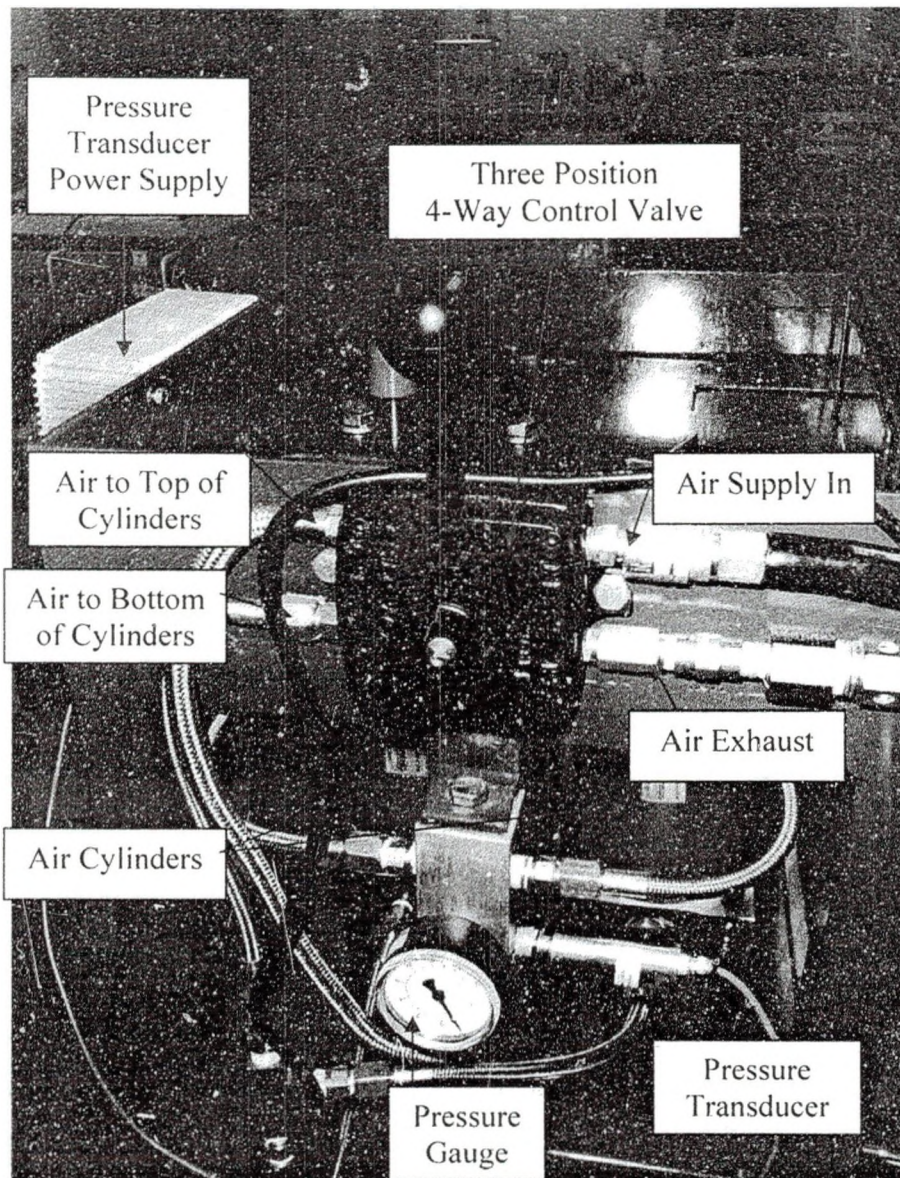


Figure 27 View of the Back Side of the S-RCF Tester's Loading Structure

The air flow to the cylinders is controlled by a three position four-way control valve located on the back side of the loading structure. The three positions are up, down and off. In the down position, air is pushed into the top of the cylinders and loading is applied to the specimen. In the up position, air is pushed into the bottom of the cylinders. In the off position, no air is allowed in or out of the cylinders. The control valve can hold

a maximum pressure of 150 psi, another limiting component for the amount of pressure possible in the S-RCF tester [16].

Air pressure can be supplied using a portable air compressor or some other external source. An air pressure regulator is used to set and maintain the air pressure in the cylinders. The regulator is rated for a maximum pressure of 150 psi and can operate at a maximum temperature of 125°F [17]. The accuracy of the regulator is ± 3 psi or better [17]. The component is the limiting factor in the amount of pressure that can be applied by the S-RCF tester.

The pressure in the cylinders can be determined in two ways, visually or electronically. On the back side of the S-RCF tester is a pressure gage. This gage allows for an approximation of the pressure in the cylinders. For a more accurate reading, a pressure transducer has been installed in the same area. The pressure transducer can measure up to 200 psi of air pressure [18]. Figure 28 is the schematic for the pneumatic system. Additional information on the transducer can be found in Appendix A: Supplemental Test Data.

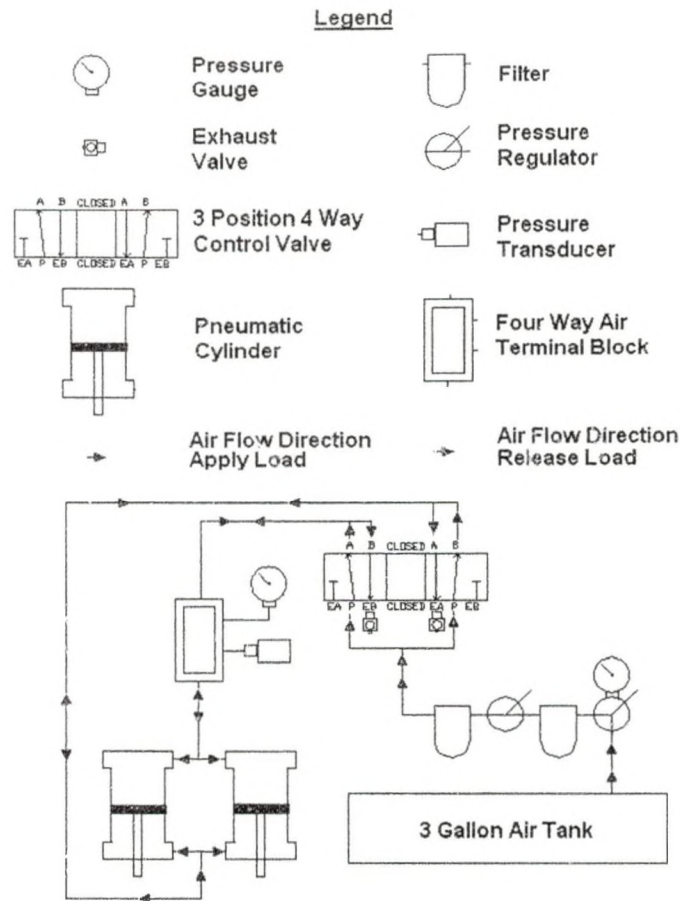


Figure 28 Pneumatic Schematic for S-RCF Tester

When the cylinder rods are lowered, pressure is applied to the top roller assembly. As previously stated, the load is transferred completely to the specimen since the only significant contact point between the top roller assembly and the specimen assembly is between the top roller and the specimen. Figure 29 is the Pro-E® model of when the top roller and specimen are in contact. Notice that a gap exists between the top roller assembly and the specimen assembly. The inner wall on the left side of the figure has been removed for clarity.

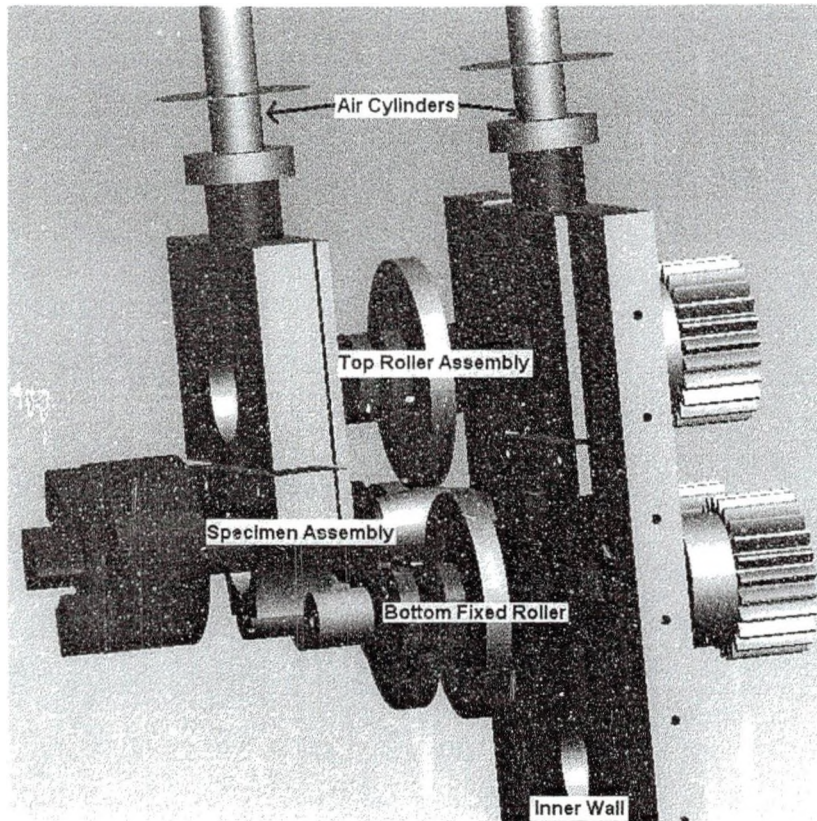


Figure 29 Pro-E® Model of Rollers and Specimen in Contact with One Inner Wall Removed

The ZF-RCF tester and the NASA gear test apparatus both use Hertzian pressure to define the amount of loading applied [13]. In converting Hertzian pressure to a radial force, a material's Young's modulus (E) is needed (see equation 5). Therefore, different materials will require different applied pressure to achieve the same Hertzian stress. A MathCAD® file in Appendix B can be used to convert Hertzian pressure to the pressure needed for the S-RCF tester. Figure 30 shows the relation for AISI 8620 steel.

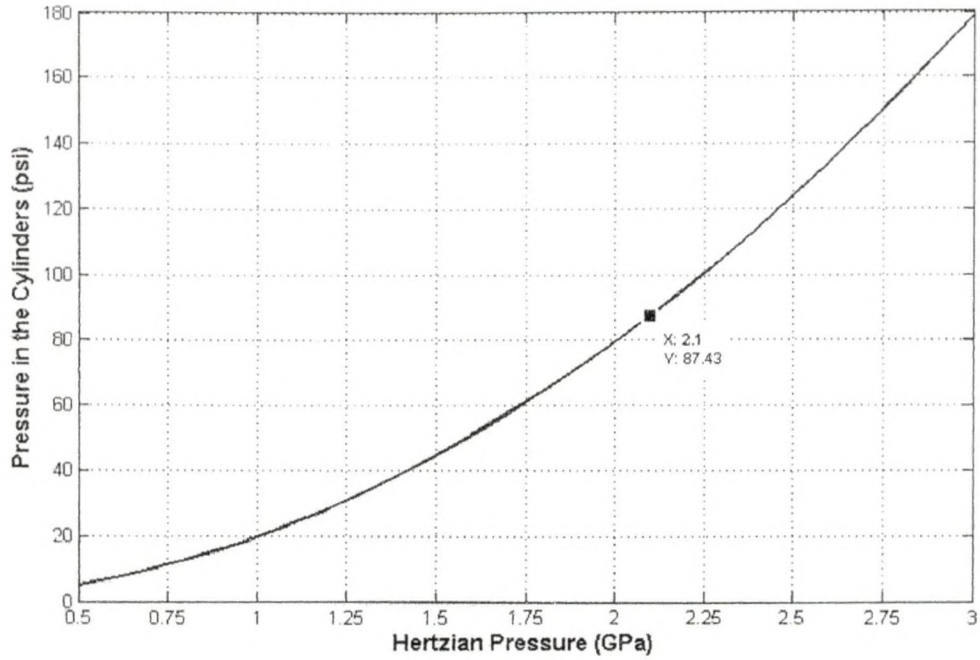


Figure 30 Hertzian Pressure Conversion to Applied Pressure of the S-RCF Tester for AISI 8620

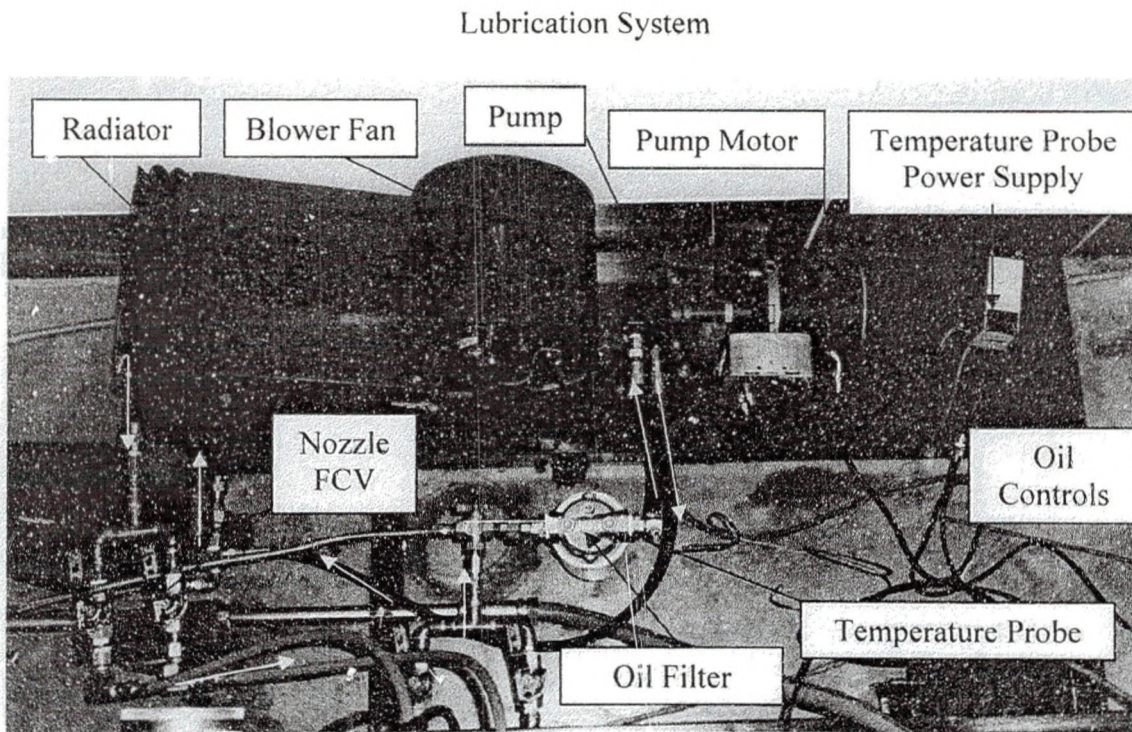


Figure 31 Lubrication System for S-RCF Tester (Oil Flow Shown in Yellow)

The lubrication system of the S-RCF tester can be seen in Figure 31 and has several functions. First, the system was designed to test in dry, film or submerged conditions. Dry and film testing is accomplished by controlling the flow of lubricant through nozzles to the internal structure. Two nozzles enter into the internal structure. The nozzle supplying lubrication to the gears needs to always be on during any test. The nozzle providing lubrication to the specimen can be turned off to perform dry testing or on to perform film testing. Figure 32 shows the two nozzles and the on/off controls for each.

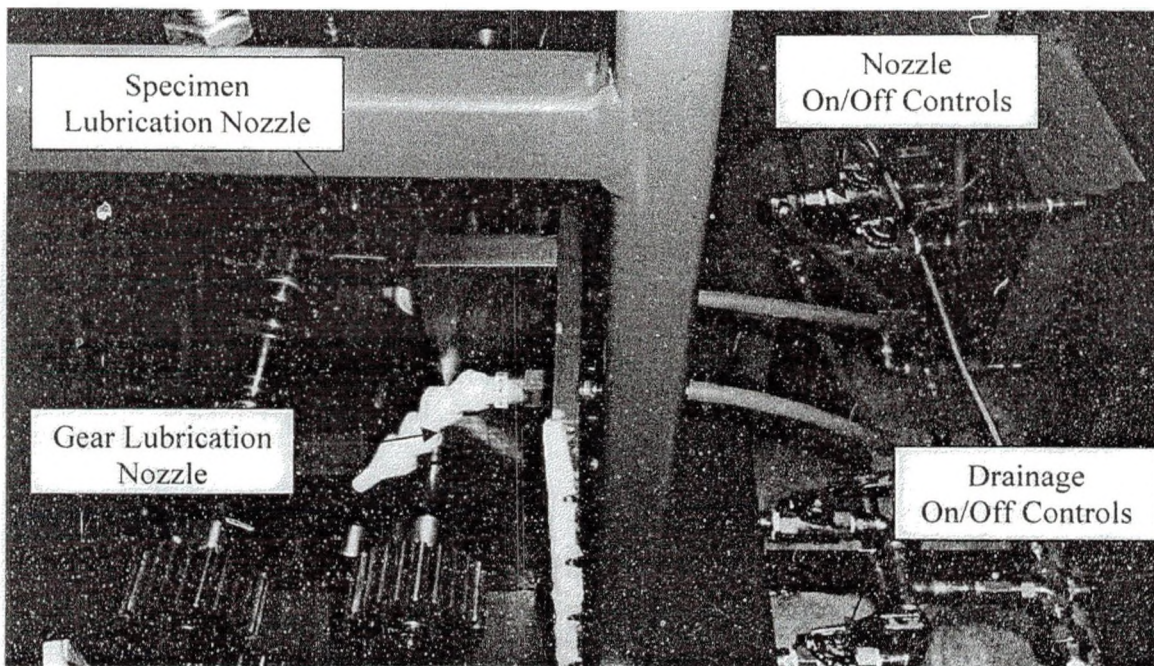


Figure 32 S-RCF Tester's Lubrication Flow Controls to Specimen and Gears

The second function of the lubrication system is to clean the lubricant and remove it from the system when the testing is completed. After leaving the internal structure, the lubricant is pumped through a three micron oil filter. The filter is placed before the pump to prevent harmful particles from entering the pump. The system can be flushed using gravity or by pumping it out. Before the filter is a three-way valve that directs the flow to

the oil filter or to a reservoir. If a large amount of lubricant needs to be flushed, a second three way valve is placed after the pump. This allows the pump to pull the lubricant out of the internal structure.

The third and final function of the lubrication system is to control and monitor the lubricant temperature. Currently, the lubrication control system is manually operated. The lubrication is pumped out of the internal structure into a filter. After leaving the filter, the lubricant's temperature is measured by a thermistor probe. Information on the temperature probe can be found in Appendix C.

After the temperature is measured, the lubricant passes through the pump and flows into a radiator. A blower fan pushes air through the radiator to cool the lubricant. The blower fan speed is controlled by a rheostat. A complete schematic of the lubrication system can be seen below in Figure 33.

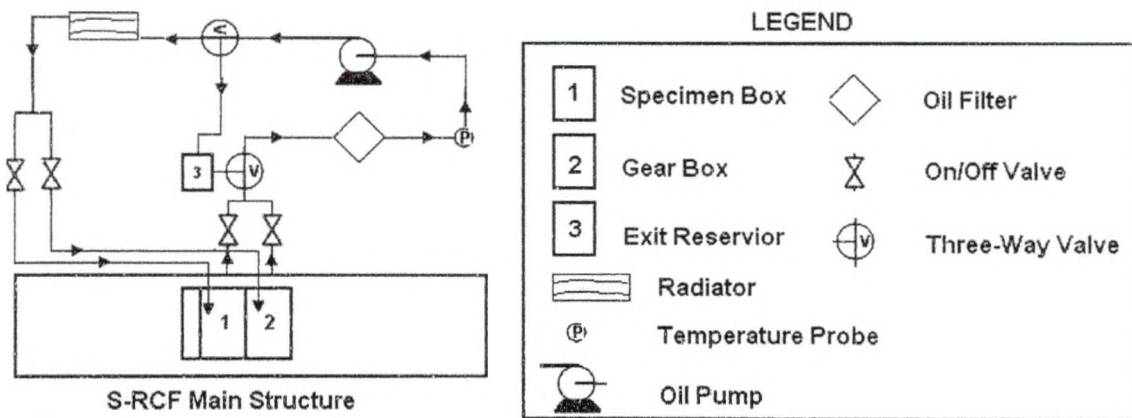


Figure 33 Schematic of the S-RCF Tester's Lubrication System

Failure Detection System

Nondestructive Inspection (NDI) Methods

Many methods are available to perform non-destructive testing and inspection.

For the S-RCF tester, a few requirements were decided upon by Penta-X. First, the

detection method needed to be portable. Secondly, the detection device would have to be capable of monitoring a spinning part. Since subsurface cracks were possible, the third requirement was that the device be able to detect these cracks. Finally, the detection method must be safe to use on a daily basis. Most of the contact fatigue testers discussed previously used vibration monitoring or eddy current monitoring for failure detection.

Table 5 shows some basic characteristics of several NDI methods available.

Table 5 Basic Characteristics of Common NDI Methods [19]

	Inexpensive	Portable	Training/Skill Required		Part Preparation Required		In Situ Monitoring	Accessible to Probe	Safety Hazard	Sensitivity		Ability to Detect Subsurface
			High	Low	High	Low				High	Low	
Visual Inspection	X	X		X		X					X	
Dye Penetrant	X	X		X	X						X	
Magnetic Particle	X	X			X					X		X
Eddy Current		X	X			X	X	X		X		X
Ultrasonic	X	X	X			X	X	X		X		X
X-Ray Radiography			X			X			X			
Isotope Radiography			X			X			X			
Vibration Monitoring	X	X		X		X					X	

Based on the criteria listed above, the two methods that seemed the most promising were the eddy current and ultrasonic methods. Both methods require reference standards, since signal interpretation takes some skill and training. Due to availability and information at the time, the eddy current method was chosen for the failure detection system in the S-RCF tester.

Eddy Current Inspection and Parameters

Eddy current inspection works on the principles of electromagnetic induction.

Therefore, materials must be electrically conductive for this method to work. Figure 34 shows the different fields that are produced in eddy current detection systems.

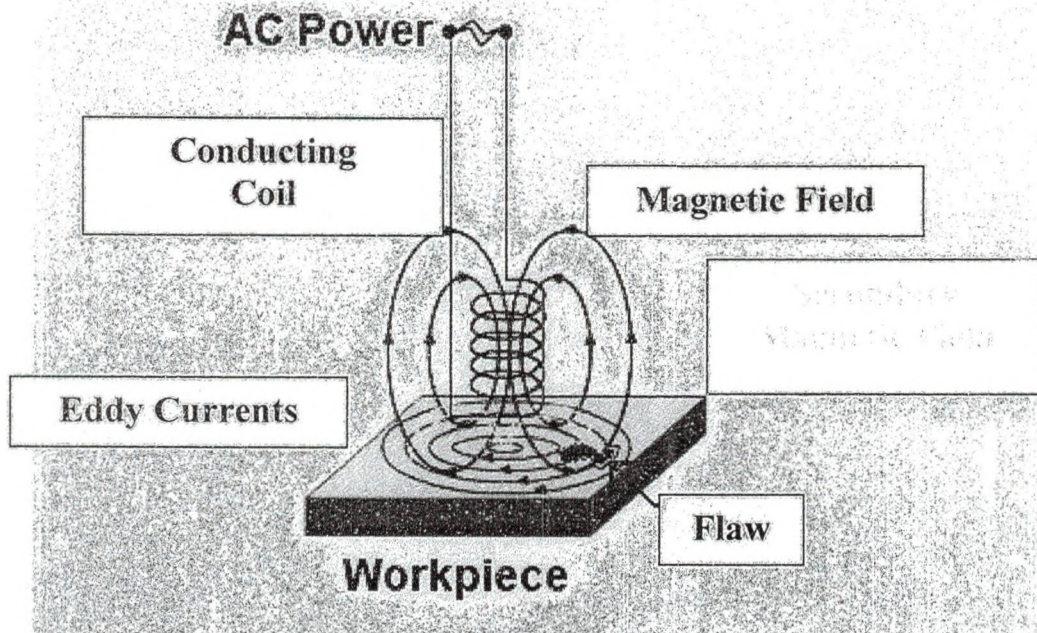


Figure 34 Basic Eddy Current Magnetic Field Description [20]

An AC current is supplied to a conducting coil. This coil produces a magnetic field (shown in blue). When a conductive material is placed close to the coil, eddy currents (shown in purple) are induced into the material. These eddy currents will produce a secondary magnetic field (shown in yellow) which opposes the magnetic field (shown in blue) of the coil. When a flaw is present on the work piece, the eddy currents are disrupted. This disruption changes the impedance of the material and can be output as a voltage change [20].

The conducting coil is placed inside a casing called a probe. Probes come in several different types: absolute, differential, reflection and hybrid. Absolute probes have

a single test coil and measure the absolute change in impedance. These probes are used in many applications including flaw detection, conductivity measurements and thickness [20]. Since there is only one coil, absolute probes are sensitive to temperature, lift-off, vibrations and conductivity [20].

Differential probes have two coils with AC current passing through them. These types of probes measure the difference in signal between the two coils. Therefore, differential probes are sensitive to flaws while being insensitive to temperature, vibrations, conductivity and lift-off [20]. Since two coils are used, signal interpretation may be more difficult. In the case of a crack wider than the spacing between the two coils, only the edges of the crack would be detected. The signal output of the two coils would be the same over the middle of the crack.

Reflection probes have two coils; however, only one coil has current passing through it (the driver coil) while the other coil senses the changes in the test material (the pickup coil) [20]. This coil configuration is used since the individual coils can be optimized for a specific purpose. The driver coil can be made to induce a strong magnetic field while the pickup coil can be designed to be sensitive to small defects [20].

Hybrid probes are usually designed for specific purposes and can act as an absolute, differential and/or reflection probe [20].

The eddy current detection system used by the S-RCF is the Foerster Defectomat® EZ 2.828. This inspection system allows for eight different inspection frequencies. Material to be inspected can pass beneath the probe at a maximum speed of 120 m/s (24,000 feet/minute). At 3,000 rpm, the S-RCF specimen is only traveling at approximately 6 m/s. Additional information about the Defectomat® EZ can be found in

Appendix C. The probe used by the S-RCF tester is a differential probe. The differential probe has the ability to monitor crack size and growth. Figure 35 shows a picture of the Defectomat® EZ, the differential probe and the probe holder.

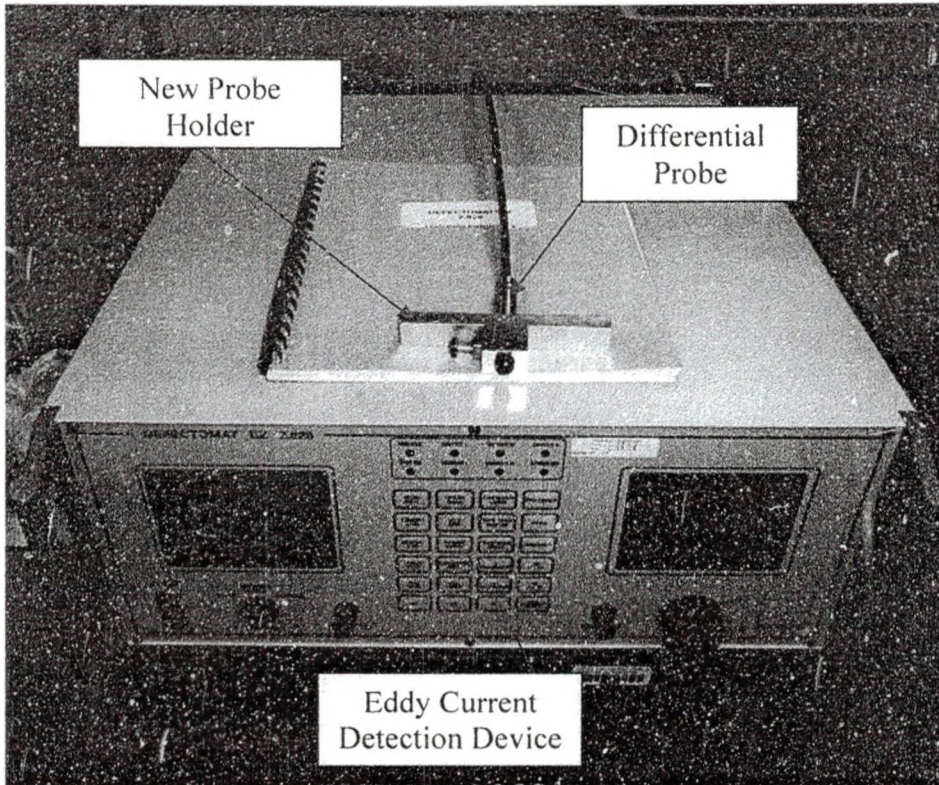


Figure 35 Foerster® Defectomat EZ 2.828 Eddy Current Detection Device

The factors affecting the eddy current detection system’s performance can be broken down into two categories. The first category is the electrical properties and surface characteristics of the material. For eddy current inspection to work, the material must be electrically conductive. The electrical conductivity of a material is influenced by the alloying, hardness, temperature, residual stresses and coatings applied to the material [21]. Surface characteristics that affect the eddy current inspection method include the surface finish, residual stresses and surface roughness. Since these parameters are material characteristics, they cannot be controlled during a test. For a batch of specimens

with the same surface characteristics, the baseline eddy current output should be similar for all of them.

The second category of factors is the setup of the eddy current inspection system. These factors include the inspection frequency and the lift-off. The inspection frequency is the frequency of the eddy current inspection system. This factor will determine the system's sensitivity to discontinuities and the depth of penetration into the material [19]. The density of eddy currents decreases exponentially as you move deeper into the material. This is demonstrated in Figure 36. The smaller the eddy current density, the less sensitive the eddy current device is to cracks.

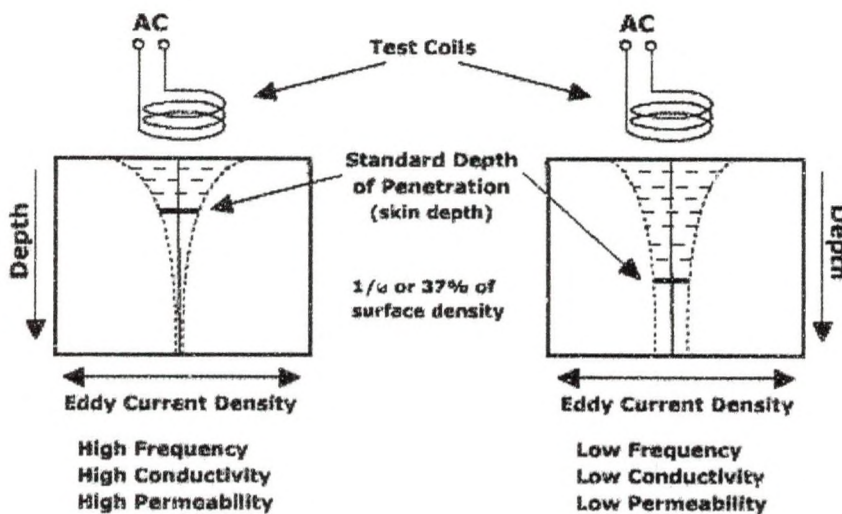


Figure 36 Eddy Current Depth of Penetration [20]

The standard depth of penetration (δ) in millimeters can be found using Equation 10. This is the depth at which the eddy current density has decreased to approximately 37%. In Equation 11, σ is the material's conductivity (mhos/m), μ_m is the magnetic permeability of the material, μ_0 is the magnetic permeability of free space and f_{Hz} is the eddy current inspection frequency (Hz).

$$\delta = \frac{1}{\sqrt{\sigma \cdot \pi \cdot \mu_m \cdot \mu_o \cdot f_{Hz}}} \quad \text{Eq. 11[22]}$$

For a curved surface, a limit (or characteristic) frequency can be calculated. The limit frequency (f_{limit}) is the inspection frequency where the strength of the magnetic field penetrating the surface is the strongest [22]. The limit frequency can be found using Equation 12.

$$f_{limit} = \frac{1}{2 \cdot \pi \cdot r_s^2 \cdot \sigma \cdot \mu_m \cdot \mu_o} \quad \text{Eq. 12[22]}$$

Lift-off is the distance between the probe and the piece being inspected [19]. As the lift-off increases, the sensitivity to impedance changes (surface and subsurface discontinuities) decreases. The sensitivity decreases because the eddy current density decreases. Therefore, it is usually preferable to minimize the amount of lift-off [19].

The impedance measured by the eddy current detection device can be broken up into two components, the resistive and the reactance. The resistive component is the real part of the impedance and the reactance component is the imaginary part. On an oscilloscope, the resistive component is usually displayed on the abscissa and the reactance component is usually displayed on the ordinate. Therefore, the resistive impedance is labeled X and the reactance impedance is labeled Y.

The Defectomat® EZ 2.828 has an oscilloscope on the front panel that can display the impedance in four different forms. Three of the displays are plotted against time on the abscissa. The first display plots the Y component on the ordinate, the second display plots Y2 on the ordinate and the third display plots the vector (V) on the ordinate. V can be found from the X and Y components of the impedance, as shown in Equation

13. The fourth type of display plots the X component on the abscissa and the Y component on the ordinate.

$$V = \sqrt{(X)^2 + (Y)^2} \quad \text{Eq. 13}$$

Data Manipulation System

Data Storage

Several test parameters are monitored and recorded during a test. These parameters include the applied loading, specimen speed, slip ratio, oil temperature and eddy current voltage readings. Recording these parameters requires eight input channels. The data is recorded using a TEAC LX-10 recording unit. Information about the channels recorded can be seen in Table 6.

Table 6 Channel Descriptions for the TEAC LX-10 Recording Unit

TEAC Channel	Channel Description	Monitoring Unit	Voltage Range	Conversion Factor	Units
1	Y-component	Defectomat® EZ-2-828	0 to 1	1	V
2	X-component	Defectomat® EZ-2-828	0 to 1	1	V
3	V	Defectomat® EZ-2-828	0 to 1	1	V
4	Y ²	Defectomat® EZ-2-828	0 to 1	1	V
5	Cylinder Pressure	Pressure Transducer PX209-200G5V	0 to 5	40.169	psi
6	Oil Temperature	Thermistor Pipe Plug THX-400-NPT-72	0 to 10	21.091	Celcius
7	Specimen Motor Speed	PowerFlex 700S	-10 to 10	416.5	RPM
8	Roller Motor Speed	PowerFlex 70	-10 to 10	416.5	RPM

The conversion factors for the cylinder pressure, oil temperature and motor speed were determined by calibrating each monitoring unit. The calibration of the pressure transducer was accomplished by using a HART® Communicator Model 275 and a Rosemount 1151DP Differential Pressure Transmitter. The air compressor, pressure transducer and HART® Communicator were all connected to the 1151DP Transmitter.

The voltage value of the pressure transducer was recorded along with the pressure value on the Hart® Communicator. These values were then plotted and a linear regression analysis was performed to determine the conversion factor. The graph and equation from this analysis can be seen in Figure 37.

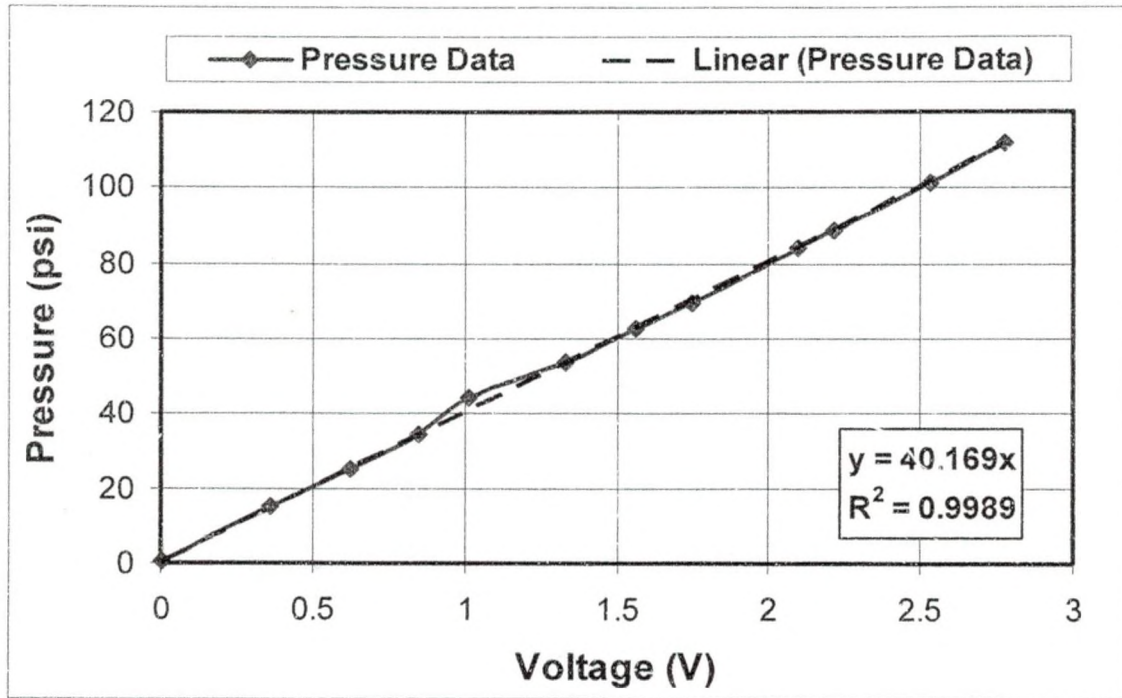


Figure 37 Calibration Results for the S-RCF Pressure Transducer

The temperature probe was calibrated using a type K thermocouple connected to a Fluke 2620 Hydra Data Acquisition Unit. The temperature probe and the thermocouple were placed in a mixture of 50% ice and 50% water. This mixture was slowly heated and the voltage from the temperature probe was recorded along with the temperature displayed on the Fluke. A linear regression analysis was performed on these values and the conversion factor was determined. The results of this analysis can be seen in Figure 38.

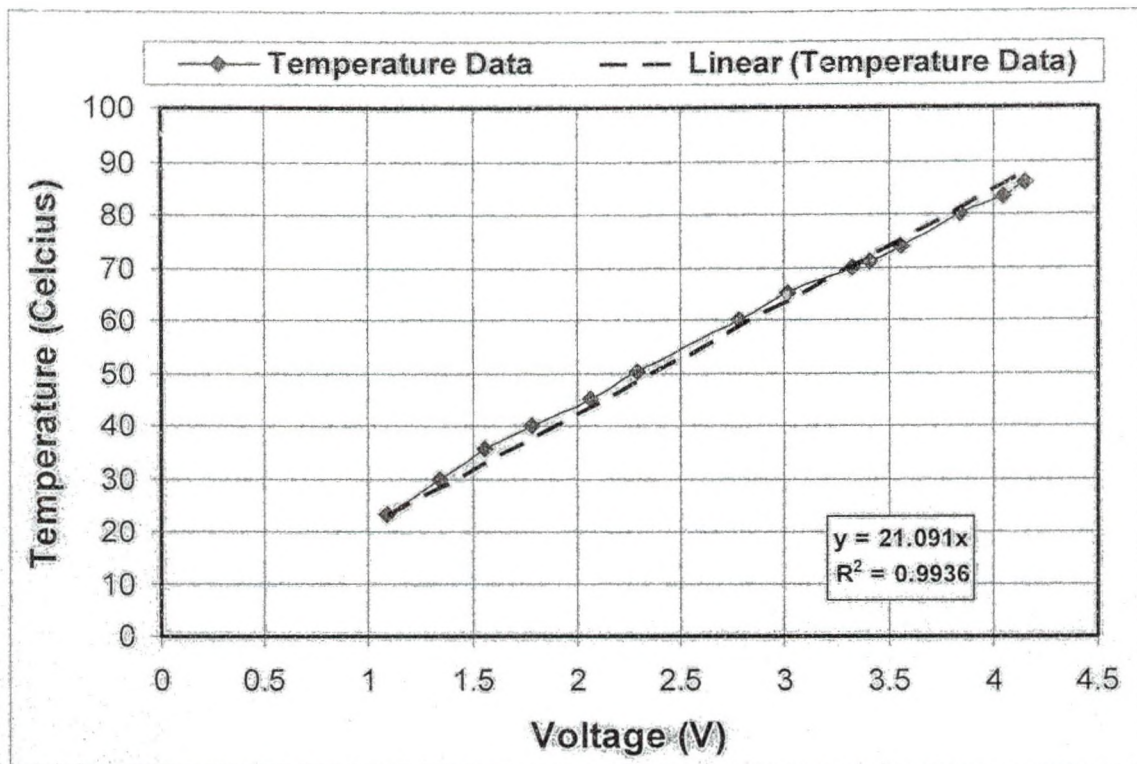


Figure 28 Calibration Results for the S-RCF Temperature Thermistor Probe

The last conversion factor to be determined was between the voltage from the motor controllers and the actual motor speed. The speed of the motors was determined by using a Strobotac 1531-A stroboscope. A signal of 1 volt was sent to the controllers and the measured motor speed was approximately 416 rpm. The conversion factor is 416.5 rpm since the maximum motor speed is 4165 and the maximum voltage into the controller is 10 volts.

After the conversion factors were determined, the next step was to decide how to record the information. As stated in the Design Requirements section, contact fatigue testing can take up to 30 million cycles. For the S-RCF tester, 30 million cycles would take approximately 48 hours of testing at 3600 rpm. Since testing takes a significant amount of time, continuous data recording and storing is not reasonable. Also, fatigue

failure does not occur suddenly. Therefore, the change between one load cycle and the next will be insignificant. Instead of continuous recording, data is taken at user specified intervals. The TEAC LX-10 comes with a program called LX-Navi that is used to record data intervals. Each data interval captured is recorded into a header (extension .hdr) and data (extension .dat) file format. The LX-Navi main window is shown in Figure 39.

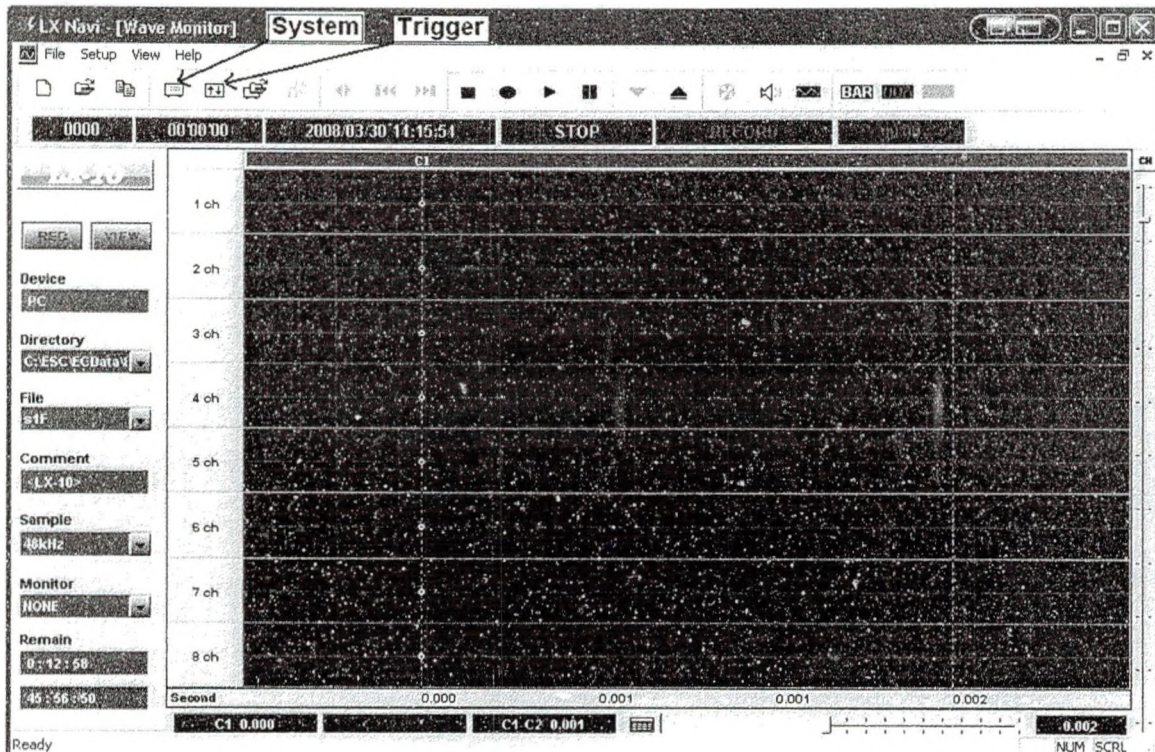


Figure 39 LX Navi Program Window

Several parameters need to be setup to record with the LX-Navi program. First, a new file must be opened for every recording session. This can be done by either pressing ctrl+n or by clicking New in the File drop box. In this new window, the user can set where to save the files, the number of zeros after the file name, the file name and what storage device to use. This window is shown in Figure 40. The file name needs to be an 's' (for specimen), followed by the specimen number, which is then followed by an 'F' (for file). Therefore, the files for the first specimen should have a filename starting with

's1F'. The storage device is the PC; hence, the PC Recording option should be selected. The number of zeros after the file names needs to be set to five. If any other value is used, the Matlab® files need to be modified. At a value of five, 32,767 files can be saved.

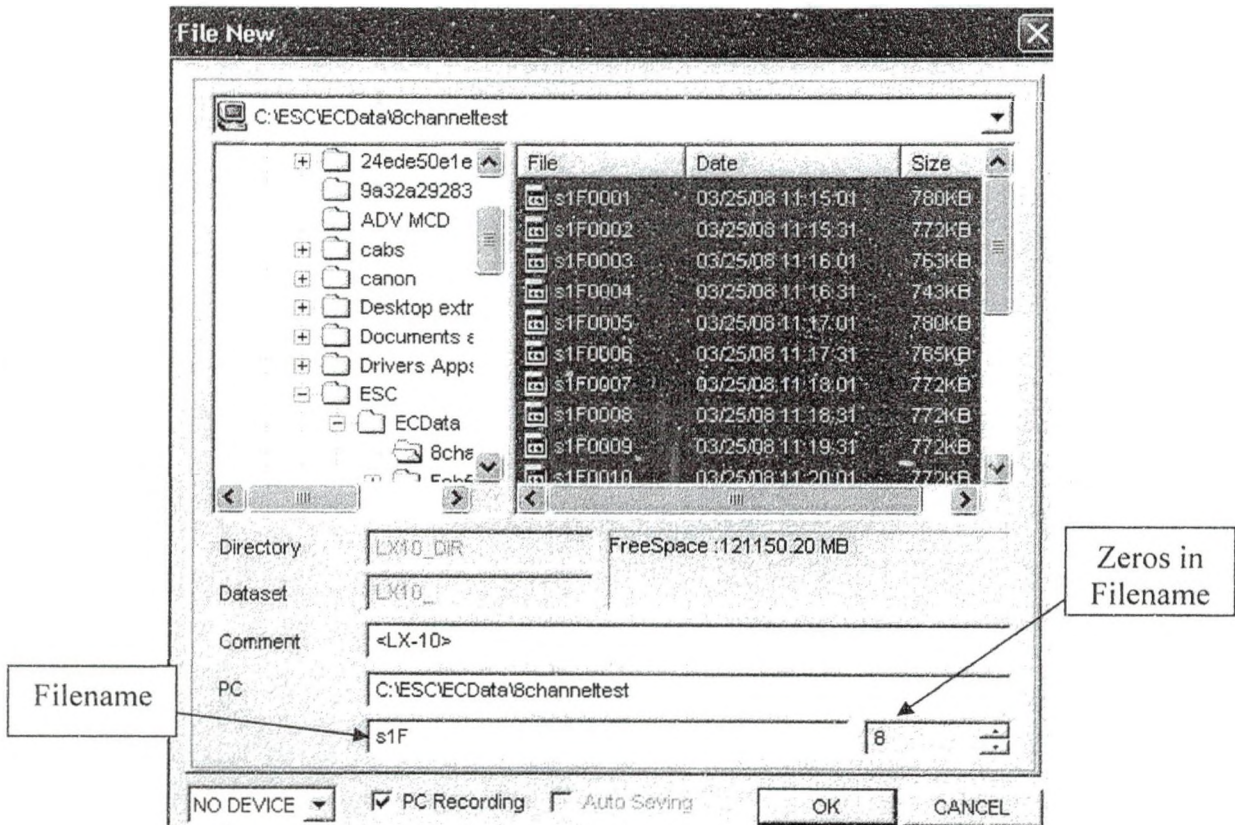


Figure 40 LX-Navi New File Window

After setting the new file options, the next parameters to set up are the system properties. This window can be reached by clicking System under the Setup tab or by selecting the System button as shown in Figure 39. In the system window, three tabs are available. For the S-RCF tester, only the system tab and Slot1 (PA-8) tabs are used. The window for the system tab in the System window can be seen in Figure 41.

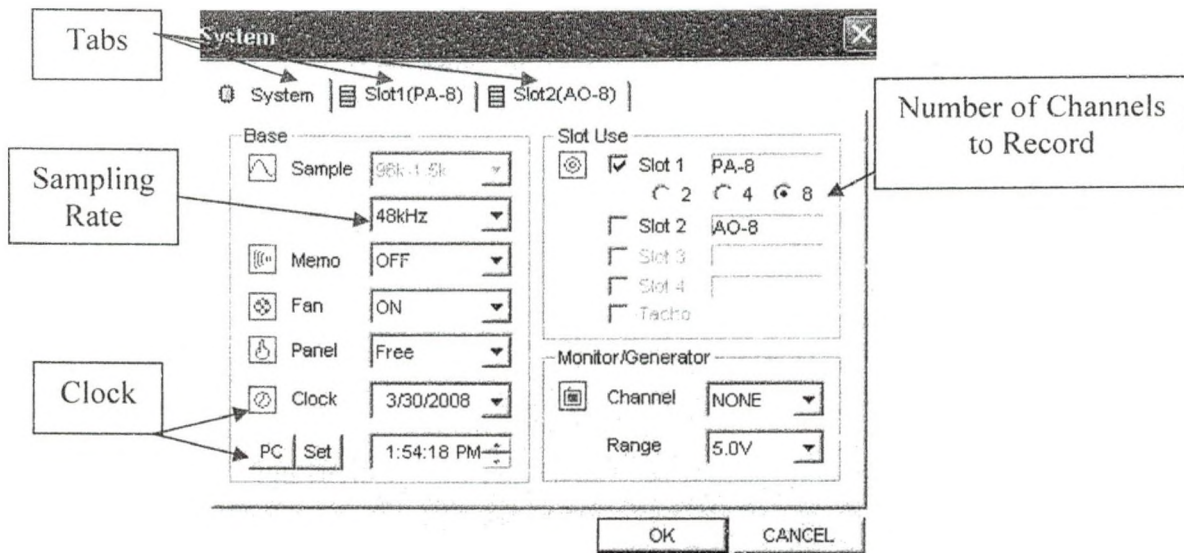


Figure 41 LX-Navi System Window System Tab Menu

Under the system tab, the sampling rate of the LX-Navi can be set. The sampling rate determines the number of points that will be recorded every second. This value depends upon the speed of the surface turning and the size of the area being recorded. The number of scans per revolution (S) needed is determined using Equation 14, where r_s is the radius of the specimen and w_d is the width each scan covers.

$$S = \frac{2 \cdot \pi \cdot r_s}{w_d} \quad \text{Eq. 14}$$

The minimum recording frequency (F_m) can be determined using Equation 15, where ω_s is the rotational speed of the specimen. A factor of two is present since the Nyquist principle states that the sampling frequency should be twice that of the actual frequency measured.

$$F_m = S \cdot \omega_s \cdot 2 \quad \text{Eq. 15}$$

For the eddy current detection system, the scanning area of the probe is five millimeters. The maximum speed of the S-RCF tester is approximately 3,600 rpm

(60Hz). Under these settings, the data is collected at a frequency of approximately 3 kHz. However, since a curved surface is being monitored, it is recommended that the defect width be taken as one millimeter. This recommendation increases the sampling frequency to approximately 14 kHz. For the LX-Navi, the closest value over 14 kHz is 24 kHz.

The other values that need to be set in the system tab are the clock and the number of channels to record. The clock can be synchronized with the PC time by clicking the PC button. Only the check box by Slot 1 should be checked since this is the slot that all the data is being input into. Under Slot 1, the number eight should be selected since this is the number of channels to be recorded.

The second tab in the System window is the Slot1 (PA-8). Figure 42 shows the window for this tab.

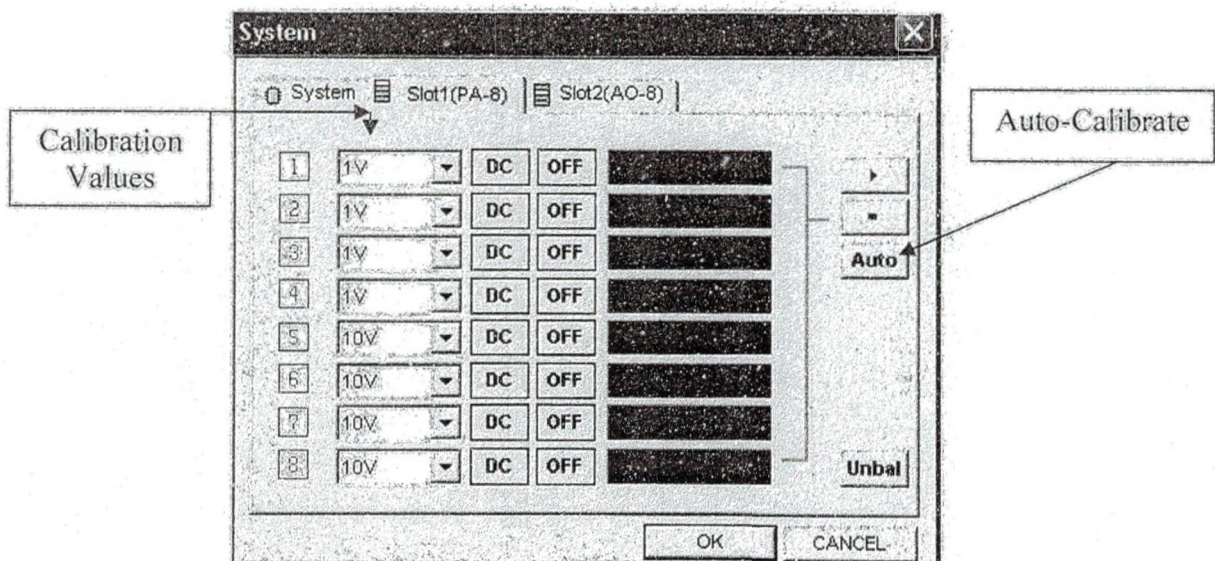


Figure-42 LX-Navi System Window Slot1 (PA-8) Tab

The Slot1 (PA-8) tab calibrates each channel manually or automatically. By clicking the Auto button, the LX-Navi measures the current voltages coming in and

calibrates itself. This method is not recommended since the signal is expected to increase as a defect or defects appear on the surface. If automatically set, the max limit may be set too low and any value above the calibration number will be cut off. Instead of the auto-calibration button, each channel can be set manually by the user. The voltage values that can be set for the LX-Navi are 0.01, 0.0316, 0.1, 0.316, 1.00, 3.16, or 10 volts. Based on the information provided in Table 6, channels one through four should be set to 3.16V and channels five through eight should be set to 10V.

Due to the volume of information being recorded, data will be taken at user specified intervals. Therefore, the last parameter to set up for the LX-Navi is the trigger for recording data. The trigger window can be accessed by either clicking on the trigger button in the main LX-Navi window or by clicking Trigger under the Setup menu. A view of the Trigger window can be seen in Figure 43.

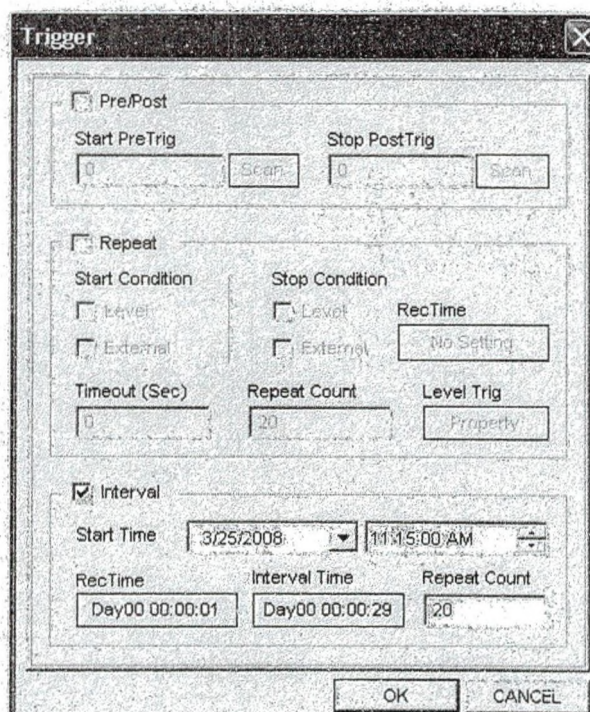


Figure 43 LX-Navi Trigger Window

In the Trigger window, the Interval check box should be selected. The interval option requires several parameters to be set. First, the start time needs to be set. This is when the first data will be recorded to the first file. Next, the RecTime and Interval Time values need to be set. The RecTime is the time that the data will be recorded and the Interval Time is the time between each recording. Each file represents the S-RCF tester values over the interval time. The number of load cycles represented by each file (LCPF) can be determined using Equation 16. The variable ω_s is the specimen speed in rpm, RL is the RecTime in seconds and IL is the Interval Time in seconds. Equation 16 has been graphed in Figure 44.

$$LCPF = \frac{\omega_s \cdot 3 \cdot (R_L + I_L)}{60}$$

Eq. 16

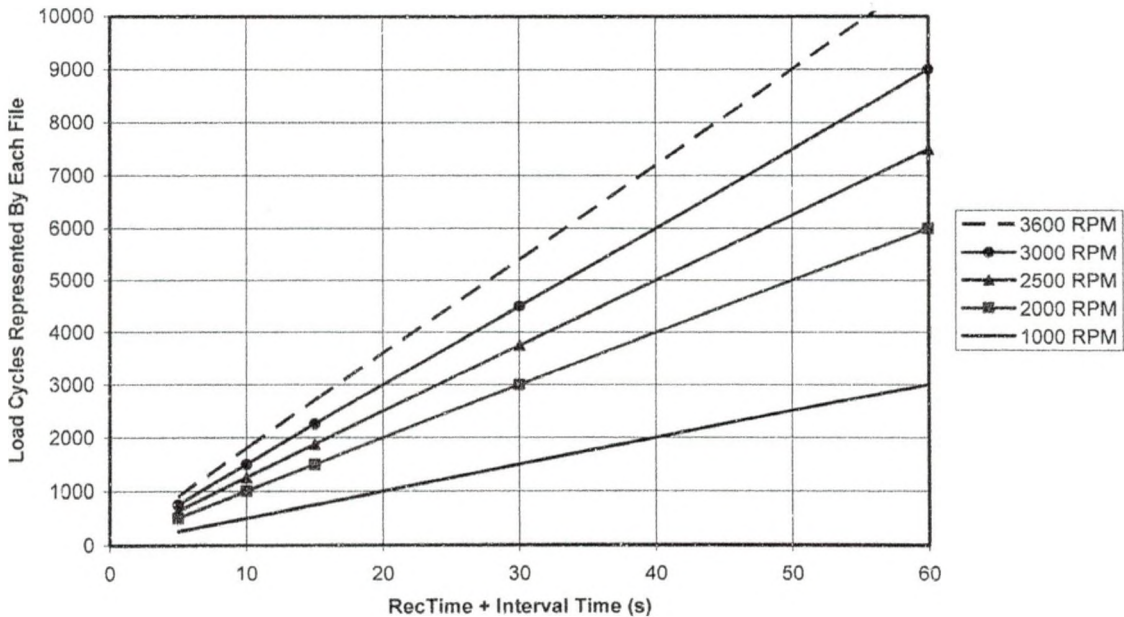


Figure 44 Number of Load Cycles Represented by Each File for Various Specimen Motor Speeds

In Figure 44, it can be seen that as the Interval Time and RecTime increase, more load cycles go unrecorded. However, since testing is expected to last several million cycles, this error would be negligible.

The number specimen revolutions stored in each file (Rev_f) can be determined by Equation 17 and has been graphed in Figure 45.

$$Rev_f = \frac{\omega_s \cdot R_t}{60} \quad \text{Eq. 17}$$

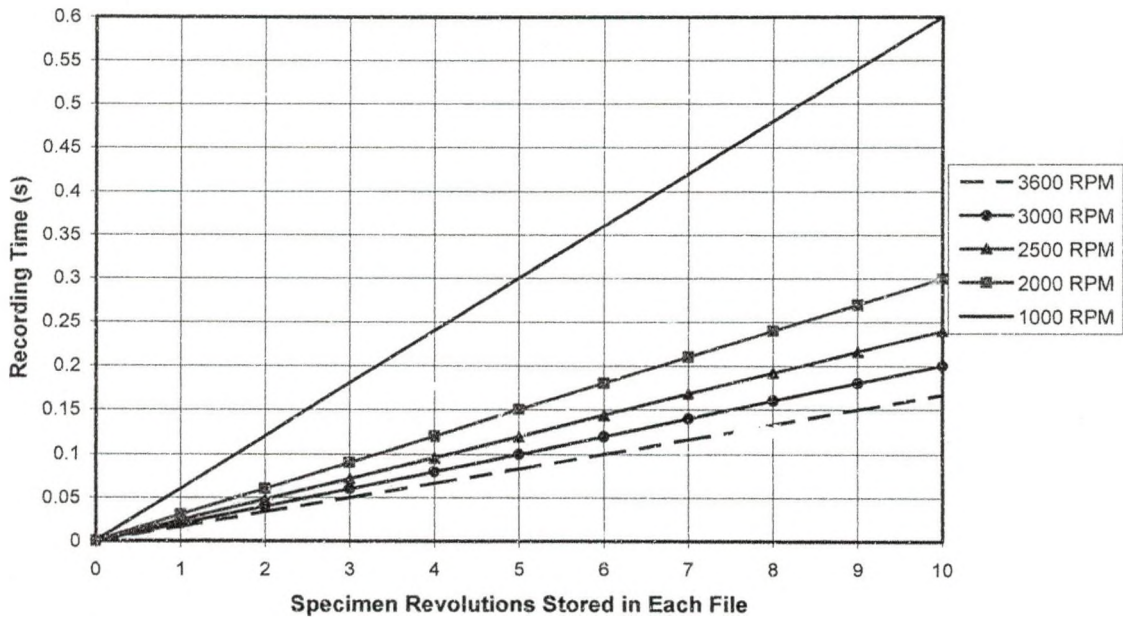


Figure 45 Recording Time Needed to Store a Given Number of Load Cycles per File for Various Specimen Motor Speeds

From Figure 45, it can be seen that as the specimen motor speed increases, less recording time is needed to get the same number of specimen revolutions in a file. It is recommended that at least five revolutions be recorded into a file. It is important to note that each specimen revolution is actually three load cycles, meaning five revolutions would be fifteen load cycles.

All of the parameters for the LX-Navi discussed need to be set before a test can be run. A summary of these parameters can be found in Table 7.

Table 7 LX Navi Setup Parameters and Description

Location	Parameter	Value	Description
File - New	Filename	s1F	s (specimen) 1(specimen number) F(file)
	Zeros	5	Sets the number of digits for the file name
	PC Recording	Check Box	Records Data to PC
System - System	Sample	48 kHz	Sets recording speed
	PC Clock	Set	Sets the LX-Navi clock to the current computer time
	Slot Use	Check Slot 1	Sets which slot to record from
8		Sets the number of channels to record on the Slot	
System - Slot1(PA-8)	Voltage Calibration Channel 1-4	3.16V	Sets the voltage range of channels 1-4 on the TEAC
	Voltage Calibration Channel 5-8	10V	Sets the voltage range of channels 5-8 on the TEAC
Trigger	Interval Setup	Check Interval Box	Sets the TEAC to record in user defined intervals
	Start Time	User defined	The time at which the TEAC will record the first file
	Record Time	1 sec	Length of time the recorded
	Interval Time	29 sec	Length of time between subsequent recordings
	Repeat	32767	Number of times the TEAC will repeat the Record Time and Interval Time

Data Analysis

Before data could be analyzed, a method needed to be developed to interpret the data that was being stored. The first method attempted was to use another program that came with the LX-10 called LX-View. LX-View is a program that allows the user to view a file created by the LX-10. The LX-View program can also export the information saved into several different file formats, including a Matlab® format. The export

function contains a batch convert option to convert many files at once. However, after experimenting with the program, it was determined that the batch option did not work.

In attempt to solve this problem, TEAC was contacted via email. A response was sent by Steve Astulfi and Bo Prum stating they were unsure why the batch option was not working. As an alternative solution, a Matlab® file was attached to the email which reads the data file created by the LX-Navi and opens them directly into Matlab®. The file has been modified several times to make it functional for the S-RCF tester. The file's name is Teac2Matlab and is located in Appendix B in the Matlab® Files section.

For a given specimen, several inputs are needed to run the Matlab® files. The determination of these values will be discussed in the Test Setup section. These input values are located in a file called *TestingParametersValues*. This Matlab® file is called upon in all the other Matlab® files; therefore, it is important to check that the values in this file are correct. A summary of the input values needed by the *TestingParametersValues* Matlab® file is presented in Table 8.

Table 8 Description of Inputs for *TestingParametersValues* Matlab® File

Variable Name	Description	Units
intervalmin	Interval time to check if crack has occurred	min
secs_to_read	Time to read of each file	s
specimennumber	Specimen test number	
reclength	Time each file is recorded	s
recinterval	Time between each file recording	s
specms	Specimen motor speed	RPM
slipratio	Slip ratio between surfaces (must be >1)	
IVc1	Initial maximum value for channel 1	V
IVc2	Initial maximum value for channel 2	V
IVc3	Initial maximum value for channel 3	V
IVc4	Initial maximum value for channel 4	V
IVc5	Initial value for channel 5	psi
IVc6	Initial value for channel 6	°C
IVc7	Initial value for channel 7	RPM
IVc8	Initial value for channel 8	RPM
deltaC1	Maximum allowable change for Channel 1	V
deltaC2	Maximum allowable change for Channel 2	V
deltaC3	Maximum allowable change for Channel 3	V
deltaC4	Maximum allowable change for Channel 4	V
deltaC5	Maximum allowable change for Channel 5	%
deltaC6	Maximum allowable change for Channel 6	%
deltaC7	Maximum allowable change for Channel 7	%
deltaC8	Maximum allowable change for Channel 8	%

The student version of Matlab® is limited in the amount of information it can store and process at one time. Due to the large amount of information to be processed, the data saved is analyzed in three stages. These stages are the failure detection stage, the screening stage and the analysis stage. For each stage, a separate Matlab® file has been generated to analyze the data. In order to work properly, the Matlab® files that are needed must be in the same folder as the files to be analyzed. The scripts of all the Matlab® files used are located in Appendix B in the Matlab® Files Section.

The failure detection stage is performed during testing and uses a file named *RealTimeDataAnalysis*. A flowchart description of the failure detection stage can be seen in Figure 46.

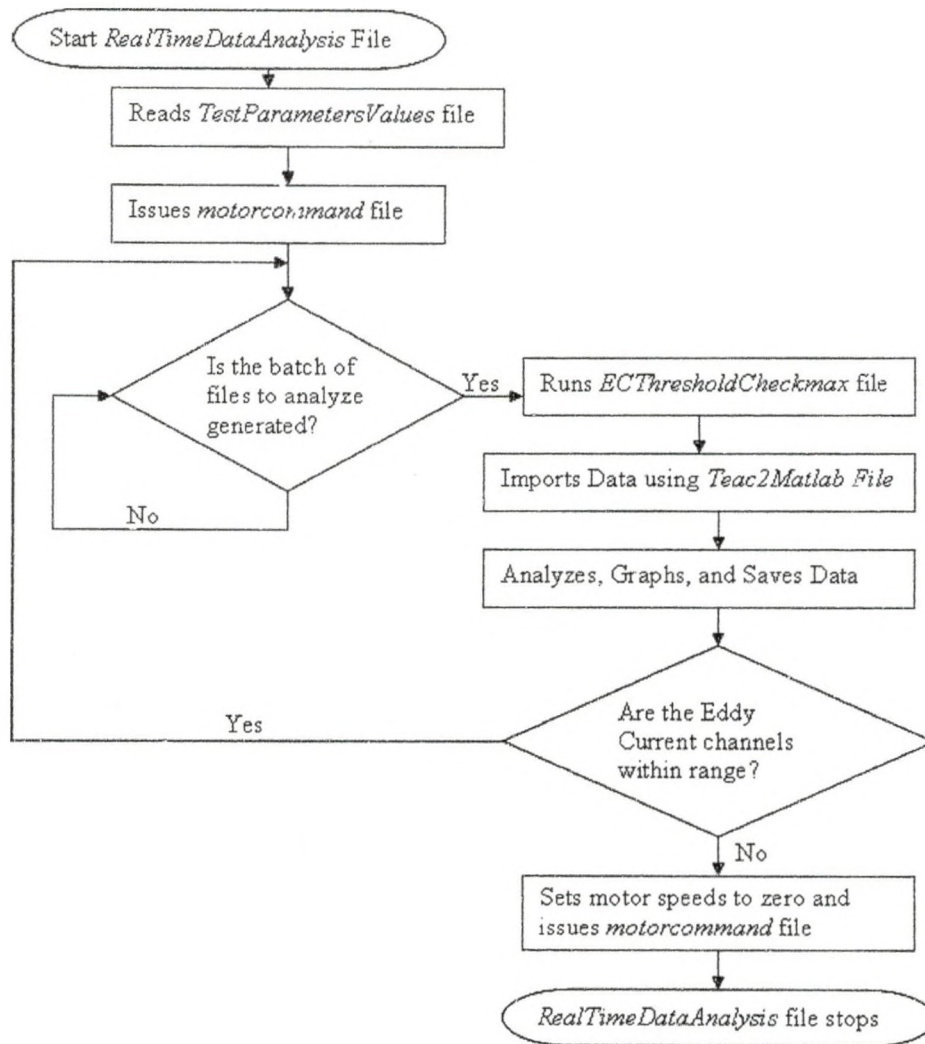


Figure 46 Flowchart Description of the Failure Detection Stage

As the *RealTimeDataAnalysis* file is started, the motor voltages (corresponding to a motor speed) are sent to the motor controllers. These voltages are sent using the *motorcommand* Matlab® file which sends the voltage values to the controllers using a NI PCI-6251 card connected to a NI BNC-2110 terminal block. After this, the computer's

clock is read and the program waits until the data file corresponding to the *intervaltimemin* variable is generated by the TEAC Recording unit.

After this data file is generated, the *RealTimeDataAnalysis* file calls upon another Matlab® file named *ECThresholdCheckmax*. The *ECThresholdCheckmax* has several functions. First, the file brings in the data using the *Teac2Matlab* file. Secondly, the values in each file are filtered down so that the absolute maximum and the absolute minimum values are stored. Next, the maximum and minimum values are processed into meaningful values using the conversion factors provided in Table 6. The third function of the *ECThresholdCheckmax* file is to plot the data. The maximum and minimum values from each file and the initial values specified by the user are plotted in two figures so the user can see what the values were. The first figure contains the plots of channels 1, 2, 3 and 4. The second figure contains the plots of channels 5, 6, 7 and 8. These figures are saved as bitmap (file extension .bmp) files in the same folder as the data being recorded. The title of each graph states the specimen name or number, the TEAC LX-10 channel being graphed and the start and stop time of the graph. Figure 47 shows a portion of one of the figures generated and saved.

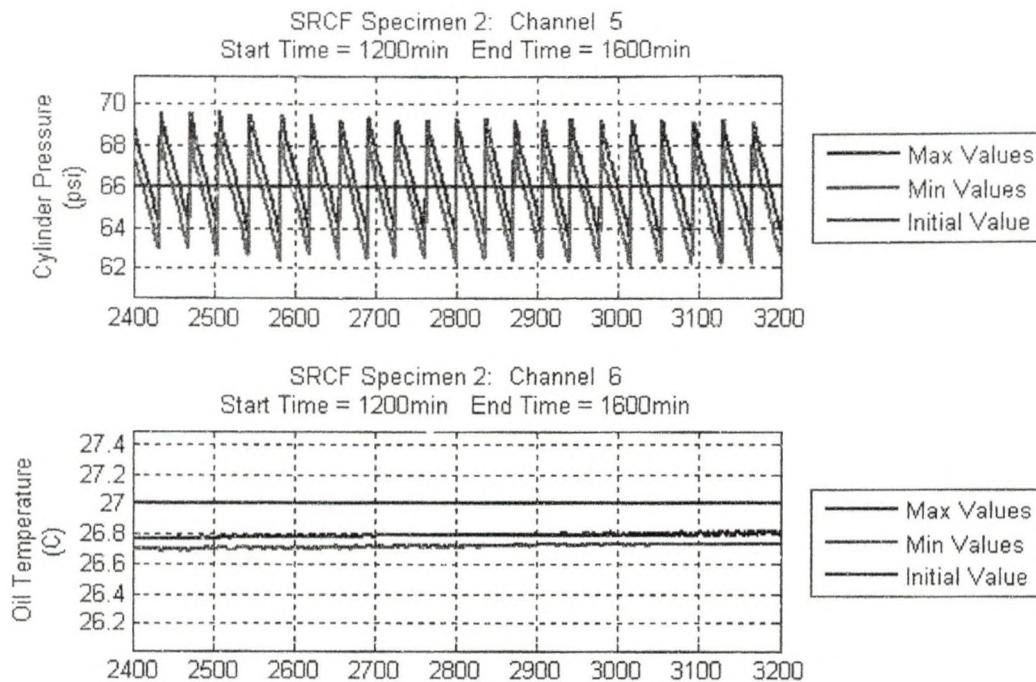


Figure 47 Example of Figures Stored during the Failure Detection Stage

The final function of the *ECThresholdCheckmax* file is to determine if failure has occurred. The maximum value on each eddy current channel is compared to its initial max value to determine if the channel is still in range. If the maximum voltage is outside the range, the program issues a stop command to the motors using the *motorcommand* file and a message appears in the Matlab command window stating which channel is out of range. If all of the values are in range, the program resets itself and waits for the next time interval to check again. At the end of the test, the figures saved can be regenerated over a larger time frame to reduce the number of figures. This is done by specifying a larger *intervaltimemin* and restarting the program. Since the program looks for the files and all the files are generated, the program will generate and store the graphs as fast as it can.

After a crack has been detected and the machine has stopped, the next stage in data analysis is the screening stage. Screening narrows down the point at which crack initiation is suspected to have taken place. The Matlab® file used is called T2Mv2Screening. The T2Mv2Screening file graphs the absolute values of the mean, minimum and maximum values of each file for a user defined interval. Instead of a time interval, this interval is based on the file numbers selected to analyze. An example of the figures generated by the screening file can be seen in Figure 48.

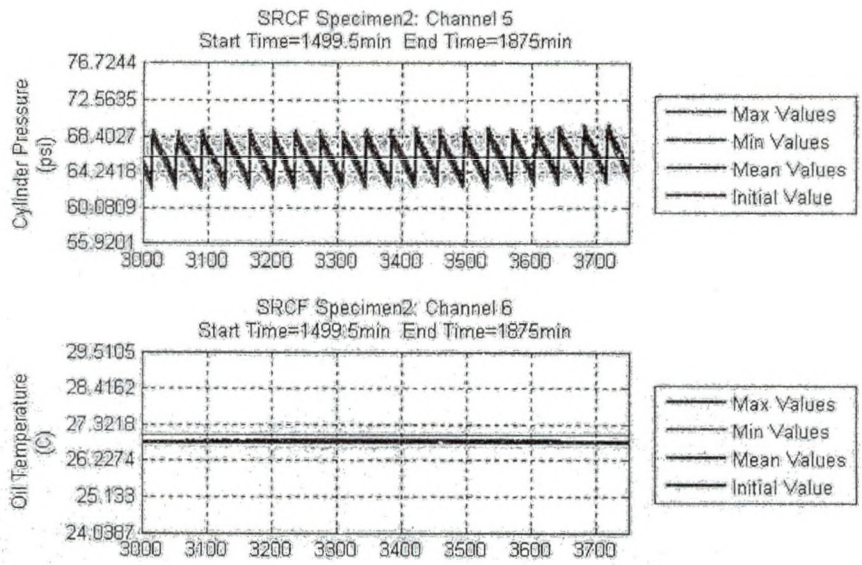


Figure 48: Example of Figures Generated during Screening Stage

The absolute maximum value is analyzed since any change in the surface needs to be detected. The eddy current voltage output for a relatively smooth, crack free surface should be constant. However, due to some variation in the surface quality, a little noise is expected. The peak values (high and/or low) of this noise will grow steadily as a crack forms. The faster the crack propagates, the quicker the increase of the peak voltage values. Since the absolute value is used, measuring the size of the crack and determining the orientation cannot be done.

After it is determined where the crack started, the final stage, the analysis stage, is to analyze the raw data using the Matlab® file called T2Mv2Analysis. This file imports the raw data over a user defined file range and plots the values on a continuous axis.

Figure 49 shows the graphs generated by the T2Mv2Analysis file.

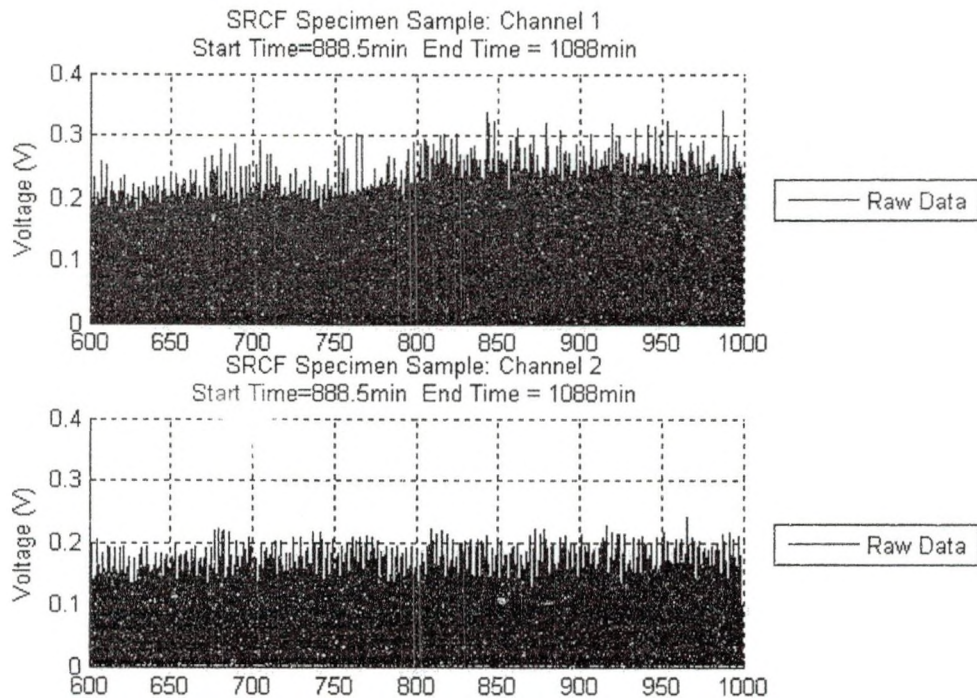


Figure 49 Example of Figures Generated during Analysis Stage

Summary of S-RCF Tester Abilities and Controls

The S-RCF tester can operate in several different conditions to test different parameters. The first condition that can be changed is the lubrication. By turning certain flow control valves (FCV) on or off, a specimen can be tested in a dry, lubricated or submerged environment. The second condition is the slip or slide ratio between the surfaces. Since two motors are used, the specimen speed and roller speed can be different. This allows for a rolling or sliding condition between the two surfaces. The

third condition that can be varied is the loading applied. The maximum allowable pressure in the pneumatic system is 150 psi.

Most of the controls for the S-RCF tester are manual. The motor speeds are entered into the Matlab® script before testing is started. Once testing has started, the speed of the machine cannot be changed. Since the speeds cannot be changed, the sliding or rolling conditions can not be varied during testing. The loading is also manually applied and maintained. The air pressure regulator is set to the desired pressure and variability. The lubrication temperature is only monitored and not controlled. The blower fan speed on the lubrication system can be varied by the rheostat; however this is not a direct control over the lubricant's temperature.

In the event of a catastrophic event during tester, the emergency button on the motor controller box should be push in. This cuts off power to the controllers, thereby stopping the machine. The machine should shut itself off since the eddy current signals would be out of range. Since the pneumatic loading system is manually controlled, loading is still being applied to the specimen.

CHAPTER 3

TESTING PROCEDURE AND CONDITIONS

This chapter documents the test setup and disassembly procedures used when performing fatigue testing with the S-RCF tester. It also describes the testing conditions and failure criteria used in performing these fatigue tests.

Test Setup Procedure

The first step in setting up a fatigue test with the S-RCF tester is to design and order the rollers and specimens to be tested. The drawings of these parts are located in Appendix D: Specimen and Roller Drawings. Along with these dimensions, several other parameters need to be specified. These parameters include the roughness, microstructure composition and hardness. The hardness and microstructure composition are affected by the type of heat treatment. The roughness depends upon the type of grinding or finishing.

The next step is to verify the properties and quality of the parts. The physical dimensions of several parts are measured using a caliper to determine if they are within tolerance. Every part must be examined visually to determine if any unacceptable scratches exist.

The surface roughness values of several parts are measured using the Surfcom 480A profilometer. The profilometer moves a stylus across the surface and measures the height change. The device gives the user a print out of several roughness parameters, the most important being the surface profile picture, the average roughness (R_a) and the maximum roughness (R_m).

The test bars manufactured are used to determine case depth and microstructure of the parts. The case depth is determined by making several hardness measurements in a line starting near the edge of the cross-section of the test bar and moving incrementally toward the center. The measurements stop when the effective hardness (the hardness of the non-carburized core) is reached. The microstructure is checked by polishing and etching the surface with different etchants. The treated surface is then placed under an SEM (scanning electron microscope) with the capability to do EDS (electron dispersion spectroscopy) analysis. The EDS determines the microstructure of the surface. Pictures of the surface also show the decarburized layer depth and if the final grinding removed this layer.

After the quality of the parts is verified, the next step is to set up the S-RCF tester. Two people and several tools are needed to setup the S-RCF tester. A detailed outline of the test setup described next is provided in Appendix E. A list of the tools needed is provided in Table 9.

Table 9: Tools Needed to Set Up the S-RCF Tester

Quantity	Tool
2	3/16 in. Allen Wrench
2	5/32 in. Allen Wrench
2	3/4 in. Socket and Racquet
1	7/16 in. Wrench
1	Rebar Rod
1	Hammer
1	Stepped Punch
1	Oil Funnel
1	Spark Plug Gap Gauge

Begin the assembly of the S-RCF tester by inserting the two bottom rollers. Each roller slides onto a shaft and sits on a keyway. The key is sitting underneath the keyed collars. After the rollers are in place, the regular collars slide onto the shaft. The bottom

roller shafts are then pushed back into the bearing while the keyed collars are lined up so the key can move through. Next, the hinged collar on each shaft is tightened around the stepped portion of the shaft. In order to remove any further slack, the tightening plate is screwed into the end of the shaft to pull the shaft and collars in that direction. Finally, the set screws in the bearings are tightened to secure the shafts in place.

After tightening the bottom rollers in place, the end oil wall on the specimen motor side is attached. PTFE (polytetrafluoroethylene) tape is located on the ends of the side oil walls to prevent oil from leaking, which may need to be replaced if it is damaged or torn. The specimen end oil wall tightens against the side oil walls using ten ¼ inch hex head screws. Then, the oil seal in the specimen end oil wall needs to be greased.

Next, the specimen sliding plates and probe holder are inserted into the S-RCF tester. The probe holder is attached to the specimen sliding plate on the specimen motor side. This assembly then slides into the inner wall. Slide the other specimen sliding plate with the small shaft and tightening plate into the other inner wall and attach it to the probe holder. The specimen shaft with the spider couple is then inserted into the oil seal located in the specimen end oil wall and the specimen sliding plate.

Insert the specimen by placing the tabs of the specimen into the slots in the shafts. The two hinged collars are tightened onto the stepped portion of each shaft. Remove any slack in the assembly by tightening the tightening plate on the end of the small shaft in the specimen sliding plate.

The next step after inserting the specimen is to move both of the motors into position. These motor require two people or a lifting mechanism to lift because they are very heavy. The specimen motor has a spider couple to drive the specimen. Align the

spider couple and then bolt this motor into place. On the roller motor side, check the PTFE tape for tears or damaged. The roller motor has a gear attached to it and needs to be lifted into place so that the teeth mesh correctly. After this, the roller motor is bolted into place. Then attach the roller end oil wall to the side oil walls.

The eddy current probe is then inserted into the probe holder. The distance from the specimen is measured using a spark plug gap gauge. The maximum distance the probe can be away from the surface is one millimeter. The nominal distance is 0.5 mm. After it is in place, secure the probe by tightening the bolt on the probe holder. If over tightened, this bolt can damage the probe. Then tighten the nut on the bolt to ensure that the bolt does not vibrate out of the spot and release the probe.

Once the probe is in place, assemble and insert the top roller assembly into the S-RCF tester. Slide the top roller onto the top roller shaft, followed with the collars and then the top roller sliding plate. Tighten the tightening plate on the end of the shaft along with set screws on the bearings. Then lift the top roller assembly into the tester and slide it slowly into the inner walls.

The S-RCF tester is now fully assembled and ready for the test parameters to be applied. These parameters include the contact force and lubricant type. The load is applied manually using the regulator on the air compressor. Plugging in the air compressor automatically starts the compressor. The gauge on the compressor is a crude estimate of the pressure in the cylinders. A more accurate reading can be done by starting the LX-Navi program and monitoring the air pressure channel and converting the voltage to a pressure.

Before adding the lubricant, check the flow control valves and the three-way control valves to ensure they are in the correct position. Lubricant must first be added into the oil filter and before connecting it into the lubrication system. Next, the lubricant is added by pouring it through a funnel into the internal structure onto the gears and specimen. Since testing will be going on for a significant amount of time, at least one gallon of lubrication should be added. The lubricant flows through the flow control valves when the handle is inline with the pipe to which it is connected. The direction the handle is pointing on the valve is the direction the lubricant flows. Plug in the pump motor for the lubrication system and flip the two yellow switches on the lubrication control box to the on position. These switches start the lubrication pump motor and the blower fan. If oil does not immediately start flowing, air may be in the system. Remove the air by turning the flow control valve for the specimen on and off several times.

After the lubricant and loading are applied, attach the cover for the S-RCF tester. Place the top cover plates top of the oil walls and bolt them down. These top cover plates prevent lubricant from spraying out of the tester during testing. A slot is present in one of the plates because a previously used probe holder reached into the internal structure. Now, because this large slot is used only for the probe cord to enter into the internal structure, there is a lot of extra space. This extra space should be covered to prevent the lubricant from splashing out of the machine

Next, power on and set up the eddy current device. Several input parameters are required for the eddy current device to provide meaningful results. These parameters include the inspection frequency, line speed, sensitivity, high pass filter value and low pass filter value. These values can be changed by pressing the setup/test button on the

front control panel of the eddy current device so that the display is flashing setup. Once the word setup is flashing, simply press the button of the value to change.

As discussed in the Eddy Current Inspection and Parameters section in Chapter 2: Failure Detection System, the inspection frequency determines how deep the eddy current penetrates into the material and the density of the current. A high frequency creates a high surface eddy current density but has a low depth of penetration. A low frequency has a low surface eddy current density but has a high depth of penetration. Also, the type of material and its properties affects the standard depth of penetration and eddy current surface density. A Mathcad® file in Appendix B: Mathcad® Files, has been created with the appropriate equations to determine the inspection frequency to use.

The line speed setting on the eddy current system lets the detection system know how fast the workpiece underneath it is moving. The line speed for the S-RCF tester is the surface velocity of the specimen. From the line speed setting, the high pass filter (HP) and low pass filter (LP) are set. The operating instruction manual for the Defectomat EZ 2.828 has the appropriate settings for the filters based on the line speed of the piece being monitored.

The sensitivity of the eddy current device determines the amount of noise picked up. The larger the sensitivity value the larger the output is for a given flaw size. The maximum value for this setting is 62.5 db. This value must be calibrated for different materials and flaw sizes.

Now that the eddy current device is on and setup, the TEAC LX-10 recording unit is powered up next. After this device is started, power on the computer. If the LX-10 is not on when the computer boots up, the computer will not recognize it.

After the computer is on, the recording program is set up. The recording program used for the S-RCF tester is called LX-Navi. Details of this program and the settings to use can be found in Chapter 2: S-RCF Design under the Data Logging section; so, only a brief description is provided here. The first step is set the file settings for all the data that is going to be saved. First, start the LX-Navi program. Once the LX-Navi program is opened, click new file under the file tab. In this window, set the filename, where to save the recorded files, number of zeros in the file name and the PC recording option. After this, set the system parameters by clicking on the system button in the main window or by clicking system in the setup drop menu. In the system window under the system tab, synchronize the clock for the LX-Navi with the PC, set the sampling rate and set the number of channels to record. Under the Slot1(PA-8) tab, set the calibration value for each channel. Finally, set up the trigger for the LX-Navi program. The properties for this are set by opening the trigger window using the trigger button in the main window or by clicking trigger in the setup drop menu. In the trigger window, check the box by the interval option. The values to set for the trigger are the record time, record interval time, repeat count and start time.

Now that the recording program is set up, seven Matlab® files are dragged into the directory where the data files will be created. The Matlab® files include *T2Mv2Screening*, *T2Mv2Analysis*, *TestParametersValues*, *Teac2Matlab*, *RealTimeDataAnalysis*, *motorcommand* and *ECThresholdCheckmax*. Only the last five files mentioned are used during testing. The first two files listed are used after a test is completed and further analysis is to be performed.

With the files in place, the monitoring devices and motors are powered on. The eddy current device should already be on and set up. The temperature probe power and the pressure transducer power are plugged into an outlet. Make sure the switches on the front panel of the controller box are in the off position. The off position ensures that any residual voltage in the controllers does not accidentally start the motors. Turn on the power to the motors and controllers by flipping the 13-15-17 and 37-39-41 breaker groups in the breaker box.

The last program to start and set up is Matlab®. Once opened, the working directory needs to be set to the folder where the Matlab® files are located. Next, open the *TestParametersValues* file and enter the values for the test to be performed. A list of the values to be entered can be found in Table 8. The initial and maximum change values have not been determined yet. Save the file once the known parameters are entered.

Determining the initial values requires the machine to be started and data to be recorded briefly. First, go to the prompt window for Matlab®, type *TestParametersValues* into the prompt and press enter. This will run the *TestParametersValues* file which places the test values into memory. Next, type *motorcommand* into the prompt window and press enter. This command sends the voltages to the motor controllers; however, since the switches are in the off position, the motors do not start. The lubrication system and air compressor should still be operating. The switches for the motors can now be turned on and the motors should begin to turn. Once they have reached the desired speed, the initial values can be read.

The initial values can be determined in two ways. The first way is to visually read the values using the digital readouts available in the LX-Navi program. The digital

readouts are activated by pressing the digit button in the main LX-Navi window or by clicking digit under the view drop box menu. Multiple digital readouts can be brought up by clicking the digit button in the digital readout window. Each readout window can be set to a specific channel. The readout will not display the current value until the *recstandby* button is clicked on. Figure 50 shows a screenshot of the digital readouts for the LX-Navi.

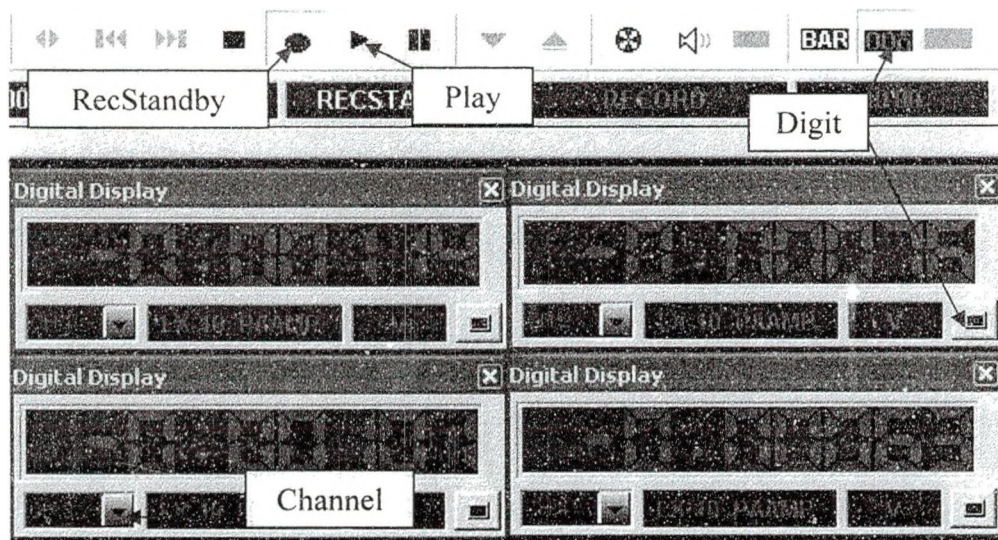


Figure 50 LX-Navi Digital Readout Windows

The second way to obtain the initial values is to actually record files to analyze. This method takes a bit more time but provides more accurate values. The files are created by simply clicking the *recstandby* button in the LX-Navi main window. This button remains depressed, indicating it is ready to record values. Clicking the play button records a file for the interval the user specified in the trigger window. Clicking play again records another file. Several files should be recorded and analyzed to achieve an accurate representation of what is occurring. The trigger does not record files at this point provided the start time set has not passed. The drawback to this method is that a

new file needs to be set up. If a new file is not setup, the file numbering will continue from the last file the user created manually when the trigger time is passed.

Once the initial values are known, turn off the motors controller switches and enter the values into the *TestParametersValues* file and then save the file. The lubrication temperature is expected to rise significantly; therefore, the initial value on this channel should be set higher than what was recorded. The S-RCF tester is not currently set up to automatically control the lubrication temperature, only to monitor and record it. The pressure value will also vary slightly due to small leaks in the system.

After the initial values are entered, the maximum allowable change for each channel must be determined. The maximum allowable change of the eddy current values (channels 1-4) determines when the machine will stop. These values are entered as an increment of voltage change from the initial value. This voltage change corresponds to a certain size defect or damage on the surface for a given set of conditions and material. Therefore, calibration of the material and different size defects should be performed prior to testing. The allowable change values for the pressure, lubrication temperature and motor speeds (channels 5-8) are not significant and only they serve to plot a line on the graphs. The maximum allowable changes for these channels are entered as a percentage of the initial value. Once all the allowable change values are entered, save the *TestParametersValues* file and close the editor.

The S-RCF tester is ready to begin testing. Clear any old data in the folder so that the only files present are the Matlab® files. In the LX-Navi, open the trigger window and set the start time to an appropriate time (approximately 2 minutes from the current time). After this, press the *teststandby* button. This button needs to be depressed in order

for the trigger option to work. Open the prompt window of Matlab®, type *RealTimeDataAnalysis* and press enter. This brings the initial values into the computer's memory and sends the motor speeds out to the controllers. A window prompt appears telling the user to start the TEAC recording system. At this point, turn the switches on the front of the controller box to on so the motors start. The motors spin up and reach the previously set speed. Click the OK button on the Matlab® pop-up window when the start time has passed.

The machine runs until the eddy current device detects a change over the user defined maximum allowable change. The machine should be monitored during the first ten minutes of operation to ensure that the graphs generated by Matlab® appear and display reasonable data. After this, check the machine periodically to ensure that it is still running correctly, nothing is out of range and enough lubricant is present in the system. If lubricant is added, record the time since this affects the lubricant temperature reading. If an emergency occurs, the large red button on the motor controller box can be pressed to stop the motors.

Test Disassembly Procedure

Before disassembling the S-RCF tester, the motors, monitoring systems and controlling programs must be turned off. Stop the motors by turning the switches on the controller box to the off position. At the computer station, the LX-Navi program may still be recording. Stop the program by clicking the stop button in the main LX-Navi window. With the Matlab® prompt window as the active window, hold the 'ctrl' button and press 'c'. This terminates the loop command occurring in the program and stop Matlab®.

Next, unplug the pressure transducer and temperature probe power supplies. The lubrication system can now be turned off. It should remain plugged in since it will be used later to remove the lubrication.

To gain access to the specimen, first release the load on the top roller. Remove the top cover to allow for a view of inside the S-RCF tester. Slide the top roller out of the tester. If it is jammed or hard to remove, reapply the load on the roller and tie a wire around the roller shaft and the push rod of the cylinder. Then, move the cylinder rods up. If connected tight enough, the wire pulls the top roller assembly up with it. The eddy current probe can be removed at this time. Next remove the top roller from the top roller assembly. The specimen is removed by taking off the hinged collars on the specimen assembly and then lifting it out.

If the specimen only needed to be visually checked and rerun, the operator checks the specimen for failure and then places the specimen back into the tester and start everything again. However, if a new specimen is to be run, then the bottom rollers need to be removed and replaced. Before this can be done, the lubricant must be drained from the system. This is accomplished both automatically and manually. Flip the valves on the lubrication system so that the flow is into the reservoir container. Then turn the lubrication system back on. The pump removes the majority of the lubricant from the tester. After no more lubricant is being pumped out, turn off the lubricant system and unplug it. Any remaining oil is drained by switching the valve in the lubrication system so that the lubricant drains out by itself. This amount of lubricant should be negligible.

The removal of the bottom rollers requires that both motors be moved so the end oil walls can be removed. Unbolt and move the specimen motor first. Then remove the

specimen shaft from the specimen end oil wall. After this, unbolt and remove the specimen end oil wall. The roller motor is attached to the roller end oil wall; therefore, this wall must be unbolted first. After this, unbolt and remove the roller motor. Remove the specimen sliding plates and the probe holder.

Next, unscrew and remove the tightening disk on the back of the bottom rollers shafts and the hinged collars. Also, loosen the set screws in the bearings. These steps allow the shaft to move axially. Push or tap the shaft axially in the direction of the gears. While the shaft is moving, the keyed collars need to be lined up with the key in the shaft to allow it to move. A ½ inch gap is all that is needed between the shaft and the bearing to slide off all the collars and rollers.

The S-RCF tester is now completely taken apart and ready to be set up for another fatigue test.

Testing Conditions and Failure Criteria

The material tested was AISI 8620 because some data on this material was available and it is a common gear material. Before a large batch was ordered, a sample specimen with no numbering was ordered and tested under a set of conditions. The heat treatment for this part and its properties were not tested or verified. After it was determined that the specimen and rollers would work, a large batch was ordered.

A description of the heat treatment for the larger batch of specimens and rollers (developed with help from Damian Wilmot) can be found in Appendix D: Heat Treatment for 8620. A total of twenty specimens, thirty rollers (ten sets) and three test bars were made by S.R.S Manufacturing Inc. located in Township, MI. The test bars are

short cylinders heat treated with the parts to allow for verification of the properties. A summary of the significant values of the heat treatment can be seen in Table 10.

Table 10 Heat Treatment and Surface Finish Specifications for AISI 8620

Property	Value
Hardness	58 to 62 HRC
Effective Hardness	50 HRC
Case depth	0.037 to 0.055 in. (.940 to 1.40 mm)
Surface Carbon	0.85 ± 0.05
Average Roughness	16 to 20 microinch
Microstructure	Martensite + Austenite Retained Austenite - 10% max Other Non-Transformed Products - 5%

Verification of the quality of the parts was performed when the parts arrived. The roughness, microstructure and hardness properties were all verified on randomly chosen parts by several machines available at UND. The roughness was verified using the Surfcom® 480A located in the hydraulics laboratory at UND. This device measured the average roughness across the grind (axially) and with the grind (circumferential). The microstructure was checked using the energy dispersive X-ray Spectroscopy (EDS) capability on the scanning electron microscope (SEM). The hardness measurements and case depth were measured using a HM-112 Mitutoyo micro-hardness tester. This tester measures the micro-hardness using a Vickers tip and then converts the value to a Rockwell C hardness value. Hardness measurements were taken incrementally from the edge until the value reached or was slightly below the effective hardness value. At this point, the distance from this point to the edge was measured as the case depth.

Most of the specimens were tested under identical conditions. However, since modifications and information changed along the way, some tests performed were slightly different. A summary of the testing conditions that each specimen was tested under can be seen in Table 11.

Table 11 Summary of S-RCF Testing Conditions for AISI 8620 Specimens

Specimen	Sample	11	2
S-RCF Tester Conditions			
Lubricant Type	10W-30	Transmission Fluid	
Lubricant Amount	Film (sprayed onto surface)		
Start Date	Feb. 5th 2008	Mar. 18th 2008	June 17th 2008
Specimen Motor Speed (RPM)	1200 [216,000 Load Cycles per Hour]		
Slip Ratio	0 (rolling)		
Average Cylinder Pressure (psi)	82	63	66
Maximum Hertzian Stress (GPa)	2.39	2.08	2.13
Material Specifications			
Material	AISI 8620		
Hardness	Unknown	See Table 10	
Heat Treatment	Unknown	See Table 10	
Roughness	16 to 20 microinch		
Eddy Current Settings			
Probe Distance (mm)	0.483		
Inspection Frequency (kHz)	1000		
Line Speed (m/s)	2.39		
High Pass Filter	5		
Low Pass Filter	7		
Sensitivity (dB)	25		
TEAC LX-10 Settings			
Interval Time (sec)	29		
Record Time (sec)	1		
Data Collection Frequency (kHz)	12	48	

The S-RCF tester conditions were chosen since similar testing on AISI 8620 was performed by Hoffman using the ZF-RCF tester [4]. The major difference between the S-RCF tester conditions and the ZF-RCF tester conditions is the amount of lubricant. The ZF-RCF tester applied a full EHL layer; whereas, the S-RCF tester applied a thin film layer. Consequently, the S-RCF specimens are expected to fail sooner than the ZF-RCF specimens.

The failure criterion for a test is determined by the user and depends upon what type of testing is to be performed. In some cases, the user may want to run the tester until a small crack or flaw has formed. Other users may want to run the tester until a larger crack or flaw has occurred. Still others may want to run until catastrophic pitting or has occurred. In any case, understanding the output signal of the eddy current device requires specimens with pre-made, pre-sized flaws in them. These flawed specimens are spun at an equivalent speed and eddy current settings to determine what the signal output is for that size of flaw. After this has been determined, the maximum allowable change in voltage can be determined and set in the Matlab® program.

The flawed specimens can be spun in the eddy current calibration device (ECCD) that has been designed. The ECCD is capable of a maximum speed of 1755 RPM. The eddy current device can monitor the specimen using the old probe holder design. The ECC was designed to spin failed specimens from the ZF-RCF tester. Therefore, it is not currently setup to monitor specimens from the S-RCF tester. Different bearings, bearing mounts, shafts and a coupler would be needed to make the ECCD capable of spinning the S-RCF tester specimens. Figure 51 is a photograph of the current state of the ECCD.

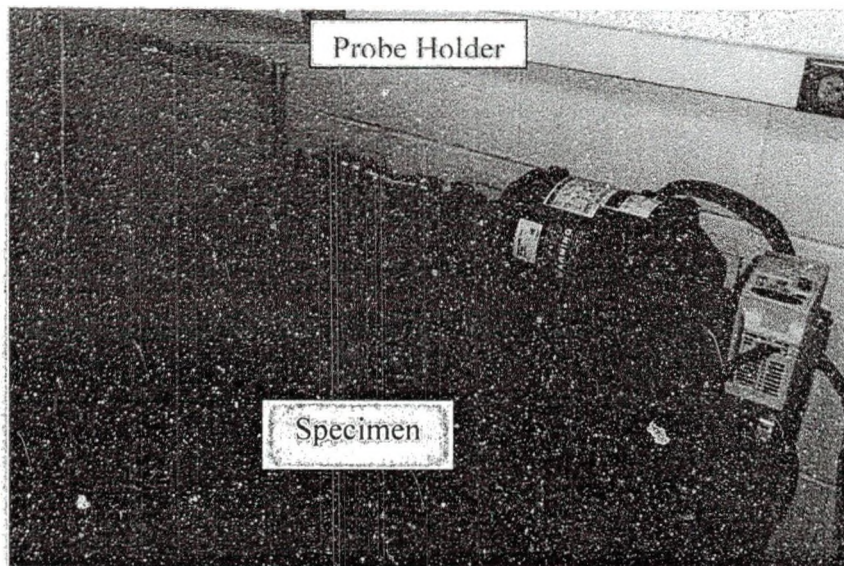


Figure 51 Eddy Current Calibration Device (ECCD)

For the sample specimen, no failure criterion was set. The machine was run until the eddy current signal reached a value believed to be failure. This value was then analyzed and damage on the specimen was examined visually. The criterion for all the other specimens was a voltage increase of 0.15 on any of the eddy current channels. This value was determined based on the results from the sample specimen.

After the voltage change occurred and the machine stopped, the specimens were taken out of the S-RCF and visually examined. A few specimens were taken to the SEM to take microscopic pictures of the damage. Also, the graphs developed during testing were examined and remade to condense the number of files. These graphs were then examined further with the T2Mv2Screening file. The screening file graphed the absolute values of the mean, minimum and maximum values for each file examined. After a point of interest is found, the raw data can be viewed using the T2Mv2Analysis file.

CHAPTER 4

RESULTS AND DISCUSSION

The preliminary test results are presented here along with a discussion of these results. The results include the verification of the properties of the specimens and rollers, the S-RCF tester's performance and the fatigue results.

Verification of Part Specifications

The properties measured include the roughness, microstructure analysis and hardness value.

In the batch of AISI 8620 material, four of the rollers had small defects along the edge and one roller had a defect across the face. The roller with the defect across the face could not be used since it would contact the test surface. The marks on the edge were determined to be far enough away from the contact zone on the roller. These defects can be seen in Figure 52 and Figure 53.

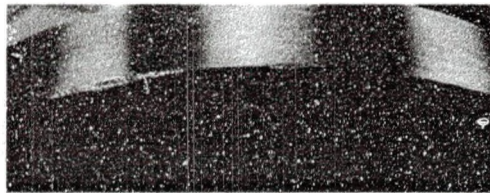


Figure 52 Defects at the Edge of the Rollers

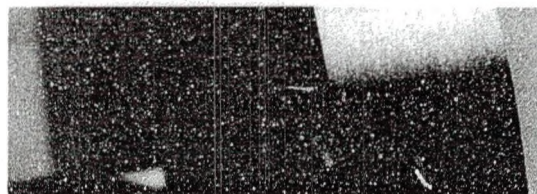


Figure 53 Defect Across the Face of the Roller

The average roughness (Ra) was measured over a distance of 0.3 inches. Three randomly chosen specimens and a randomly chosen set of rollers (3) were measured. Each part was measured in four random locations in the axial and circumferential directions. The axial direction goes across the faces of the part (across the grinding marks) and the circumferential direction goes around the part (with the grinding marks). As expected, measuring in the axial direction on a part gave a higher value than in the circumferential direction. The Ra values of the rollers were consistently less than the values for the specimens. In Table 12, the data shows that Ra values of the individual parts and the sample group are all less than the maximum specified value of $20 \mu''$ (see Table 10) with 95% confidence.

Table 12 Roughness Measurements of Randomly Chosen Specimens and Rollers

		Specimen/Roller Number	13	4	3	4A	4B	4C
Axial Ra	Individual	Average (μ'')	15.28	13.65	13.46	11.35	7.08	9.39
		95% Confidence Interval (μ'')	± 2.30	± 1.81	± 3.36	± 0.62	± 1.05	± 0.72
	Group	Average (μ'')	14.13			9.27		
		95% Confidence Interval (μ'')	2.48			5.31		
Circumferential Ra	Individual	Average (μ'')	10.86	10.41	10.70	5.99	4.59	5.75
		95% Confidence Interval (μ'')	± 1.54	± 2.43	± 4.86	± 2.12	± 0.56	± 1.65
	Group	Average (μ'')	10.66			5.44		
		95% Confidence Interval (μ'')	0.57			1.86		

A photograph of the testing surface of the specimen is shown in Figure 54. This photo was taken with the SEM microscope at UND at a magnification of 85. The marks on the surface are the grind marks from the manufacturer grinding the parts down to the specified roughness.



Figure 54 Specimen Testing Surface (Untested)

The microstructure analysis was performed by Dr. Ranko Todorovic of the Engineered Surface Center (ESC) and Damian Wilmot of Alion Science and Technology. The analysis was performed on the test bars that were heat treated the same but not polished or ground to a finish like the actual parts. Therefore, a decarburized layer is present on the test bars. The decarburized layer can be seen in Figure 55 and Figure 56. The depth of the decarburized layer is approximately 0.3mm. In a private communication with Damian Wilmot, it was determined that the manufacturer ground away this layer.

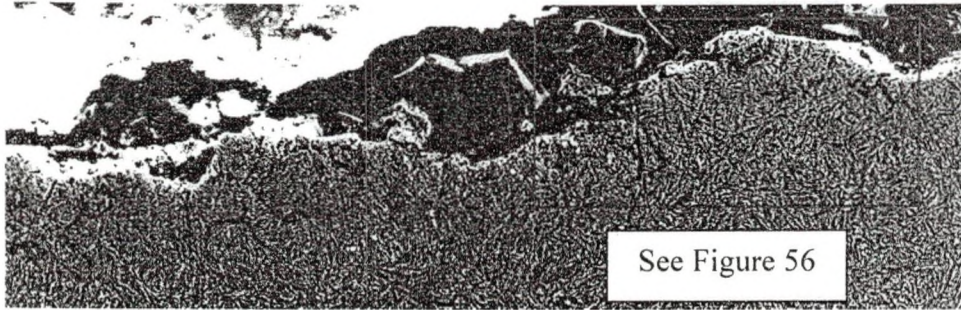


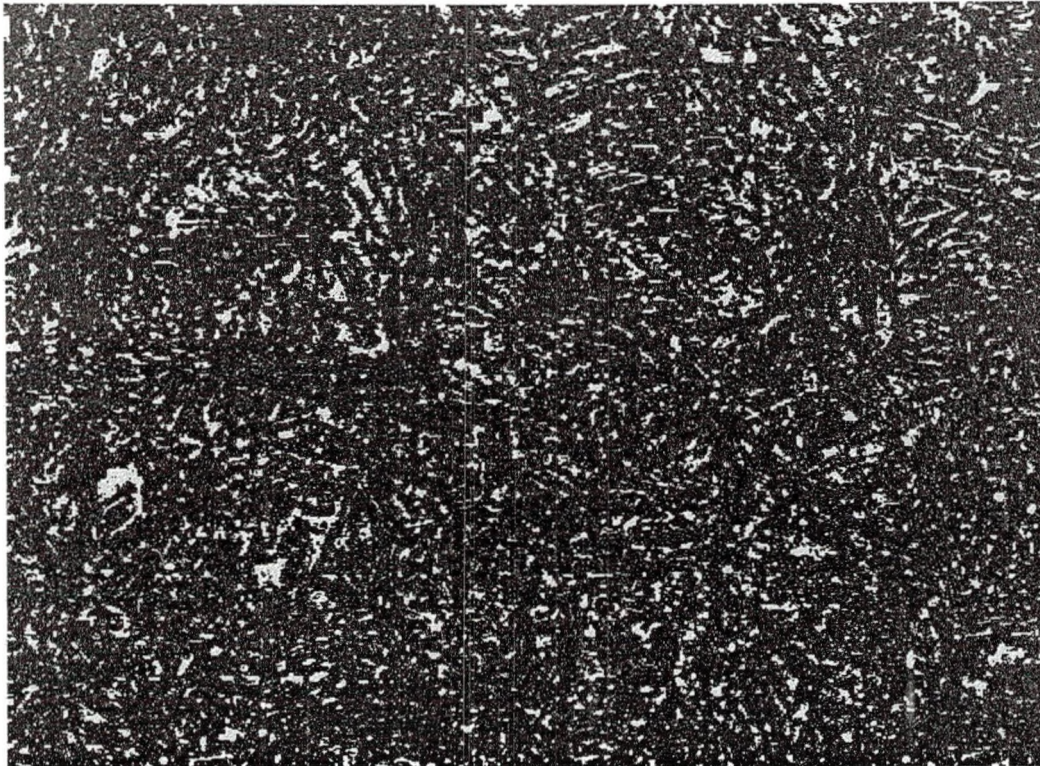
Figure 55 Decarburized Layer of AISI 8620 Test Cylinder at a Magnification of 500



Figure 56 Decarburized Layer of AISI 8620 Test Cylinder at a Magnification of 1000

Several pictures of one of the test bars were taken to determine the microstructure at different depths away from the surface. Figure 57 shows the analysis taken 20 microns from the edge, which was the maximum value of all the spots analyzed. The amount of retained austenite and other non-transformed products in Figure 57 (shown in yellow) is 15.13%. The maximum set forth in the specifications was 15%. Additional pictures are located in Appendix A: Supplemental Data from Tests in the Microstructure Pictures and Composition Analysis section.

Segmentation for Image: 1



Segment	Description	Area
■		15.13
■		84.87

Figure 57 Microstructure Analysis 20 Microns from the Edge

Hardness measurements were taken incrementally every 15mm on one of the test bars. The first hardness measurement was taken at a distance of 15mm from the edge. Measurements stopped when the effective hardness value (50 HRC) was reached. The distance from this point to the edge was then measured. The data is shown in Figure 58.

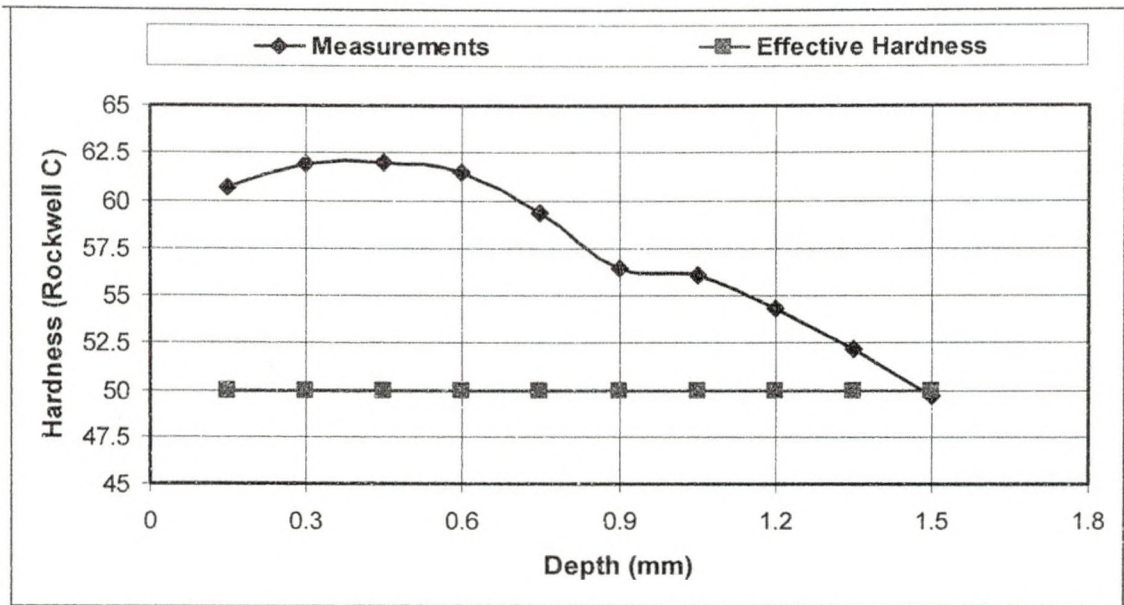


Figure 58 Hardness Measurements for Verifying the Case Depth

Since the test bars were not polished or finished, the de-carburized layer is still present. Therefore, the hardness measurements rise until the de-carburized layer is passed. Past this point, the hardness decreases due to decreasing strength of the heat treatment. The hardness measurements drop below the effective hardness at around 1.5 mm. In both the microstructure pictures (Figure 55 and Figure 56) and Figure 58, the de-carburized layer is approximately 0.3mm deep. The case depth is then 1.2mm, which is within the range specified in Table 10.

All of the measurements taken indicated that the batch of AISI 8620 material was within specifications. Therefore, preliminary testing on these parts could begin.

S-RCF Tester Performance

The sample specimen was the first specimen to be tested on the S-RCF tester. Testing was performed on February 5th 2008 until February 8th 2008. The total testing time was forty hours.

The data storage and analysis systems performed adequately. The data taken was stored correctly by the LX-10 at the user specified interval (wait twenty-nine seconds then record for one second). At the time, Matlab® analyzed these files after the user defined time (five minutes) had passed. A problem developed since the LX-10 and Matlab® were not set to the same clock. Therefore, the LX-10 was gradually creating files later and later than it should have. Matlab® would reach the amount of time to wait and look for a file that was not created yet. This discrepancy would cause an error in Matlab® and force the *RealTimeDataAnalysis* file to stop. This problem was temporarily fixed by starting the *RealTimeDataAnalysis* file twenty minutes behind the time the LX-10. Also, the automatic stop was not yet set up; therefore, the tester could not turn off the motors if a crack was detected.

The lubrication and pneumatic loading system both performed well. The leaking from the pneumatic loading system was very minimal. Some hissing was heard, but disappeared after the connections were tightened. Lubrication leaked out of the machine in several spots. After the lubricant was drained and filled back into the containers, approximately 1.5 quarts of lubricant leaked out or was still in the lines. The S-RCF tester originally had about 1 gallon of lubricant in the reservoir during testing.

After the sample specimen was removed and the bottom and top rollers taken off, the damage to the machine was assessed. All of the shafts had grooves on them from where they sat in the bearings. These grooves made removal of the rollers and collars difficult. The top roller shaft had developed a chip in it near the keyway. The damage to the top roller can be seen in Figure 59.

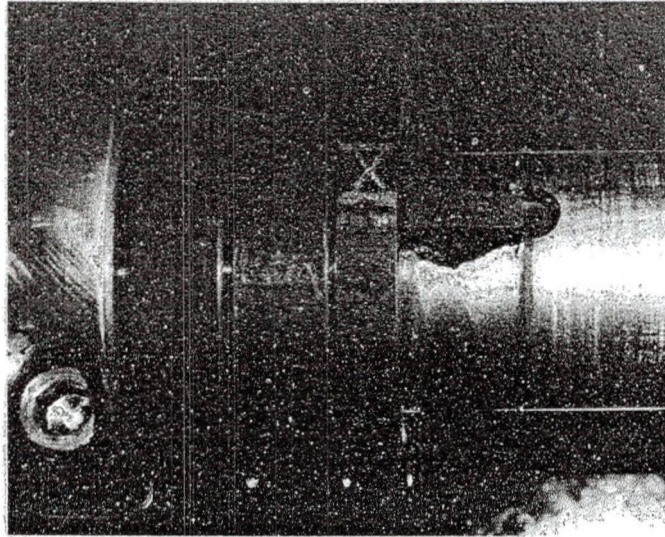


Figure 59 Keyway Damage to the Top Roller Shaft

The old probe holder used reached inside the S-RCF tester to monitor the specimen surface. The idea was that this isolated the eddy current probe from the vibrations in the tester. However, vibrations from the tester and from surrounding machinery were causing more vibrations in the floor than previously thought. Therefore, a new probe holder was designed for the next test to help reduce this vibration problem. The new probe holder sets inside the machine and is attached to the specimen sliding walls. A picture of the old and new probe holder can be seen in Figure 60.

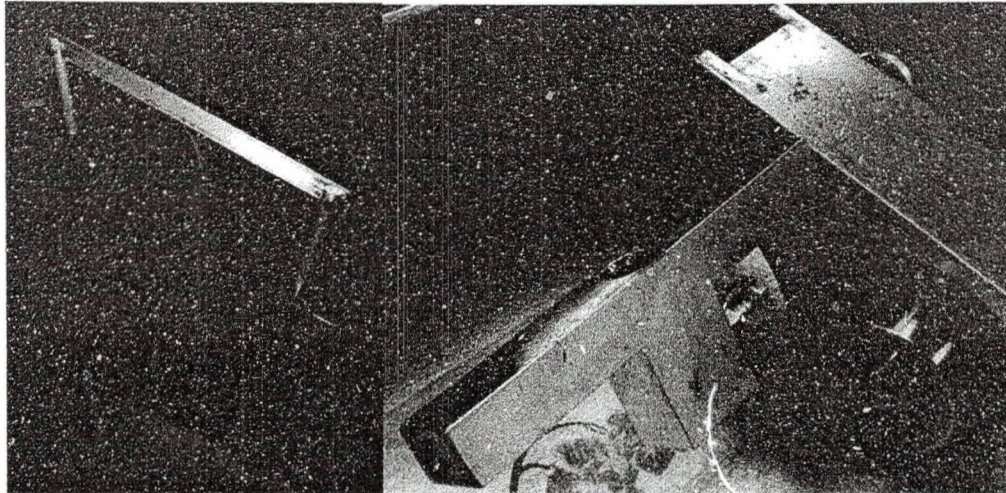


Figure 60 S-RCF Tester Eddy Current Probe Holders: Old (left) and New (right)

The next specimen tested was specimen 11 on April 18th thru April 22nd. The total testing time was approximately ninety-six hours.

Like the sample specimen testing, this testing required that the file creation and analysis be offset by approximately twenty minutes to prevent Matlab® from stopping unexpectedly. Since testing took significantly longer than the sample specimen, the offset had to be monitored and reset if necessary. The automatic stop was setup in the RealTimeDataAnalysis file and was tested several times to ensure it worked correctly.

The lubrication and pneumatic systems performed in much the same way. The pneumatic system continued to leak minimally and the lubrication system lost about the same amount of lubricant as the sample specimen test. The lubrication system worked well except for the temperature probe. At several points during testing, the probe seemed to have turned off or lost power as it drops to zero for no apparent reason. After this problem was discovered, the power to the temperature probe was reset and the probe worked correctly. The cause of this loss of power is unknown.

The new probe holder did well and no damage was done to the probe. The signal output from the probe was also much lower this time than the previous test. This can be seen by looking at the values of the graphs generated at the start of each test (graphs located in Appendix A: Supplemental Test Data in their respective section).

After testing was completed, the S-RCF tester was examined. There was no further evidence of wear on the top roller shaft and the shafts still had slight grooves in them. The PTFE tape used to seal the lubricant compartment was still holding in place and preventing lubricant from leaking. The oil seal in the specimen motor end oil wall had become wore and was tearing out of place.

Before specimen 2 was tested, several adjustments were made. First, under a higher loading, it appeared that the gear on the top roller was meshing too tightly with the gear on the roller motor. A new batch of top rollers was ordered with the diameter two millimeters larger than before. All other properties were kept the same. By only changing the diameter of the top roller, it now spins slightly faster than the other rollers. For a specimen speed of 1200 rpm and rolling conditions, the top roller surface velocity is 95.9 in./sec (2.44 m/s) whereas the bottom rollers surface velocities are 94.2 in./sec (2.39m/s). This difference is negligible when compared to the variability in the motors speeds during testing.

Secondly, it was determined that the motor mounts were to flexible and causing excessive noise and vibration. The metal adapter plate and motor mounts were removed and replace with two 10" channel irons. These channel irons provided a very solid and rigid base.

Testing on specimen 2 began on June 17th 2008 and ran continuously for about 29 hours. The new motor mounts installed reduced the noise and vibration considerably. The lubrication and pneumatic system performed the same as they did in the previous tests. The temperature probe turned off and on again several times for an undetermined reason.

After testing was completed, specimen 2 was removed so that specimen 3 could be run. The rollers were left on since specimen 3 was going to be used to test the ability to apply a slip ratio. With the tester back together, the motors were turned on with slip. Under loading, the roller motor would not turn on or ramp up to speed. The specimen motor tried to turn the whole system, but could only reach a speed of 400 RPM (it was set at 1200 RPM). If it was not under loading, the system worked fine and both motors turned up to speed. The S-RCF tester was taken apart and examined to determine the cause of the motor problem. After the bottom rollers were removed, it was discovered that a shaft had broken. Under loading, the gear on the broken shaft would bind the gear driving assembly. Due to the broken shaft, further testing could not be performed at the time. A picture of the broken bottom roller shaft can be seen in Figure 61.

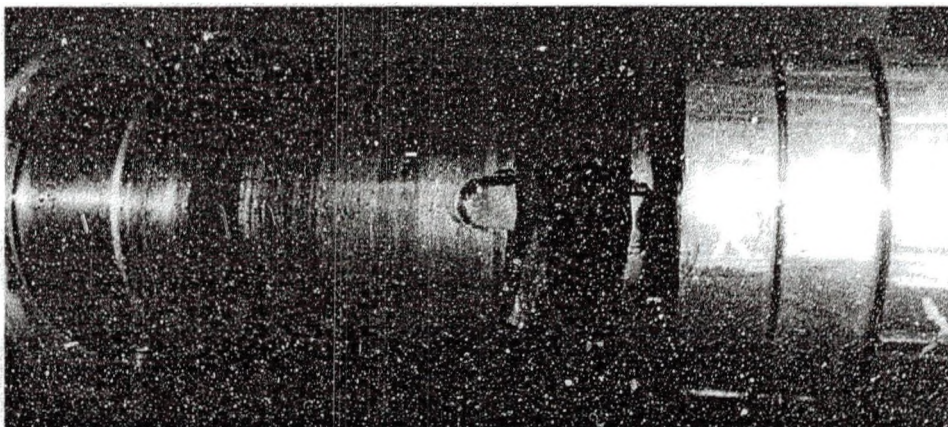


Figure 61 Broken Bottom Roller Shaft

After several modifications and additions during testing, the various systems of the S-RCF tester functioned adequately. These systems performed their tasks with a few minor problems that have been or can be fixed. These problems did not inhibit the ability of the tester to perform fatigue tests. The only major breakdown was the shaft on the bottom roller breaking. However, this failure was attributed to the fact that the shafts were made here at UND by a student and were not heat treated. New shafts are on order that will be precision machined and heat treated.

S-RCF Specimen Test Results

The graphs generated during the first stage of analysis (real time data analysis) for each specimen are located in Appendix A: Supplemental Test Data under the appropriate section. Table 13 presents the fatigue results of the AISI 8620 S-RCF specimens. The results of each specimen are presented in further detail in their respective sections. Each fatigue test was performed with new rollers.

Table 13 AISI 8620 S-RCF Specimen Test Results

Specimen	Test Dates	Failure Detected	Elapsed Time (hrs)	Load Cycles	Average Cylinder Pressure (psi)	Maximum Hertzian Stress (GPa)
Sample	Feb 5-8	Yes	40	8.64E+06	83	2.39
11	Apr 18-22	No	93	2.01E+07	63	2.08
2	Jun 17-18	Yes	29	6.26E+06	66	2.13

Sample Specimen

The sample specimen was the first specimen tested in the S-RCF tester. This specimen was made from AISI 8620, but had an unknown heat treatment and its properties were not verified. The cylinder pressure was approximately 82 psi (2.39 GPa maximum Hertzian stress). Since the automatic shutoff for the Matlab® files was not set up correctly at the time, the tester continued to run and was manually stopped at 40 hours

(8.64 million load cycles). Since the specimen was overrun, the exact time and location of the first signs of failure can only be determined by analyzing the data from the eddy current device. The specimen is hypothesized to have begun failure at approximately 27.8 hours of testing. The total number of load cycles at this point is about 6 million.

Since testing was not run continuously, there are several files that have the same number. Therefore, the testing time at the top of each graph is not accurate. The appropriate time for the graph is located in the titles.

During the first 18 hours of testing, no significant eddy current voltage change was detected. After 18 hours, the voltages on the Y and V channels began to gradually rise. This rise indicates that an irregularity or flaw is present on or near the surface which is disrupting the eddy currents induced into the material. This section of data was analyzed using the screening Matlab program. Figure 62 and Figure 63 are the figures developed from the screening program.

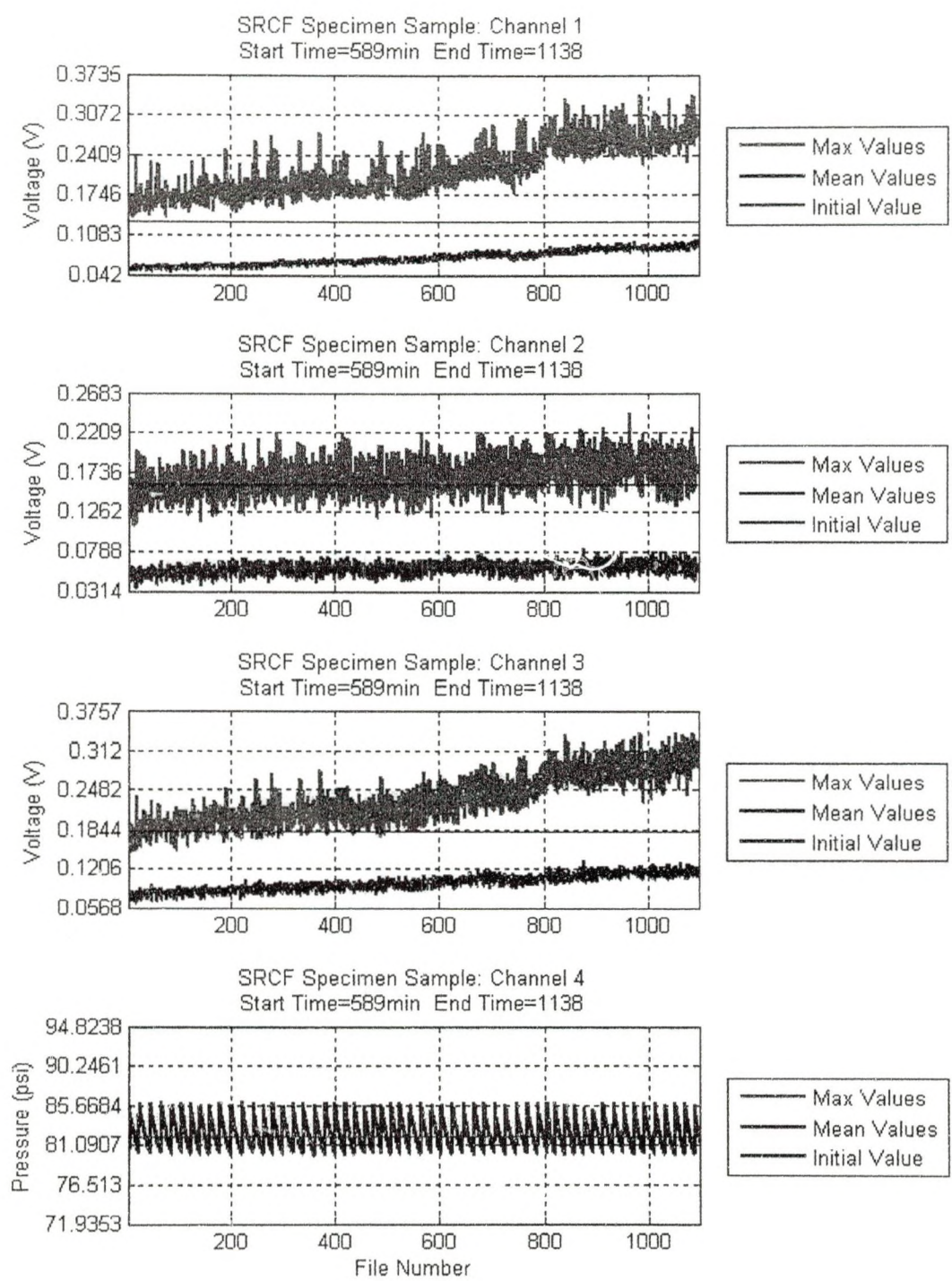


Figure 62 Screening Figure 1 for Sample Specimen (Testing Time 18 - 27.8 hrs)

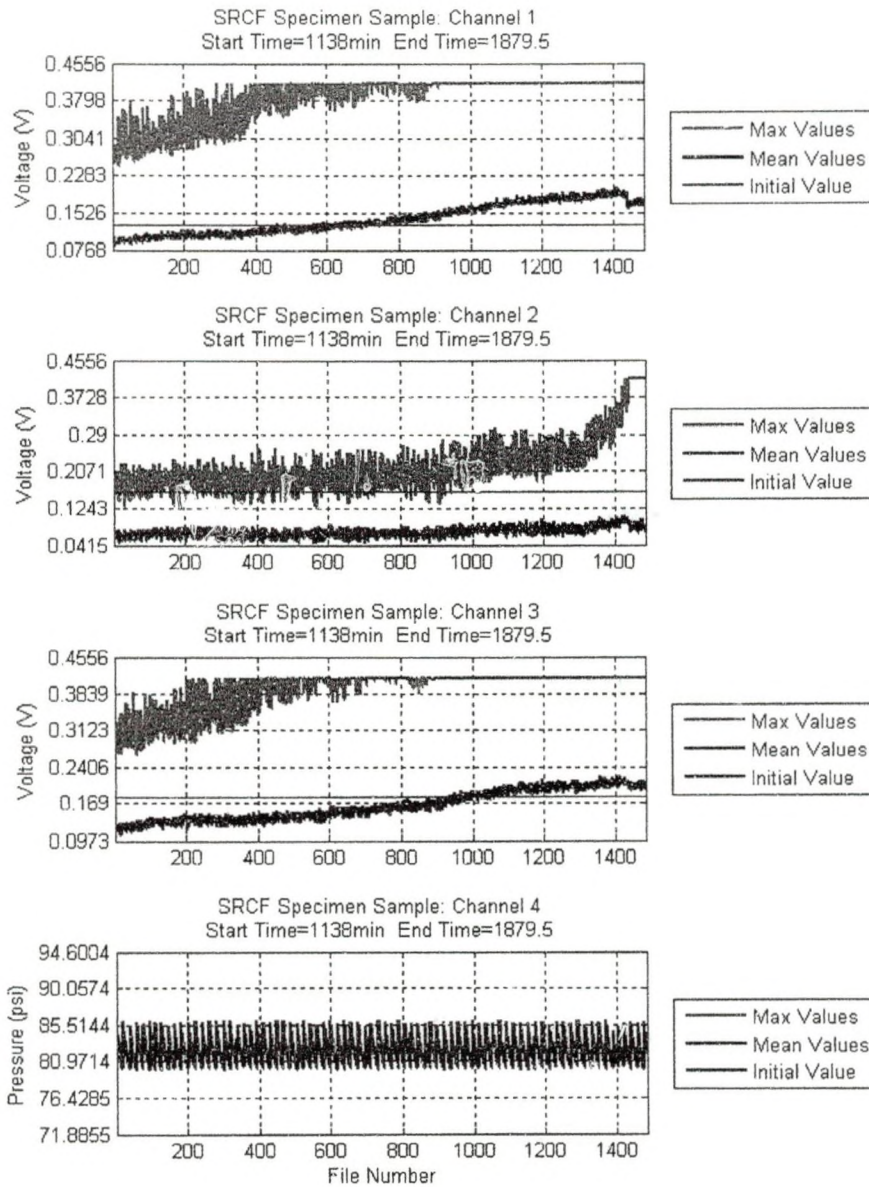


Figure 63 Screening Figure 1 for Sample Specimen (Testing Time 27.8 - 40 hrs)

In Figure 63, it can be seen that the signal levels off into a line. This is because the LX-Navi range was not calibrated correctly and the signal reached a maximum allowable value. Even with this data cut off, a significant voltage change was detected (see Table 14). Since the change went undetected, testing on the sample specimen was not stopped at the appropriate time.

Table 14 Summary of Eddy Current Voltage Changes for Sample Specimen

	Channel	0 hours	18 hours	27.8 hours	29.8 hours
Voltage Values (V)	Y	0.16	0.175	0.31	0.38
	X	0.15	0.174	0.22	0.23
	V	0.17	0.18	0.31	0.41
	Channel	0 to 0 hours	0 to 18 hours	18 to 27.8 hours	27.9 to 29.8 hours
Voltage Change (mV/hr)	Y	0.00	0.83	13.78	35.00
	X	0.00	1.33	4.69	5.00
	V	0.00	0.56	13.27	50.00

Severe pitting was found on the surface when the sample specimen was removed from the S-RCF tester. A photograph of the damage can be seen in Figure 64. A SEM photograph of the damage at a magnification of thirty-five is shown in Figure 65.

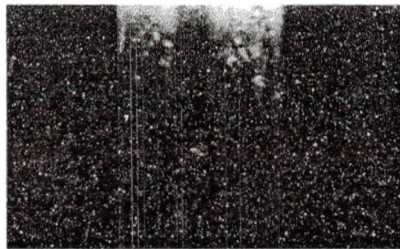


Figure 64 Pitting on S-RCF Sample Specimen

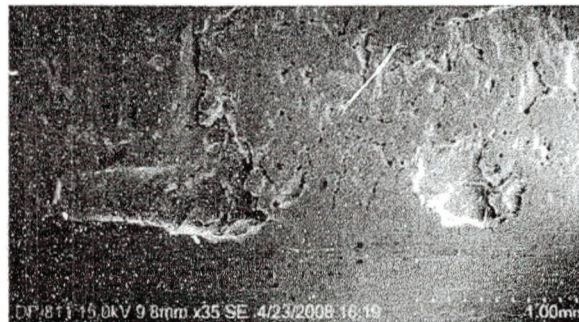


Figure 65 SEM 35x Photograph of the Sample Specimen

The SEM photograph shows that the damage is on the scale of millimeters. Since the specimen has not been cut, the origin of the pitting could not be determined. However, since the specimen was tested in a thin EHL layer, most likely the damage is a point-surface origin pit, severe micropitting, or a combination of both.

Specimen 11

Specimen 11 was the second specimen tested, but was the first specimen tested from the batch of material ordered. Specimen 11 was used in place of specimen 1 since specimen 1 had a flaw on the surface which made it unusable. Testing was performed continuously from April 18th to April 22nd and suspended after 93 hours since failure was not detected. The specimen was loaded at a cylinder pressure of 63 psi (2.08 GPa maximum Hertzian stress).

Since no failure was detected, testing was stopped and the specimen was taken out and inspected. The test surface on the specimen showed a wear track on the surface; however, no crack or flaw could be seen. A photograph of the wear track on the test surface can be seen in Figure 66.

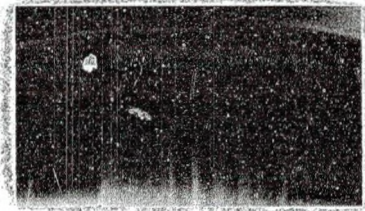


Figure 66 S-RCF Specimen 11 Test Surface Wear Track

The SEM was used to examine the surface in finer detail. A comparison of an untested surface with the tested surface of specimen 11 can be seen in Figure 67. The tested surface of specimen 11 appears cleaner and has fewer bumps on it. The bumps on the untested surface are from the grinding process and were eroded off during testing. The few nicks and scratches that can be seen on both surfaces are also from the grinding process. No further analysis of the data was performed.

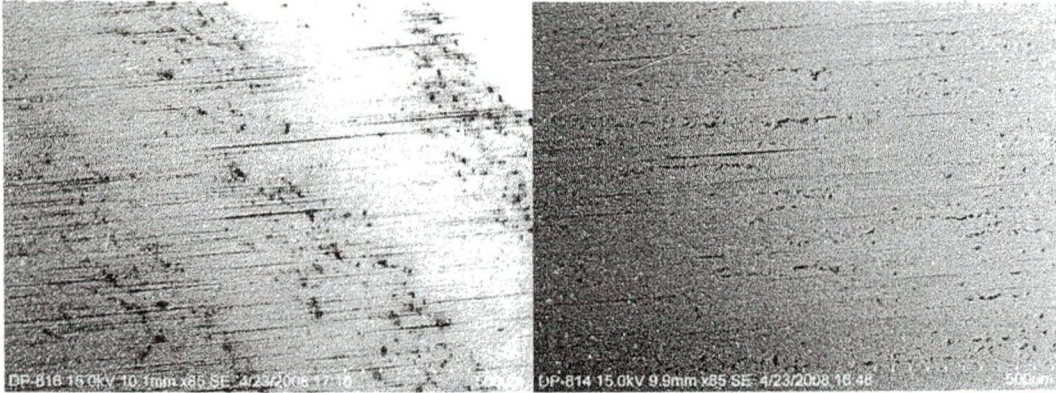


Figure 67 Comparison between an Untested S-RCF Specimen Test Surface (left) and the Tested Test Surface of Specimen (right)

Specimen 2

Specimen 2 was the second specimen tested from the batch of material ordered. The specimen was loaded at a cylinder pressure of 66 psi (2.13 GPa maximum Hertzian stress). Testing was performed continuously from June 17th to June 18th. On June 18th, one of the eddy current channels observed a signal outside of the allowable range. The motors were turned off automatically, but the applied loading and file creation continued to operate. Figure 68 shows the graphs for specimen 2 generated during stage 2 (screening stage) from the start to 33 hours into testing.

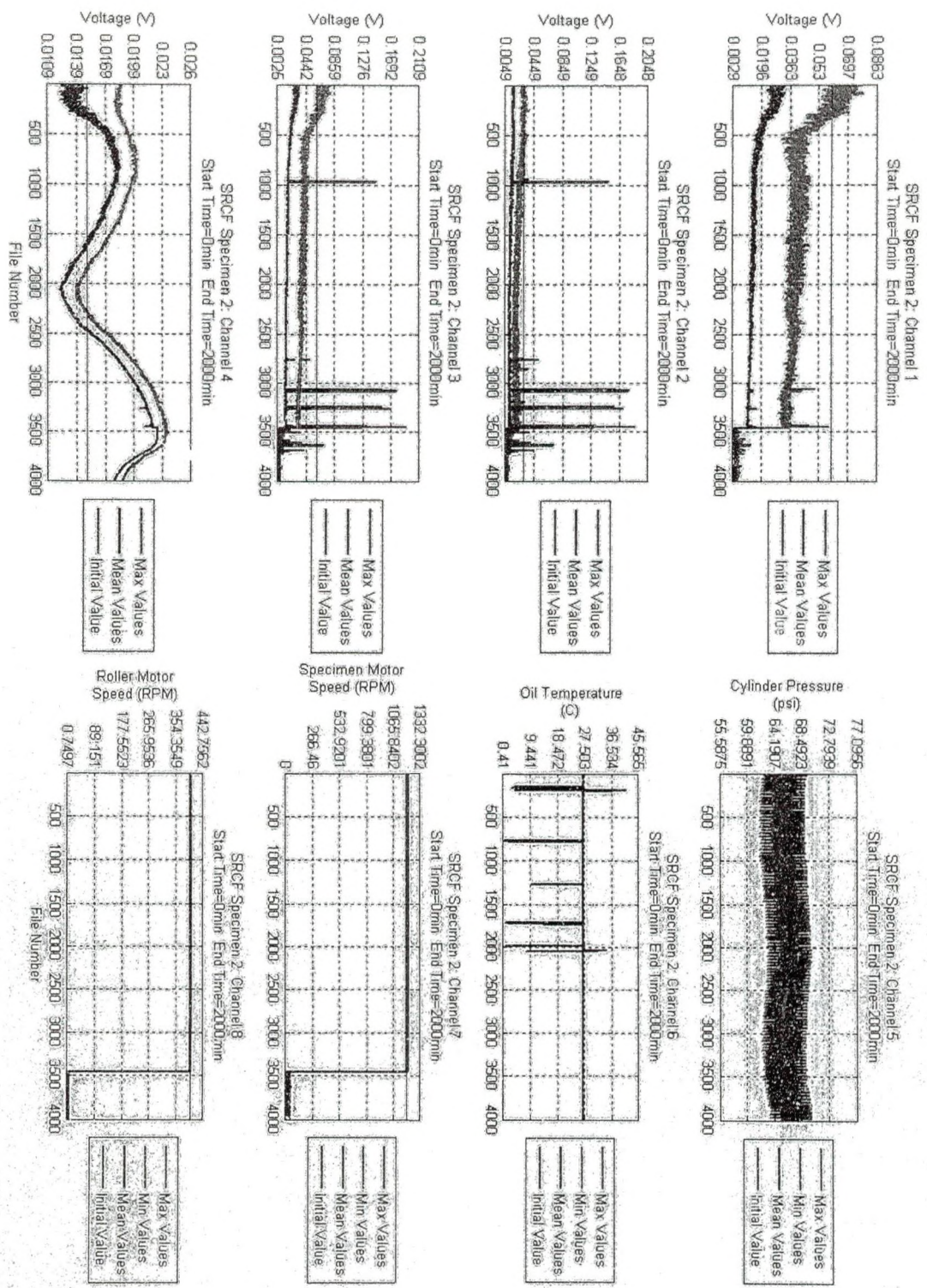


Figure 68-Screening Figures 1 and 2 for Specimen 2 (Testing Time: 0 to 33 hrs)

From Figure 68, it can be seen that channels 1, 2 and 3 (the Y, X and Vector eddy current signals, respectively) experienced a sharp rise in voltages at several points. The reason for these sharp rises in voltage was not determined until the tester was taken apart. As previously mentioned, one of the bottom roller shafts was found to be broken. The peaks in voltages were probably the bottom shaft moving out of position. The largest peak on the second channel was the reason the motors turned off. This occurred after approximately 29 hours of testing (6.26 million load cycles).

Specimen 2 was removed from the S-RCF tester and examined for signs of wear and damage. Tiny pits had begun forming on only one edge of the testing surface. Since the damage is only on one side of the test surface, it is possible that a misalignment is present in the system. Also, the area around the testing surface had a darker coloring to it than the rest of the metal. The discoloring did not occur on the previous specimens. A picture of specimen 2 can be seen in Figure 69.

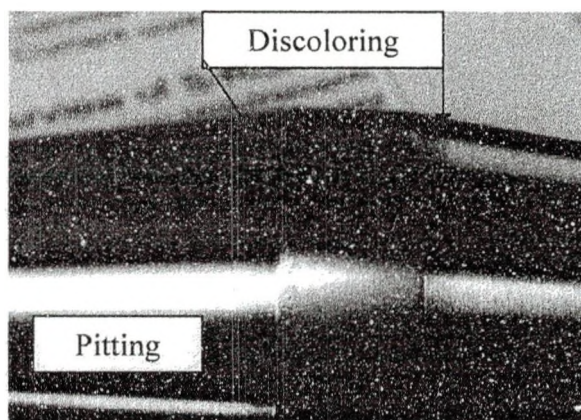


Figure 69 S-RCF Specimen 2 Photograph of Tested Surface

The specimen was then put into the SEM to obtain a closer look at the damage. After trying for several hours with Dr. Ranko, the SEM would not give a clear image of the surface. The specimen was then taken to an optical microscope with photographing

capabilities in the ESC. The microscope showed small pits at one edge of the test surface. The damaged edge is 1.21 millimeters wide and the largest pit is almost $\frac{1}{2}$ a millimeter wide. The optical microscope photograph can be seen in Figure 70.

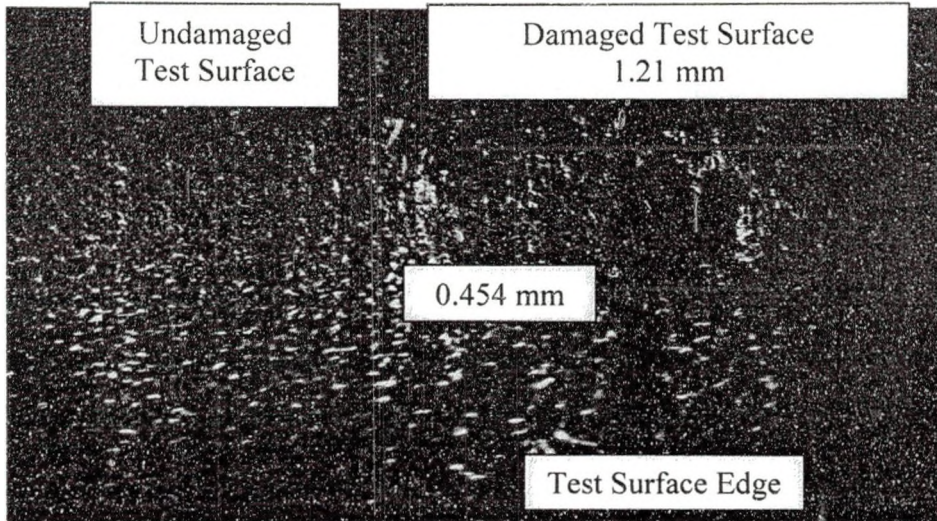


Figure 70 S-RCF Specimen 2 Optical Microscope Photograph Tested Surface

The damage on one side of the test surface and not the other suggests that the loading across the test surface is not equal. The cause for this unequal loading is probably due to the poor machining of the shafts and the collars. The three rollers are not perfectly inline; therefore, a slight bending moment is occurring at the specimen. This bending would cause the pressure distribution to be uneven at higher loadings. Thus, one side of the surface is under higher pressure than the others. The uneven loading is also present on the sample specimen since one side is damaged more than the other (see Figure 64). However, since the sample specimen was overrun, damage had begun to form on both sides.

CHAPTER 5

CONCLUSIONS AND RECOMMENDATIONS

Many different testers for sliding and/or rolling contact fatigue exist in the industry. Each tester is used for a specific application and has different limitations. The S-RCF tester was designed to be a fatigue tester that could perform contact fatigue tests under a wide range of conditions. These different conditions can be controlled and monitored by the tester. A method for determining the relevant properties of the material was also developed. The analysis program created gives the user a way to determine when failure has started and if it is growing. The only condition not functioning correctly is the ability to apply a slip ratio. This problem is a controller issue and will need to be addressed in the future. Although the limits of the tester's capability were not performed, the basic systems of the machine were tested and function properly.

The pneumatic system applied loading with some small scale variability (about 3 psi). This variability is due to small leaking and the cylinders having to be recharged. The lubrication system lost lubricant during testing but did not affect the tester's ability. The reason for leaking is due to poor machining of the oil walls. Submerged testing can not be performed due to a broken oil seal in one of the end oil walls. The eddy current detection device worked well during all of the tests. Failure was detected on the first test (sample specimen) and removing the specimen showed pitting had occurred. The second test (specimen 11) did not show any signs of failure and no significant voltage change was found. The Matlab® scripts that have been developed and revised give the user a

way to analyze the data. This data can be analyzed both during testing and after testing. The broken shaft was probably due to a roller misalignment due to poor machining of the collars and shafts. Precision machined and hardened shafts and collars should fix this problem.

After performing tests and working with the S-RCF tester, several improvements and ideas have been developed. These suggestions could either be used on the current tester or on a second generation version of the tester. It is recommended that work on the current tester be continued until it is fully determined that the concepts behind it will work.

The first set of improvements concern the pneumatic loading system of the S-RCF tester. Originally, the loading structure was to be removable so that the user could access the specimen and rollers easily. However, the frame warped when it was welded and now the frame catches on the bolt heads. A quick solution for this is to use hex bolts in place of the socket head cap screws (SHCS) currently in use. The hex bolt heads have a lower profile and will allow the loading frame to be removed.

The application of the loading is performed manually by flipping a three-position four-way control valve. Therefore, when failure is detected and the motors stop turning, the load is still being applied. It is recommended that the loading be controlled by the computer as well as manually. The manual switch would act as a safety measure if something were to go wrong. The computer controlled method would allow Matlab® to automatically remove the loading when failure has been detected.

The lubrication system has several improvements that would make it function better. The lubricant leaking that occurred during this test did not hinder or affect the

tests; however, it did make quite a mess. The leaking problem is due to the poor machining of the end oil walls and a slight dip in the center of the base. These machining problems would be best corrected by designing a new machine. The leaking problem could also be solved by drilling large holes in the base to allow the lubricant to store in a separate reservoir. This separate reservoir would also allow the user to determine the amount of lubricant in the system and if more needs to be added. Lubricant was added to the S-RCF tester by removing the top cover and pouring it into the top. A separate reservoir would make adding lubricant easier and safer.

An explanation for the temperature probe turning off and on at random could not be found. It is possible that the power supply is overheating or that the bare wires are touching. In either case, the temperature probe needs to be fixed or replaced. The probe should also be moved closer to the specimen to get a more accurate reading. The current location of the temperature probe measures the bulk lubricant temperature after the lubricant has been sitting inside the tester for while. The temperature of interest in fatigue testing is the temperature of the contacting surfaces. Deng, Nakanishi and Kato used a type K thermocouple which hovered just above the surface to measure the surface temperature [7]. The thermocouple would measure the temperature of the lubricant film on the contacting surface. Although this is not the actual surface temperature, it is a closer approximation than the method currently used.

Another area of improvement is the user controls of the S-RCF tester. The tester is currently controlled by Matlab® and requires some skill in programming if changes are to be made. Labview® (a more graphical programming language) was tried but it did not function correctly. It is recommended that a combination of both the programs be used

together. Labview® has the capability of calling up and running a Matlab® script. The user defined inputs could then be on a Labview® control board. The user could then start the Labview® program and it would automatically run the Matlab® scripts.

Although significant work and several modifications have been made to the Matlab® scripts, there is still a lot that could be done. If the loading was computer controlled, then the user could generate a load history script to vary the loading during testing. The slip could be varied during testing as well once it is possible to perform slip.

The graphs generated during the real time data analysis stage (stage 1) display a small window of time. While this shows when a failure occurs, it does not show the long term trend of the data. Since Matlab® is limited on the amount of information it can process, graphing all of the data is not a feasible solution. A solution for this problem is to remove old data from the memory and replace it with the new data. The data matrix with all of the information can be manipulated so that the first column of data is deleted and the new data is concatenated to the end of the data matrix. Preliminary trials in Matlab® show promise that this method will work.

The final set of improvements concern the procedure for the assembly and disassembly of the S-RCF tester. Currently, the user must manually lift out the top roller to gain access to the specimen. Even after performing this task several times alone, it is not easy to do. Since the top roller must be removed after every test performed, it should be made easier to do. This can be accomplished by designing a connection between the air cylinder rods and the top roller assembly. With this connection, the air cylinders can lift the top roller out of the inner walls.

Another task that must be performed after every test is the changing of the bottom rollers. This task is complicated due to the fact that both motors must be disengaged and moved and both end oil walls must be unbolted. A couple of improvements could be made to make this task easier. First, the motors could be placed on a linear motion system than lock into place. Secondly, the bottom rollers could be made to slide out like the top roller. Therefore, the rollers could be changed outside the machine like the top roller.

Most of these improvements would serve best on a second generation S-RCF tester. It is recommended that testing continue on the current S-RCF tester to test all of its capabilities. If it is determined that all the systems of the tester can function properly together, a second generation tester with improvements should be designed and built.

In comparison to other testers available, the S-RCF tester does not currently function as well as them. The biggest shortcoming of the S-RCF tester is that it cannot perform a contact fatigue test under a full EHL condition. However, the other testers have been around for several years and worked on longer. The potential capabilities of the S-RCF tester is the same or better than most tester available. The most promising potential is the ability to run at any slip ratio. Other potential capabilities include a dynamic load history, surface temperature monitoring and lubricant temperature control.

APPENDICES

APPENDIX A

Supplemental Test Data

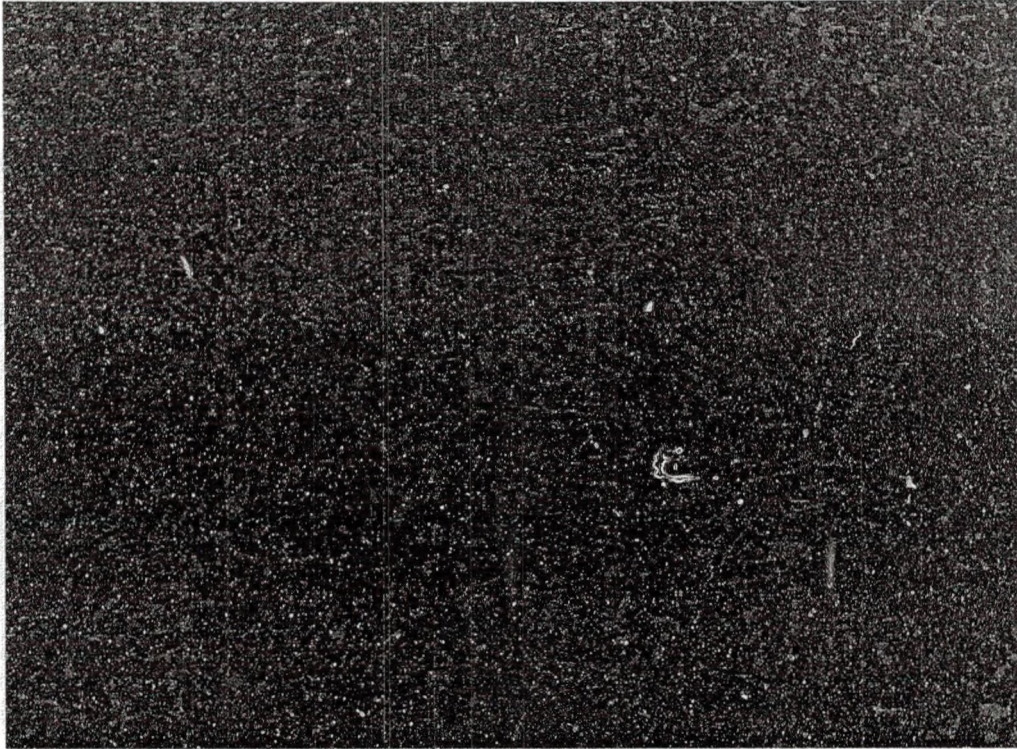
Roughness Measurements of AISI 8620

Axial Roughness Measurements	Measured Values	Specimen/Roller Number	13	4	3	4A	4B	4C	
		Ra1 (μ'')	16.73	14.86	13.85	10.85	7.44	10.02	
		Ra2 (μ'')	13.38	14.36	12.27	11.49	7.79	8.99	
		Ra3 (μ'')	15.97	12.79	11.47	11.78	6.76	9.16	
	Ra4 (μ'')	15.02	12.57	16.26	11.28	6.33	9.40		
	Individual	Average (μ'')	15.28	13.65	13.46	11.35	7.08	9.39	
		Sample Standard Deviation (μ'')	1.44	1.14	2.11	0.39	0.66	0.45	
		95% Confidence Interval (μ'')	± 2.30	± 1.81	± 3.36	± 0.62	± 1.05	± 0.72	
	Group	Average (μ'')	14.13			9.27			
		Sample Standard Deviation (μ'')	1.69			1.88			
		95% Confidence Interval (μ'')	2.48			5.31			
	Circumferential Roughness Measurements	Measured Values	Specimen/Roller Number	13	4	3	4A	4B	4C
			Ra1 (μ'')	10.37	9.76	8.86	6.14	4.60	7.02
Ra2 (μ'')			11.07	12.60	7.63	7.54	4.12	5.78	
Ra3 (μ'')			9.88	9.11	14.40	4.28	4.65	4.48	
Ra4 (μ'')		12.11	10.15	11.92	5.98	4.97	5.70		
Individual		Average (μ'')	10.86	10.41	10.70	5.99	4.59	5.75	
		Sample Standard Deviation (μ'')	0.97	1.52	3.05	1.34	0.35	1.04	
		95% Confidence Interval (μ'')	± 1.54	± 2.43	± 4.86	± 2.12	± 0.56	± 1.65	
Group		Average (μ'')	10.66			5.44			
		Sample Standard Deviation (μ'')	1.86			1.11			
		95% Confidence Interval (μ'')	0.57			1.86			

Microstructure Pictures and Composition Analysis

Image Distance: 100 Microns from the edge

Segmentation for image: 1

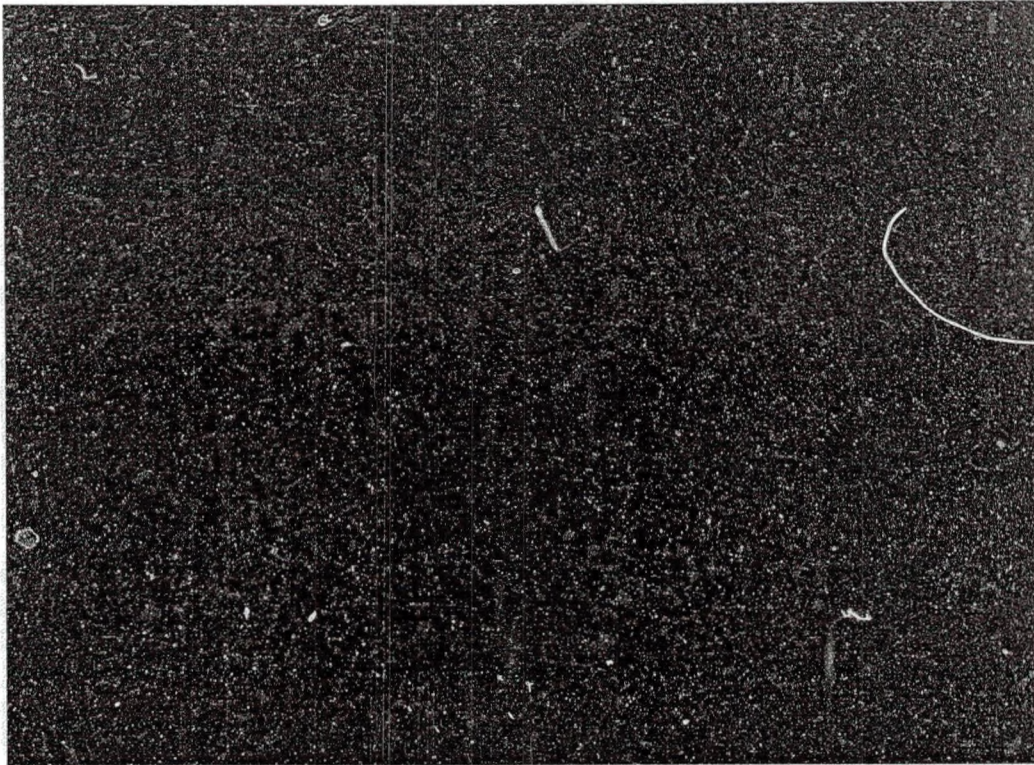


Segment	Description	Area
1		12.10
2		87.90

Retained Austenite and Other Non-Transformed Products: 12.10 % (Volume)

Image Distance: 200 Microns from the Edge

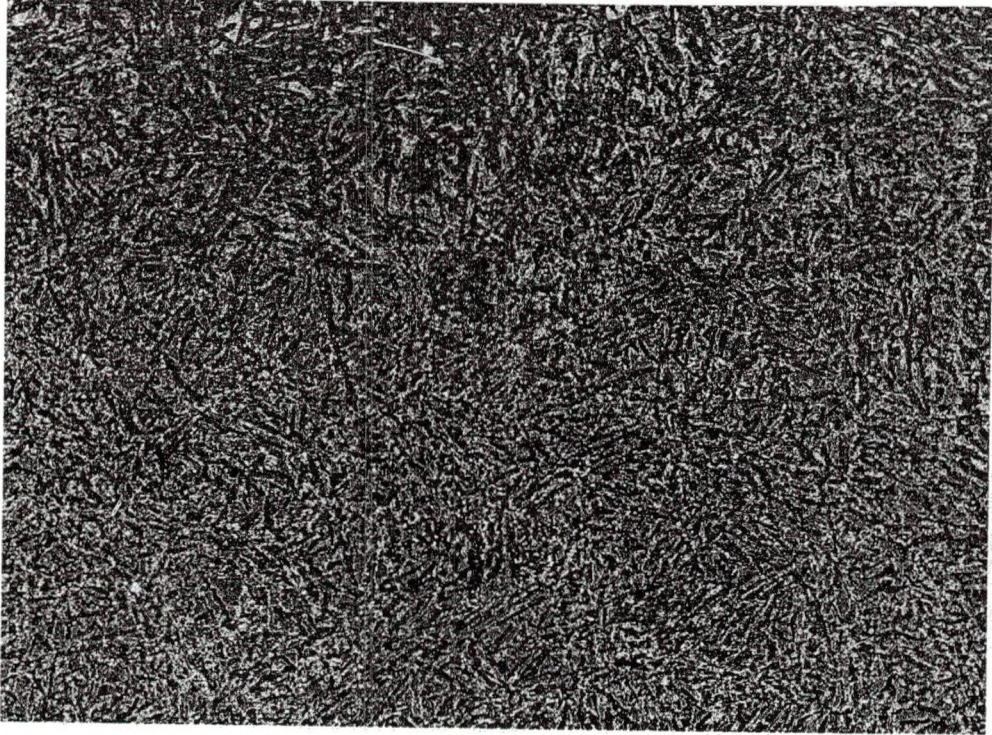
Segmentation for Image: I



Segment	Description	Area
1		7.64
2		92.36

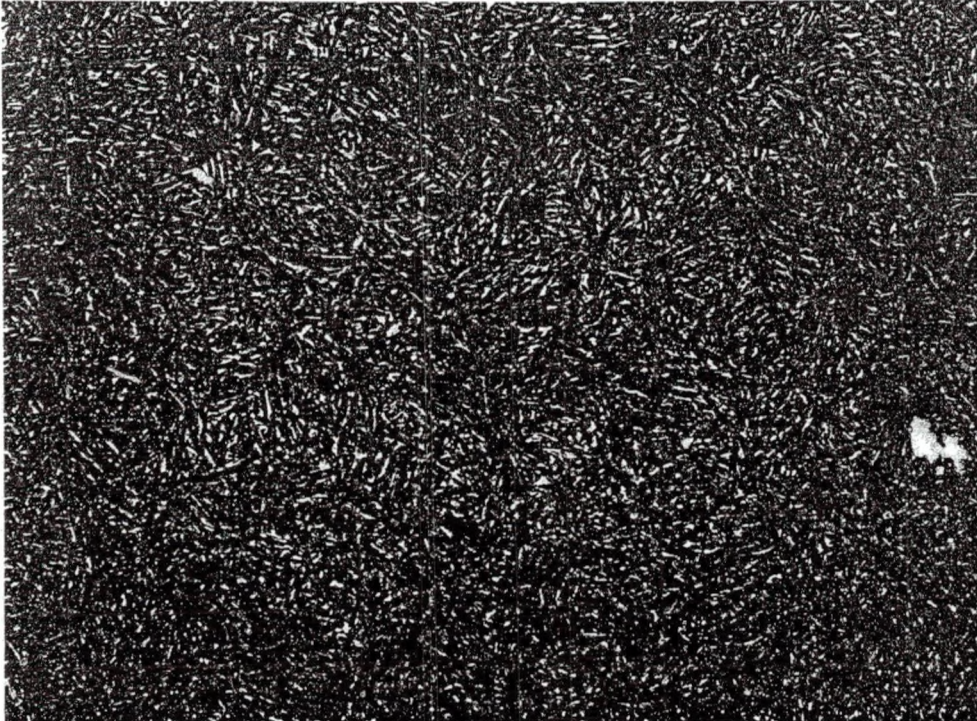
Retained Austenite and Other Non-Transformed Products: 7.64 % (Volume)

Unknown Image of Test Bar at an Unknown Distance



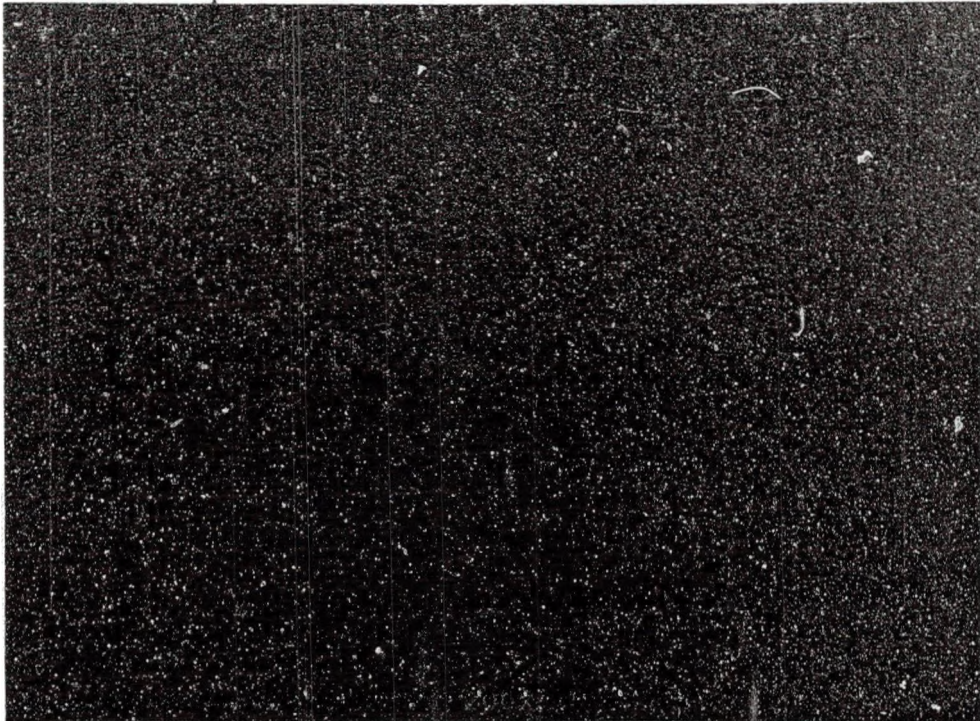
Retained Austenite and Other Non-Transformed Products: 15.59% (Volume)

Elemental Composition Area 1



Component	Conc.						
Si	0.683	wt.%					
Cr	0.447	wt.%					
Mn	0.403	wt.%					
Fe	96.605	wt.%					
Ni	1.208	wt.%					
Cu	0.653	wt.%					
	100.000	wt.%	Total				
Elt.	Line	Intensity (c/s)	Error 2-sig	Atomic %	Atomic Ratio	Conc	
Si	Ka	5.50	1.048	1.351	1.0000	0.683	wt.%
Cr	Ka	3.81	0.873	0.478	0.3536	0.447	wt.%
Mn	Ka	1.76	0.593	0.408	0.3018	0.403	wt.%
Fe	Ka	311.71	7.895	96.050	71.1126	96.605	wt.%
Ni	Ka	2.37	0.688	1.143	0.8464	1.208	wt.%
Cu	Ka	0.95	0.435	0.570	0.4224	0.653	wt.%
				100.000		100.000	wt.%
							Total
kV	15.0						
Takeoff Angle	35.0°						
Elapsed Livetime	20.0						

Elemental Composition Area 2



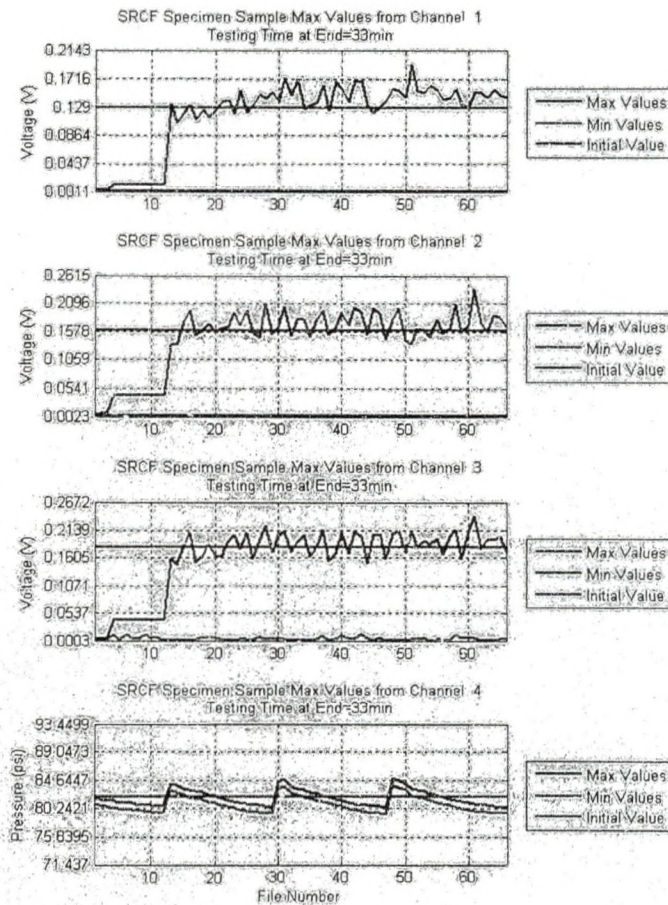
Component	Conc.	
Si	0.639	wt.%
Cr	0.751	wt.%
Mn	0.794	wt.%
Fe	96.178	wt.%
Ni	0.967	wt.%
Cu	0.670	wt.%
	100.000	wt.%
		Total

El.	Line	Intensity (c/s)	Error 2-sig	Atomic %	Atomic Ratio	Conc
Si	Ka	10.33	1.437	1.264	1.0000	0.639 wt.%
Cr	Ka	12.09	1.555	0.802	0.6349	0.751 wt.%
Mn	Ka	6.83	1.169	0.802	0.6349	0.794 wt.%
Fe	Ka	623.14	11.163	95.631	75.6695	96.178 wt.%
Ni	Ka	3.81	0.872	0.915	0.7242	0.967 wt.%
Cu	Ka	1.95	0.625	0.586	0.4635	0.670 wt.%
				100.000		100.000 wt.%
						Total

kV	15.0
Takeoff Angle	35.0°
Elapsed Livetime	20.0

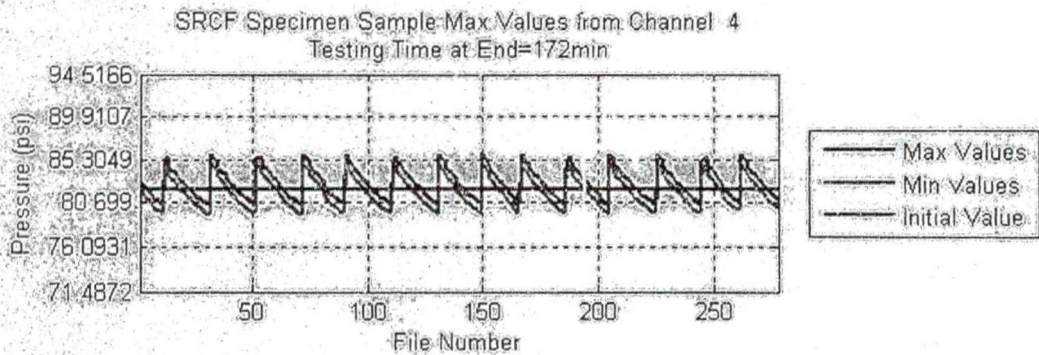
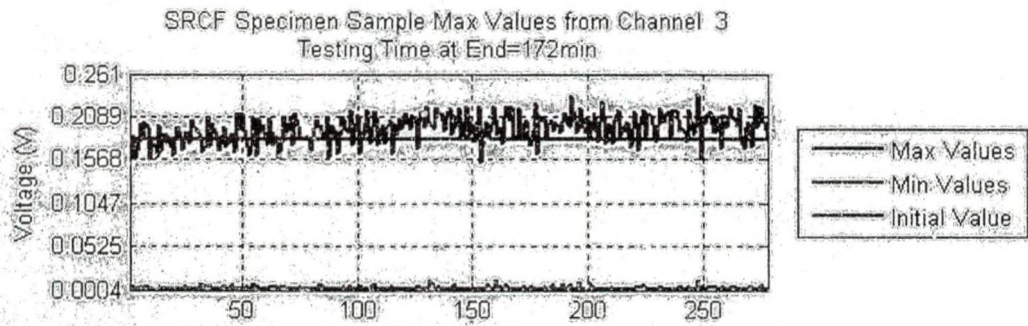
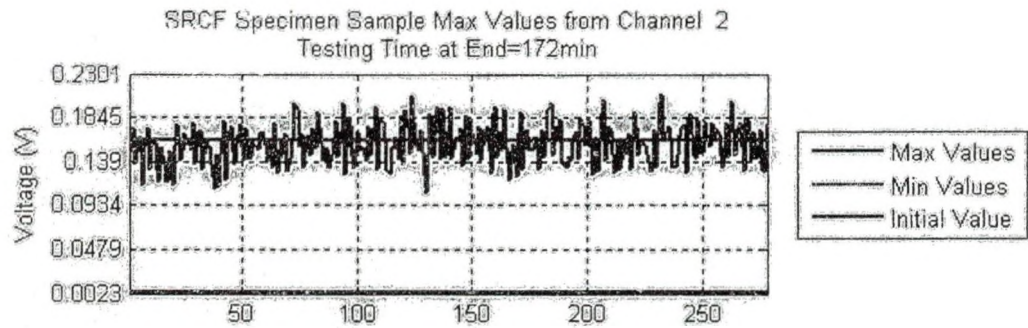
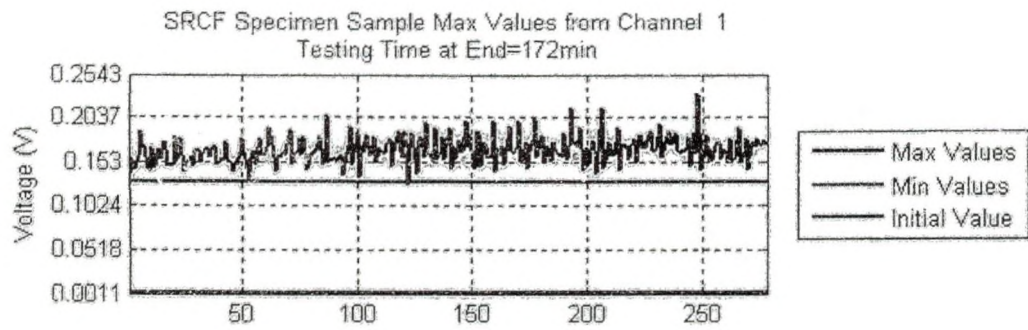
Sample Specimen

For the sample specimen, channels 1, 2 and 3 were the eddy current channels. Channel 1 was the Y-component, channel 2 was the X component and channel 3 was the V (vector) component. Channel 4 was the pressure as measured by the pressure transducer. Eight hours of testing occurred before these graphs were generated; therefore, the time at the top of the graph needs to have nine hours added to it to achieve the testing time.

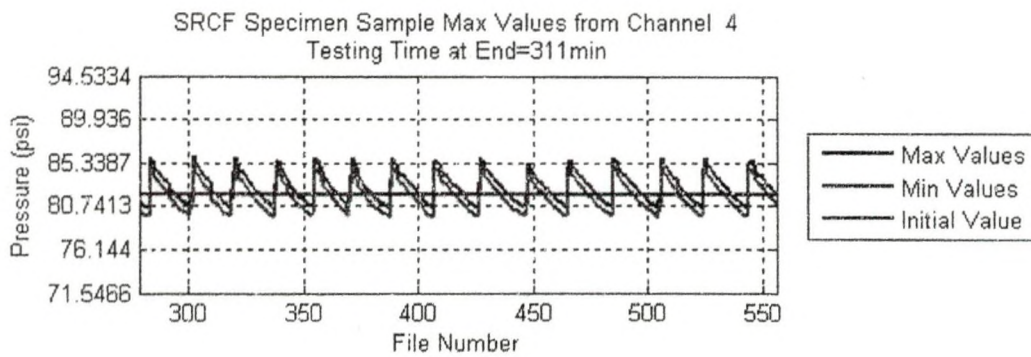
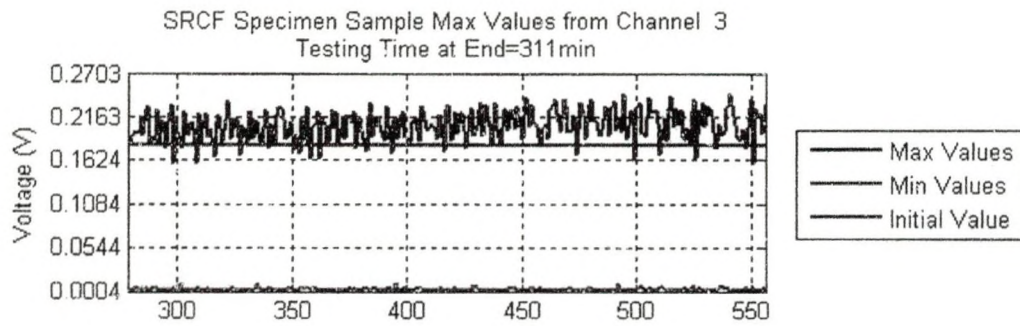
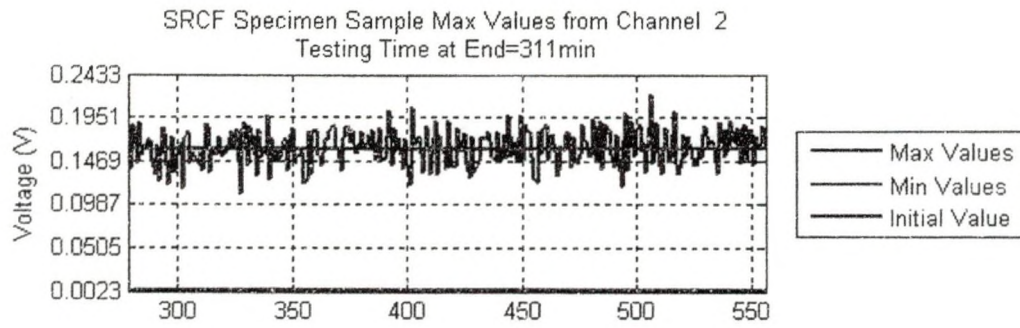
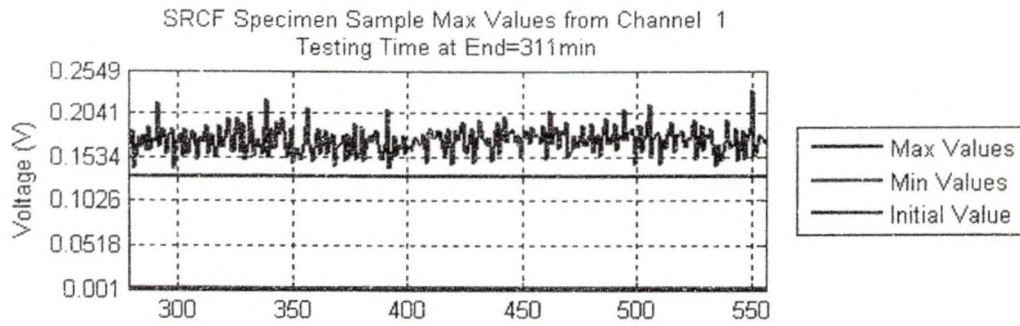


Testing Time: 9hr to 9.5hr

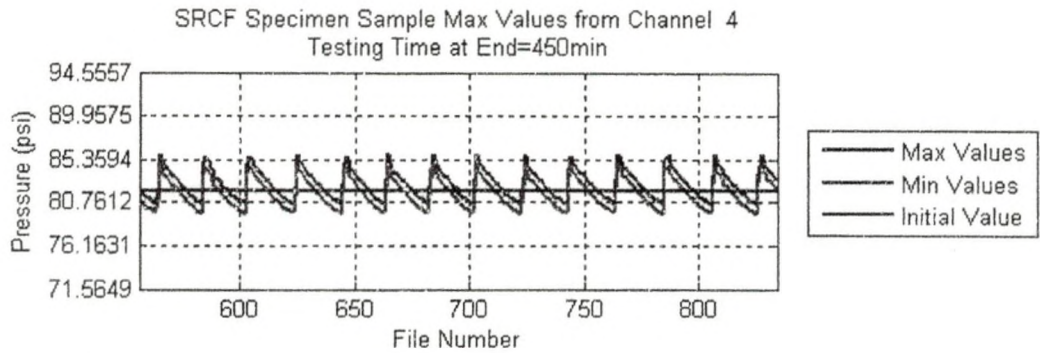
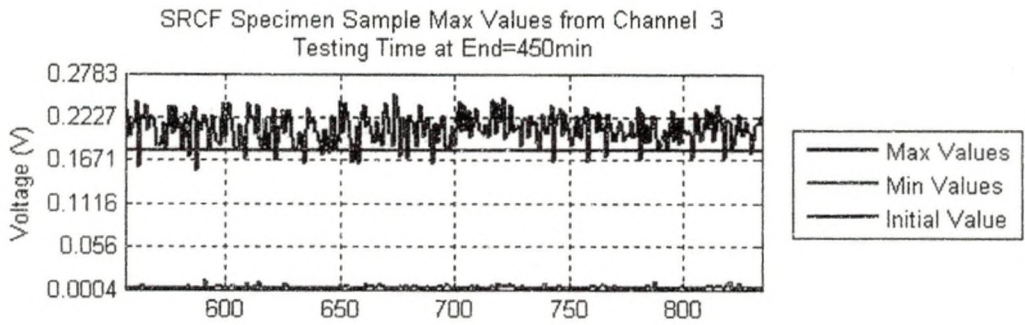
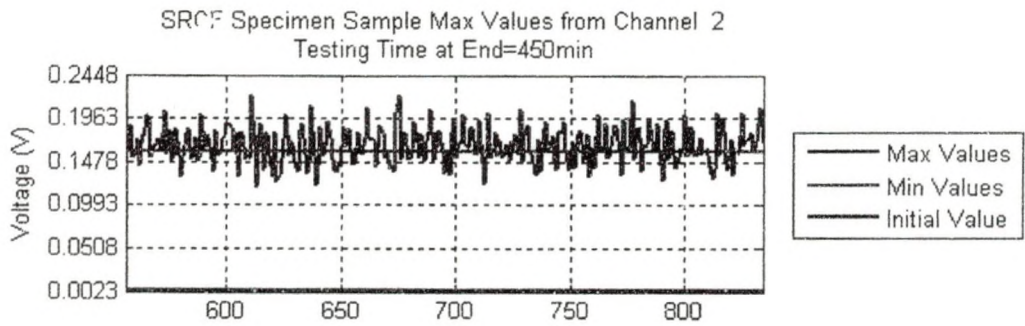
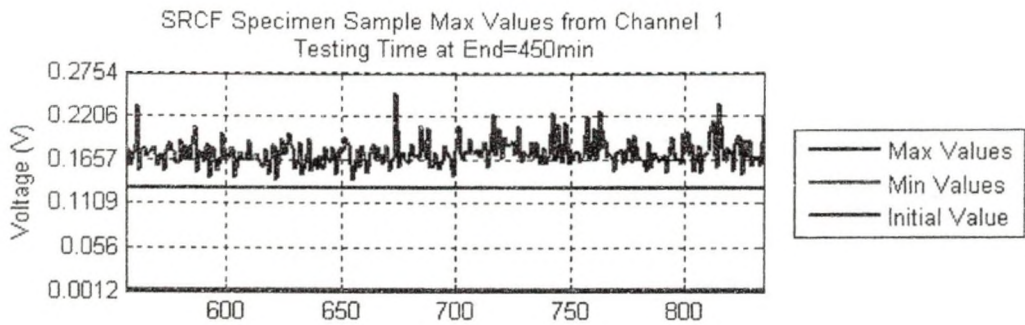
The low values at the start of the graphs for channels 1, 2 and 3 are because the motors were not turned on yet.



Testing Time: 9.5 hr to 11.75hr

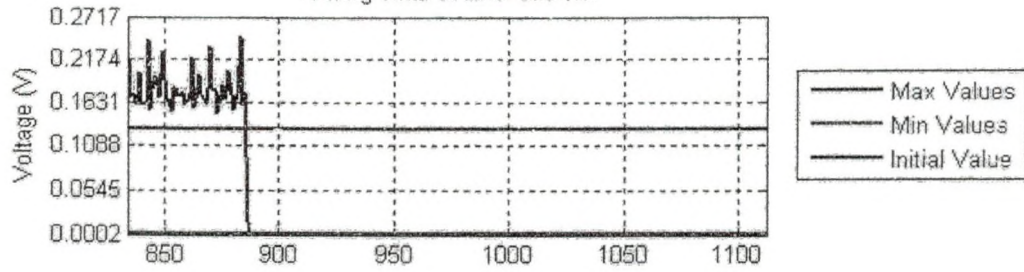


Testing Time 11.75hr to 14hr

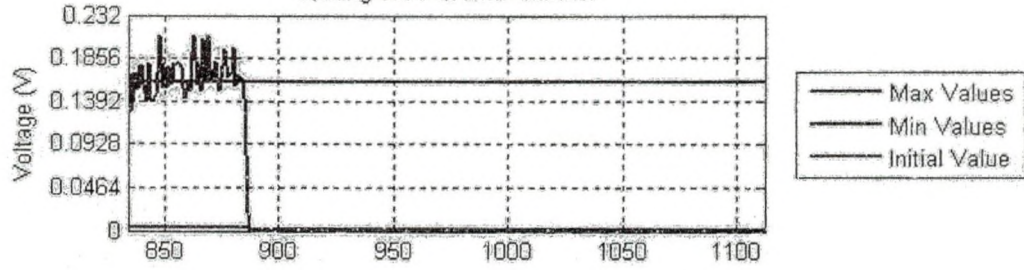


Testing Time: 14hr to 16.35hr

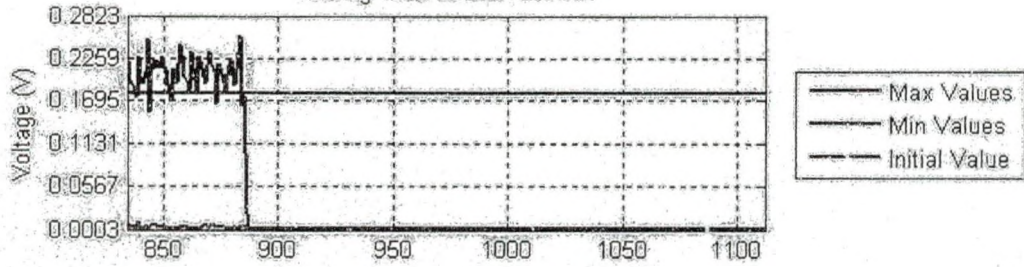
SRCF Specimen Sample Max Values from Channel 1
Testing Time at End=589min



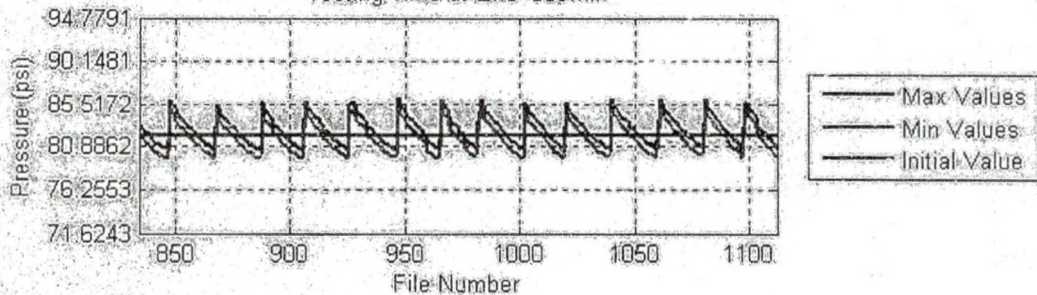
SRCF Specimen Sample Max Values from Channel 2
Testing Time at End=589min



SRCF Specimen Sample Max Values from Channel 3
Testing Time at End=589min

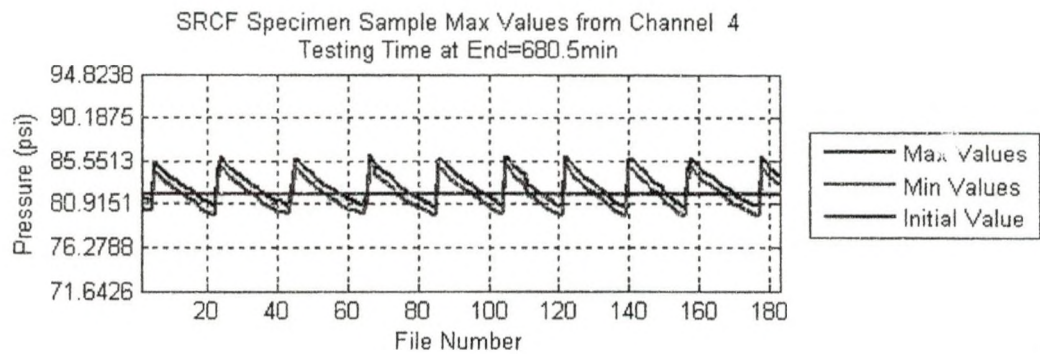
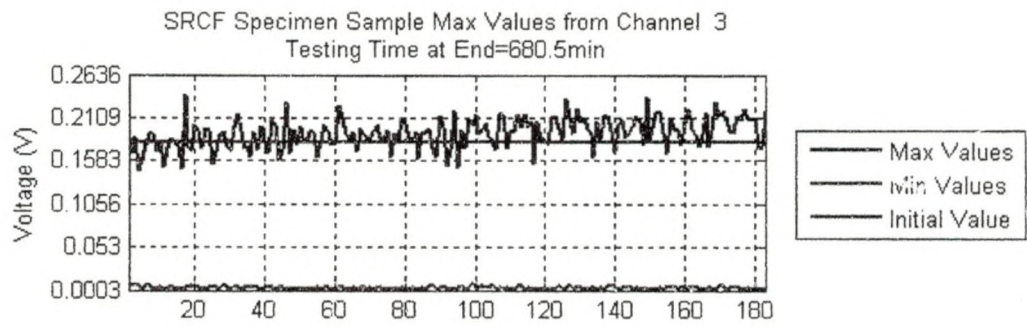
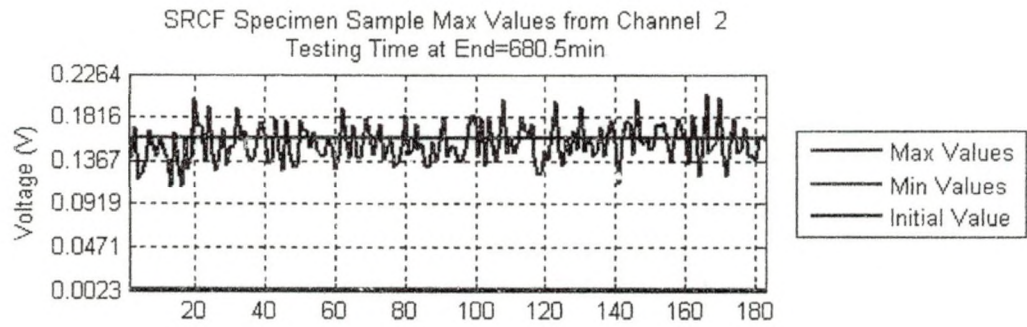
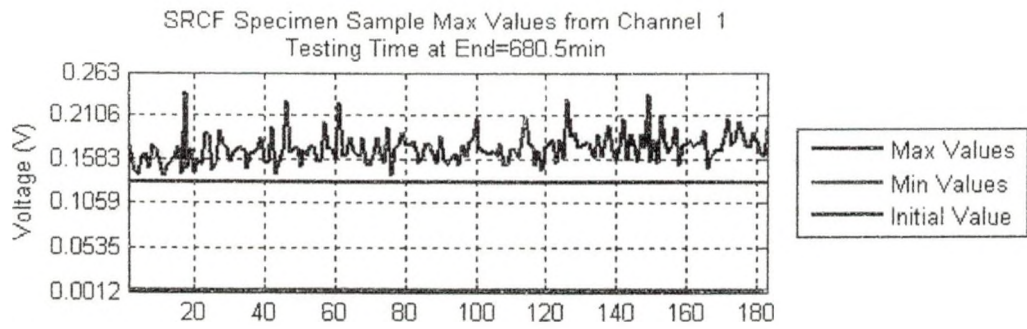


SRCF Specimen Sample Max Values from Channel 4
Testing Time at End=589min

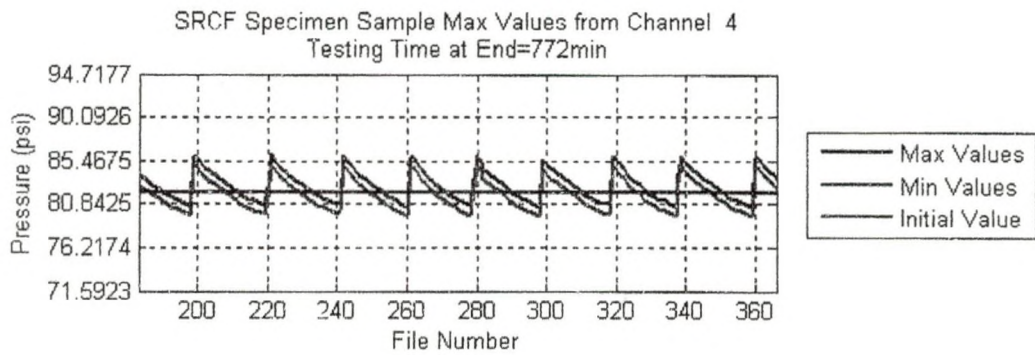
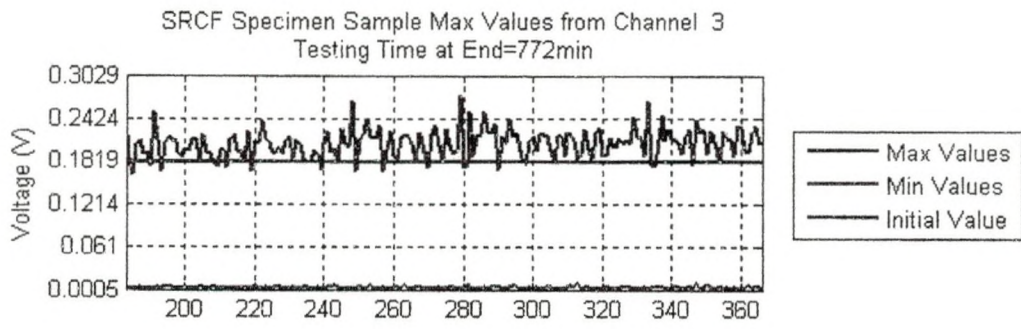
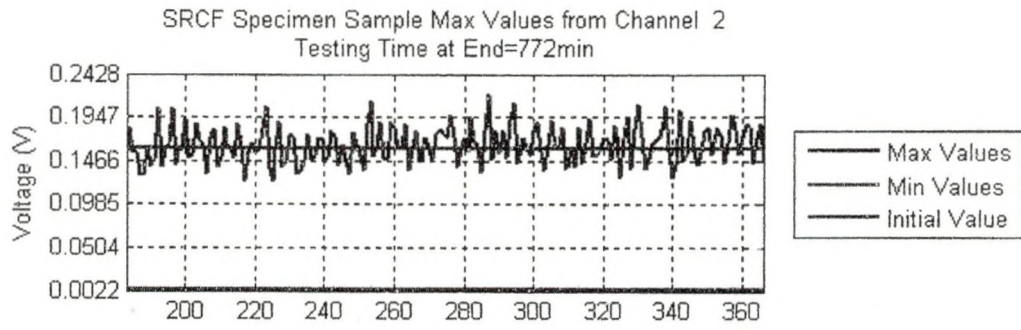
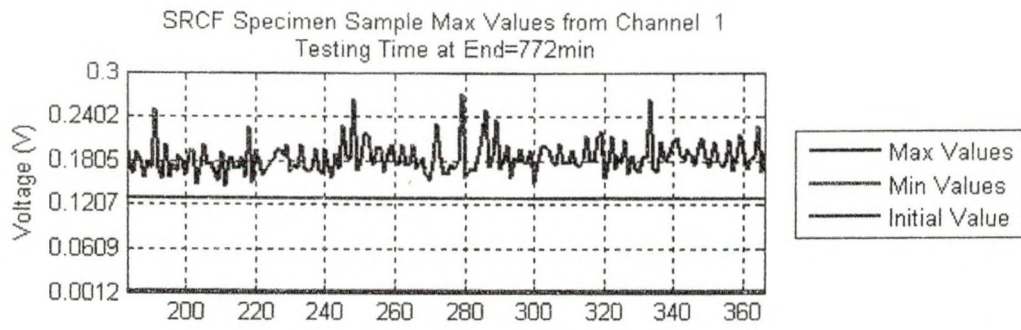


Testing Time: 16.35hr to 18.67hr

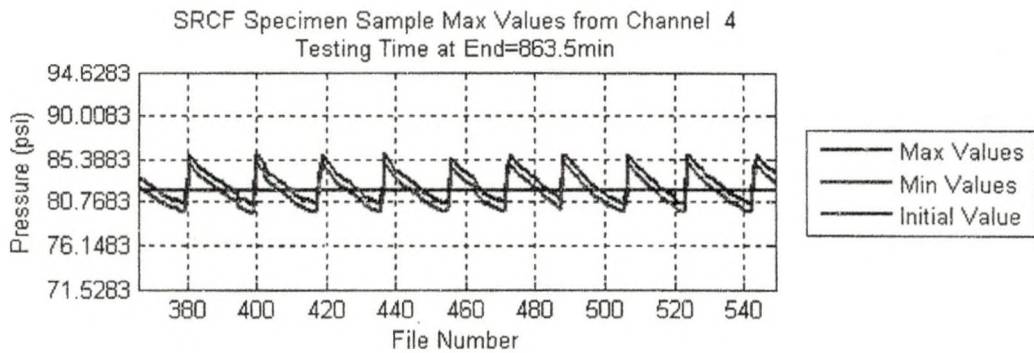
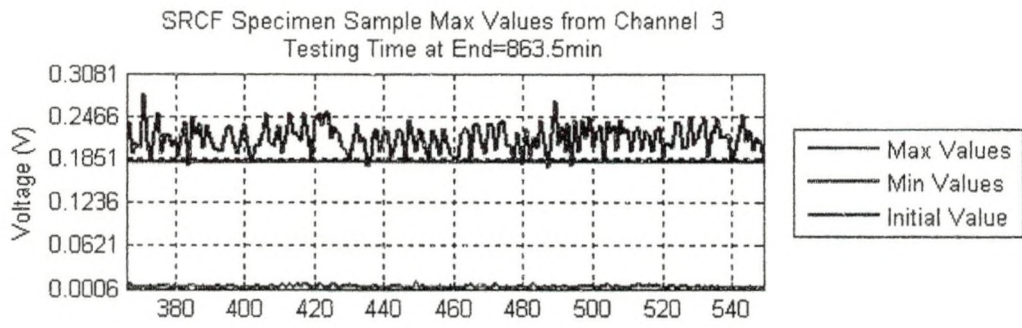
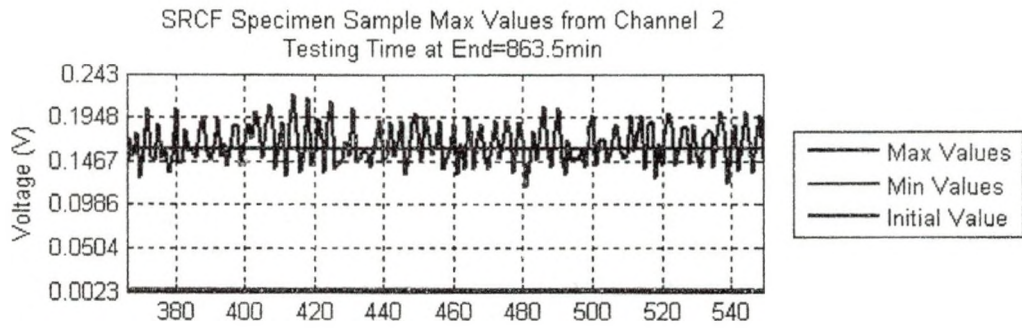
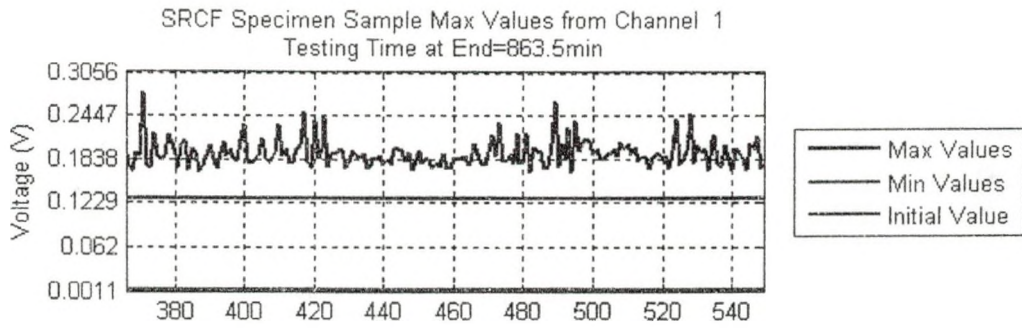
The drop off in channels 1, 2 and 3 are because the eddy current device was accidentally shut off.



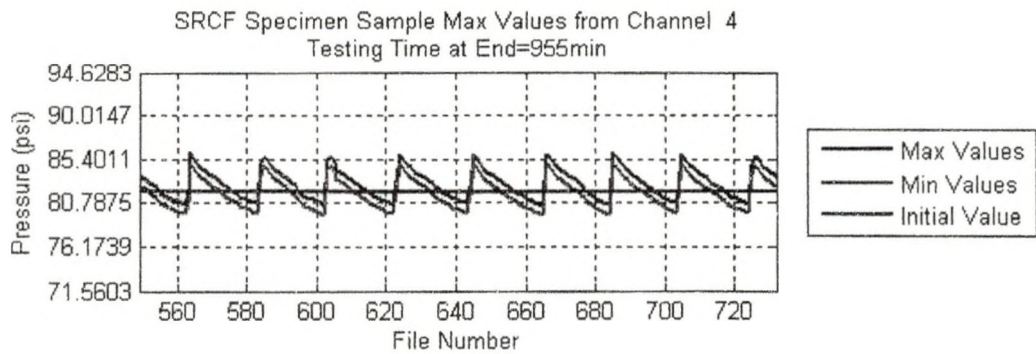
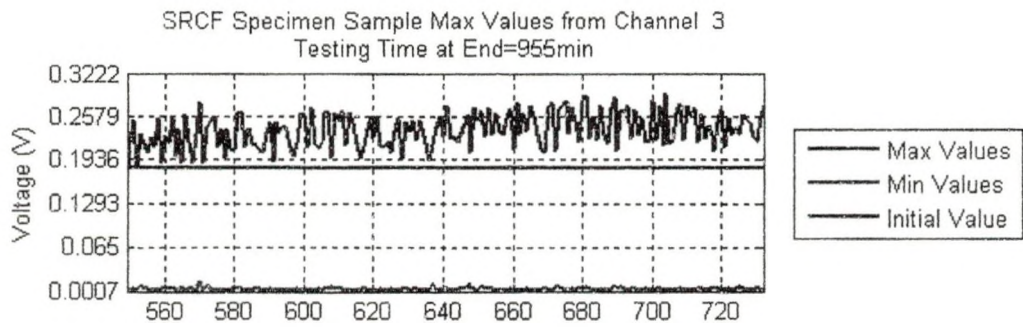
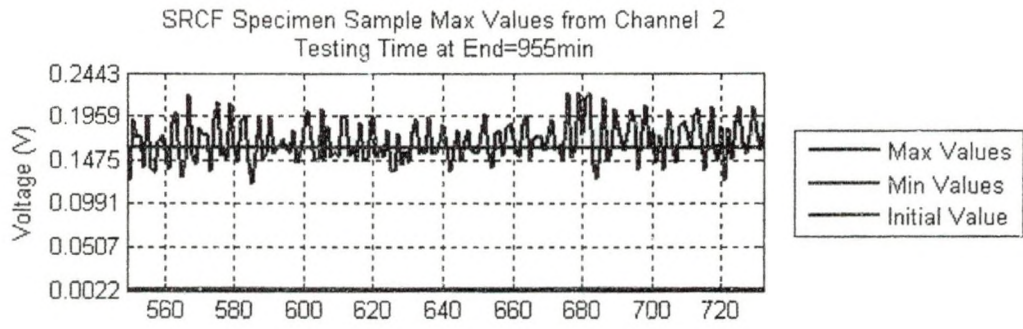
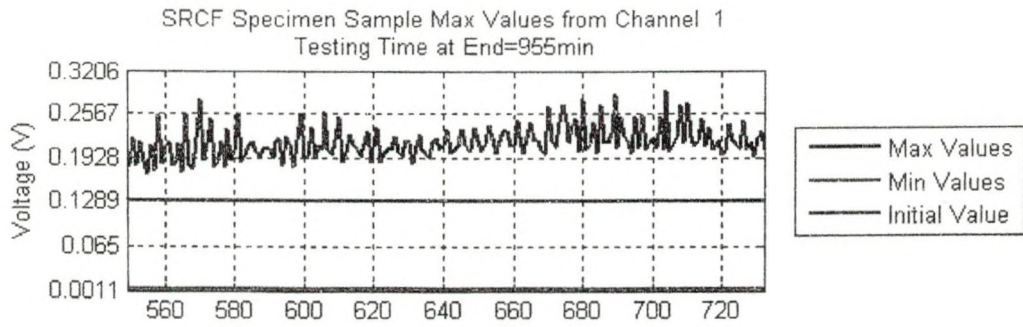
Testing Time: 18.67hr to 20.2hr



Testing Time: 20.2hr to 21.73hr

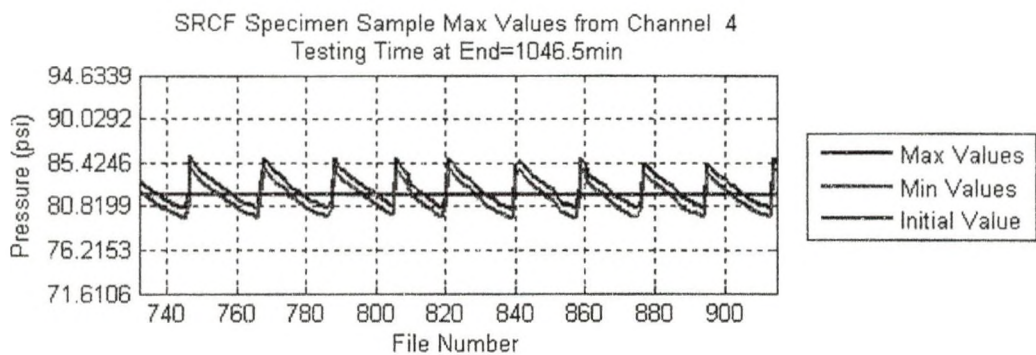
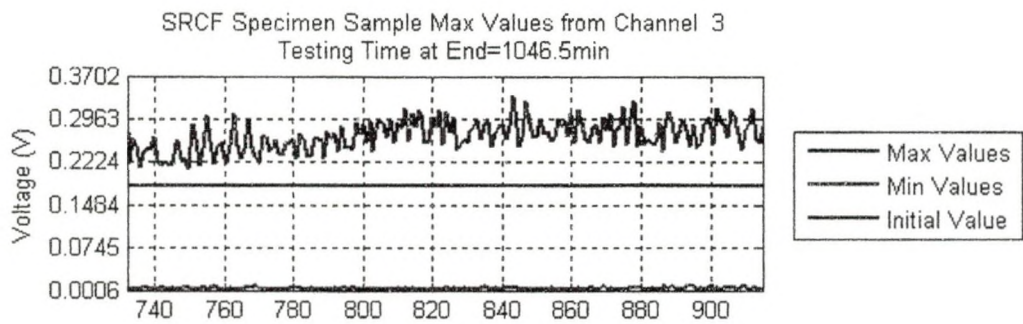
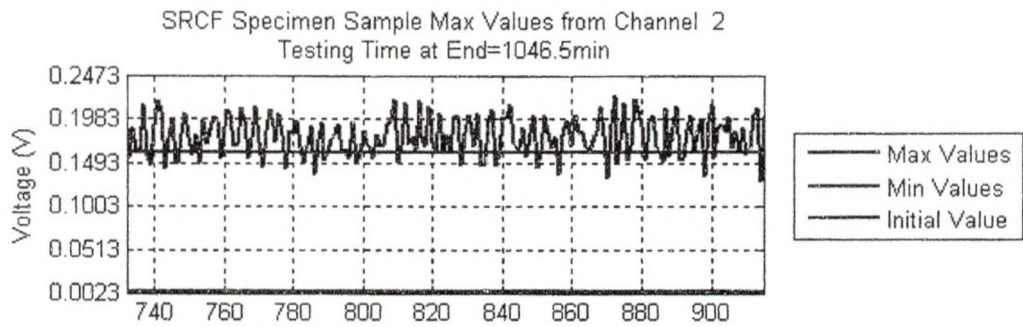
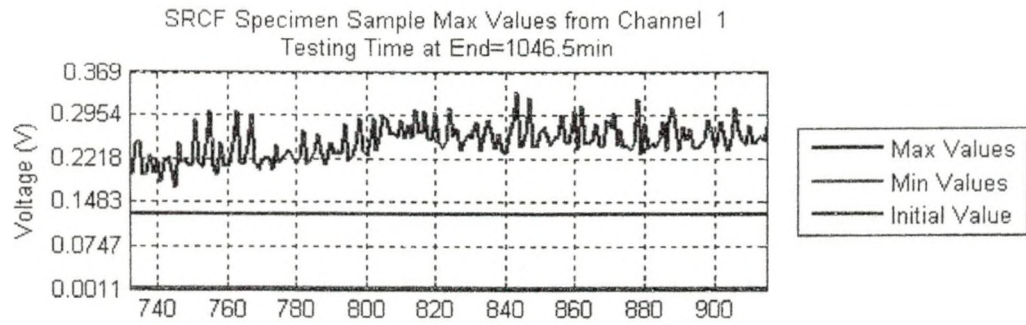


Testing Time: 21.73hr to 23.25



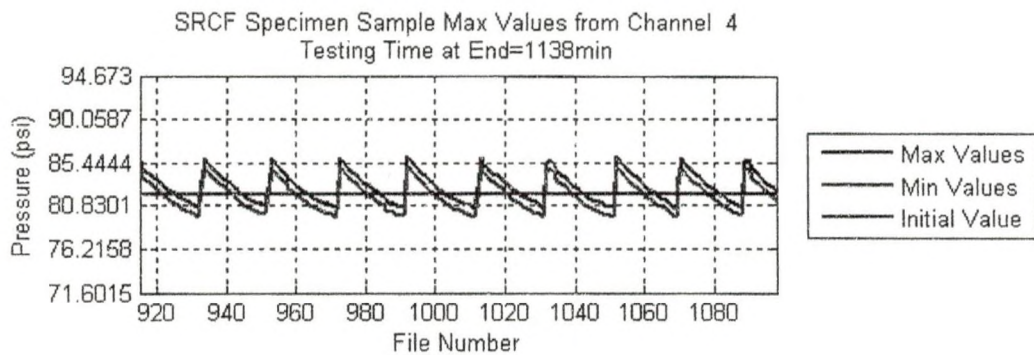
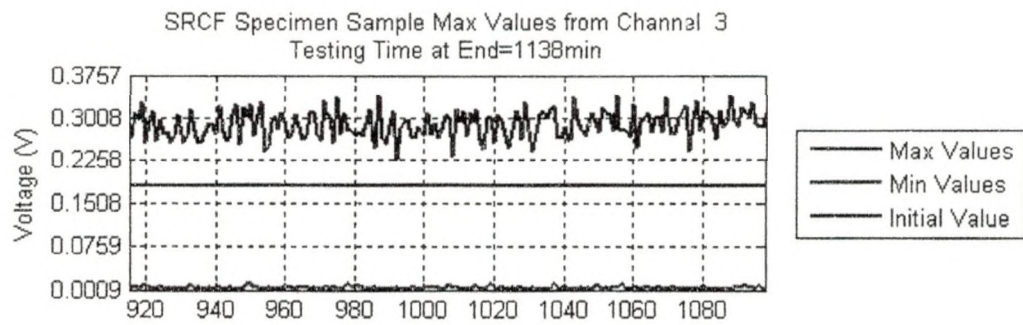
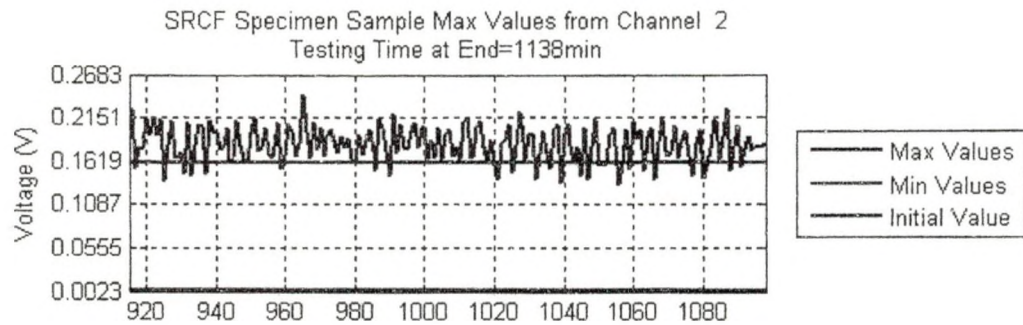
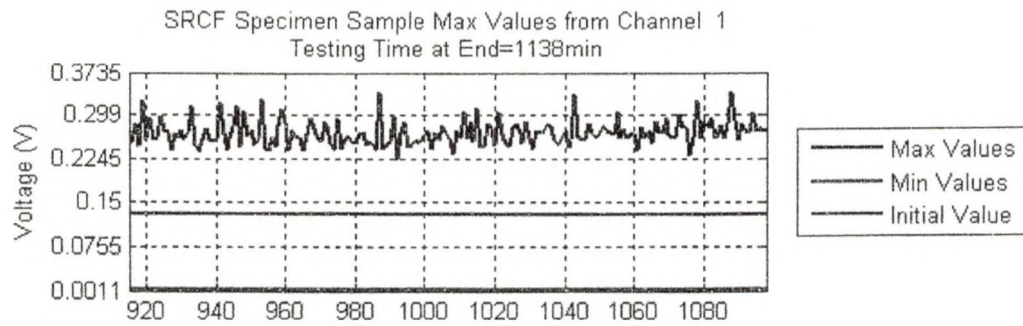
Testing Time: 23.25hr to 24.76hr

In channel 1, the signal has started to increase significantly from the initial value.

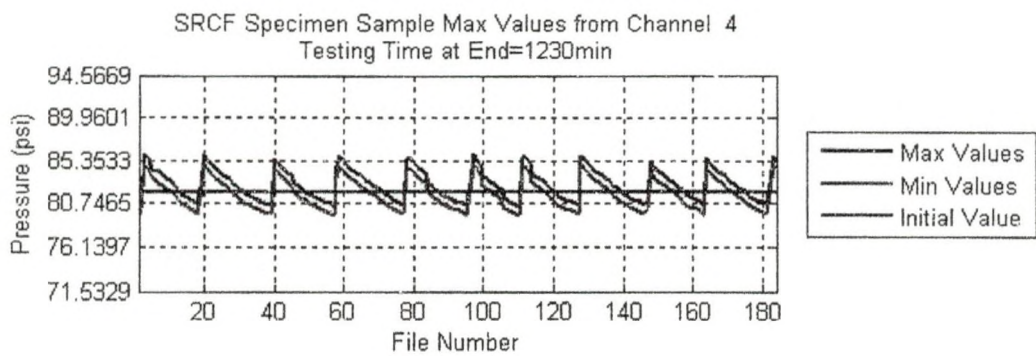
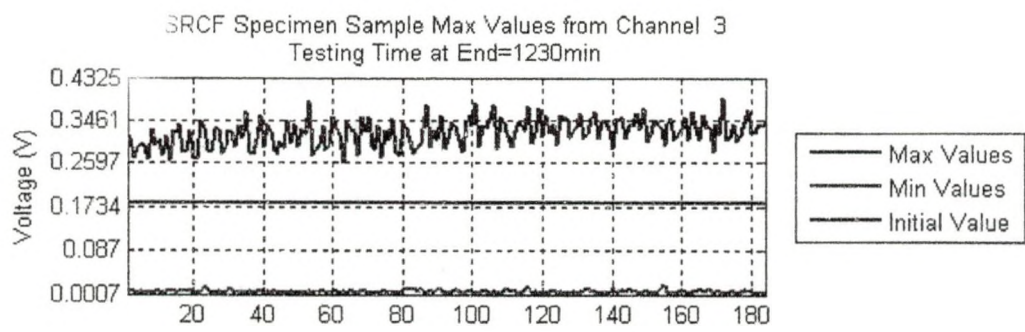
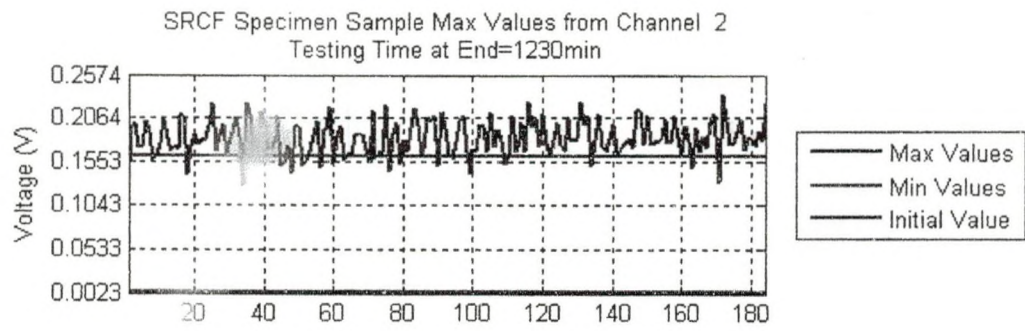
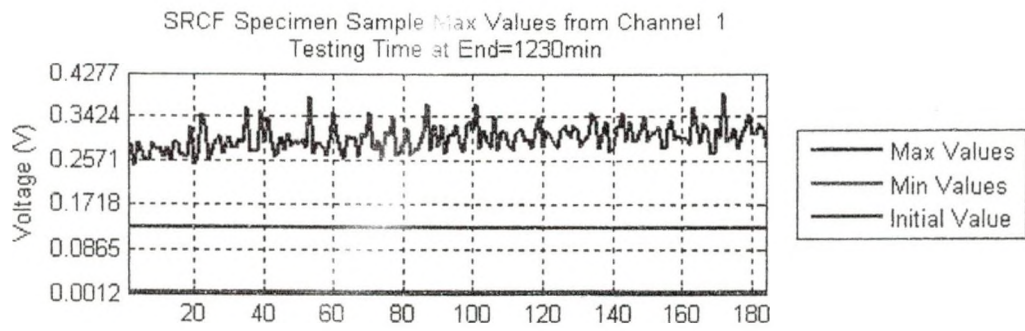


Testing Time: 24.76hr to 26.3hr

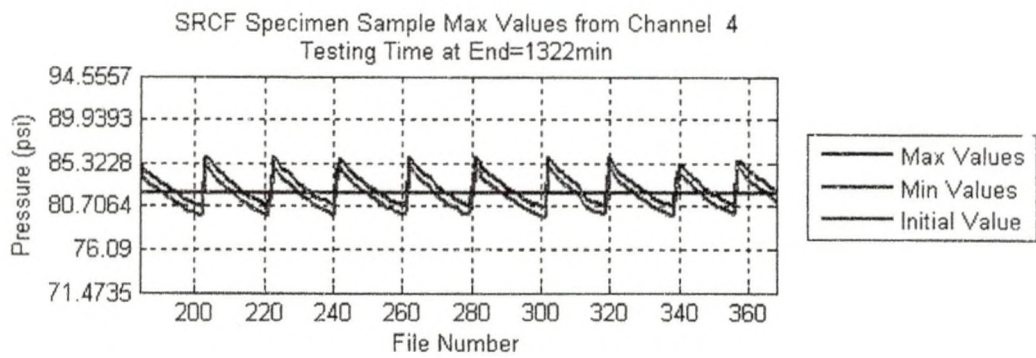
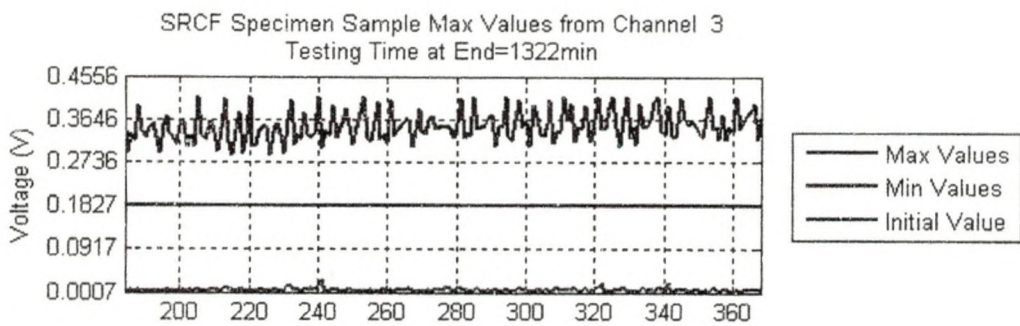
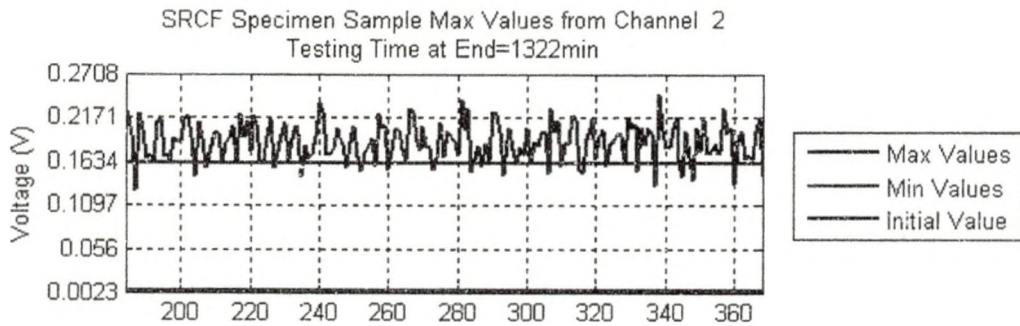
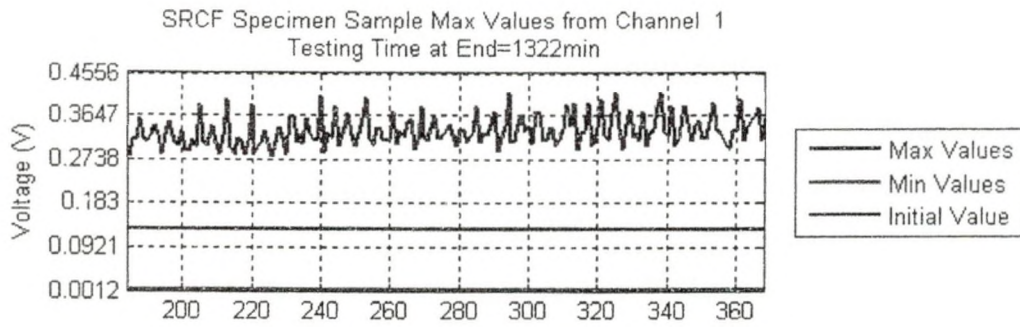
In channel 1, the jump in the voltage at file 815 signals that an irregularity in the surface has formed. This can also be seen in the graph of channel 3.



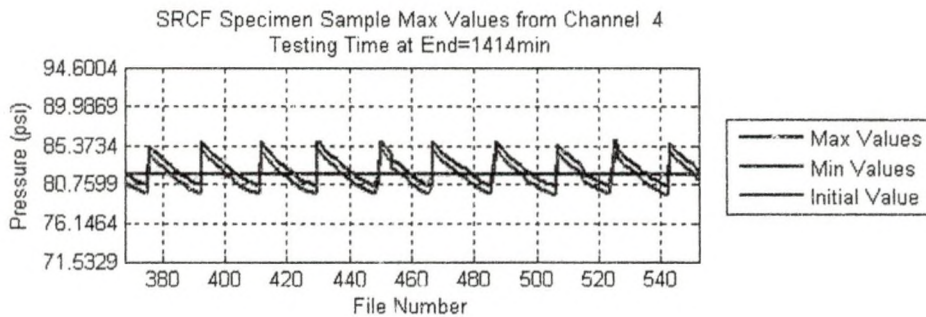
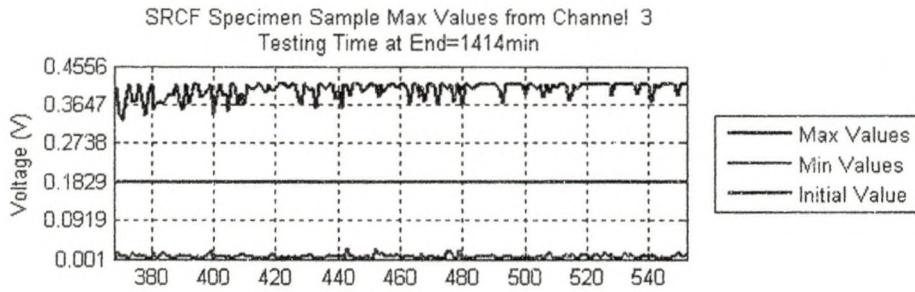
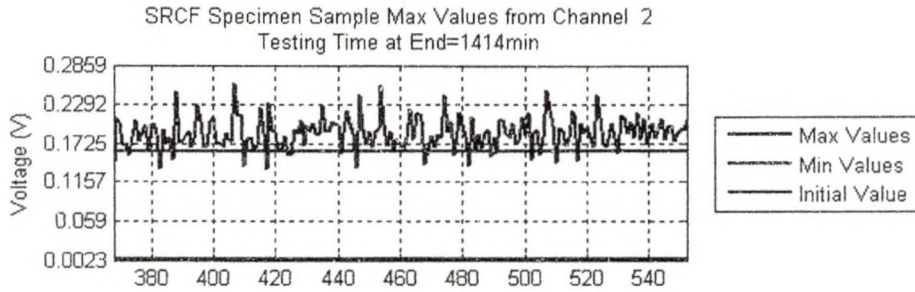
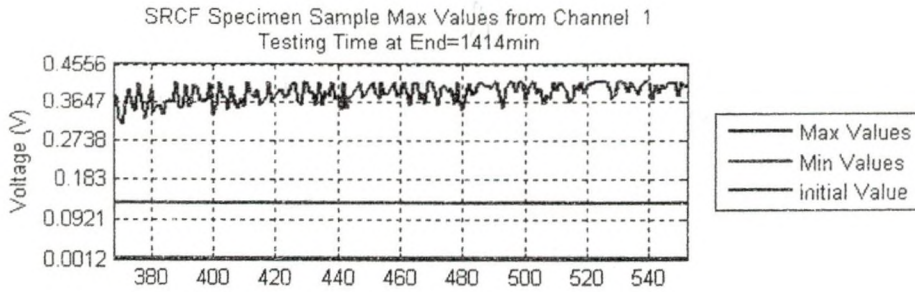
Testing Time: 26.3hr to 27.825hr



Testing Time: 27.825 hr to 29.35 hr

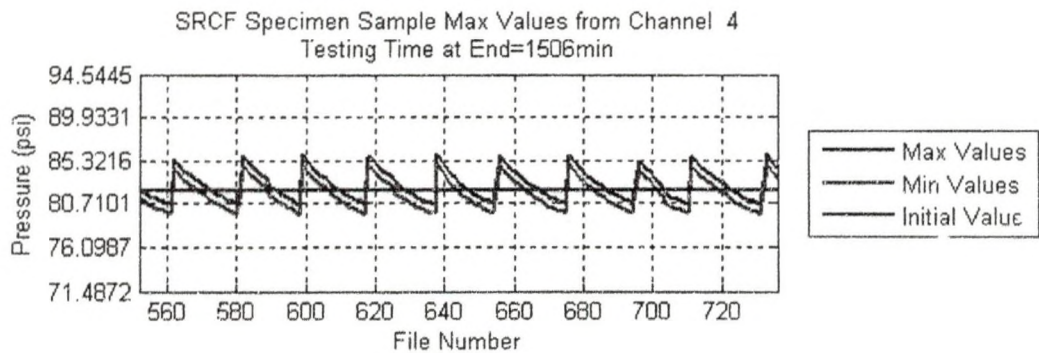
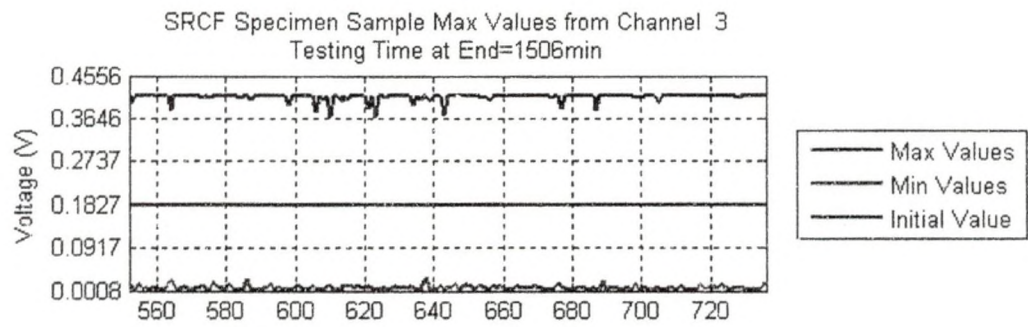
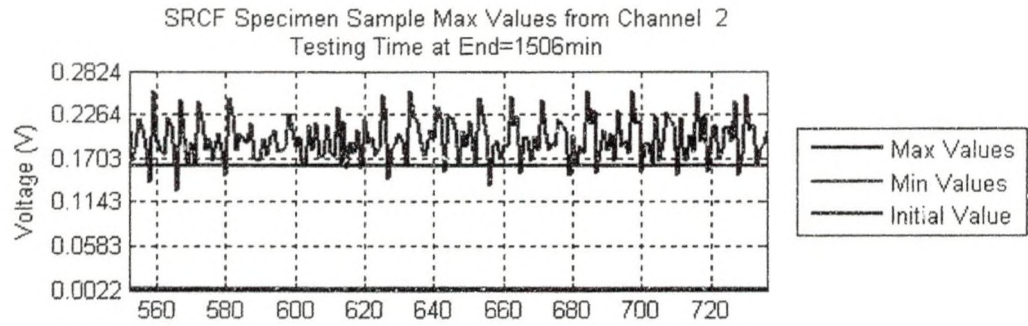
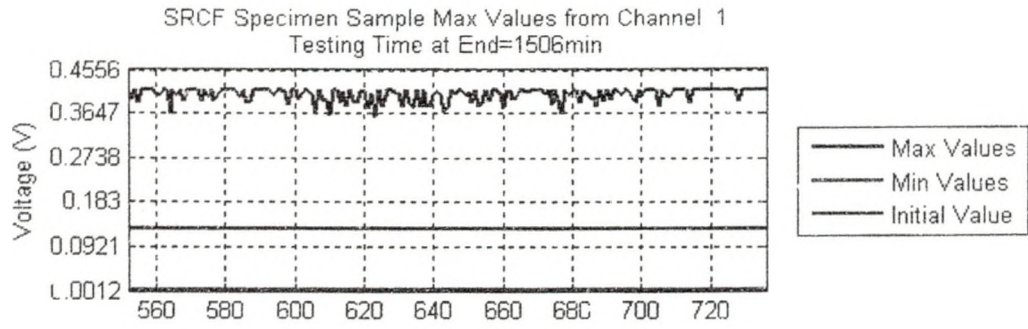


Testing Time: 29.35 hr to 30.875 hr

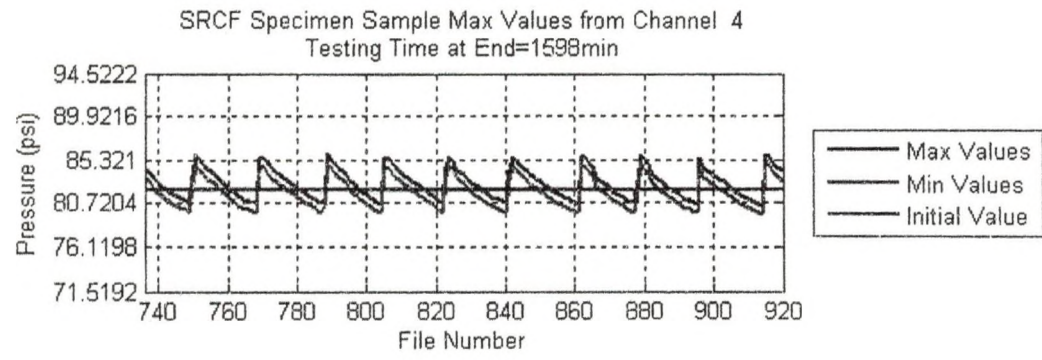
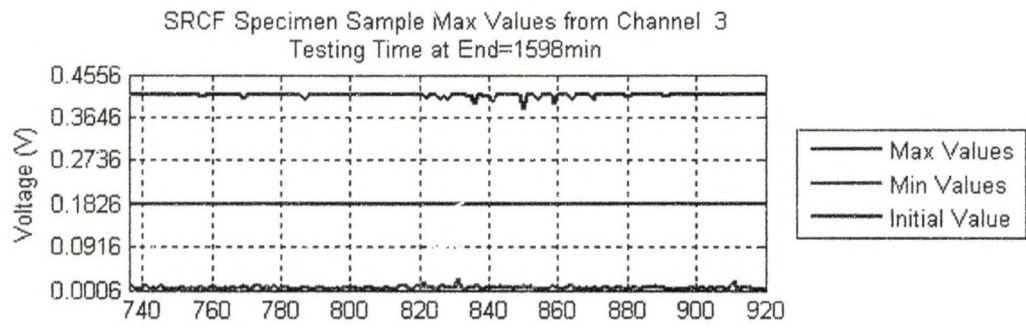
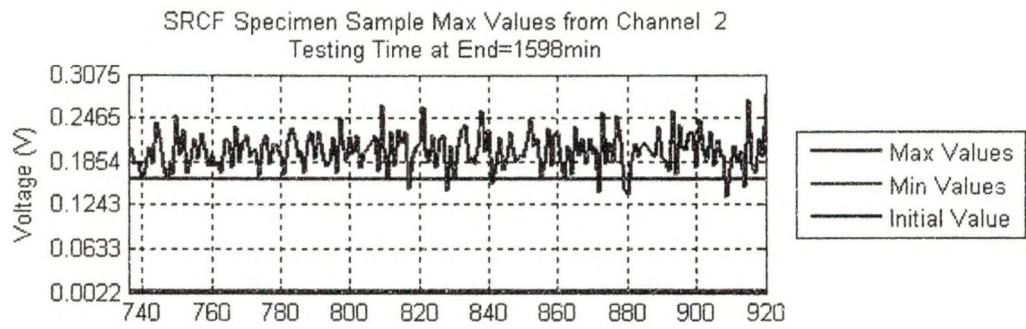
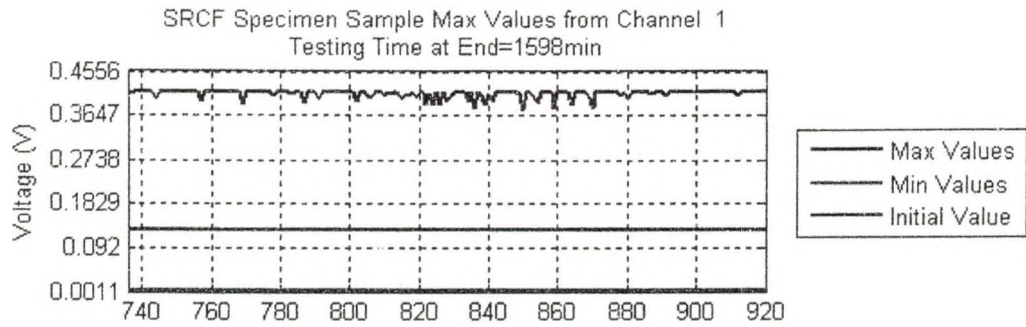


Testing Time: 30.875 hr to 32.4 hr

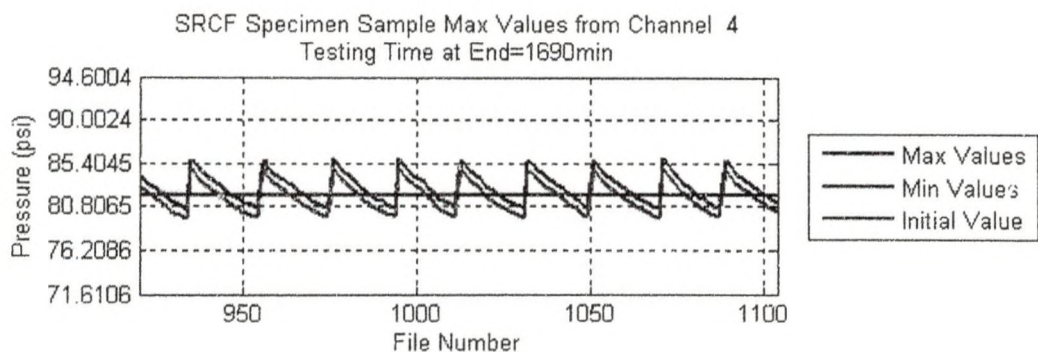
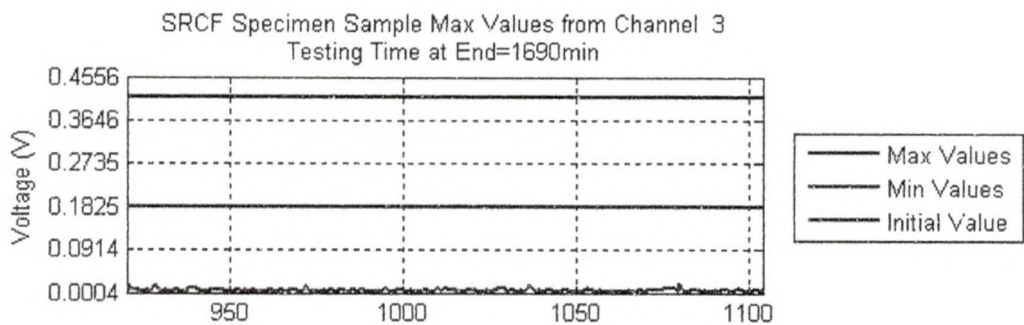
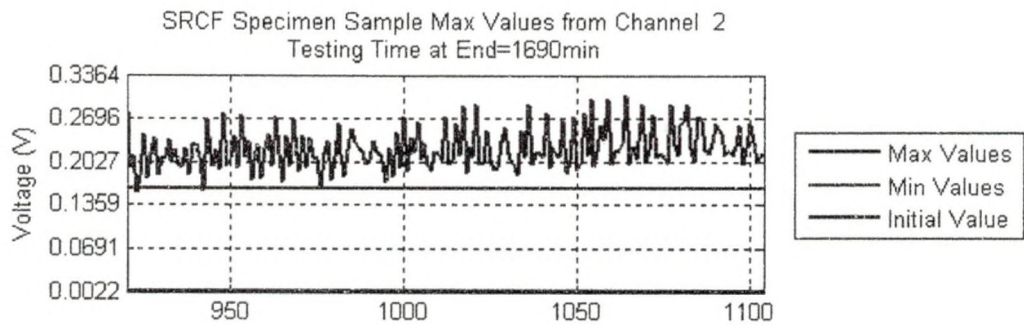
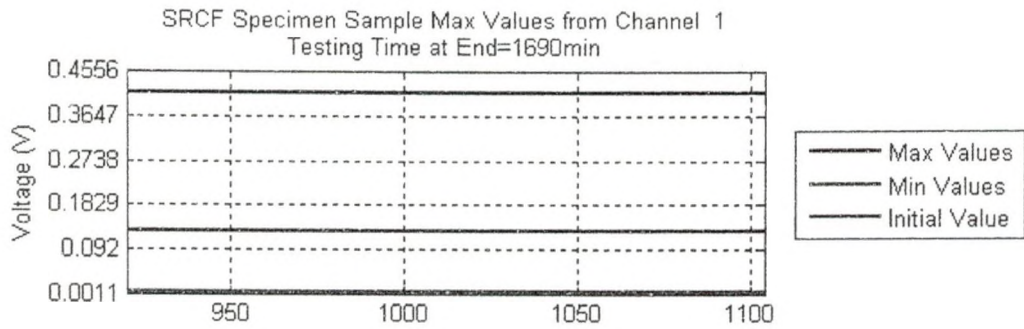
The values for channel 1 and channel 3 peak and flatten out because the LX-10 was auto-calibrated instead of manually. Therefore, it was calibrated for the initial values and not what the potential future values could be.



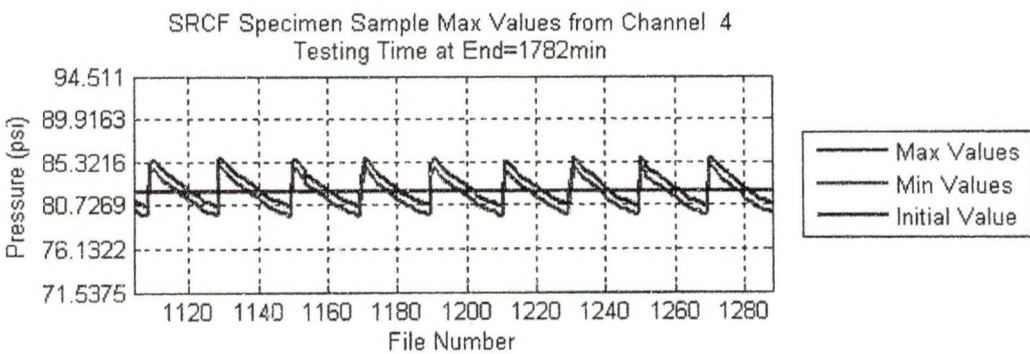
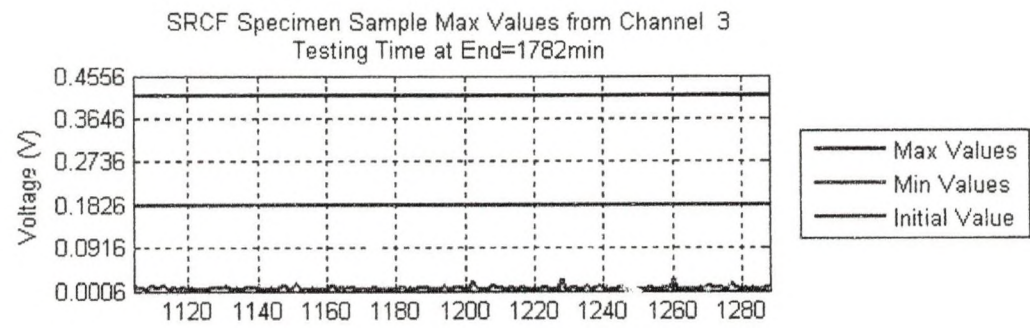
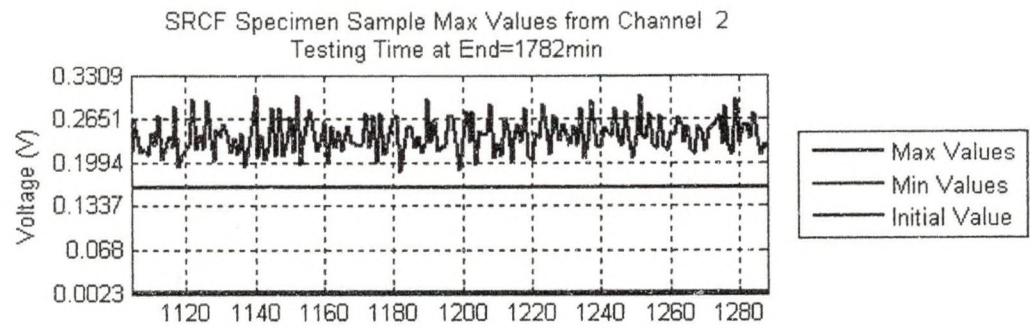
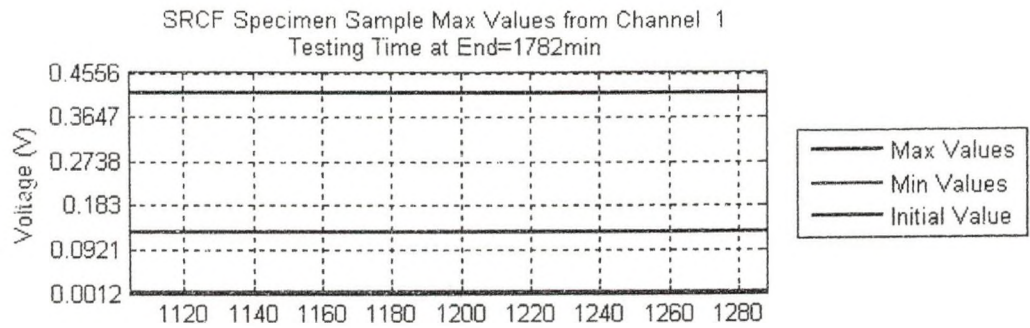
Testing Time: 32.4 hr to 33.9 hr



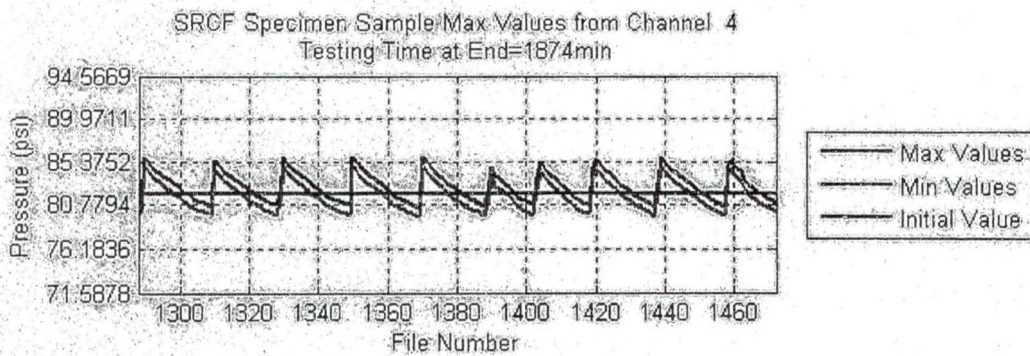
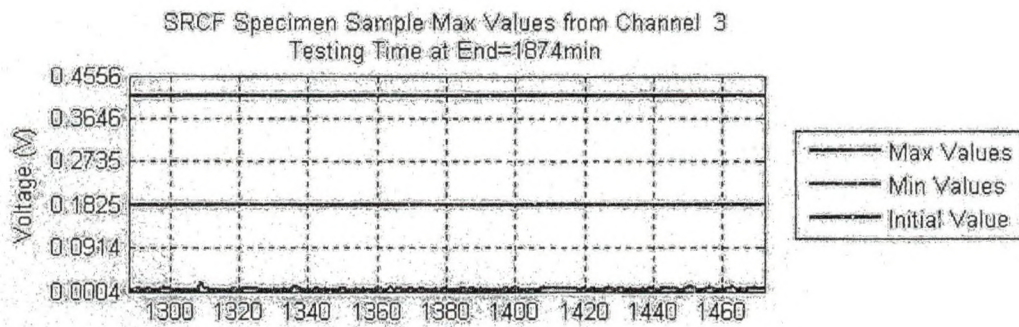
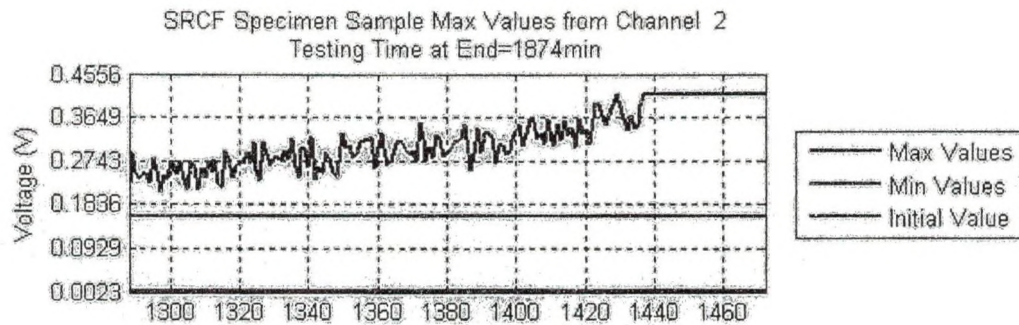
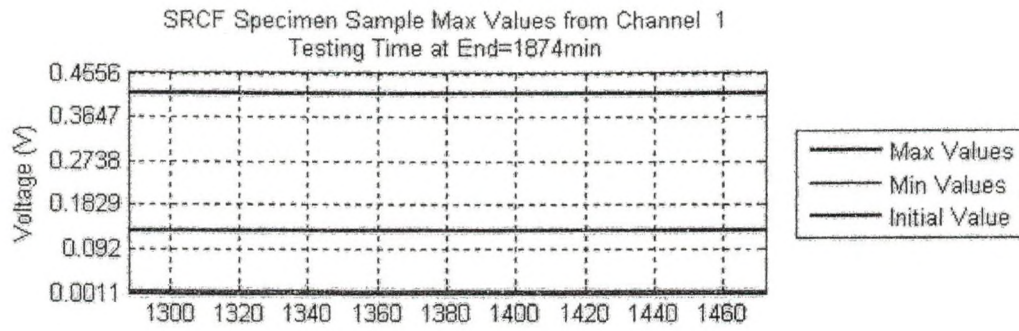
Testing Time: 33.9 hr to 35.45 hr



Testing Time: 35.45 hr to 37 hr



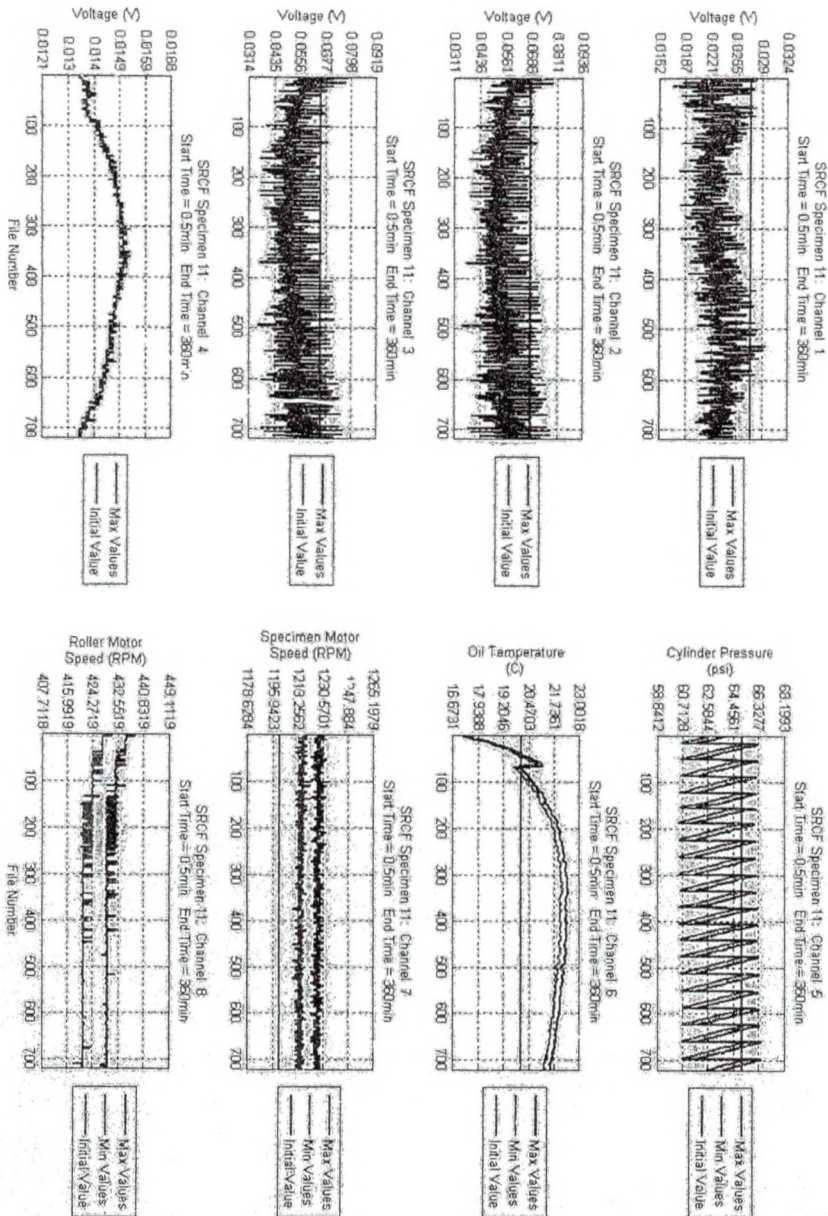
Testing Time: 37 hr to 38.5 hr



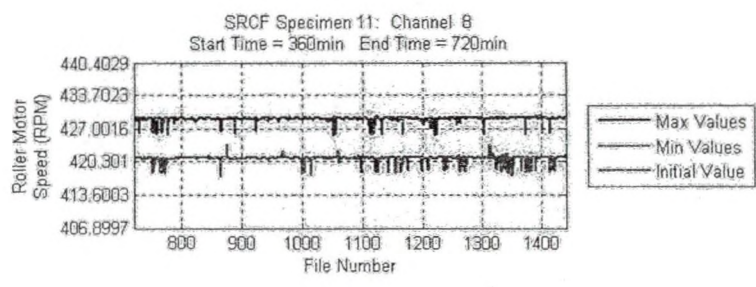
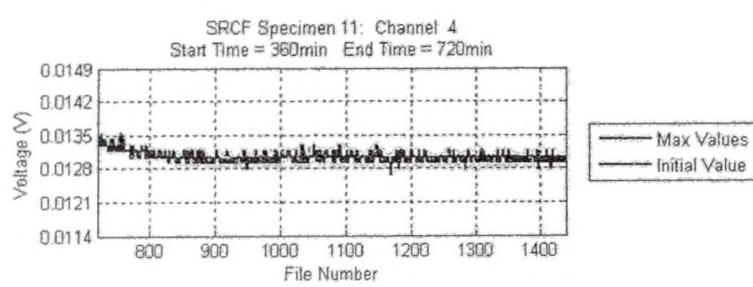
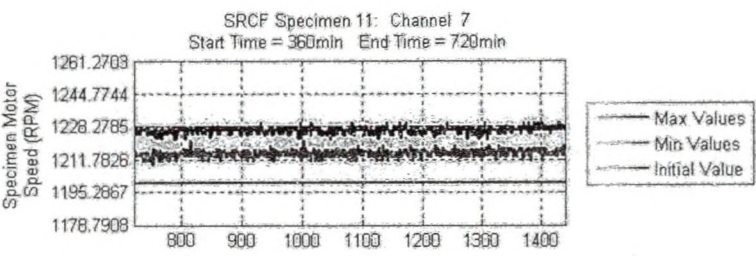
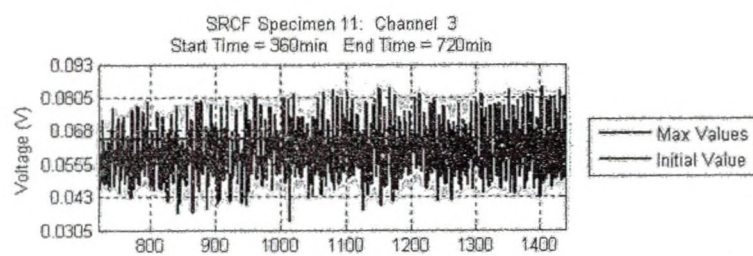
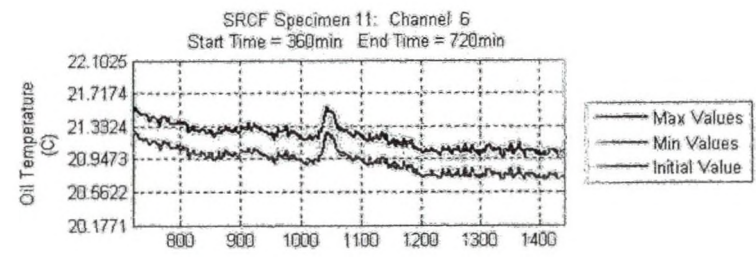
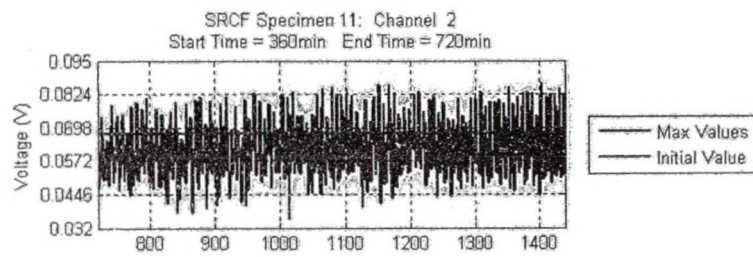
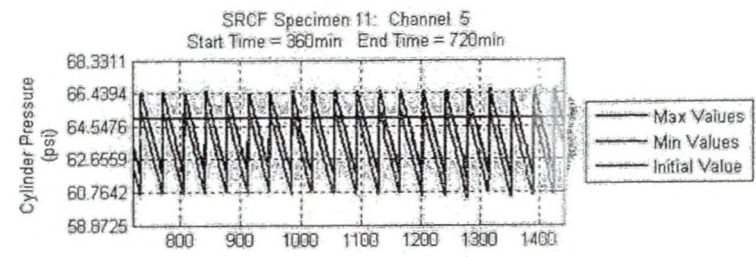
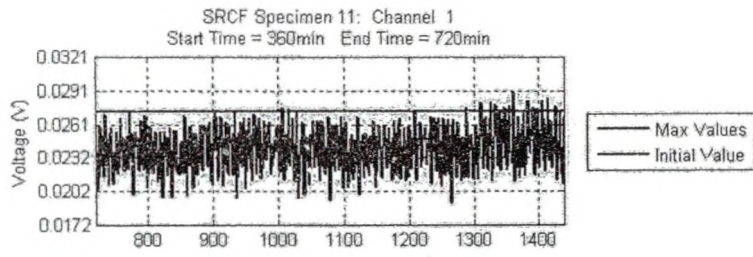
Testing Time: 38.5 hr to 40 hr

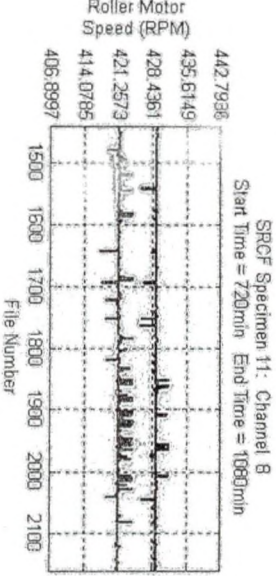
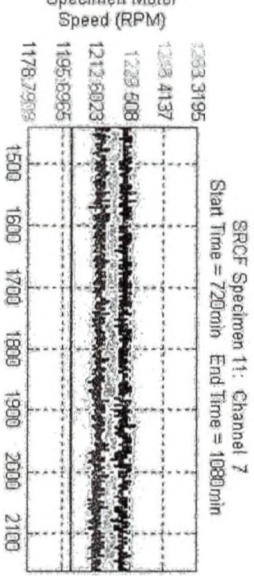
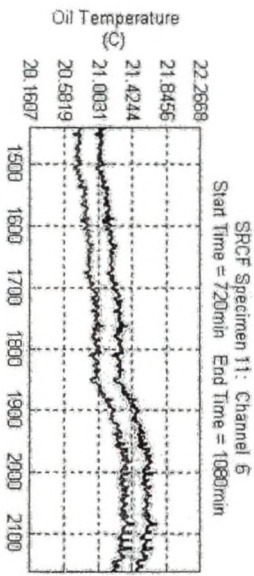
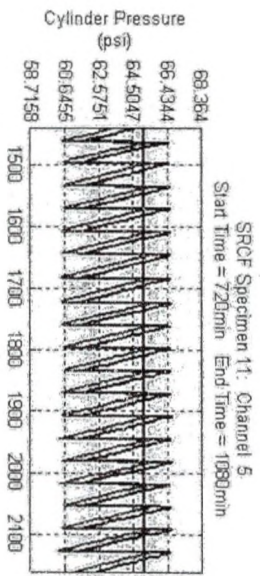
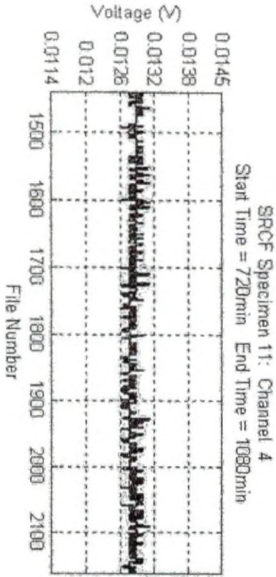
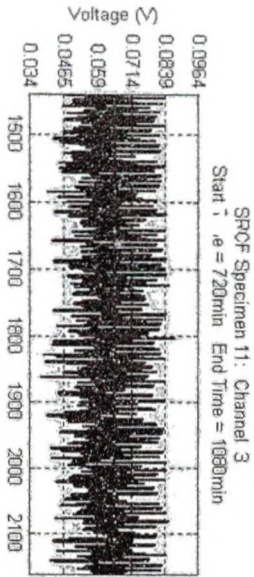
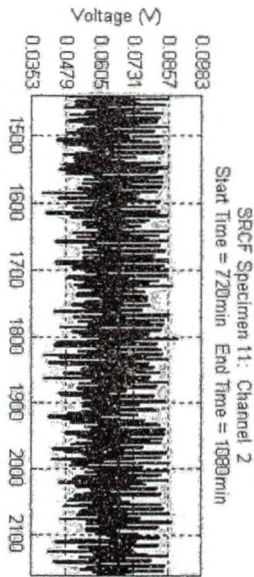
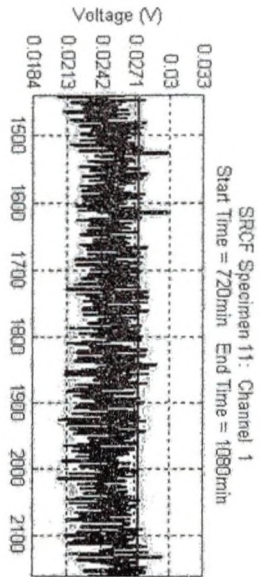
Channel 2 begins to increase significantly and eventually peaks and flattens like channels 1 and 3 due to the calibration error.

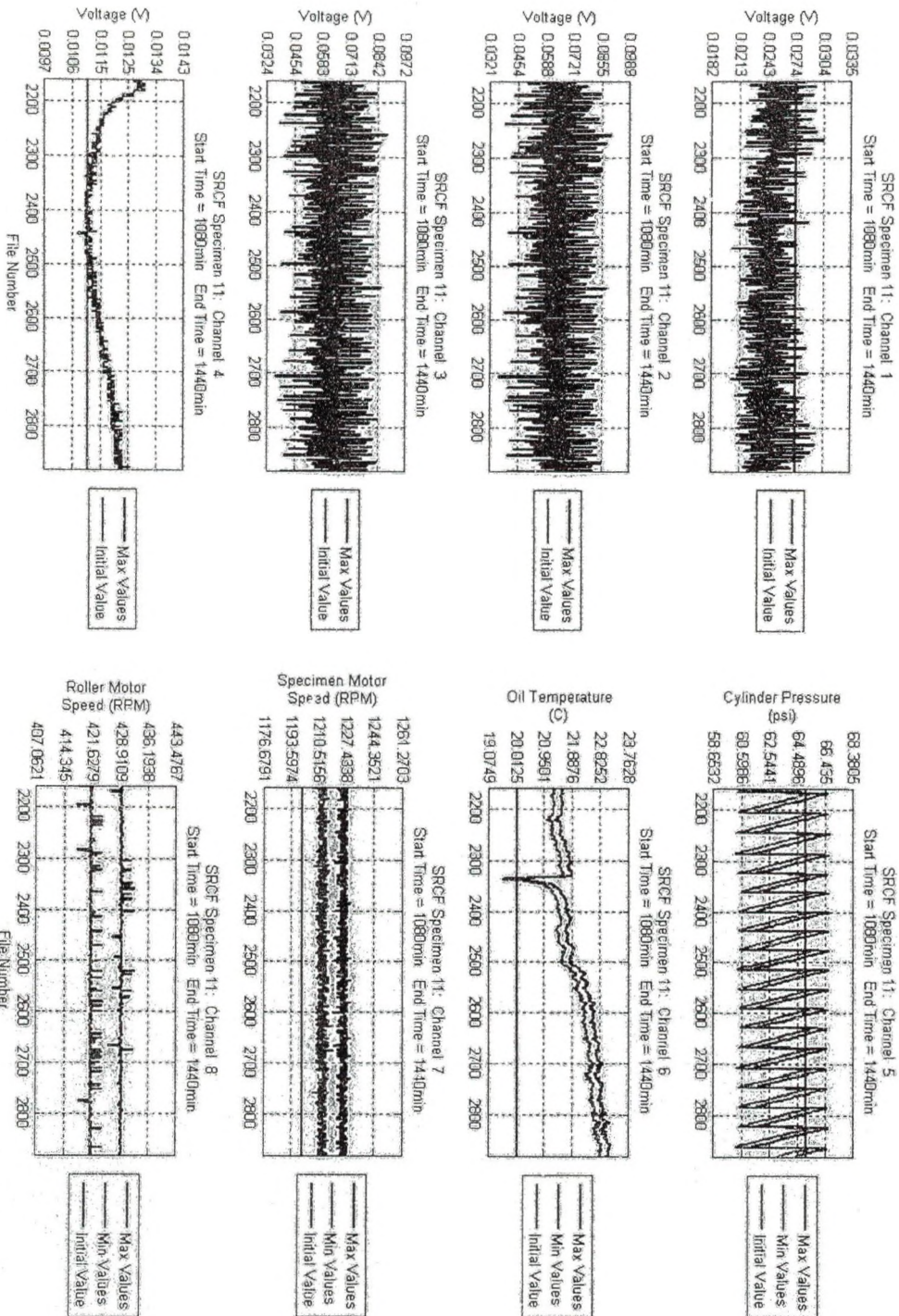
Specimen 11



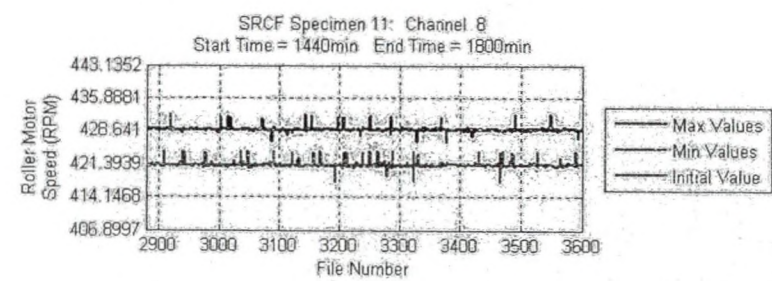
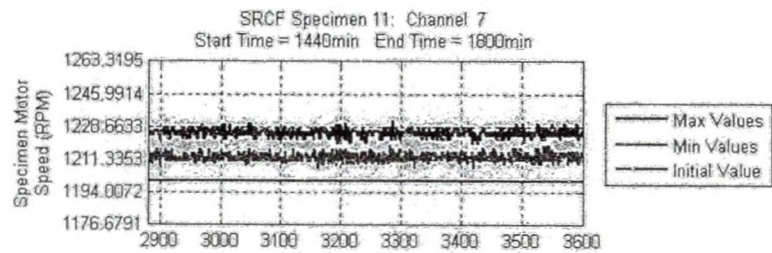
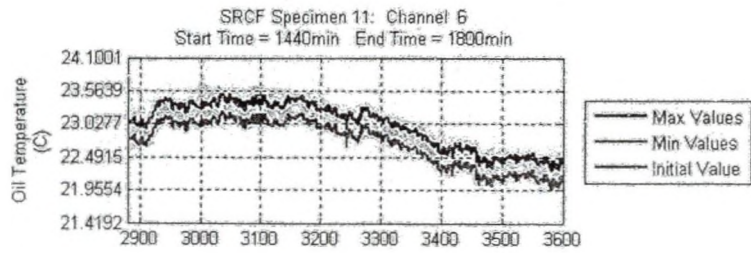
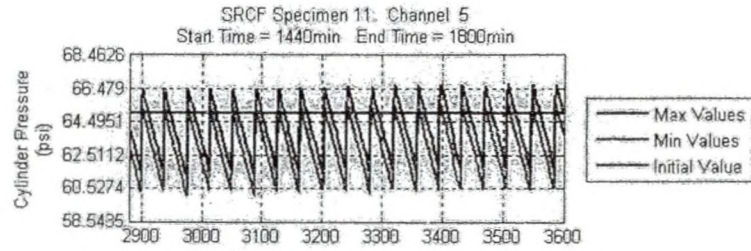
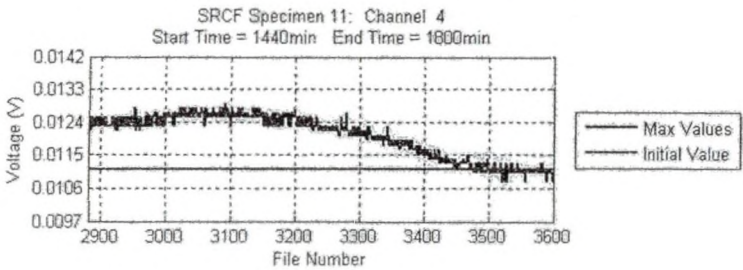
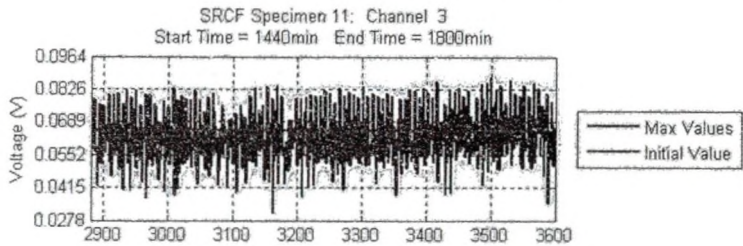
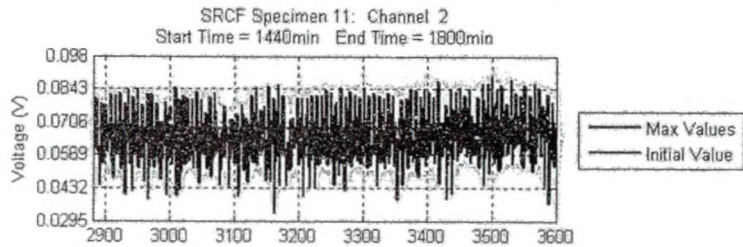
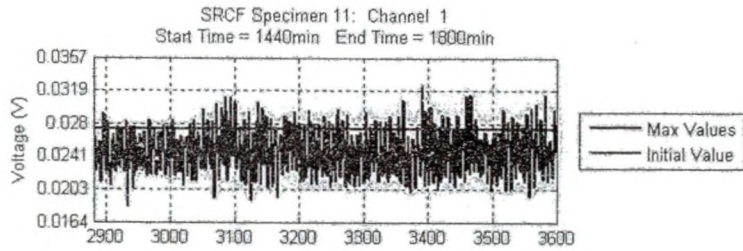
The channel 6 rises significantly since the temperature of the lubricant has not reached equilibrium yet. It is unclear why channel 4 is curving at the beginning of the test. It also appears that both motors are running slightly faster than expected (Channel 7 should be 1200 RPM and Channel 8 should be 400 RPM). Also, the initial value for the pressure is slightly higher than the average value.



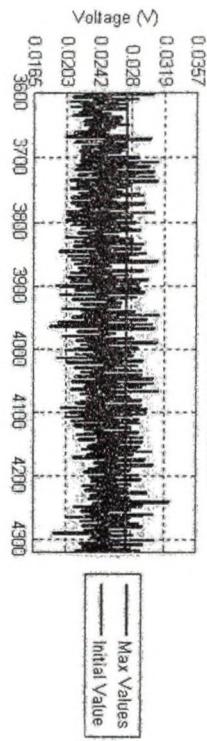




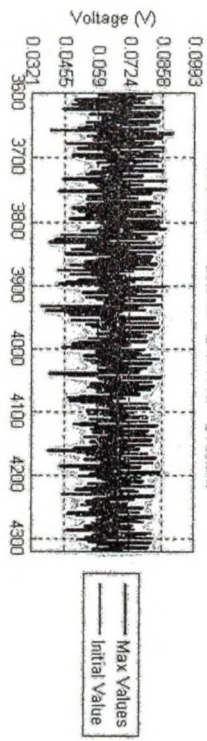
The drop in signal in channel 6 at approximately file 2325 (created April 19th 2008 at 11:07 am) is because oil at room temperature was added to the system to replace lost oil due to minor leaking.



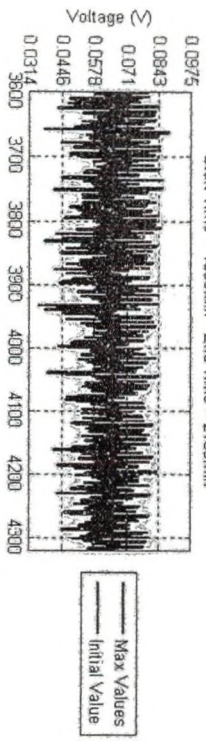
SRCF Specimen 11: Channel 1
Start Time = 1800min End Time = 2180min



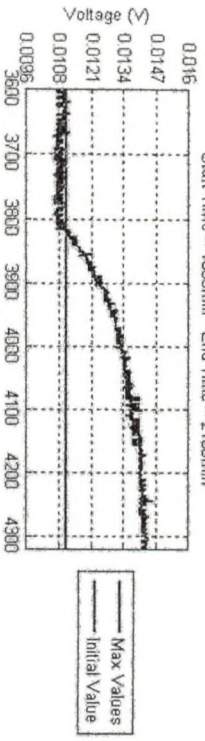
SRCF Specimen 11: Channel 2
Start Time = 1800min End Time = 2180min



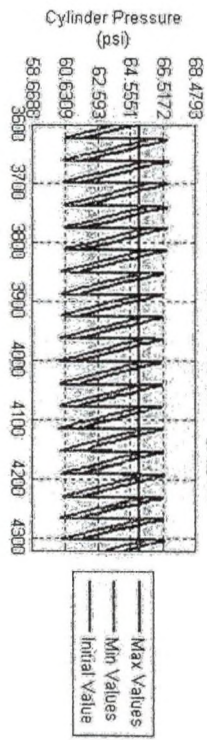
SRCF Specimen 11: Channel 3
Start Time = 1800min End Time = 2180min



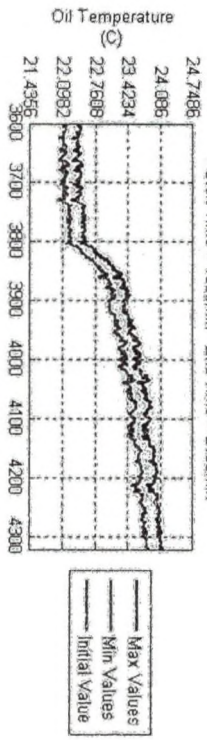
SRCF Specimen 11: Channel 4
Start Time = 1800min End Time = 2180min



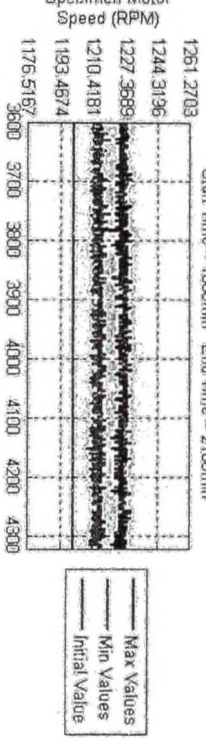
SRCF Specimen 11: Channel 5
Start Time = 1800min End Time = 2180min



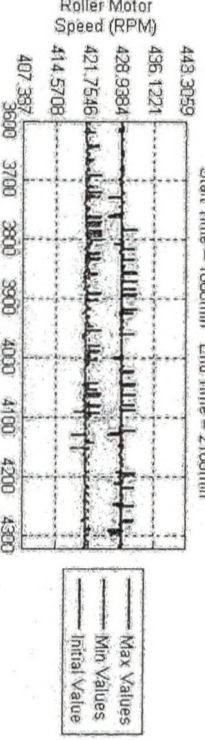
SRCF Specimen 11: Channel 6
Start Time = 1800min End Time = 2180min

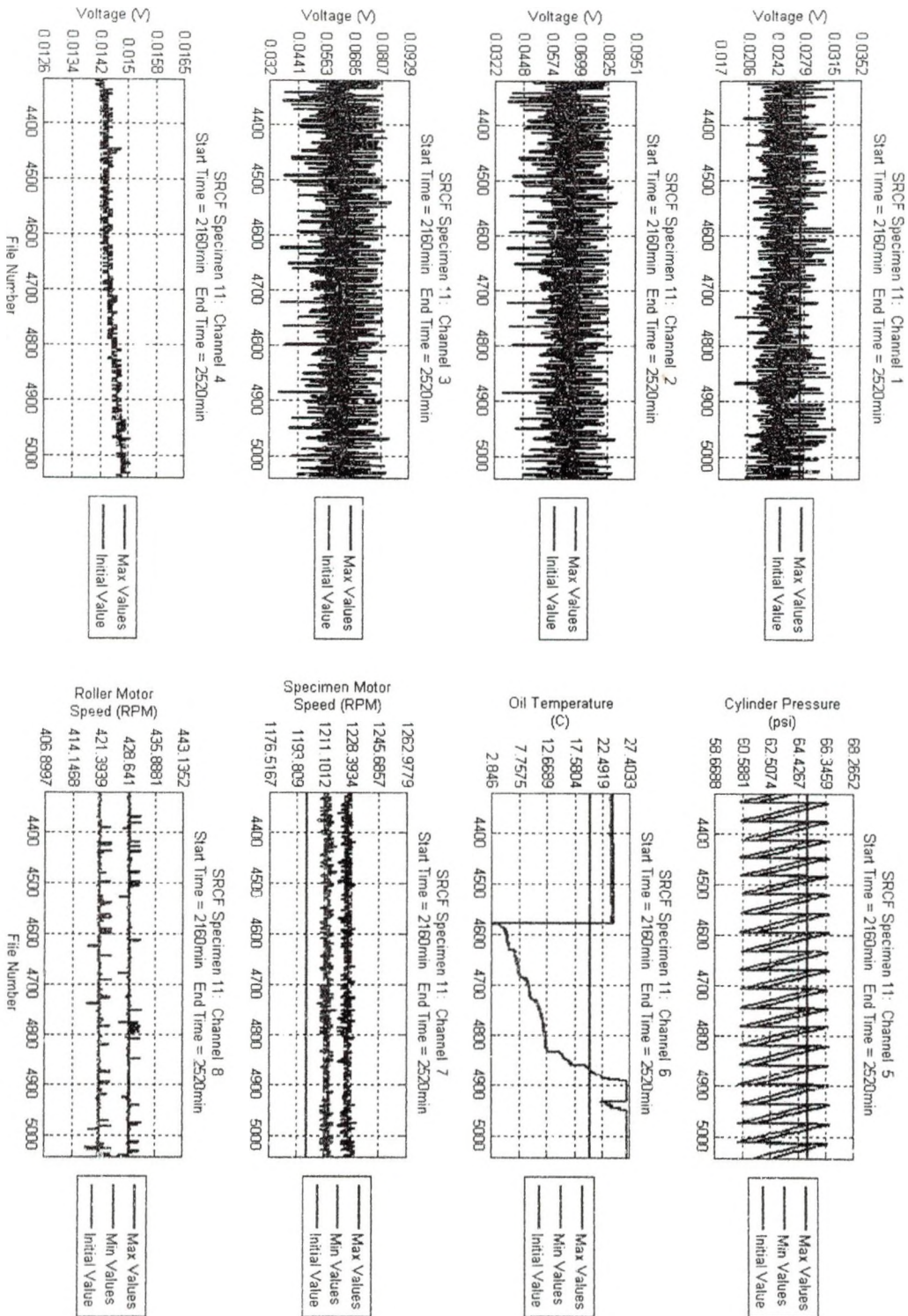


SRCF Specimen 11: Channel 7
Start Time = 1800min End Time = 2180min

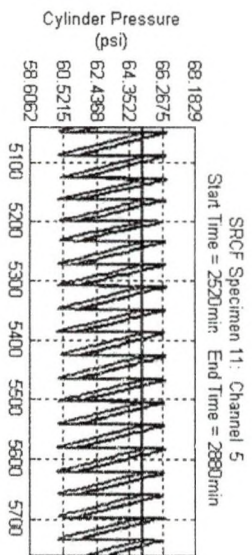
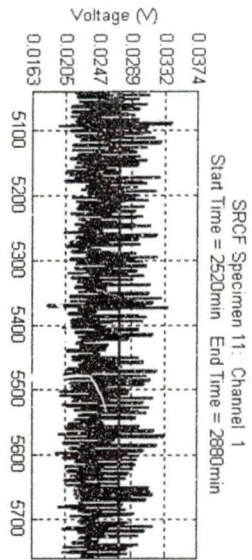


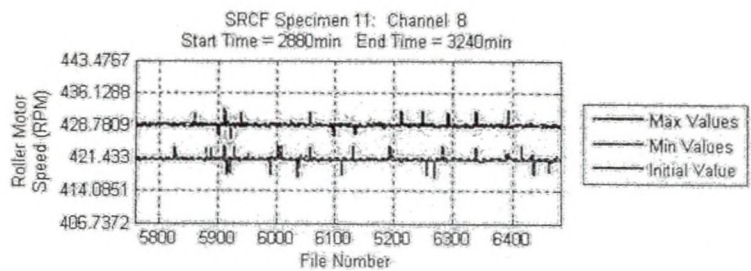
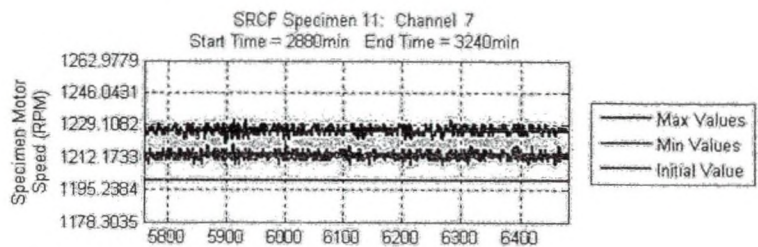
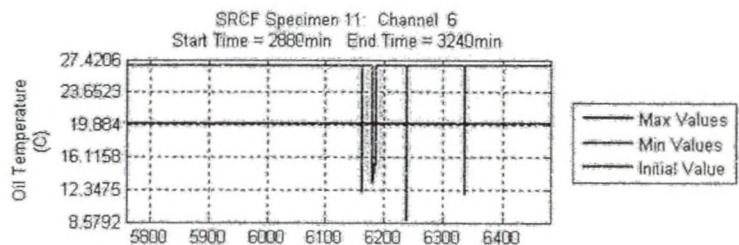
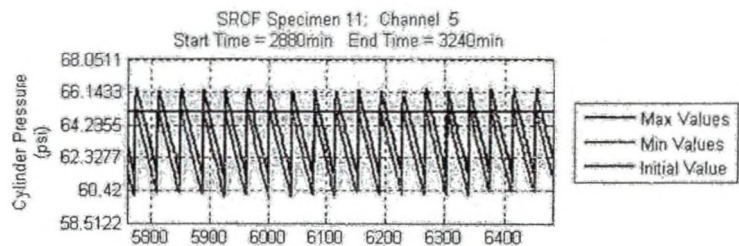
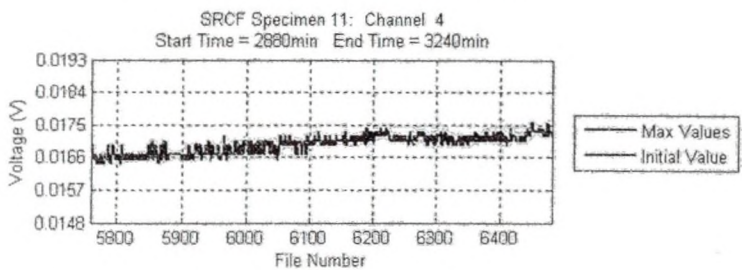
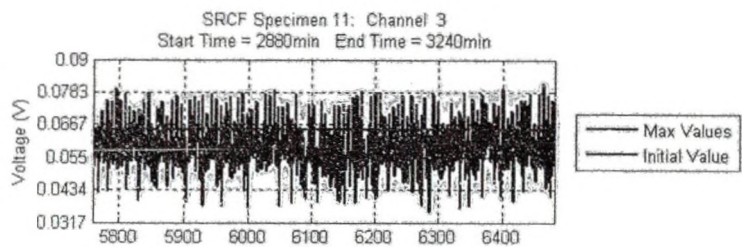
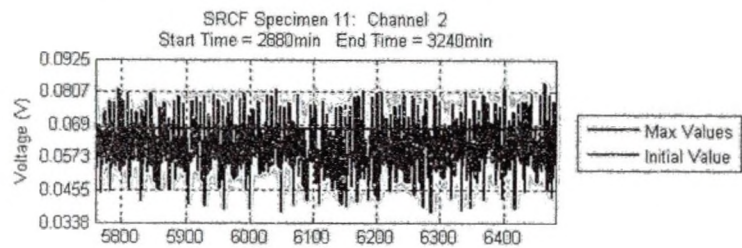
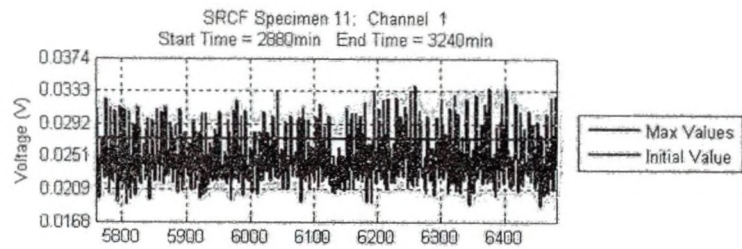
SRCF Specimen 11: Channel 8
Start Time = 1800min End Time = 2180min

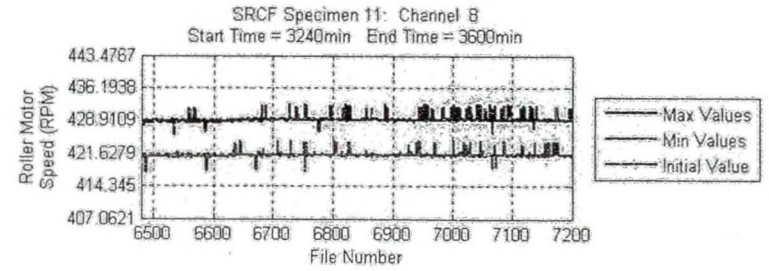
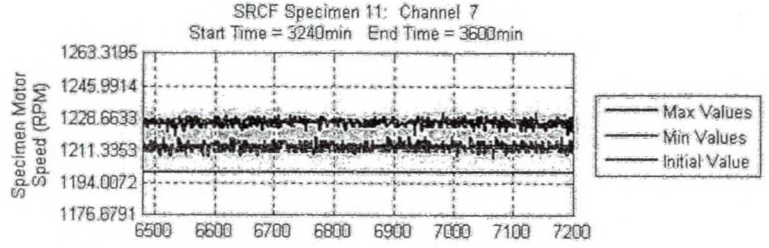
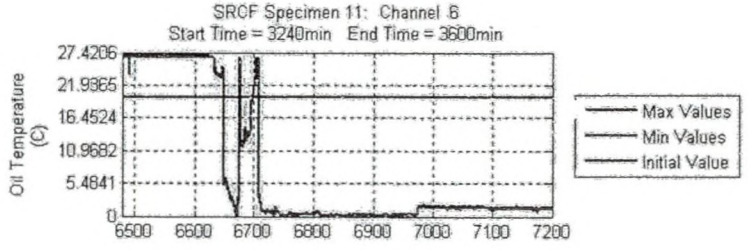
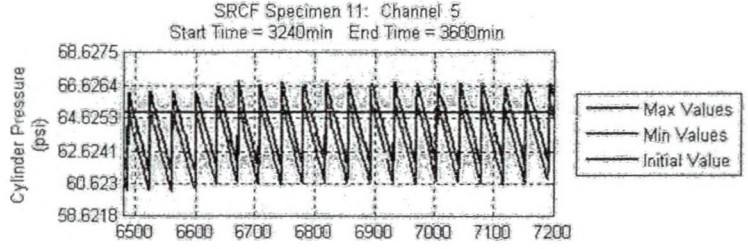
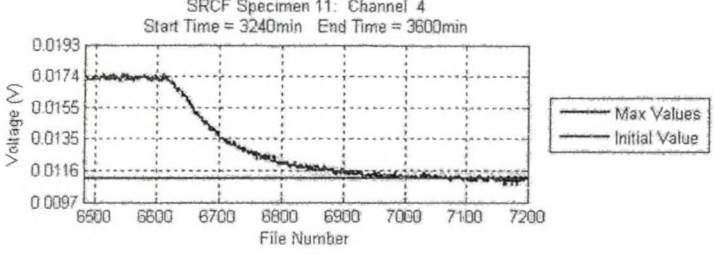
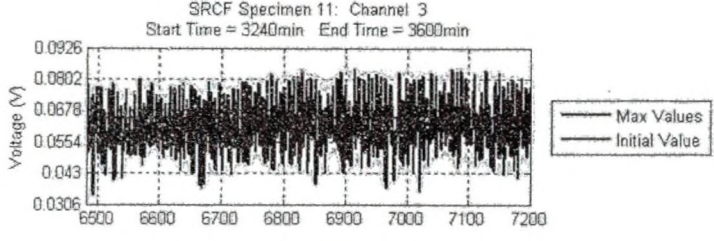
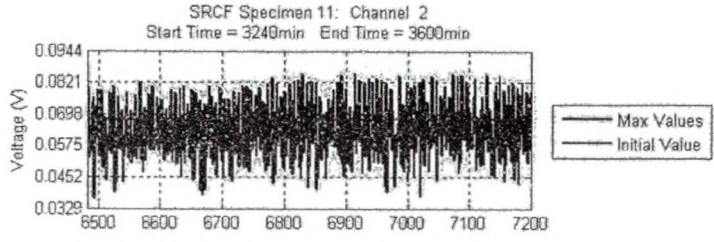
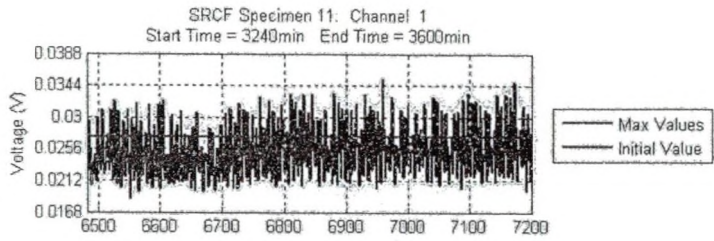


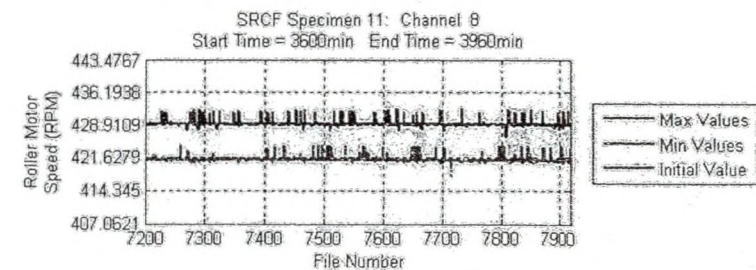
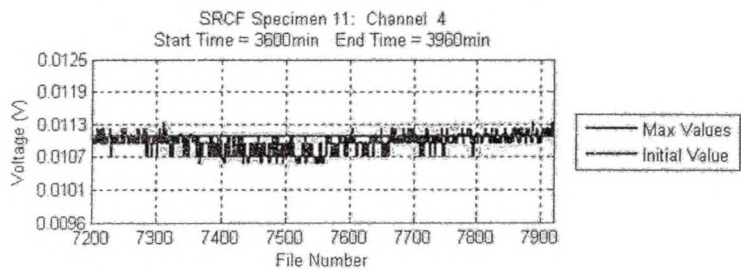
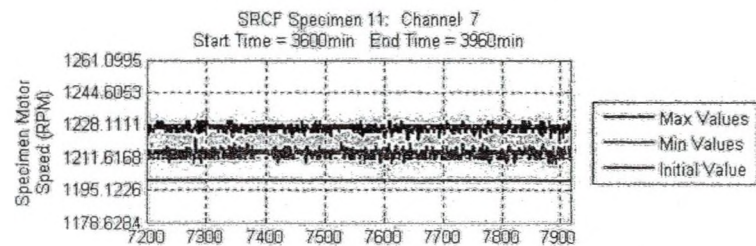
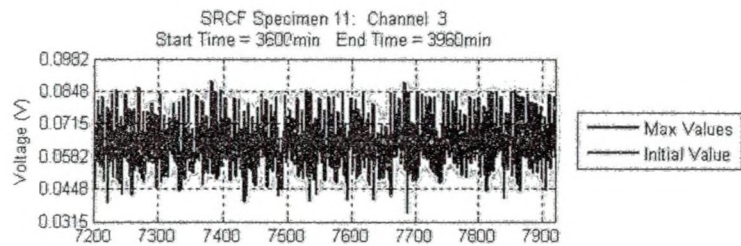
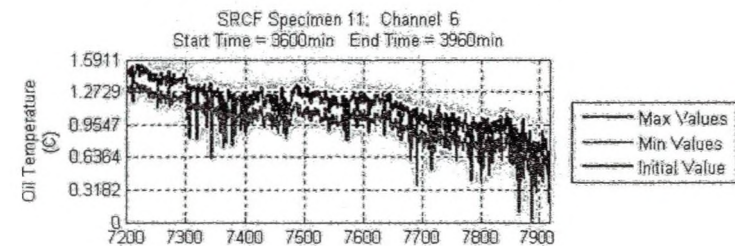
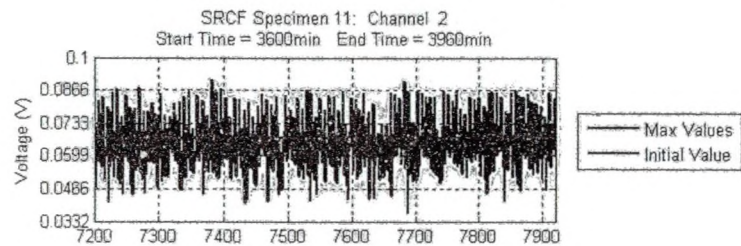
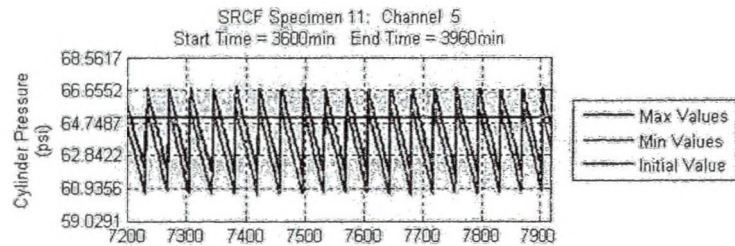
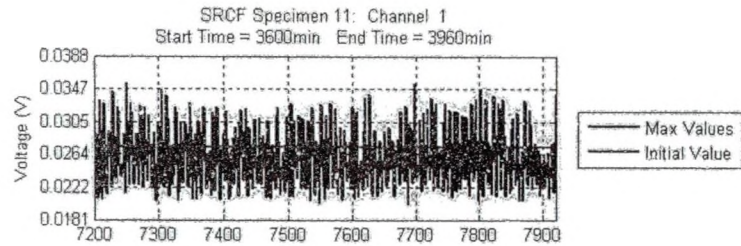


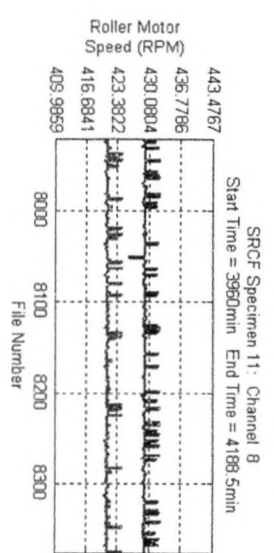
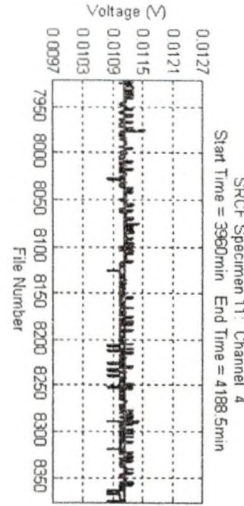
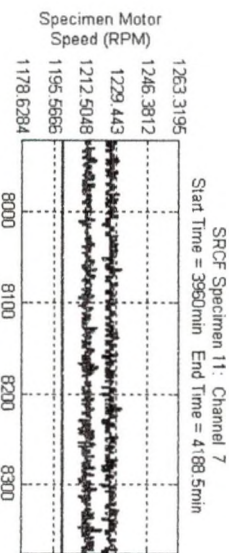
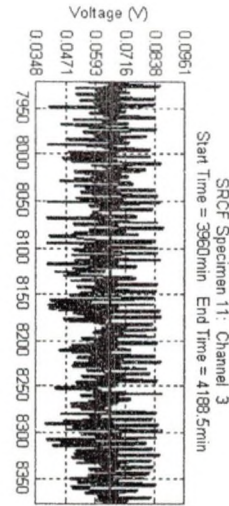
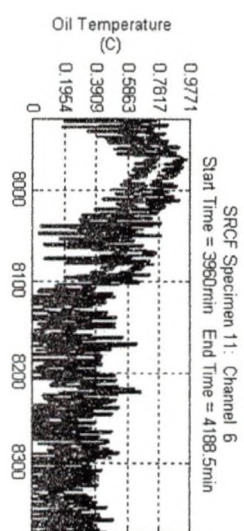
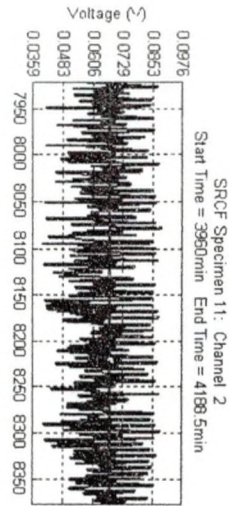
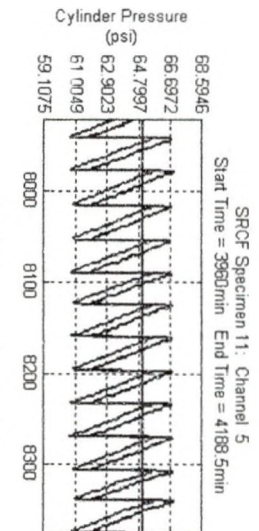
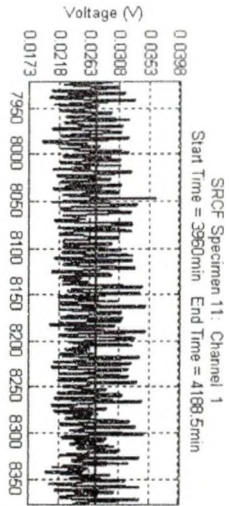
It is unclear as to why the signal on channel 6 dropped so dramatically. File 4600 was created on April 20th 2008 at about 6:49 am.

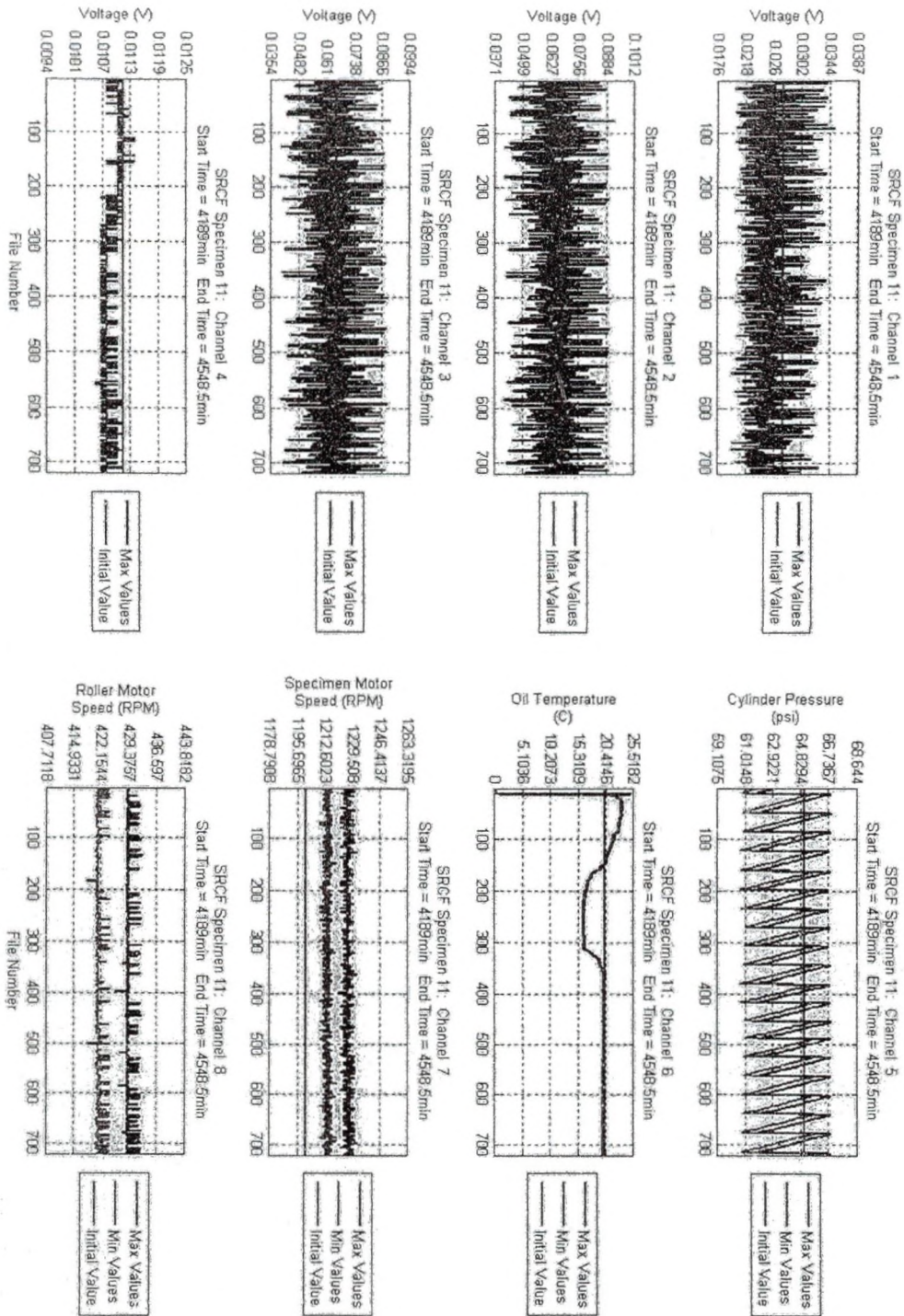




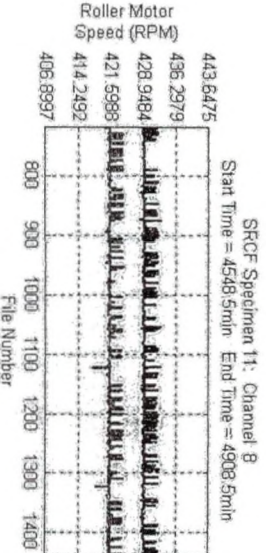
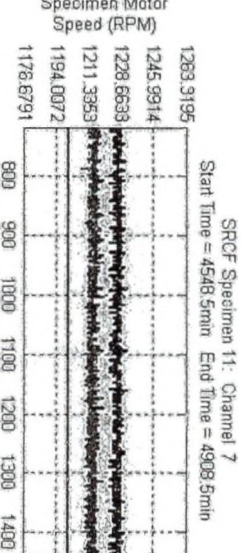
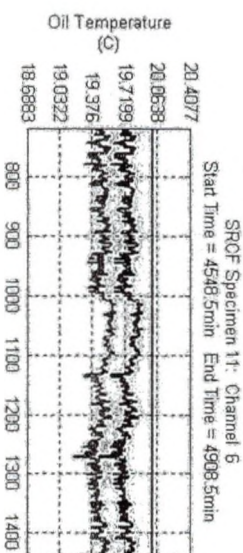
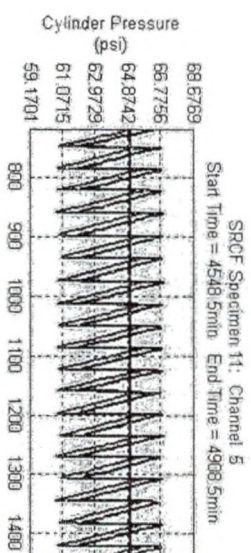
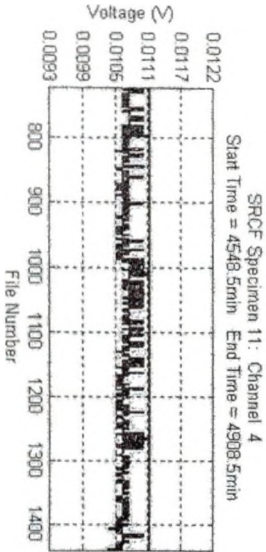
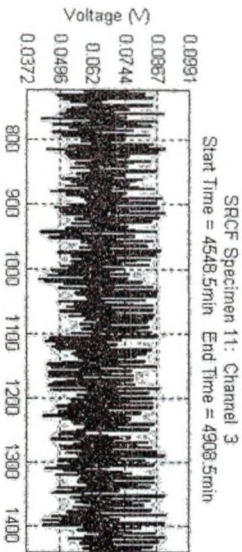
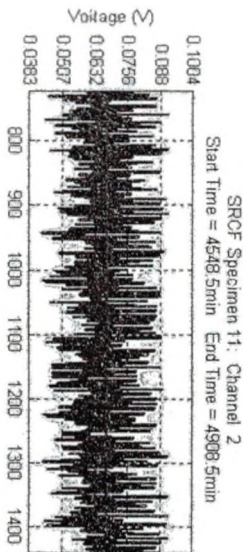
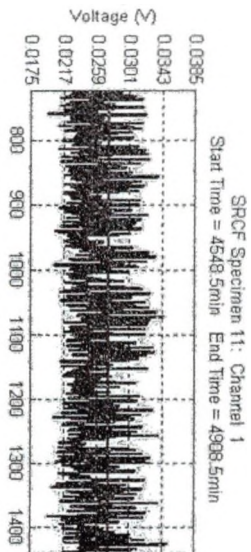


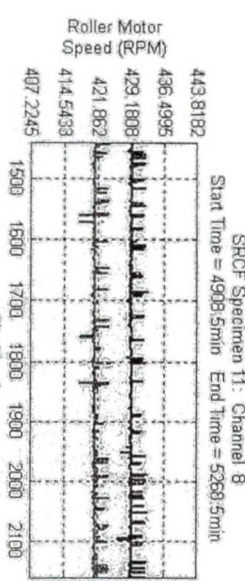
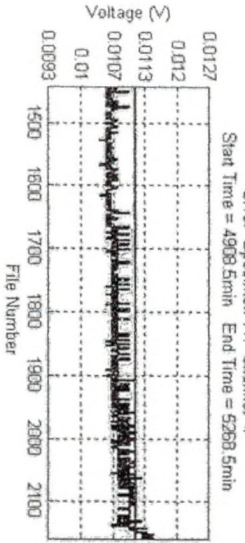
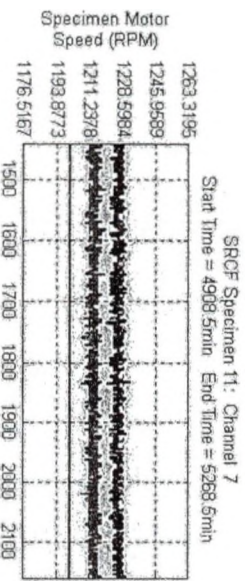
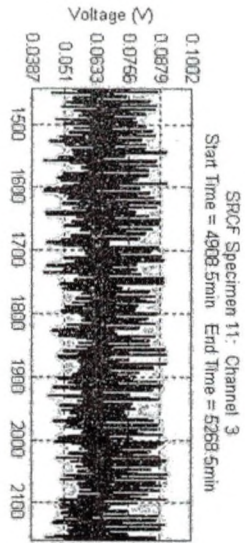
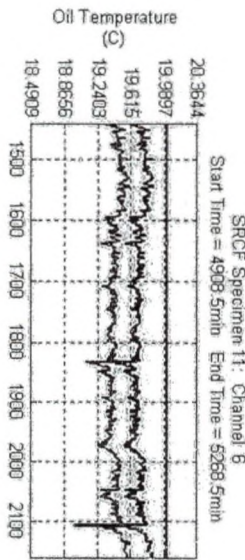
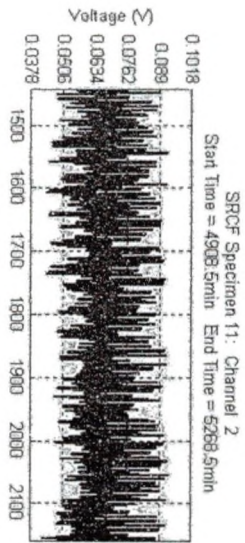
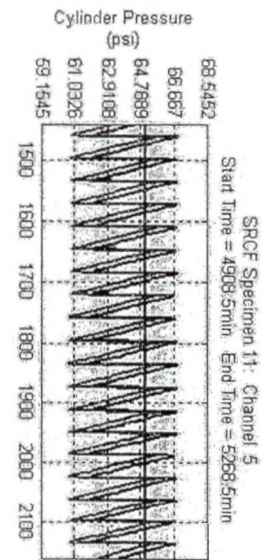
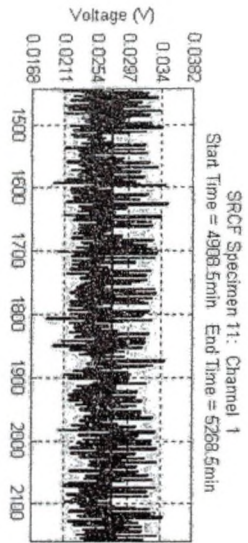


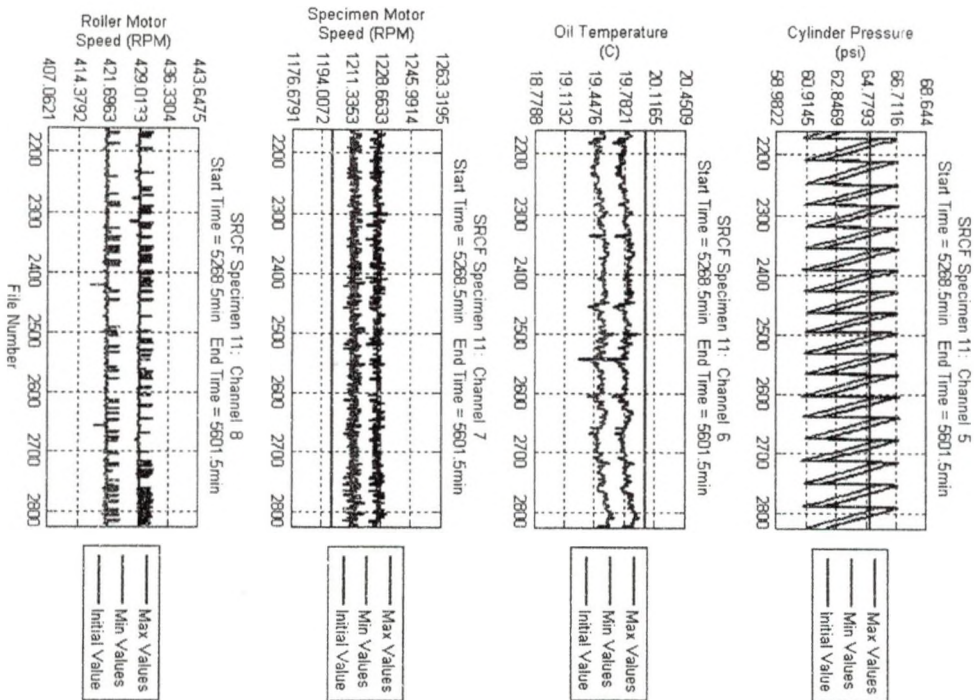
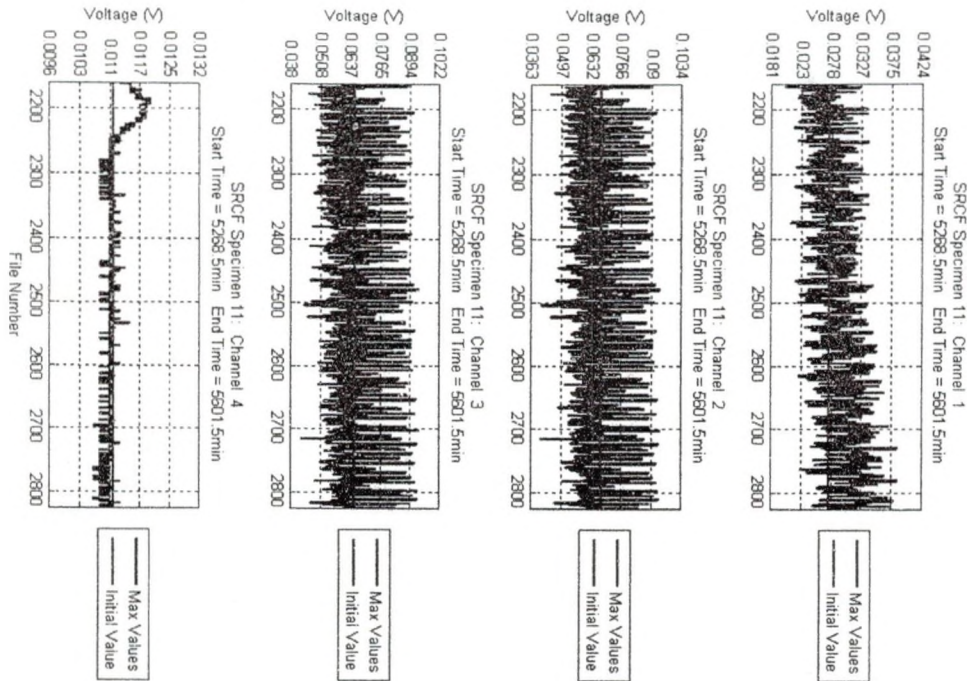




At the start of file 1, the temperature probe was reset by unplugging it then plugging it back into the outlet. This seemed to reset the probe and it began to work correctly again.

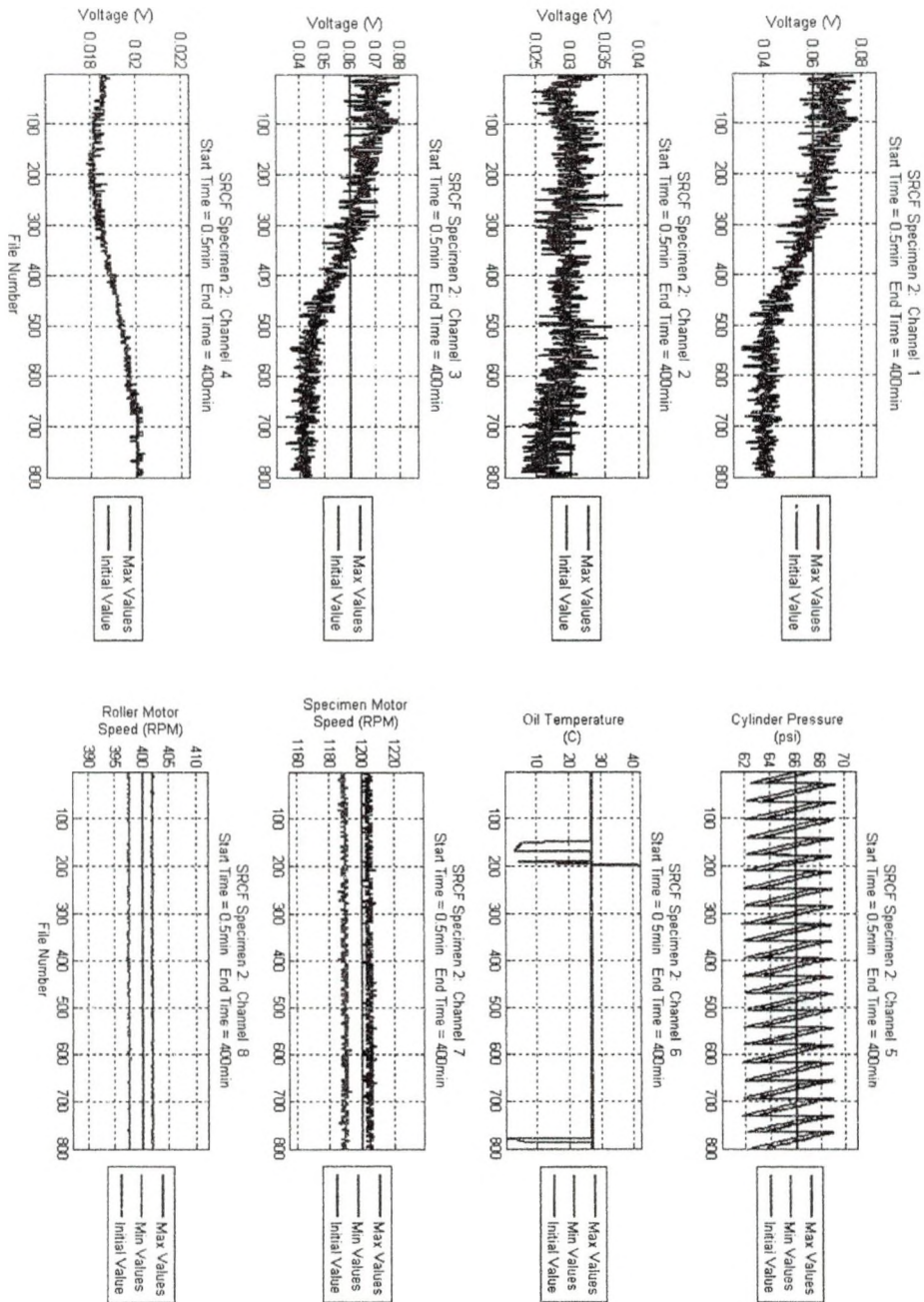


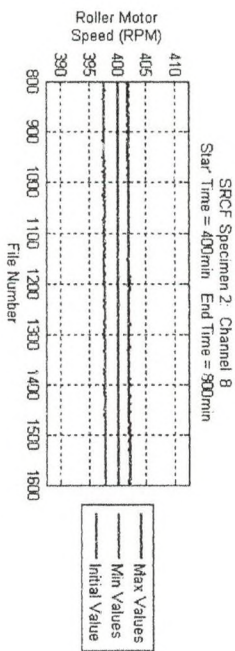
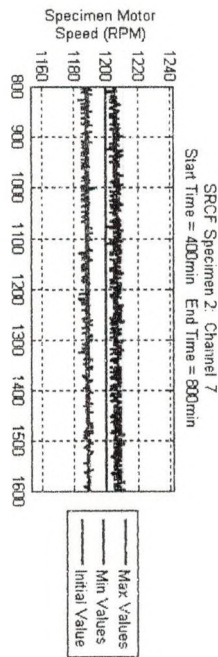
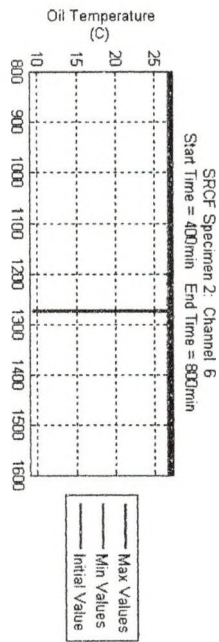
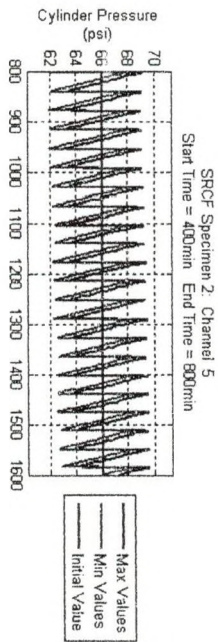
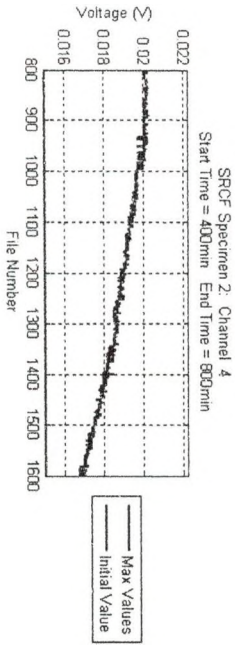
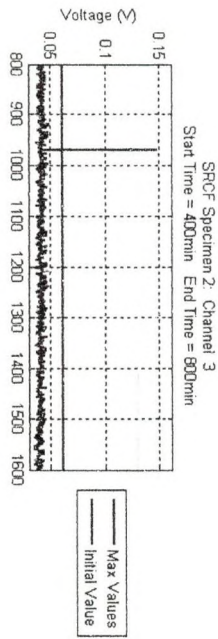
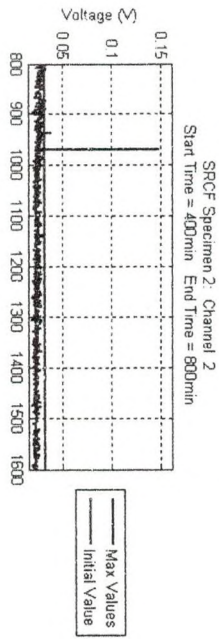
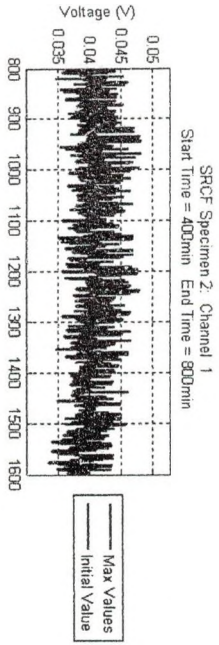


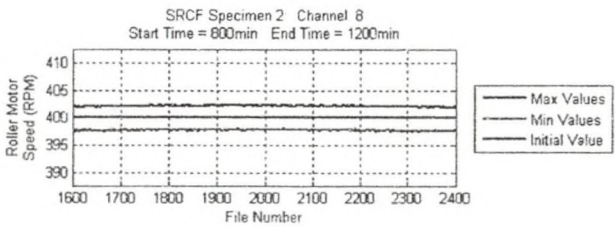
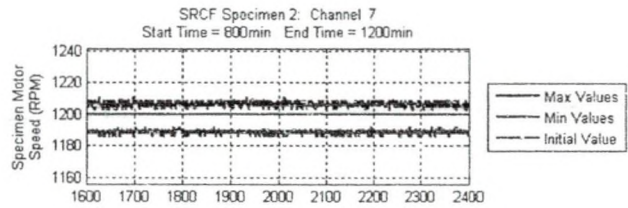
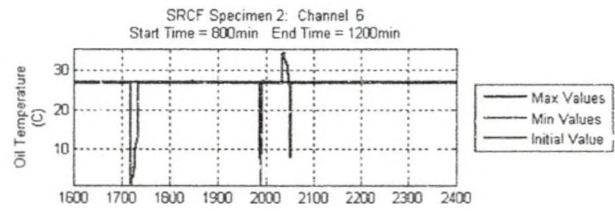
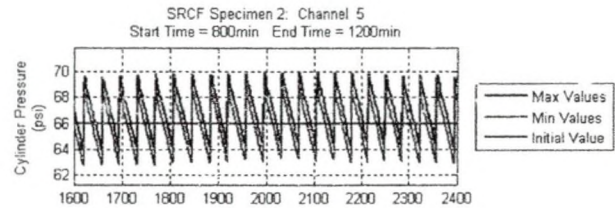
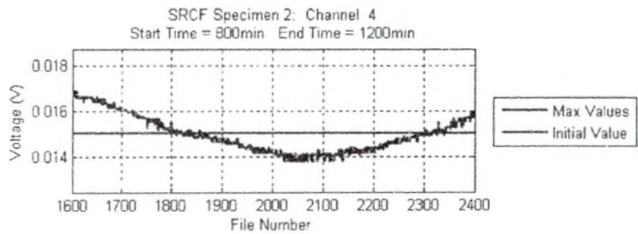
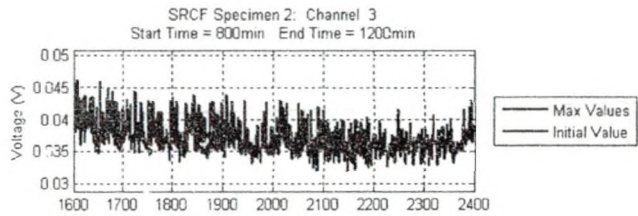
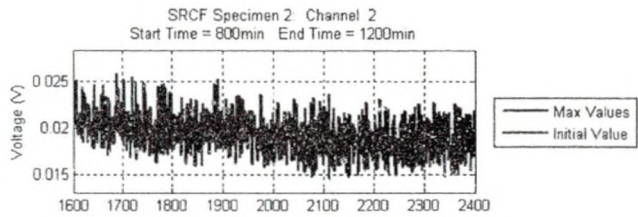
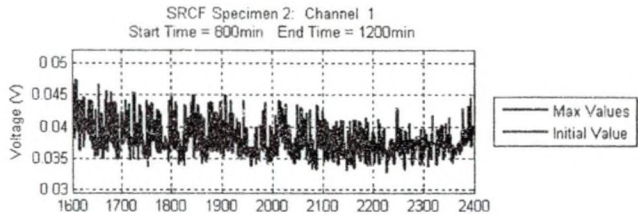


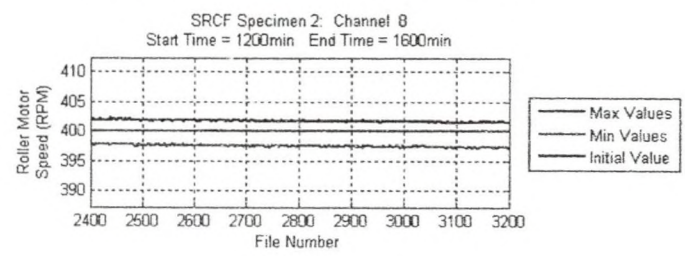
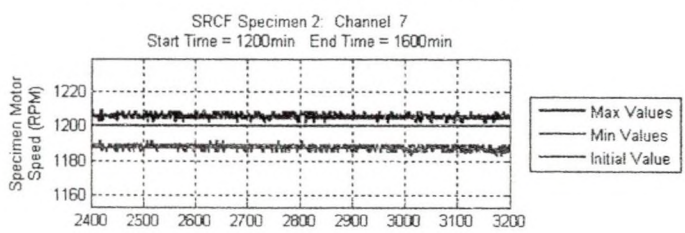
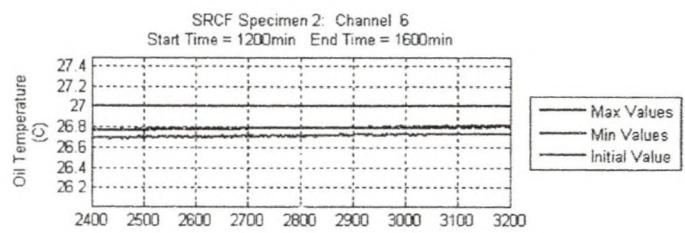
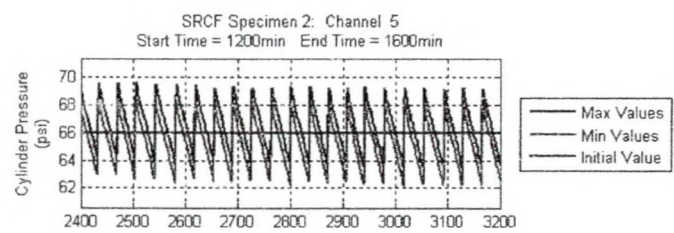
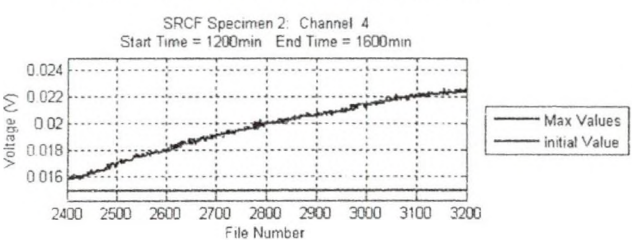
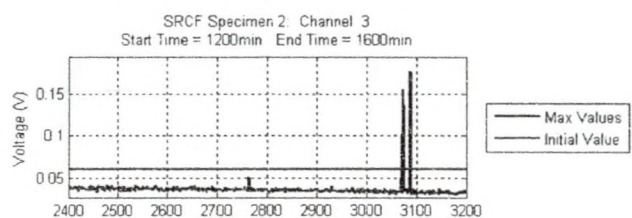
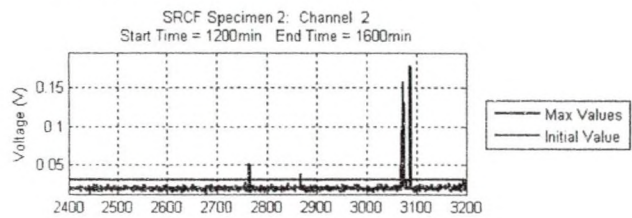
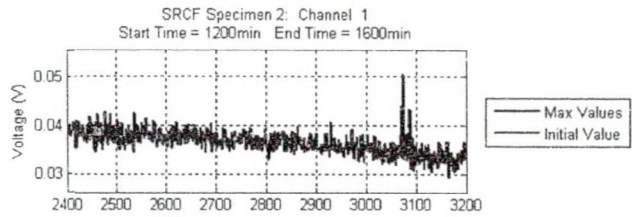
Testing was suspended on April 22nd 2008 at about 4:00 pm. However, it would appear that channel 1 was beginning to show signs of a surface irregularity since the signal began increasing steadily.

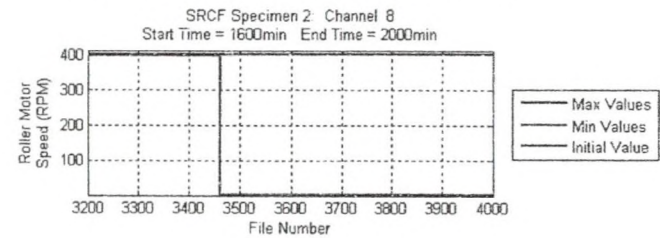
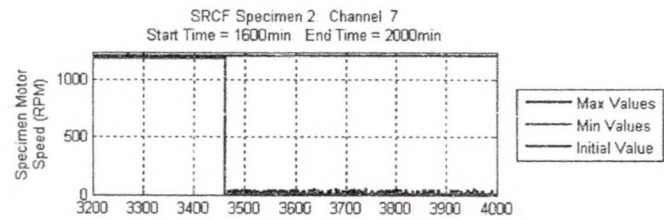
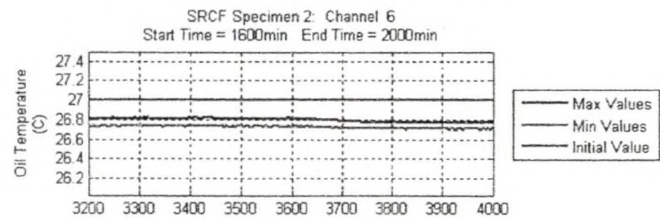
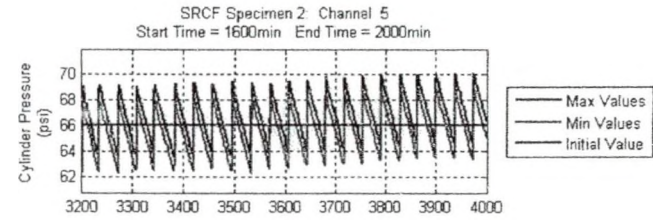
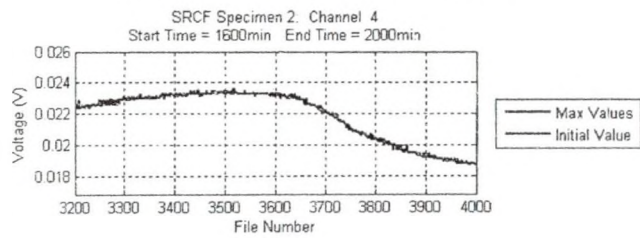
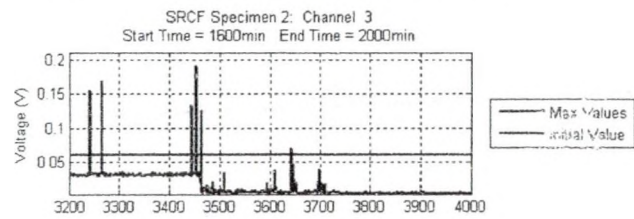
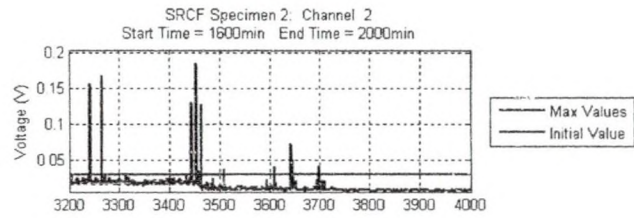
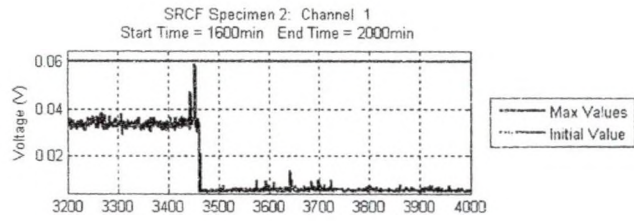
Specimen 2











APPENDIX B

Mathcad® Files

Mathcad® File for Converting Hertzian Stress to a Cylindrical Pressure

Fixed Machine Values

Radius of Specimen:	$r_s := .75 \text{ in}$	Radius of Roller:	$r_r := 3 \cdot r_s$
Air Cylinder Diameter:	$d_c := 4.5 \text{ in}$	Roller to Wall Distance:	$L_{\text{wall}} := 2.5 \text{ in}$
Contact Length:	$L := 5 \text{ mm}$	Shaft Diameters:	$d_{\text{shaft}} := 1 \frac{1}{8} \text{ in}$
Air Cylinder Area:		$A_c := \pi \cdot \frac{d_c^2}{4}$	
$\text{GPa} := 10^9 \text{ Pa}$		$\text{MPa} := 10^6 \text{ Pa}$	
$\text{kN} := 10^3 \text{ N}$		$\text{ksi} := 10^3 \text{ psi}$	

Material Properties (Taken from CES 2007)

$E_s := 2 \cdot 10^{11} \text{ Pa}$	$\nu_s := .29$	$E_r := 2 \cdot 10^{11} \text{ Pa}$	$\nu_r := .29$
$K_s := \frac{1 - \nu_s^2}{\pi \cdot E_s}$	$K_s = 1.458 \times 10^{-3} \frac{1}{\text{GPa}}$	$K_r := \frac{1 - \nu_r^2}{\pi \cdot E_r}$	$K_r = 1.458 \times 10^{-3} \frac{1}{\text{GPa}}$

Force to Maximum Hertzian Pressure:

Input: Pressure in cylinders: $P_c := 66 \text{ psi}$

Calculations:

Force Applied:	$F_{\text{app}} := 2 \cdot A_c \cdot P_c$	$F_{\text{app}} = 9.338 \text{ kN}$	$F_{\text{app}} = 2.099 \times 10^3 \text{ lbf}$
Corrected radius:	$R := \frac{r_s \cdot r_r}{r_s + r_r}$	$R = 14.287 \text{ mm}$	$R = 0.563 \text{ in}$
Width of Band of Contact:	$B := \sqrt{\frac{16 \cdot F_{\text{app}} \cdot (K_s + K_r) \cdot R}{L}}$	$B = 1.116 \text{ mm}$	$B = 0.044 \text{ in}$
Max Hertzian Stress	$P_{\text{Hz}} := \frac{4 \cdot F_{\text{app}}}{L \cdot \pi \cdot B}$	$P_{\text{Hz}} = 2.131 \text{ GPa}$	$P_{\text{Hz}} = 309.14 \text{ ksi}$
Mean Hertzian Stress:	$P_{\text{Hz.mean}} := \frac{\pi}{4} \cdot P_{\text{Hz}}$	$P_{\text{Hz.mean}} = 1.674 \text{ GPa}$	$P_{\text{Hz.mean}} = 242.799 \text{ ksi}$
Maximum Hertzian Shear Stress:	$\tau_{\text{max}} := .295 \cdot P_{\text{Hz}}$	$\tau_{\text{max}} = 628.778 \text{ MPa}$	$\tau_{\text{max}} = 91.197 \text{ ksi}$
Depth of Max Shear Stress:	$z := .393 \cdot B$	$z = 0.438 \text{ mm}$	$z = 0.017 \text{ in}$

Mathcad® File for Expected Testing Time

Expected Testing Time: $\text{rpm} := \frac{1}{\text{min}}$

Input: Cycles for Failure: $C_{\text{fail}} := 8 \cdot 10^6$
Speed of Tester: $\omega_s := 1200 \text{rpm}$

Fixed Machine Values:

Loading Points: $L_p := 3$

Calculations:

Loads Per Hour: $\text{LPH} := \omega_s \cdot L_p$ $\text{LPH} = 2.16 \times 10^5 \frac{1}{\text{hr}}$

Expected Failure Time: $\text{EFT} := \frac{C_{\text{fail}}}{\text{LPH}}$ $\text{EFT} = 37.037 \text{hr}$
 $\text{EFT} = 1.543 \text{day}$

Eddy Current Settings:

Material Properties:

Magnetic Permeability of Air: $\mu_{Air} := 1.256 \cdot 10^{-6} \frac{H}{m}$ NDT Website

Relative Magnetic Permeability of Material: $\mu_{Material} := 400 \cdot 10^{-6}$

Electrical Resistivity of Material: $\rho_{Material} := 3 \cdot 10^{-7} \text{ohm}\cdot\text{m}$ CES

Electical Conductivity:

$\sigma_{Material} := \frac{1}{\rho_{Material}}$ $\sigma_{Material} = 3.333 \times 10^6 \frac{S}{m}$

Limit Frequency:

$f_{limit} := \frac{1}{2 \cdot \pi \cdot r_s^2 \cdot \mu_{Air} \cdot \mu_{Material} \cdot \sigma_{Material}}$ $f_{limit} = 261.88 \text{kHz}$

Depth of Penetration:

Assuming a Planar Surface δ is the depth at which eddy current density is reduced by $1/e=36.8\%$
 $i := 0..7$

$f_{available} := \begin{pmatrix} 1 \\ 3 \\ 10 \\ 30 \\ 100 \\ 300 \\ 1000 \\ 3000 \end{pmatrix} \text{kHz}$

$\delta_{available_i} := \frac{1}{\sqrt{\pi \cdot f_{available_i} \cdot \mu_{Air} \cdot \mu_{Material} \cdot \sigma_{Material}}}$

$\delta_{available} = \begin{pmatrix} 435.974 \\ 251.71 \\ 137.867 \\ 79.598 \\ 43.597 \\ 25.171 \\ 13.787 \\ 7.96 \end{pmatrix} \text{mm}$ $\delta_{available} = \begin{pmatrix} 17.164 \\ 9.91 \\ 5.428 \\ 3.134 \\ 1.716 \\ 0.991 \\ 0.543 \\ 0.313 \end{pmatrix} \text{in}$

Line Speed:

$\omega_s = 20 \text{Hz}$

Line Speed: $LS := \omega_s \cdot 2r_s \cdot \pi$ $LS = 2.394 \frac{m}{s}$ $LS = 7.854 \frac{ft}{s}$

Use Chart on Page 26 of Defetomat EZ 2.828 Operating Instructions to set HP and LP.

Mathcad® File for Data Frequency Collection Calculation

Frequency of Data:

Input: Size of defect to detect: $w_d := .5\text{mm}$

Calculations:

Circumference: $C_s := 2 \cdot \pi r_s$

Scans per Revolution: $S := \frac{C_s}{w_d}$ $S = 239.389$

Frequency of Measurements: $F_m := S \cdot \omega_s \cdot 2$ $F_m = 9.576\text{kHz}$

Matlab® Files

Matlab® Teac2Matlab File

```
function
[x,dt,date,time]=Teac2Matlab(mins_offset,secs_offset,secs_to_read,fname,EndFile);
clc
close all
%cd c:\matlab\GX-1\    % DADISP_GX.M
% Copy of the file TAffmat_gx.m sent by Steve Astulfi
% Additions by C.S. Hayek, JHU/APL, 10/16/02
% This is the working copy to install improvements

% Input variables:
% Scalars-
%   mins_offset - the number of minutes to skip before starting to read the data
%   secs_offset - the number of seconds to skip before starting to read the data
%   secs_to_read the number of seconds of data to read

% Output variables:
% Matrices-
%   dt - time sequence of data for all channels, in original engineering units
% Vectors -
%   x - time, in seconds

%[fname, pname] = uigetfile('C:\DATA\Spring2008\ESC\TeacMatlab\*.hdr');
%addpath(pname);
% fid = fopen(fname, 'r');
% fid = fopen(fname, 'r');
fileExist=0;
while fileExist==0;
    try
        fileExist=1;
        fid = fopen(fname, 'r');
        fseek(fid, 0, 1);
    catch
        fileExist=0;
        if EndFile>=15000;
            fileExist=1;
        end
    end
end
end
% fseek(fid, 0, 1);
fsize = ftell(fid);
fseek(fid, 0, -1);
```



```

%fprintf('Reading header info...\n')

[F,count] = fread(fid, [1,fsize], 'char');
s = setstr(F);

fclose(fid);

p = findstr(s, 'DATASET');
for q = p : fsize
    if F(q) ~= 13
        else
            break
        end
end
dataset = s(p + 8: q - 1);

p = findstr(s, 'VERSION');
for q = p : fsize
    if F(q) ~= 13
        else
            break
        end
end
version = s(p + 8: q - 1);

p = findstr(s, 'SERIES');
for q = p : fsize
    if F(q) ~= 13
        else
            break
        end
end
series = s(p + 7: q - 1);

p = findstr(s, 'DATE');
for q = p : fsize
    if F(q) ~= 13
        else
            break
        end
end
date = s(p + 5: q - 1);

p = findstr(s, 'TIME');
for q = p : fsize
    if F(q) ~= 13

```

```

    else
        break
    end
end
time = s(p + 5: q - 1);

p = findstr(s, 'RATE');
for q = p : fsize
    if F(q) ~= 13
        else
            break
        end
    end
end
rate = s(p + 5: q - 1);

p = findstr(s, 'VERT_UNITS');
for q = p : fsize
    if F(q) ~= 13
        else
            break
        end
    end
end
vert_units = s(p + 11: q - 1);

p = findstr(s, 'HORZ_UNITS');
for q = p : fsize
    if F(q) ~= 13
        else
            break
        end
    end
end
horz_units = s(p + 11: q - 1);

p = findstr(s, 'NUM_SERIES');
for q = p : fsize
    if F(q) ~= 13
        else
            break
        end
    end
end
num_series = s(p + 11: q - 1);

p = findstr(s, 'STORAGE_MOD');
for q = p : fsize
    if F(q) ~= 13
        else

```



```

        break
    end
end
storage_mod = s(p + 12: q - 1);

p = findstr(s, 'NUM_SAMPS');
for q = p : fsize
    if F(q) ~= 13
        else
            break
        end
    end
end
num_samps = s(p + 10: q - 1);

p = findstr(s, 'FILE_TYPE');
for q = p : fsize
    if F(q) ~= 13
        else
            break
        end
    end
end
file_type = s(p + 10: q - 1);

p = findstr(s, 'SLOPE');
for q = p : fsize
    if F(q) ~= 13
        else
            break
        end
    end
end
y_slope = s(p + 6: q - 1);

p = findstr(s, 'X_OFFSET');
for q = p : fsize
    if F(q) ~= 13
        else
            break
        end
    end
end
x_offset = s(p + 9: q - 1);

p = findstr(s, 'Y_OFFSET');
for q = p : fsize
    if F(q) ~= 13
        else
            break
        end
    end
end

```

```

    end
end
y_offset = s(p + 9: q - 1);

% disassemble series
nch = str2num(num_series);
p = 1;
q = findstr(series, ',');
for I = 1 : nch - 1
    label(I) = cellstr(series(p : q(I) - 1));
    p = q(I) + 1;
end
sz = size(series);
label(nch) = cellstr(series(p : sz(2)));

% disassemble unit
p = 1;
q = findstr(vert_units, ',');
for I = 1 : nch - 1
    y_unit(I) = cellstr(vert_units(p : q(I) - 1));
    p = q(I) + 1;
end
sz = size(vert_units);
y_unit(nch) = cellstr(vert_units(p : sz(2)));
% sampling frequency
sampF = str2num(rate);
% horizontal unit
x_unit = horz_units;
% slope
p = 1;
q = findstr(y_slope, ',');
for I = 1 : nch - 1
    slope(I) = str2num(y_slope(p : q(I) - 1));
    p = q(I) + 1;
end
sz = size(y_slope);
slope(nch) = str2num(y_slope(p : sz(2)));
% offset
p = 1;
q = findstr(y_offset, ',');
for I = 1 : nch - 1
    offset(I) = str2num(y_offset(p : q(I) - 1));
    p = q(I) + 1;
end
sz = size(y_offset);
offset(nch) = str2num(y_offset(p : sz(2)));

```



```

% read data file
p=size(fname);
fname=fname(1:p(2)-4);

fname = strcat(fname, '.dat');
fid = fopen(fname, 'r');

% Compute the number of bytes to skip into the data, based on user's input (S. Hayek,
10/16/02)
secs_into_data=(mins_offset*60)+secs_offset;
nbyteskip=secs_into_data*sampF*nch*2; % The 2 is to allow for 2 byte data words
statusR = fseek(fid,nbyteskip,'bof');
if statusR==-1
    message = ferror(fid)
    return
end;
% Compute the number of ELEMENTS (not bytes) to read, based on user's input (S.
Hayek, 10/16/02)
nelread=secs_to_read*sampF;

%fprintf('Reading data ...\n')

% [dt,count]=fread(fid,[nch,inf], 'int16'); % Astulfi's original
[dt,count]=fread(fid,[nch,nelread], 'int16');
fclose(fid);

% convert data
for I = 1 : nch
    dt(I,:) = (dt(I,:) * slope(I) + offset(I));
end

% calculate data number
ndata = count / nch;

% create X
% x = linspace(0, ndata / sampF, ndata); % Astulfi's original
%x = linspace(0, ndata * sampF, ndata);
x = linspace(secs_into_data, secs_into_data+(ndata / sampF), ndata);

```

Matlab® RealTimeDataAnalysis File

```

clear all
close all
clc
%-----
%user inputs (create a load file for these values)
TestParametersValues
speedup=30; % (s)FOR TESTING ONLY SET TO 1 OTHERWISE
intervaltimemin=intervaltimemin/speedup;
%-----

StartFile=1; %First File to Read on the first Loop
%need to subtract off the pause time for the graphs
%-----
%Send Start Command
motorcommand %calls up .m file to send motor voltages
%voltages are maintained at the last value?
%-----
%Pause to Start TEAC recording
fprintf('Please Start TEAC Recording. \n\n')
prompt={'Press any button to begin Analyzing Data'};
title='Start Test';
lineNo=1;
inputparam=inputdlg(prompt,title,lineNo);
%-----
starttime=clock; %Start time of the program
%-----
%Data analysis to determine if machine should stop
MyStop=0; %Machine Stop command
intervalcount=1; %Counts the number of times the data is checked
EndFile=StartFile-1+intervaltimemin*speedup*60/(reclength+recinterval);
    %End File for first loop
while MyStop==0;
%   elapsedtime=etime(clock,starttime); %elapsed time in seconds
%   if elapsedtime>=intervaltimemin*60*intervalcount;
        %command to start at interval mark
%       while elapsedtime>=intervaltimemin*60*intervalcount;
            ECThresholdCheckmax %file to load and check max value
            StartFile=EndFile; % New First file is the last loops EndFile
            EndFile=EndFile+intervaltimemin*speedup*60/(reclength+recinterval);
                %New Last File Header to Read
            intervalcount=intervalcount+1; %Looping count number
%       end
%   end
end

```



```
%-----  
%issure stop command  
specms=0;  
rollms=0;  
motorcommand %calls up .m file to send motor voltages
```

Matlab® motorcommand File

%Machine Values

rspec=.0381/2; %(m) Radius of Specimen

rroll=rspec*3; %(m) Radius of a Roller

RPMtoVolt=416.5; %Converts RPM to Voltage

specsv=specms/60*(2*pi*rspec); %(m/s) specimen surface velocity

rollsv=specsv*slipratio; %(m/s) roller surface velocity

rollms=rollsv/(2*pi*rroll)*60; %(RPM) Roller Motor Speed

specmv=specms/RPMtoVolt; %(V) Specimen Motor Voltage

rollmv=rollms/RPMtoVolt; %(V) Roller Motor Voltage

ao=analogoutput('nidaq','Dev2'); %specifies the device type and ID number

channels=addchannel(ao,[0 1]); %specifies channels to use for ao

set(ao, 'SampleRate', 8000); %sets the sample rate property

t=linspace(0,1,16000); %linear space from a to b with n points

y=specmv*ones(1,size(t,2)); %voltage data for specimen

y1=rollmv*ones(1,size(t,2)); %voltage data for motors

putdata(ao, [y' y1']); %queue data to be sent on each channel

set(ao, 'TriggerType', 'Immediate'); %when to start the data flow

start(ao);

wait(ao,5);

clear y y1 ao channels t

Matlab® ECThresholdCheckmax File

```

clc
%
%Inputs
%-----
tc=0; %min Time correction value if time went
%unrecorded and for a second group of files
%-----
%This section reads the header files and brings in the data
mins_offset=0;
secs_offset=0;
for j=StartFile:EndFile;
    if j<10;
        fname=['s',int2str(specimennumber),'F0000',int2str(j),'.hdr'];
    elseif j>9 && j<100;
        fname=['s',int2str(specimennumber),'F000',int2str(j),'.hdr'];
    elseif j>99 && j<1000;
        fname=['s',int2str(specimennumber),'F00',int2str(j),'.hdr'];
    elseif j>999 && j<10000;
        fname=['s',int2str(specimennumber),'F0',int2str(j),'.hdr'];
    elseif j>9999 && j<100000;
        fname=['s',int2str(specimennumber),'F',int2str(j),'.hdr'];
    else
        fname=['s',int2str(specimennumber),'F',int2str(j),'.hdr'];
    end
    [RunTime,SingleData,Date,Time]=...
        Teac2Matlab(mins_offset,secs_offset,secs_to_read,fname,EndFile);
    TestData=[SingleData;RunTime];
    DateTimeStamp(j,:)=[' ',Date,' ',Time];
    MaxV(:,j)=max(abs(SingleData),[],2);
    MinV(:,j)=min(abs(SingleData),[],2);
clear SingleData RunTime TestData
end
Results=[num2str(MaxV(1:totalchannelsread,:)) Date TimeStamp];
clear title
t0=clock;
%Max Values from each channel
for i=channelstart:channelend;
    V(i,:)=MaxV(i,:);
    Values(i,:)=V(i,:)*channelconversions(i,:);
    intervalMaxValues(i,:)=max(Values(i,:));
    changefrominitial(i,:)=intervalMaxValues(i,:)-initialvalues(i,:);
end
%Min Values from each channel
for i=5:8

```

```

V2(i,:)=MinV(i,:);
Values2(i,:)=V2(i,:)*channelconversions(i,:);
intervalMinValues(i,:)=min(Values2(i,:));
changefrominitial2(i,:)=intervalMinValues(i,:)-initialvalues(i,:);
end

%-----
%This section plots the data desired
correctionxaxis=[0:1:StartFile-2]*0;
xaxis1=[StartFile:1:EndFile];
xaxis=cat(2,correctionxaxis,xaxis1);
yaxisplotcorrection=ones(totalchannelsread,length(xaxis));
for i=channelstart:channelend;
    changefrominitialplot(i,:)=...
        yaxisplotcorrection(i,:)*changefrominitial(i,:);
    initialvaluesplot(i,:)=yaxisplotcorrection(i,:)*initialvalues(i,:);
    maxlimitplot(i,:)=yaxisplotcorrection(i,:)*maxlimit(i,:);
    minlimitplot(i,:)=yaxisplotcorrection(i,:)*minlimit(i,:);
end
%-----
%Plotting Loop for Max Values
abovemax=1.1; %Percentage above max Y value
belowmin=.9; %Percentage below min Y value
scrsz = get(0,'ScreenSize');
figure('Position',[0 scrsz(4)*.04 scrsz(3)*.5 scrsz(4)*.88])
%[distance from left, distance from bottom, width, height]
for i=1:4;
    Ymax(i)=max(Values(i,StartFile:EndFile));
    Ymin(i)=min(Values(i,StartFile:EndFile));
    subplot(4,1,i)
    plot(xaxis,Values(i,:),'-k',...
        xaxis,initialvaluesplot(i,:),'-b','Linewidth',1.5);
    axis([StartFile EndFile belowmin*Ymin(i) abovemax*Ymax(i)]);
    TITLE1L1=['SRCF Specimen ',num2str(specimennumber),': ',...
        ' Channel ',num2str(i)];
    TITLE1L2=['Start Time = ',...
        num2str((reclength+recinterval)*StartFile/60+tc),'min End Time = ',...
        num2str((reclength+recinterval)*EndFile/60+tc),'min'];
    title({TITLE1L1;TITLE1L2});
    ylabel('Voltage (V)')
    grid;
    hold;
    legend('Max Values','Initial Value','Location','EO');
% set(gca,'YTick',belowmin*Ymin(i):...
% (abovemax*Ymax(i)-belowmin*Ymin(i))/5:abovemax*Ymax(i));
end

```



```

xlabel('File Number')
FileTitle1=['Figure1_',num2str((reclength+recinterval)*EndFile/60+tc),...
'minute.bmp'];
saveas (figure(1),FileTitle1);
%-----
abovemax=1.025; %Percentage above max Y value
belowmin=.975; %Percentage below min Y value
figure('Position',[scrsz(3)*.5 scrsz(4)*.04 scrsz(3)*.5 scrsz(4)*.88])
%[distance from left, distance from bottom, width, height]
for i=5:8;
    Ymax(i)=max(Values(i,StartFile:EndFile));
    Ymin(i)=min(Values2(i,StartFile:EndFile));
    subplot(4,1,i-4)
    plot(xaxis,Values(i,:),'-k',...
        xaxis,Values2(i,:),'-m',...
        xaxis,initialvaluesplot(i,:),'-b','Linewidth',1.5);
    axis([StartFile EndFile belowmin*Ymin(i) abovemax*Ymax(i)]);
    TITLE1L1=['SRCF Specimen ',num2str(specimennumber),' ',...
        ' Channel ',num2str(i)];
    TITLE1L2=['Start Time = ',...
        num2str((reclength+recinterval)*StartFile/60+tc),'min End Time = ',...
        num2str((reclength+recinterval)*EndFile/60+tc),'min'];
    title({TITLE1L1;TITLE1L2});
    if i==5;
        ylabel({'Cylinder Pressure';'(psi)'});
    elseif i==6;
        ylabel({'Oil Temperature';'(C)'});
    elseif i==7;
        ylabel({'Specimen Motor';'Speed (RPM)'});
    elseif i==8;
        ylabel({'Roller Motor';'Speed (RPM)'});
    end
    grid;
    hold;
    legend('Max Values','Min Values',...
        'Initial Value','Location','EO');
    % set(gca,'YTick',belowmin*Ymin(i):...
    % (abovemax*Ymax(i)-belowmin*Ymin(i))/5:abovemax*Ymax(i));
end
xlabel('File Number');
FileTitle2=['Figure2_',num2str((reclength+recinterval)*EndFile/60+tc),...
'minute.bmp'];
saveas (figure(2),FileTitle2);
clear MaxV V Values MinV V2 Values2
%-----
%Statement to Stop if EC change is too large

```

```

if intervalMaxValues(1,*)>maxlimit(1,);
    MyStopC1=1;
    fprintf('\nEC Channel 1 Outside Range\n\n');
else MyStopC1=0;
end
if intervalMaxValues(2,*)>maxlimit(2,);
    MyStopC2=1;
    fprintf('EC Channel 2 Outside Range \n\n');
else MyStopC2=0;
end
if intervalMaxValues(3,*)>maxlimit(3,);
    MyStopC3=1;
    fprintf('EC Channel 3 Outside Range \n\n');
else MyStopC3=0;
end
if intervalMaxValues(4,*)>maxlimit(4,);
    MyStopC4=1;
    fprintf('EC Channel 4 Outside Range \n\n');
else MyStopC4=0;
end
MyStopC1_4=[MyStopC1; MyStopC2; MyStopC3; MyStopC4];
clear MyStopC1 MyStopC2 MyStopC3 MyStopC4
if max(MyStopC1_4)>=1;
    MyStop=1;
else MyStop=0;
end
clear MyStopC1_4 yaxisplotcorrection ...
    changefrominitialplot initialvaluesplot...
    maxlimitplot minlimitplot

pause(1); %time to pause so graphs can pop up

```


Matlab® T2Mv2Screening File

```

clear all
close all
clc
%
fprintf('This program reads the max value from each interval recorded. \n\n');
%Inputs
prompt={'First File to Read: ', 'Last File to Read: ',...
        'Specimen Number: '};
title='Input Parameters';
lineNo=1;
inputparam=inputdlg(prompt,title,lineNo);
StartFile=str2double(inputparam(1,1));
EndFile=str2double(inputparam(2,1));
specimennumber=str2double(inputparam(3,1));
%-----
%Inputs global test values
TestParametersValues
%-----
%This section reads the header files and brings in the data
t0 = clock;
for j=StartFile:EndFile;
    if j<10;
        fname=['s',int2str(specimennumber),'F0000',int2str(j),'.hdr'];
    elseif j>9 && j<100;
        fname=['s',int2str(specimennumber),'F000',int2str(j),'.hdr'];
    elseif j>99 && j<1000;
        fname=['s',int2str(specimennumber),'F00',int2str(j),'.hdr'];
    elseif j>999 && j<10000;
        fname=['s',int2str(specimennumber),'F0',int2str(j),'.hdr'];
    elseif j>9999 && j<100000;
        fname=['s',int2str(specimennumber),'F0',int2str(j),'.hdr'];
    else
        fname=['s',int2str(specimennumber),'F',int2str(j),'.hdr'];
    end
    [RunTime,SingleData,Date,Time]=...
        Teac2Matlab(mins_offset,secs_offset,secs_to_read,fname);
    TestData=[SingleData;RunTime];
    DateTimeStamp(j,:)=[' ',Date, ', ',Time];
    MaxV(:,j)=max(abs(SingleData),[],2);
    MinV(:,j)=min(abs(SingleData),[],2);
    MeanV(:,j)=mean(abs(SingleData),2);

end
Results=[num2str(MaxV(1:4,:)) DateTimeStamp];

```

```

matlabtime=etime(clock,t0)/60
clear t0 title
t0=clock;
for i=1:8;
    V(i,:)=MaxV(i,:);
    V2(i,:)=MinV(i,:);
    V3(i,:)=MeanV(i,:);
    V(i,:)=V(i,:)*channelconversions(i,:); %Correction Factors
    V2(i,:)=V2(i,:)*channelconversions(i,:); %Correction Factors
    V3(i,:)=V3(i,:)*channelconversions(i,:); %Correction Factors
end
%-----
%This section plots the data desired
correctionxaxis=[0:1:StartFile-2]*0;
xaxis1=[StartFile:1:EndFile];
xaxis=cat(2,correctionxaxis,xaxis1);
abovemax=1.1; %Percentage above max Y value
belowmin=.9; %Percentage below min Y value
scrsz=get(0,'ScreenSize');
figure('Position',[0 scrsz(4)*.04 scrsz(3)*.5 scrsz(4)*.88]);
%Plotting Loop for Max Values
figure(1)
for i=1:4;
    Ymax(i)=max(V(i,StartFile:EndFile));
    Ymin(i)=min(V3(i,StartFile:EndFile));
    subplot(4,1,i)
    plot(xaxis,V(i,:),'-r',xaxis,V3(i,:),'-k',...
        xaxis,initialvalues(i,:),'-b','LineWidth',1.5);
    axis([StartFile EndFile belowmin*Ymin(i) abovemax*Ymax(i)]);
    TITLE1L1=['SRCF Specimen ',num2str(specimennumber),': Channel ',num2str(i)];
    TITLE1L2=['Start Time=',...
        num2str((StartFile-1)/2+timeoffset),'min End
Time=',num2str(EndFile/2+timeoffset), 'min'];
    title({TITLE1L1,TITLE1L2});
    ylabel('Voltage (V)')
    grid
    set(gca,'YTick',belowmin*Ymin(i):...
        (abovemax*Ymax(i)-belowmin*Ymin(i))/5:abovemax*Ymax(i));
    legend('Max Values','Mean Values','Initial Value','Location','EO');
end
xlabel('File Number')
FileTitle1=['Figure1 Screening_s',num2str(specimennumber),...
    'Time_',num2str((StartFile-1)/2+timeoffset),'to',...
    num2str((EndFile)/2+timeoffset),'min','.bmp'];

figure('Position',[scrsz(3)*.5 scrsz(4)*.04 scrsz(3)*.5 scrsz(4)*.88]);

```



```

figure(2)
for i=5:8;
    Ymax(i)=max(V(i,StartFile:EndFile));
    Ymin(i)=min(V2(i,StartFile:EndFile));
    subplot(4,1,i-4)
    plot(xaxis,V(i,:),'r',xaxis,V2(i,:),'g',xaxis,V3(i,:),'k',...
        xaxis,initialvalues(i,:),'b','LineWidth',1.5);
    axis([StartFile EndFile belowmin*Ymin(i) abovemax*Ymax(i)]);
    TITLE1L1=['SRCF Specimen ',num2str(specimennumber),' Channel ',num2str(i)];
    TITLE1L2=['Start Time=',...
        num2str((StartFile-1)/2+timeoffset),'min End
Time=',num2str((EndFile-1)/2+timeoffset),'min'];
    title({TITLE1L1,TITLE1L2});
    if i==5;
        ylabel({'Cylinder Pressure';'(psi)'});
    elseif i==6;
        ylabel({'Oil Temperature';'(C)'});
    elseif i==7;
        ylabel({'Specimen Motor';'Speed (RPM)'});
    elseif i==8;
        ylabel({'Roller Motor';'Speed (RPM)'});
    end
    grid
    set(gca,'YTick',belowmin*Ymin(i):...
        (abovemax*Ymax(i)-belowmin*Ymin(i))/5:abovemax*Ymax(i));
    legend('Max Values','Min Values','Mean Values','Initial Value','Location','EO');
end
xlabel('File Number')
FileTitle2=['Figure2Screening_s',num2str(specimennumber),...
    'Time_',num2str((StartFile-1)/2+timeoffset),'to',...
    num2str((EndFile)/2+timeoffset),'min','.bmp'];

savefileinput=input('Save Figures to File? (1 is Y, 0 is N): ');
if savefileinput==1;
    saveas(figure(1),FileTitle1);
    saveas(figure(2),FileTitle2);
end

findtime=input('Find File Time and Cycles? (1 is Y, 0 is N): ');
while findtime==1;
    filenumbermax=input('Value on X-Axis: ');
    DateTimeStamp(filenumbermax,:);
    CyclesCompleted=...
        (filenumbermax-1)*(reclength+recinterval)*(specimenrpm*3)/60
    findtime=input('Find Maximum Time (1 is Y, 0 is N): ');
end

```

```
clear StartFile EndFile channelend channelstart fname lineNo prompt...
specimenrpm specimennumber totalchannelsread secs_offset...
secs_to_read t0 xaxis xaxis1 j i findtime filenumbermax...
reclength recinterval mins_offset Ymin Ymax
```


Matlab® T2Mv2Analysis File

```

clear all
close all
clc
fprintf('This program reads all the raw data for a set of intervals recorded. \n\n');
%Inputs
prompt={'First File to Read: ', 'Last File to Read: ',...
        'Specimen Number: '};
title='Input Parameters';
lineNo=1;
inputparam=inputdlg(prompt,title,lineNo);
StartFile=str2double(inputparam(1,1));
EndFile=str2double(inputparam(2,1));
specimennumber=str2double(inputparam(3,1));
%-----
%Inputs global test values
TestParametersValues
%-----
%This section reads all the data in
mins_offset=0;
secs_offset=0;
t0 = clock;
for j=StartFile:EndFile;
    if j<10;
        fname=['s',int2str(specimennumber),'F0000',int2str(j),'.hdr'];
    elseif j>9 && j<100;
        fname=['s',int2str(specimennumber),'F000',int2str(j),'.hdr'];
    elseif j>99 && j<1000;
        fname=['s',int2str(specimennumber),'F00',int2str(j),'.hdr'];
    elseif j>999 && j<10000;
        fname=['s',int2str(specimennumber),'F0',int2str(j),'.hdr'];
    elseif j>9999 && j<100000;
        fname=['s',int2str(specimennumber),'F0',int2str(j),'.hdr'];
    else
        fname=['s',int2str(specimennumber),'F',int2str(j),'.hdr'];
    end
    [RunTime,SingleData,Date,Time]=...
        Teac2Matlab(mins_offset,secs_offset,secs_to_read,fname);
    TestData(:,j)=[SingleData;RunTime];
    DateTimeStamp(j,:)=[' ',Date,' ',Time];
end
matlabtime=etime(clock,t0)/60
fprintf('\n minutes \n\n')
clear t0 matlabtime mins_offset secs_offset title

```

```

t0=clock;

for j=StartFile:EndFile;
    %timefix(:,j)=(j-1)*(reclength+recinterval); In equation below
    globaltime(1,:,j)=RunTime(1,:)+(j-1)*(reclength+recinterval);
    globalloadcycles(:,j)=globaltime(:,j)*(specimenrpm*3)/60;
    %continuousxaxis(:,j)=TestData(5,:,j)+j-(j-StartFile)*(reclength-secs_to_read);
    for k=1:size(TestData,2);
        continuousxaxis(:,k,j)=RunTime(1,k)*1/(secs_to_read)+j;
    end
end
%-----
%Voltage to Values

for i=1:8;
    V(i,:)=(TestData(i,:,:));
    V(i,:)=V(i,:)*channelconversions(i,:); %Conversion Factors
    Ymax(i)=max(V(i,:));
    Ymin(i)=min(V(i,:));
end
%-----
%Plot
Xmin=continuousxaxis(1,1,StartFile);
Xmax=continuousxaxis(1,size(TestData,2),EndFile);
abovemax=1.1;
belowmin=.9;
scrsz=get(0,'ScreenSize');
figure('Position',[0 scrsz(4)*.04 scrsz(3)*.5 scrsz(4)*.88]);
figure(1);
for i=1:4;
    subplot(4,1,i)
    grid
    hold on
    for j=StartFile:EndFile;
        plot(continuousxaxis(1,:,j),V(i,:,j));
        TITLE=['Raw Data for SRCF Specimen ',num2str(specimennumber),' from Channel
',num2str(i)];
        title(TITLE);
        ylabel('Voltage (V)');
    end
    % axis([Xmin Xmax Ymin(i)*belowmin Ymax(i)*abovemax]);
    % set(gca,'YTick',belowmin*Ymin(i):...
    % (abovemax*Ymax(i)-belowmin*Ymin(i))/5:abovemax*Ymax(i));
end
xlabel('File Number');

```



```

figure('Position',[scrsz(3)*.5 scrsz(4)*.04 scrsz(3)*.5 scrsz(4)*.88]);
figure(2);
for i=5:8;
    subplot(4,1,i-4)
    grid
    hold on
    for j=StartFile:EndFile;
        plot(continuousxaxis(1,:j),V(i,:j));
        TITLE=['Raw Data for SRCF Specimen ',...
            num2str(specimennumber),' from Channel ',num2str(i)];
        title(TITLE);
        ylabel('Voltage (V)');
    end
    if i==5;
        ylabel({'Cylinder Pressure';'(psi)'});
    elseif i==6;
        ylabel({'Oil Temperature';'(C)'});
    elseif i==7;
        ylabel({'Specimen Motor';'Speed (RPM)'});
    elseif i==8;
        ylabel({'Roller Motor';'Speed (RPM)'});
    end
    % axis([Xmin Xmax Ymin(i)*belowmin Ymax(i)*abovemax]);
    % set(gca,'YTick',belowmin*Ymin(i):...
    % (abovemax*Ymax(i)-belowmin*Ymin(i))/5:abovemax*Ymax(i));
end
xlabel('File Number');
hold off

matlabtime=etime(clock,t0)/60
fprintf('\n minutes \n\n')

FileTitle1=['Figure1 Analysis_s',num2str(specimennumber),...
    'Files',num2str(StartFile),'_',num2str(EndFile),'.bmp'];
FileTitle2=['Figure2 Analysis_s',num2str(specimennumber),...
    'Files',num2str(StartFile),'_',num2str(EndFile),'.bmp'];

savefileinput=input('Save Figures to File? (1 is Y, 0 is N): ');
if savefileinput==1;
    saveas(figure(1),FileTitle1);
    saveas(figure(2),FileTitle2);
end

findcycles=input('Find Approximate Cycles and Time Stamp(1 is Y, 0 is N): ');
while findcycles==1;

```

```
valueonxaxis=input('Value on X-Axis of Figure 1 (Whole Number): ');
DateTimeStamp(valueonxaxis,:)
globalloadcycles(1,1,valueonxaxis)
findcycles=input('Approximate Cycles and Time Stamp(1 is Y, 0 is N): ');
end
```

```
clear findcycles valueonxaxis Date Time TITLE...
channelend channelstart lineNo prompt recinterval reclength...
secs_to_read specimennumber specimenrpm t0 totalchannelsread
clear i j k fname
```

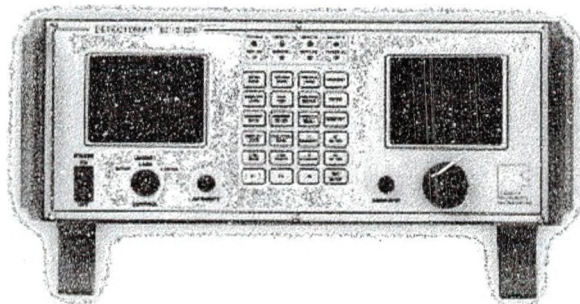

S-RCF Tester Supplemental Information

Foerster Defectomat® EZ 2.828 Information [23]

DEFECTOMAT® EZ 2.828

An innovative, easy-to-use eddy current test instrument for detecting surface defects in a variety of applications

- The DEFECTOMAT EZ is an innovative addition to Foerster's line of eddy current testing instruments. The DEFECTOMAT EZ is used in conjunction with the appropriate test coil system to detect surface defects in:
 - Ferrous and nonferrous bar, wire and tubing in the diameter range of 0.010" - 7.000"
 - Mass produced parts with simple or complex geometries
 - In-service structures and equipment



The DEFECTOMAT EZ can be installed in the production line or in an off-line application for determination of product surface quality. Examples of typical in-line applications include drawing and rolling lines, welded tube lines, hot wire and rod mills, finishing lines and grinding lines. Examples of off-line applications include inspection lines, research and development, and maintenance inspection.

Test results are clearly presented on the DEFECTOMAT EZ display for analysis.

• Benefits

- Improved quality assurance through 100% continuous automatic inspection
- Highly reliable and repeatable inspection results by eliminating the subjectivity of visual inspection techniques
- Reduced scrap and reject levels and on-time deliveries of customer orders through early detection of surface defects
- Optimized production through improved process control and high throughput speeds
- Simplified operator setup and standardization procedures

• Features

- Wide test frequency range permits accurate testing of products in various sizes, shapes and materials
- Compatible with test coil systems designed for the DEFECTOMAT family
- Automatic monitoring of the test coil
- High flaw resolution
- Optional speed matching filter card
- Optional card to transfer defect counts to a remote PC
- Built-in signal generator for troubleshooting and instrument verification
- Two paint marking outputs
- Sorting into three classes via an optional remote PLC
- Raw analog and pulse-expanded outputs available for strip chart recording
- Program memory for easily reproducible test settings
- Optional analog CRT for signal display
- Multiple channel capability; common analog CRT
- Optional flaw signal processing
- Automatic test coil balancing

DEFECTOMAT EZ 2.828 Eddy Current Testing Instrument

Technical Data

Coil Systems IMD encircling and segmental coils; HD and HMD encircling coils; transformer, bridge and parameter type probes (adapter may be required); rotating probes Ro50, HRo and StaRo.

Optional Cards Data collection card to transfer defect count data to a PC; AutoFilter card to automatically vary filter setting as a function of testing speed.

Transceiver 1/3/10/30/100/300/1000/3000 Khz switchable.

Phase Selector 0-360 degrees in 1 degree steps.

Filtering Separate LP and HP filter settings in 16 steps. Manual adjustment standard; automatic adjustment via optional card.

Sensitivity Setting 0-69.5 dB in 0.5 dB steps.

Y-Enhancement For phase dependent evaluation, Y (vertical) gain adjustable 0, 6, 12, 18 dB.

X-Attenuation For phase dependent evaluation; attenuation of X signal adjustable 0, -6, -12, -18 dB.

Oscilloscope Display Analog CRT; Phase amplitude (flying dot) or Y/L for eddy current signal display.

Settings Display Back lit LCD display

Operator Interface Sealed front panel keyboard, EZ Knob to change variable settings.

Evaluation Modes Phase dependent $\frac{1}{2}Y\frac{1}{2}$ or $\frac{1}{2}Y\frac{1}{2}$, phase dependent $\frac{1}{2}Y\frac{1}{2}$.

Flaw Thresholds Three independent thresholds, S, M and L adjustable in 5% steps.

System Monitoring Automatic monitoring of test coil and instrument.

Storage Medium Internal RAM, battery buffered; 10 stored settings possible.

Test Speed Range 0-120 m/s (0-24,000 FPM).

Inputs Test ON/OFF; external motion clock; external motion clock freeze; rotary synchronization.

Interface RS232 Interface for control by a host computer.

Outputs Three instantaneous flaw outputs (S, M and L); two independent marking outputs (M and L); interface for sorting via optional PLC; analog outputs X, Y, V and $\frac{1}{2}Y\frac{1}{2}$; line speed clock output; Test ON/OFF output.

Dimensions
HxWxD: 7.75" x 17.75" x 26.75"
Foldable front legs.

Weight 50 lbs.

Operating Temperature
32° - 105° F

Storage Temperature
0° - 120° F

Available Test Coil Systems

H40/H90

Testing of 0.3-100 mm diameter cold ferrous and nonferrous bar, wire and tubing (to 180° F) without magnetic solution.

H40/H90 PM

Testing of 0.3-100 mm diameter cold ferrous and nonferrous bar, wire and tubing (to 180° F) with saturation magnetization by permanent magnet.

H40-H90 PMT

Water cooled version of H40/H90 PM for testing of materials at elevated temperatures.

M40/90/170

Testing of 0.3-180 mm diameter cold ferrous and nonferrous bar, wire and tubing (to 180° F) with saturation magnetization by electromagnet.

Transmitter T

Testing of 5-125 mm diameter hot ferrous and nonferrous bar, wire and tubing (to 2200° F).

HRo

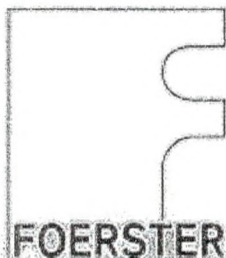
Testing of ferrous and nonferrous materials with a hand held rotating probe scanner.

StaRo

Testing of ferrous and nonferrous materials with an automated rotating probe scanner.

Probes

Testing of ferrous and nonferrous materials using hand held or automated probe systems.

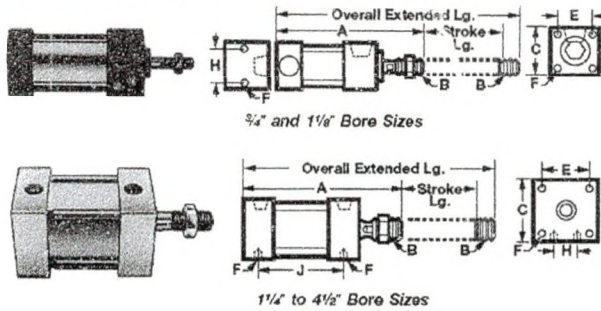


FOERSTER INSTRUMENTS INCORPORATED
140 Industry Drive, RIDC Park West, Pittsburgh, Pennsylvania, U.S.A. 15275-1028
800/635-0613 FAX: 412/788-8984 Outside the U.S.: 412/788-8976
E-Mail: sales@foerstergroup.com www.foerstergroup.com

Part No.
2.828
Ident. No.
902 621 5 8/00

Tie Rod Air Cylinders

Aluminum Tie Rod Air Cylinders



External tie rods, which are made of steel, protect the cylinder barrel while still allowing easy disassembly for repairs. To make repairs, use the replacement seal kits. All of these cylinders are an economical choice for high-force output when the cylinder is working against simple horizontal loads, with no side loading. They are double acting—they have two compressed air ports: one to extend in the “push” direction and another to retract in the “pull” direction. They are not interchangeable with NFPA-footprint cylinders. Maximum pressure is 250 psi (except for 3/4” and 1 1/8” bore sizes, which is 150 psi). Temperature range is 10° to 200° F (except for 3/4” and 1 1/8” bore sizes, which is 0° to 180° F). **To Order:** For all cylinders, please specify stroke length in 1/2” increments from the ranges listed.

Cylinders and Cylinders with Cushion—Have an aluminum barrel, rod bearing, and end caps; chrome-plated steel piston rod. They are not switch ready.

Switch-Ready Cylinders—Have an aluminum barrel. For 3/4” and 1 1/8” bore sizes: rod bearing is bronze, piston rod is Type 303 stainless steel, and end caps are steel. For all other sizes: rod bearing and end caps are aluminum; piston rod is chrome-plated steel.

Additional Information: For additional information about these products, go to our web site, www.mcmaster.com, and search for 6491KAC, or fax us at 630-782-3800 and request 6491KAC.

Bore Size	Force @ 100 psi, lbs.	Port Pipe Size, Female	Rod, Thread Size x Lg. (B)	(C)	(E)	Mounting Holes (F)	(H)	(J) ♦
3/4"	39	1/8" NPT	1/4"-28 x 5/8"	1"	0.75"	6-32	3/4"	
1 1/8"	88	1/8" NPT	3/8"-24 x 5/8"	1 1/2"	1.125"	10-32	1 1/8"	
1 1/4"	112	1/8" NPT	3/8"-16 x 1"	1 3/4"	1.281"	1/4"-28		2 1/32" + Stroke Lg.
1 3/4"	196	1/4" NPT	3/4"-10 x 1 1/2"	2 3/8"	1.718"	5/16"-24	2 5/32"	2 3/8" + Stroke Lg.
2"	269	1/4" NPT	3/4"-10 x 1 1/2"	2 3/8"	1.875"	1/4"-28 ▲	2 5/32"	2 3/8" + Stroke Lg.
2 1/2"	447	3/8" NPT	3/4"-10 x 1 1/2"	2 7/8"	2.206"	5/16"-24	1 1/4"	2 3/8" + Stroke Lg.
3"	662	3/8" NPT	3/4"-10 x 1 1/2"	3 3/8"	2.625"	5/16"-24	1 1/4"	2 3/8" + Stroke Lg.
3 1/2"	884	1/2" NPT	1"-8 x 1 5/8"	4 1/8"	3.224"	1/2"-20	1 27/32"	3 7/8" + Stroke Lg.
4 1/2"	1512	1/2" NPT	1"-8 x 1 5/8"	5 1/8"	4.024"	1/2"-20	2 1/2"	3 7/8" + Stroke Lg.

♦ For cylinders with cushion, add 1". ▲ 5/16"-24 for mounting holes on the side of the cylinder.

Pressure Transducer (PX209-200G5V) Specifications [18]

SPECIFICATIONS

Voltage Output

Excitation: 24 Vdc @ 15 mA (7 to 35 Vdc for 5 V output, 12 to 35 for 10 V output)

Output: 0 to 5 Vdc or 0 to 10 Vdc $\pm 1.5\%$ (3-wire)

Zero Balance: 0 Vdc $\pm 2\%$ FSO

4 to 20 mA Output

Excitation: 24 Vdc (7 to 35 Vdc) reverse polarity protected

Output: 4 to 20 mA $\pm 1\%$ FSO (2-wire)

Zero Balance: 4 mA $\pm 2\%$ FSO

Max. Loop Resistance: 50 x (supply voltage -10) Ohms

Common Specifications

Accuracy: 0.25% BFSL (including linearity, hysteresis and repeatability)

Operating Temperature: -54 to 121°C (-65 to 250°F)

Compensated Temperature: -20 to 80°C (-4 to 176°F)

Thermal Effects: 0.04% FS/°C (0.02% FS /°F)

Proof Pressure: 150%

Burst Pressure: 300% range max.

Response Time: 2 mS typical

Vibration Sensitivity: At 20 g peak sinusoidal vibration from 10 Hz to 2000 Hz (1.2" D.A.), the output shall not exceed 0.04% FS/g for 15 psi range to 0.005% FS/g for 100 psi and above

Natural Frequency: >35 kHz for 100 psi range

Gage Type: Diffused silicon strain gages

Wetted Parts: 316 SS, borosilicate glass, silicon nitride, epoxy

Pressure Port: 1/4-18 NPT

Electrical Connections:

PX209: 1 m (36") shielded 4-conductor cable

PX219: DIN 43650 Plug Connector Supplied

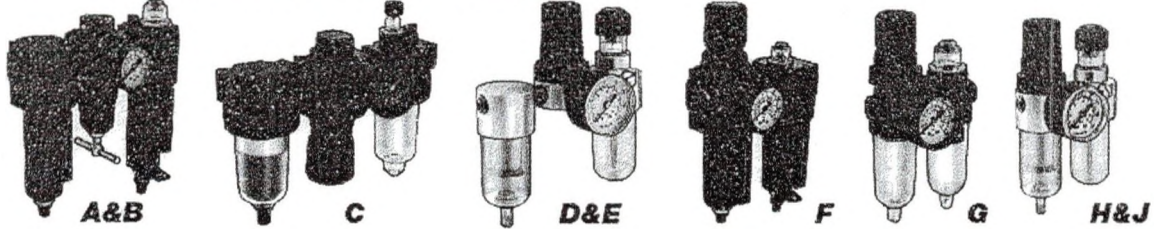
Weight: 128 g (4.5 oz)

PSI Range	BAR Range	CABLE STYLE*	CONN. STYLE	COMPATIBLE METERS
GAGE PRESSURE RANGES (psig) WITH 0 to 5 Vdc OUTPUT				
0 to 15	0 to 1.0	PX209-015G5V	PX219-015G5V	DPi8, DP41-E, DP25B-E
0 to 30	0 to 2.1	PX209-030G5V	PX219-030G5V	DPi8, DP41-E, DP25B-E
0 to 60	0 to 4.1	PX209-060G5V	PX219-060G5V	DPi8, DP41-E, DP25B-E
0 to 100	0 to 6.9	PX209-100G5V	PX219-100G5V	DPi8, DP41-E, DP25B-E
0 to 200	0 to 13.8	PX209-200G5V	PX219-200G5V	DPi8, DP41-E, DP25B-E
0 to 300	0 to 20.7	PX209-300G5V	PX219-300G5V	DPi8, DP41-E, DP25B-E

Air Filter/Regulator/Lubricators (FRLs)

For information about air preparation, see page 935.

Air Filter/Regulator/Lubricators (FRLs)



Just connect the ends to your system—we've already selected matching components and assembled them as one unit, threaded together with pipe nipples. Regulators include a gauge and are relieving style, which reduces downstream pressure through a vent port when your system is blocked. Accuracy is ± 3 psi or better. Lubricators have a sight glass; 10W nondetergent oil (ISO Grade 32) is recommended. Mounting brackets are sold separately (unless noted) and include hardware. Inlet and outlet connections are NPT female. *Stacked* units combine a filter and regulator into one "piggyback" device, with a lubricator at the side.

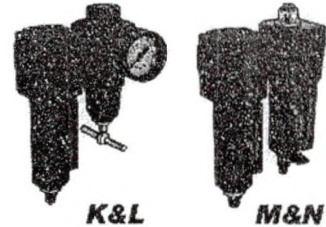
(A, K, M) **Standard**—Filters have a polypropylene element that removes particles as small as 5 microns. Drain is automatic. Body and bowl are zinc.

(B, F, L, N) **Lightweight**—Filters have a polypropylene (unless noted) element that removes particles as small as 5 microns. Drain is automatic. Body and bowl are aluminum.

(C, G) **Easy View**—A clear polycarbonate bowl lets you see what's being filtered. Filters have a polyethylene element, except stacked units which have a polypropylene element. All remove particles as small as 5 microns. Drain is automatic. Body is zinc. Style C has a steel bowl guard.

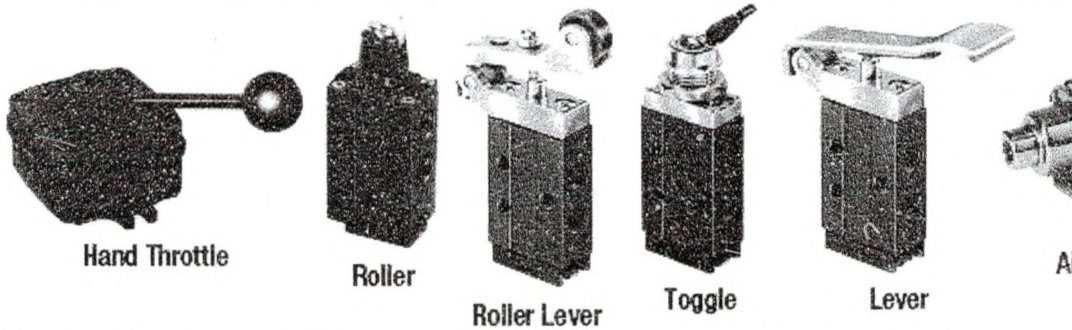
(D, H) **Lightweight Easy View**—A clear polycarbonate bowl lets you see what's being filtered, while an aluminum body makes the unit lightweight. Filters have a polypropylene element that removes particles as small as 20 microns (unless noted). Drain is manual (unless noted).

(E, J) **Chemical Resistant**—Have increased chemical compatibility. A clear polyurethane bowl lets you see what's being filtered and won't crack in systems heavy with synthetic compressor oils. Filters have a polypropylene element that removes particles as small as 20 microns. Drain is manual. Body is brass.



	Pipe Size	Max. scfm @ 100 psi	Regulating Range, psi	Oil Cap., oz.	Max. Temp.	Max. Pressure	O'all Size, Ht. x Wd.	Complete Units Each	Repl. Filter Elements Each	Mounting Brackets Each			
Filter/Regulator/Lubricators													
A	1/4	49	5-150	2.2	150° F	150 psi	7.44" x 6.46"	4957K53	\$103.58	4958K81	\$2.46	4957K61	\$5.01
A	3/8	49	5-150	2.2	150° F	150 psi	7.44" x 6.46"	4957K54	109.06	4958K81	2.46	4957K61	5.01
B	1/2	60	5-150	3.5	175° F	250 psi	8" x 9.13"	4957K58	148.87	4958K82	3.91	4957K62	5.52
B	3/4	116	5-150	7	175° F	250 psi	8.8" x 10.52"	4957K87	178.09	4958K95	5.57	4910K98	5.72
B	1	116	5-150	7	175° F	250 psi	8.8" x 10.52"	4957K88	181.89	4958K95	5.57	4910K98	5.72
B	3/4	168	5-125	.32	175° F	250 psi	12.78" x 14.75"	4957K27	337.40	4958K97	24.61	4957K77	30.60
B	1	168	5-125	.32	175° F	250 psi	12.78" x 14.75"	4957K28	316.04	4958K97	24.61	4957K77	30.60
B	1 1/4	168	5-125	.32	175° F	250 psi	12.78" x 14.75"	4957K29	368.19	4958K97	24.61	4957K78	34.11
C	1/4	45	2-125	2.9	125° F	150 psi	7.93" x 9.45"	41555K51	143.20	41555K81	3.79	41555K41	5.33
C	3/8	65	2-125	2.9	125° F	150 psi	7.93" x 9.45"	41555K52	143.20	41555K81	3.79	41555K41	5.33
C	1/2	65	2-125	2.9	125° F	150 psi	7.93" x 9.45"	41555K53	143.20	41555K81	3.79	41555K41	5.33
C	3/4	95	2-125	6	125° F	150 psi	9.38" x 10.74"	41555K54	161.49	41555K82	5.58	41555K74	5.33

Heavy-Duty Mechanically Operated Air Valves



Heavy-duty high flow mechanically operated valves are constructed with corrosion-resistant materials. Types of mechanical operators including foot, palm, hand locking and air actuated.

Mfr's #	Inlet/Outlet Size (NPT)	Valve Type	Actuator Type	CV Rate	Working Pres. psi		Order #	Price Ea.
					Min.	Max.		
PL25	1/4	4-Way, 3 Position	Hand Throttle	2.2	0	150	01228873	\$142.24
PL37	3/8	4-Way, 3 Position	Hand Throttle	2.6	0	150	01228881	142.24
PL50	1/2	4-Way, 3 Position	Hand Throttle	5.3	0	150	01228899	186.39
410211000	1/8	4-Way, 2 Position	Roller Lever	0.2	32	175	01228907	62.64

Hand Throttle

- 1/4", 3/8" and 1/2" NPT 4-way, 3 position rotary disc air valves operate with a 90° lever movement
- Ground & lapped bronze disc and cast iron surface provide a leakproof seal
- Air pressure from inlet port seals tighter as pressure increases
- Only 15 Lbs. pressure required to move lever at 100 psi
- Detent for easy location of neutral position
- Excellent for inching of double acting cylinders
- Rated at 0-150 psi, 18-200°F. CV up to 5.3

Temperature Probe (THX-400-NPT-72) [24]

Pipe Plug Thermistor Probe

ALL MODELS AVAILABLE FOR FAST DELIVERY!

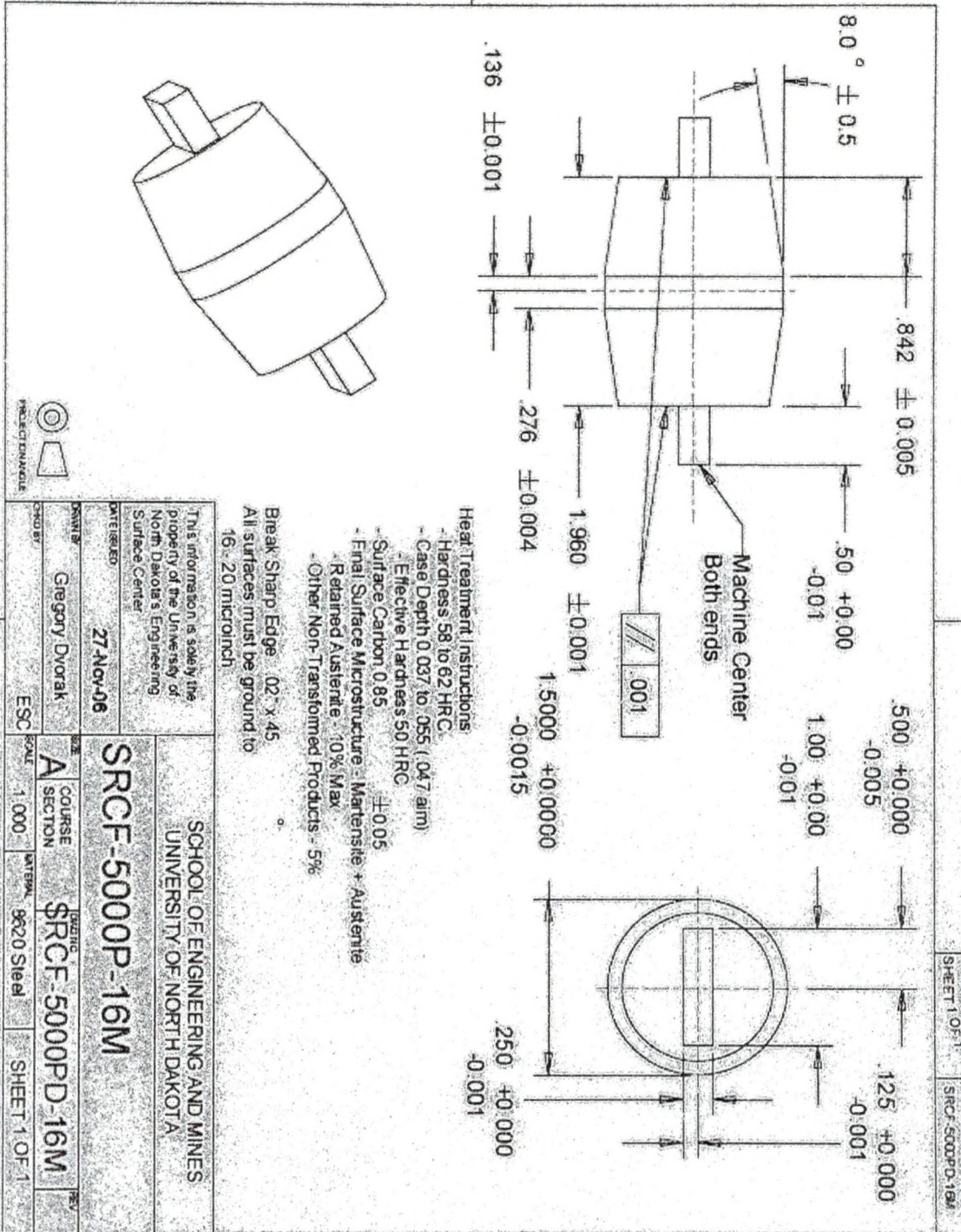
This high-pressure plug sensor is ideal for vessel applications, pressurized containers, and applications requiring NPT-mounted security for fixed readings. This accurate thermistor probe is 225 Ω @25°C. Its 304SS sheath has a 6.0 mm (0.25") dia. probe pipe plug, with 2 m (80") of 26-AWG Teflon®-insulated stainless steel overbraided stranded wire with stripped leads. Pressure rating is 2500 psi (172 bar). The hex flats are 14.1 mm (0.56") apart, and 16.0 mm (0.63") across points. Hex flats width is 6.0 mm (0.23").



APPENDIX D

Specimen and Roller Drawings

S-RCF Specimen Pro-E® Drawing

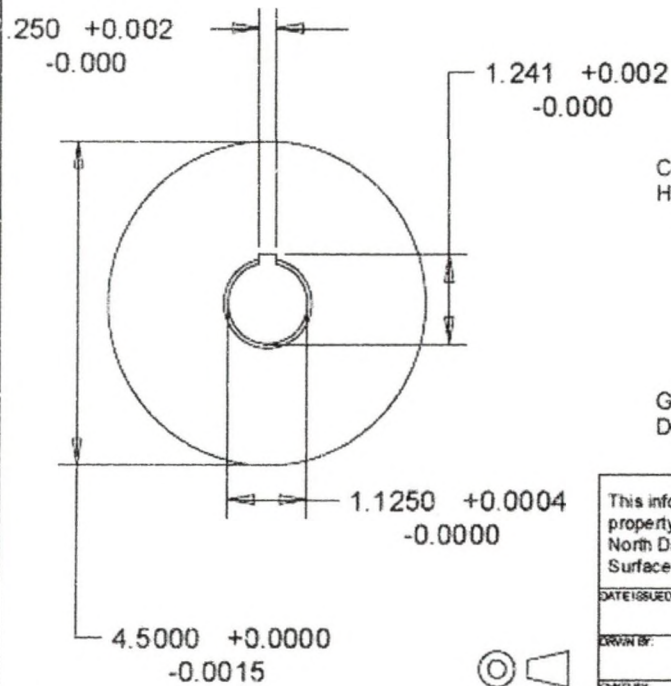
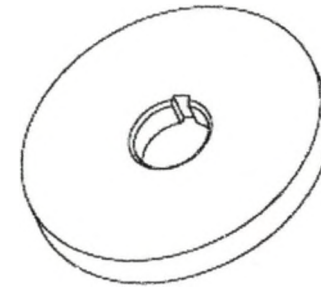
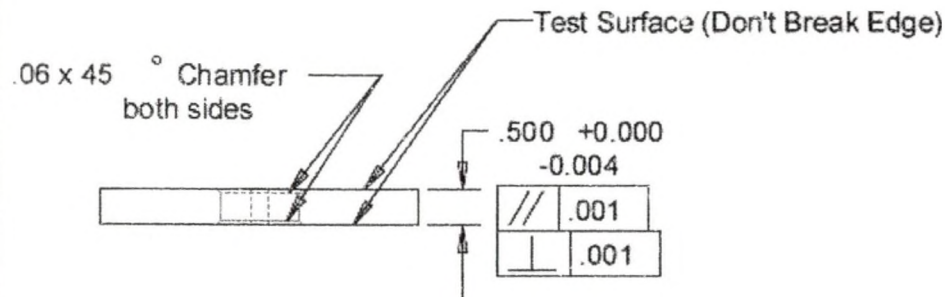


Heat Treatment Instructions:

- Hardness 58 to 62 HRC
- Case Depth 0.037 to 0.055 (0.47 aim)
- Effective Hardness 50 HRC
- Surface Carbon 0.85 ± 0.05
- Final Surface Microstructure - Martensite + Austenite
- Retained Austenite - 10% Max
- Other Non-Transformed Products - 5%

Break Sharp Edge .02" x 45°
 All surfaces must be ground to
 16-20 microninch

This information is solely the property of the University of North Dakota's Engineering Surface Center DATE ISSUED: 27-Nov-06 DRAWN BY: Gregory Dvorak ESC		SCHOOL OF ENGINEERING AND MINES UNIVERSITY OF NORTH DAKOTA SRCF-5000P-16M COURSE SECTION: SRCF-5000PD-16M SCALE: 1:000 MATERIAL: 9620 Steel SHEET 1 OF 1	
---	--	--	--



Concentric ID and OD .0005 inches
 Heat Treatment Instructions
 - Hardness 58 to 62 HRC
 - Case Depth 0.037 to 0.055 (.047 aim)
 - Effective Hardness 50 HRC
 - Surface Carbon 0.85 ± 0.05
 - Final Surface Microstructure - Martensite + Austenite
 - Retained Austenite - 10% Max
 - Other Non-Transformed Product - 5% Max
 Ground to 16 - 20 microinches
 Don't break test surface edge

This information is solely the property of the University of North Dakota's Engineering Surface Center.

SCHOOL OF ENGINEERING AND MINES
 UNIVERSITY OF NORTH DAKOTA

DATE ISSUED: 24-Apr-07

SRCF-5000P-04M

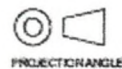
DRWN BY: Gregory Dvorak

SIZE: A COURSE SECTION: SRCF-5000PD-04M-R01

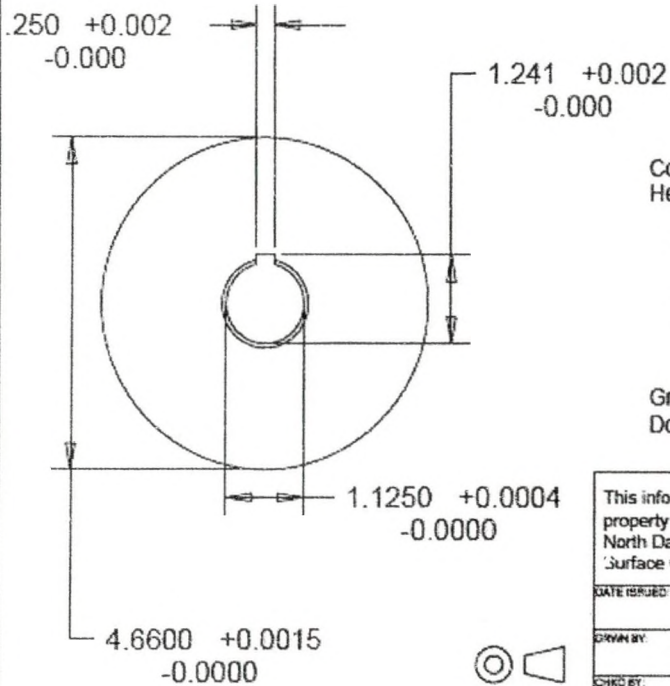
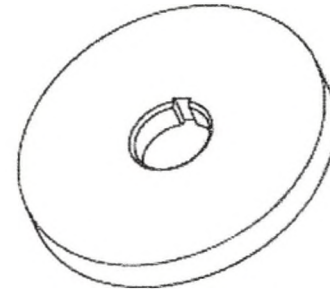
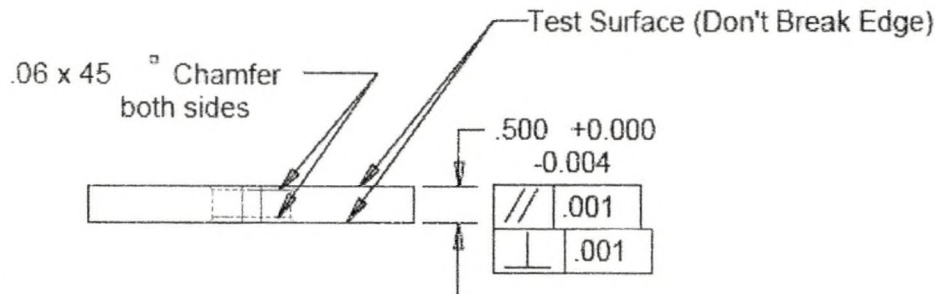
CHKD BY: ESC

SCALE: 0.500 MATERIAL: 8620 Steel

SHEET 1 OF 1



S-RCF Bottom Roller Pro-E® Drawing



Concentric ID and OD .0005 inches
 Heat Treatment Instructions
 - Hardness 58 to 62 HRC
 - Case Depth 0.037 to 0.055 (.047 aim)
 - Effective Hardness 50 HRC
 - Surface Carbon 0.85 ± 0.05
 - Final Surface Microstructure - Martensite + Austenite
 - Retained Austenite - 10% Max
 - Other Non-Transformed Product - 5% Max
 Ground to 16 - 20 microinches
 Don't break test surface edge

S-RCF Top Roller Pro-E® Drawing

This information is solely the property of the University of North Dakota's Engineering Surface Center.

DATE ISSUED: 24-Apr-07

DRAWN BY: Gregory Dvorak

CHKD BY:

SCHOOL OF ENGINEERING AND MINES
 UNIVERSITY OF NORTH DAKOTA

SRCF-5000P-04M Top Roller

SIZE: A	COURSE SECTION: SRCF-5000PD-04M-R01	DMG NO:	REV:
---------	-------------------------------------	---------	------

SCALE: ESC	MATERIAL: 8620 Steel	SHEET 1 OF 1
------------	----------------------	--------------



Heat Treatment for 8620

Final Requirements for Specific Part

Heat Treatment of 8620 RCF Coupons

- Hardness – 58 to 62 HRC
- Case Depth - .037 to .055 (.047 aim) with Effective hardness 50 HRC
- Surface Carbon- 0.85 ±0.05
- Final Surface Microstructure- Martensite plus Austenite
- Retained Austenite - 10% Max
- Other Non-Transformed Products- 5% Max

Quality Check

Insert (2) test bars of #8620 steel ½” in diameter and 3” long into work load prior to going into the carburizing cycle. These bars will be removed, hardened, cut, polished, acid etched and the carburized depth measured on a microscope to ensure the correct carbon depth before the load is hardened.

Carburize cycle

1. Carburize to desired depth with:
Set furnace carbon potential: 0.85% and wait until furnace has reached the proper carbon potential
Carburizing Set Temperature: 1700 Degrees F
Load parts and after furnace temperature recovers, set cycle time to:
Time at temperature:
5 hours = 0.037” effective case depth
6 hours = 0.040” effective case depth
7 hours = 0.043” effective case depth
8 hours = 0.046” effective case depth
9 hours = 0.049” effective case depth
2. Gas quench cool by:
Drop furnace temperature to 1475° F before moving parts to gas quench vestibule or top cool to 450 ° F.
3. Austenitize and quench harden parts by:
Set furnace carbon potential to be at 0.50%
Set furnace temperature to 1550° F and when furnace temperature indicators reach the set temperature, load parts into furnace.
When furnace temperature recovers, set cycle time to 1 hour.
At the end of the hour quench parts into agitated oil that has been controlled at a temperature of 120° F. Leave parts in oil for at least ½ hour.

4. Clean oil off parts.
5. Subzero parts to ensure at least 85% transformation of austenite to martensite. Set subzero to at least -120° F., load parts and after subzero returns to -120° F, set cycle time for 2 hours.
NOTE: If cryogenic unit is available, set unit to -320° F, load parts and after unit returns to set temperature, set cycle time for 2 hours.
6. Temper parts to remove stress. Set oven temperature to 300° F. When oven reaches set temperature, load parts and when oven temperature recovers to set temperature, set cycle time for 2 hours. After cycle has been run, remove parts and allow the parts to cool to be able to safely handle.
7. Clean parts in a glass bead machine and check parts for hardness.

Joseph Shenosky
January 20, 2006
Revised July 14, 2006

Dr. Ranko Torodvic
Updated for 8620
February 18, 2008

APPENDIX E

Outline for S-RCF Test Setup Procedure

1. Insert bottom rollers.
 - a. Slide rollers onto each shaft.
 - b. Slide regular collars onto each shaft.
 - c. Push shaft into place.
 - i. Align the key on the shaft with the keyways in the collars.
 - d. Place and tighten a hinged collar on the stepped portion of each shaft.
 - e. Tighten tightening plate at the end of each shaft.
 - f. Tighten set screws on the bearings of each shaft.
2. Attach specimen end oil wall.
 - a. Check PTFE tape, reapply if necessary.
 - b. Place plate into position and tighten ten hex head bolts.
 - c. Grease oil seal in specimen end oil wall.
3. Insert probe holder and specimen.
 - a. Attach probe holder to one of the specimen sliding plates.
 - b. Slide probe holder and specimen sliding plate assembly into the inner wall.
 - c. Insert the other specimen sliding plate with the short shaft and tightening plate into the inner wall.
 - i. Attach the probe holder to the other specimen sliding plate.
 - d. Insert the shaft with the spider couple into the oil seal located in the specimen end oil wall and the specimen sliding plate.

- e. Place the specimen into the S-RCF tester by sliding the tabs on the specimen into the slots on the shaft.
 - f. Secure the specimen in place by placing hinged collars (2) over the tab slot interface.
 - g. Tighten the tightening plate on the back of the specimen short shaft to remove any slack.
 - h. Tighten the set screws on bearing collars for the specimen assembly.
4. Attach the specimen and roller motor.***
- ***Two people are needed for this step.
- a. Move the specimen motor into place and align it the spider couple.
 - i. Bolt tightly into place.
 - b. Move the roller motor into place by lifting it onto the gears.
 - i. Bolt tightly into place.
 - ii. Screw roller end oil wall into place.
 - 1. Check PTFE tape, replace if necessary.
5. Insert eddy current probe.
- a. Insert the eddy current probe into the probe holder device.
 - b. Set the distance of the probe away from the specimen using the spark plug gap gauge.
 - i. Maximum distance is 1mm - Nominal distance is ½ mm.
 - c. Tighten the screw on the side of the probe holder to secure the probe.
 - i. Do not over tighten as this will damage the probe.
 - ii. Tighten the nut on the screw to prevent the screw from vibrating out.

6. Assemble and insert top roller.
 - a. Slide the rollers and collars on to the top roller shaft.
 - b. Slide the top roller sliding wall on the top roller shaft.
 - c. Screw the tightening plate into the top roller shaft.
 - d. Tighten the set screws on the bearings of the top roller assembly.
 - e. Lift the top roller assembly into the machine and slide it slowly into the inner walls.
 - i. It may require two people to insert the wall (1 for each side).
7. Apply loading.
 - a. Plug in the air compressor.
 - b. Set the pressure on the air compressor.
 - i. The gage on the compressor can be used as a crude approximation.
 - ii. Use the LX-Navi voltage to achieve a more accurate representation.
8. Add lubrication and begin lubrication system.
 - a. Check the direction of all the three-way control valves and the flow control valves.
 - b. Add lubricant to the oil filter and attach the oil filter.
 - c. Add the lubricant into the specimen and gears compartments.
 - i. At least one gallon of lubricant should be added.
 - d. Plug in the oil system.
 - e. Flip the switches on the lubrication control box to the on position.

- i. If lubricant does not immediately begin flowing, prime the system by turning the flow control valve to the specimen on and off quickly several times. Repeat until oil begins to flow.
9. Setup eddy current detection device.
 - a. Several settings need to be entered into the Defectomat EZ. These settings can be determined using the appropriate Mathcad® file located in Appendix C: Mathcad® files.
 - i. Inspection frequency.
 - ii. Line speed.
 - iii. High pass and low pass filter values.
 - iv. Sensitivity.
10. Power on TEAC LX-10.
11. Power on personal computer.
12. Setup LX-Navi program (see Table 7 for a list of parameters).
 - a. Create a folder for all the data to be saved into.
 - b. Open the LX-Navi program.
 - c. In the main window, click the New File button or click new file in the file drop box menu.
 - i. Set the options for the new file.
 1. Set the directory to the folder created in step a.
 2. Set the file name (ex: s1F).
 3. Set the number of zeros in the file name.
 4. Check the PC recording option.

- d. In the main window, click the System button or click system in the setup drop box menu.
 - i. Under the system tab, set the system values.
 1. Set the sampling rate.
 2. Synchronize the LX-Navi clock with the PC clock.
 3. Check Slot 1.
 4. Set number of channels for Slot 1.
 - ii. Under the Slot1(PA-8) tab, set the channel values.
 1. Set the calibration value for every channel.
 - a. Channels 1-4: 3.16V.
 - b. Channels 5-8: 10V.
 - e. In the main window, click the Trigger button or click trigger in the setup drop box menu.
 - i. Set the trigger options.
 1. Check the interval check box.
 2. Set the record time.
 3. Set the interval time.
 4. Set the repeat count value.
 5. Set the start time.
13. Set up and power on monitoring and controlling devices.
- a. Drag the Matlab® files into the directory that the files from the TEAC will be created in.

- i. Files: TestParametersValues, Teac2Matlab, T2Mv2Screening, T2Mv2CrackMeasurements, T2Mv2Analysis, REalTimeDataAnalysis, motorcommand and ECThresholdCheckmax.
 - b. Plug in the power for the pressure transducer and the temperature probe.
 - c. Turn the control switches on the face of the motor controller box to off.
 - d. Flip the two breakers in the breaker box to power up the motor controllers.
 - i. Breaker group 13-15-17 and 37-39-41.
14. Acquire initial values.
- a. Turn on the lubrication system and the air compressor if they are not already on.
 - b. Open Matlab®.
 - i. Set Matlab® working directory to the folder the files are located.
 - ii. Open the TestParametersValues file.
 - iii. Edit the values and set them to the current values known, Save the file.
 - iv. In the Matlab® prompt window type TestParametersValues.
 - v. In the Matlab® prompt window type motorcommand.
 - c. Flip the switches on the front of the controller box to on to start the motors.
 - i. Let the motors power up to full speed.
 - d. Determine the initial values by:
 - i. Open the LX-Navi digital readouts and visually record max value.
 - ii. Record several files and analyze with T2Mv2Analysis file.
 - 1. If this option is used, a new file must be setup in the LX-Navi.
 - e. Turn the switches on the front of the controller box to off to stop the motors.

- f. Open the TestParametersValues file and enter the initial values.
 - i. The oil temperature value will vary significantly since it will not be at equilibrium until testing has been running for awhile.
 - ii. Based on the initial values, set the maximum allowable change on each channel.
 - 1. For channels 1-4 (eddy current channels) the value is a voltage change. This voltage change can either be determined by performing calibration tests on parts with know defect sizes or by observing the noise in the base signal and determining an appropriate value.
 - 2. For channels 5-8, the value entered is a percentage of the initial value. These values do not stop the machine; therefore, the value entered is up to the user's discretion.
 - iii. Save the TestParametersValues file.

15. Start the S-RCF tester.

- a. Clear any old data files created in the folder.
- b. Set the start time in the LX-Navi trigger menu.
 - i. Set to approximately two minutes from the current time.
- c. Enter RealTimeDataAnalysis into the Matlab® prompt window and press enter.
 - i. Pop-up window will appear displaying a message.
- d. Turn the switches on the front of the motor controller box to on.

- e. Allow the motors to reach full speed and then click OK on the pop-up window.
- f. Monitor the tester for the first ten minutes to ensure that the graphs appear and display reasonable information.
- g. Periodically check the machine to determine if more lubrication is needed.
 - i. Record time that oil is added.

Outline for S-RCF Test Disassembly Procedure

1. Stop power to the motors.
 - a. Turn the switches on the motor controller box to off, even if the motors are already stopped.
2. Stop the LX-Navi and Matlab® programs.
 - a. In the LX-Navi window, click the stop button to cancel further recording.
 - b. In the prompt window of Matlab®, hold the 'ctrl' button and press 'c'.
 - i. This will terminate the while loop in the program.
3. Switch off the lubrication and monitoring systems.
 - a. Unplug the power supply for the pressure transducer and the lubrication temperature probe.
 - b. Turn the lubrication system off using the switches on the lubrication system control panel.
4. Open the S-RCF tester.
 - a. Remove the load on the top roller.
 - b. Remove the top covers.
5. Remove the specimen.
 - a. Slide out the top roller assembly.
 - i. If it is jammed, use the air cylinders to lift the assembly out.
 - b. Remove the hinged collars on the specimen assembly.
 - c. Slide out the specimen.
 - d. Disassemble the top roller assembly to remove the top roller.
6. Remove eddy current probe

7. Drain the lubricant from the system.
 - a. Flip the valves on the lubricant system so that the lubricant flows into the reservoir container.
 - b. Turn the lubricant system back on.
 - c. Pump the lubricant until no more flows out of the hose.
 - d. Turn the lubricant system off and unplug it.
 - e. Flip the valves on the lubricant system so that the lubricant drains out by gravity into a reservoir container.
 - i. The flow should be minimal.

8. Remove motors.***

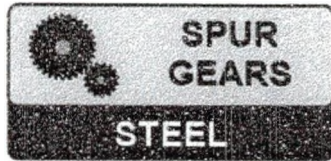
***Two people will be needed to lift the motors

- a. Unbolt the specimen motor and lift it out of the way.
 - b. Remove the specimen shaft with the spider couple on it.
 - i. Loosen the set screw in the bearing to remove this shaft.
 - c. Unbolt specimen end oil wall and remove.
 - d. Lift out specimen sliding plates and probe holder.
 - e. Unbolt roller end oil wall.
 - f. Unbolt roller motor and lift the motor out of the way.
9. Remove bottom rollers.
 - a. Remove the tightening plate on the back of each shaft.
 - b. Remove the hinged collar on the shafts.
 - c. Loosen the set screws in the bearings holding the shafts.
 - d. Move the shaft axially towards the gear side.

- i. Line up the keyway in the keyed collars with the key on the shaft.
- e. After a $\frac{1}{2}$ gap is present between the bearing and shaft, remove the regular collars.
- f. Slide the rollers off.

Replacement Parts

Spur Gears for Roller Motor and Roller Shafts (Y412) from the Browning Catalog, ordered through Tri-Steel in Grand Forks, North Dakota.



14-1/2° PA gears will not operate with 20° PA gears!

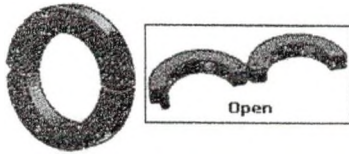
14-1/2° PA PART NO	20° PA PART NO	T E E T H	S T Y L E	PITCH DIA	FACE	BORE	HUB DIA	HUB PROJ
S411	TS411	11	B	3.000	2.00	1.125	2.25	.88
A411	F411	11	A	3.000	2.00	1.125	---	---
S412	TS412	12	B	3.000	2.00	1.125	2.25	.88
A412	F412	12	A	3.000	2.00	1.125	---	---
	Y412	12	B	3.000	3.50	1.063	2.25	1.00
	Z412	12	A	3.000	3.50	1.063	---	---
S414	TS414	14	B	3.500	2.00	1.125	2.75	.88
A414	F414	14	A	3.500	2.00	1.125	---	---
	Y414	14	B	3.500	3.50	1.063	2.75	1.00
	Z414	14	A	3.500	3.50	1.063	---	---
S415	TS415	15	B	3.750	2.00	1.125	3.00	.88
A415	F415	15	A	3.750	2.00	1.125	---	---
	Y415	15	B	3.750	3.50	1.063	3.00	1.00
	Z415	15	A	3.750	3.50	1.063	---	---
S416	TS416	16	B	4.000	2.00	1.125	3.25	.88
A416	F416	16	A	4.000	2.00	1.125	---	---
	Y416	16	B	4.000	3.50	1.313	3.25	1.00
	Z416	16	A	4.000	3.50	1.313	---	---
S418	TS418	18	B	4.500	2.00	1.125	3.75	.88
A418	F418	18	A	4.500	2.00	1.125	---	---
	Y418	18	B	4.500	3.50	1.313	3.75	1.00
	Z418	18	A	4.500	3.50	1.313	---	---
S420	TS420	20	B	5.000	2.00	1.125	4.25	.88
A420	F420	20	A	5.000	2.00	1.125	---	---

FAX: 1-800-635-6273

Hinged One-Piece Clamp-On Shaft Collar (ordered from McMaster)

Shaft Collars

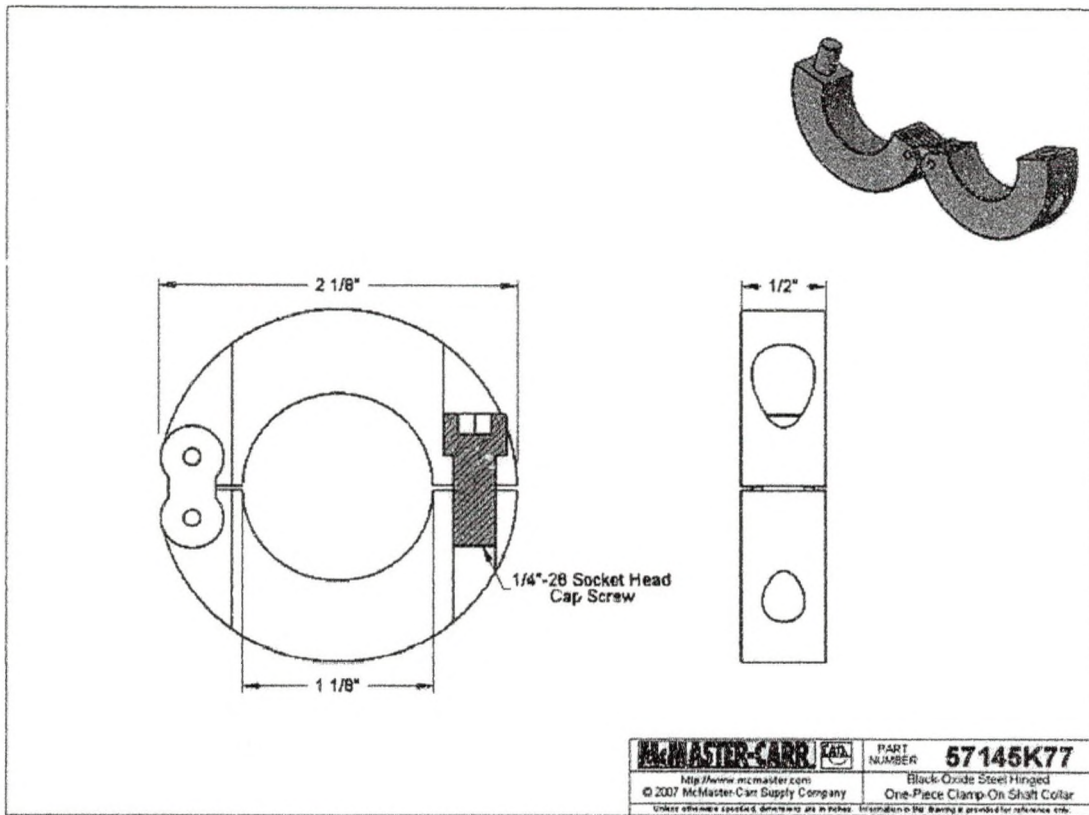
This product matches all of your selections.



Part Number: 57145K77

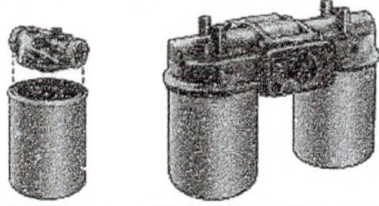
\$11.23 Each

Type	Hinged One-Piece Clamp-On
System of Measurement	Inch
Material	Steel
Steel Material	Carbon Steel
Finish	Black-Oxide
Bore Size	1-1/8"
Outside Diameter	2-1/8"
Width	1/2"
Screw Size	1/4"-28
Set/Cap Screw Material	Alloy Steel
Specifications Met	Not Rated



Hydraulic Oil Filter for S-RCF Tester Lubrication System (ordered from McMaster)

Spin-On Hydraulic Oil Filters



3/4" to 1 1/4"
Pipe Sizes

1 1/2" Pipe Size with Side-by-Side
Filter Cartridges

Changing filter cartridges is a snap—simply spin them on and off in seconds since there are no bolts to remove. Install these filters in return lines as well as in off-line filtration and lubrication systems. They have a Buna-N seal, a steel cartridge housing, and include one filter cartridge (two filter cartridges where noted).

All have a built-in bypass valve. When the pressure differential between the inlet and outlet reaches the set limit, indicating a clogged cartridge, the valve routes the oil away from the cartridge to prevent pressure build-up in your line.

Connections: NPT female.

Note: Filters with 1 1/2" pipe size also have 2" SAE 4-bolt flange ports. Horizontal bolt hole center-to-center is 3 1/8"; vertical center-to-center is 1 1/8". Bolt holes are 1/2"-13 UNC.

Standard filters are nominal-rated and use cellulose paper media for filtering.

High-efficiency filters use fiberglass media for more precise filtering. They are absolute-rated to 99% efficiency (they'll stop 99% of particles larger than their micron rating).

Optional Filter Gauge—With a range of 0-60 psi, these gauges tell you when it's time for a new filter cartridge. Available only for 44185K series.

To Order: For filters and replacement cartridges, please specify your required micron rating from those listed.

Pipe Size	Max. psi	Bypass Valve Set Limit, psi	Max. Temp.	Max. Flow, gpm	Port-to-Port Lg.	O.D. Ht.	Available Micron Ratings	Filters		Replacement Cartridges	
								Each	Each	Each	Each
Standard											
3/4"	120	25	250° F	15	3 1/8"	6 1/8"	3, 10, 25	4453K11	\$33.12	4453K19	\$12.05
3/4"	150	15	225° F	15	3 3/8"	7 3/4"	3, 10, 25	44185K65	31.61	44185K41	17.11
1"	120	25	250° F	15	3 1/8"	7 3/8"	3, 10, 25	4453K12	33.83	4453K19	12.05
1 1/4"	120	25	250° F	30	5 3/8"	9 1/8"	3, 10, 25	4453K13	52.04	4453K29	22.59
1 1/4"	150	15	225° F	50	4 1/2"	9 1/2"	3, 10, 25	44185K66	64.02	44185K42	31.98
1 1/2"	120	25	250° F	60	6 1/2"	10 3/8"	3, 10, 25	4453K14	170.32	4453K29	22.59
High Efficiency											
3/4"	120	43	250° F	15	3 1/8"	6 1/8"	5, 10, 20	4358K41	69.41	4358K39	49.38
3/4"	150	15	225° F	15	3 3/8"	7 3/4"	10, 20	44185K67	68.19	44185K43	56.06
1"	120	43	250° F	15	3 1/8"	7 3/8"	5, 10, 20	4358K42	75.19	4358K39	49.38
1 1/4"	120	43	250° F	30	5 3/8"	9 1/8"	5, 10, 20	4358K43	131.41	4358K49	87.27
1 1/4"	150	15	225° F	50	4 1/2"	9 1/2"	10, 20	44185K68	111.75	44185K44	79.23
1 1/2"	120	43	250° F	60	6 1/2"	10 3/8"	5, 10, 20	4358K44	309.83	4358K49	87.27
Optional Filter Gauge for 44185K									44185K11	Each	\$20.04

■ Has two side-by-side filter cartridges. Overall width is 12 1/8".

Micron rating: 3

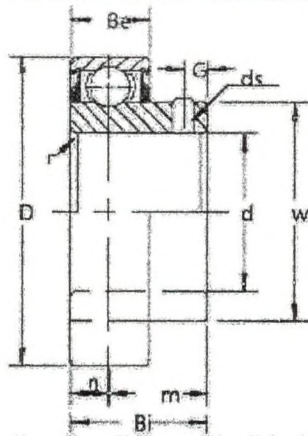
Part Number: 4453K11

Cartridge: 4453K19

Insert Bearings FHSR200 Series Set Screw Locking (Peer Bearings)

- Standard load capacity
- Narrow inner ring with cylindrical outer ring
- Non-lubricatable bearing is standard (shown)
- Nylon patched class 3A set screws are standard
- Standard seal: RST tight riding, full cover, metal shroud seals

Optional seals: See page B3

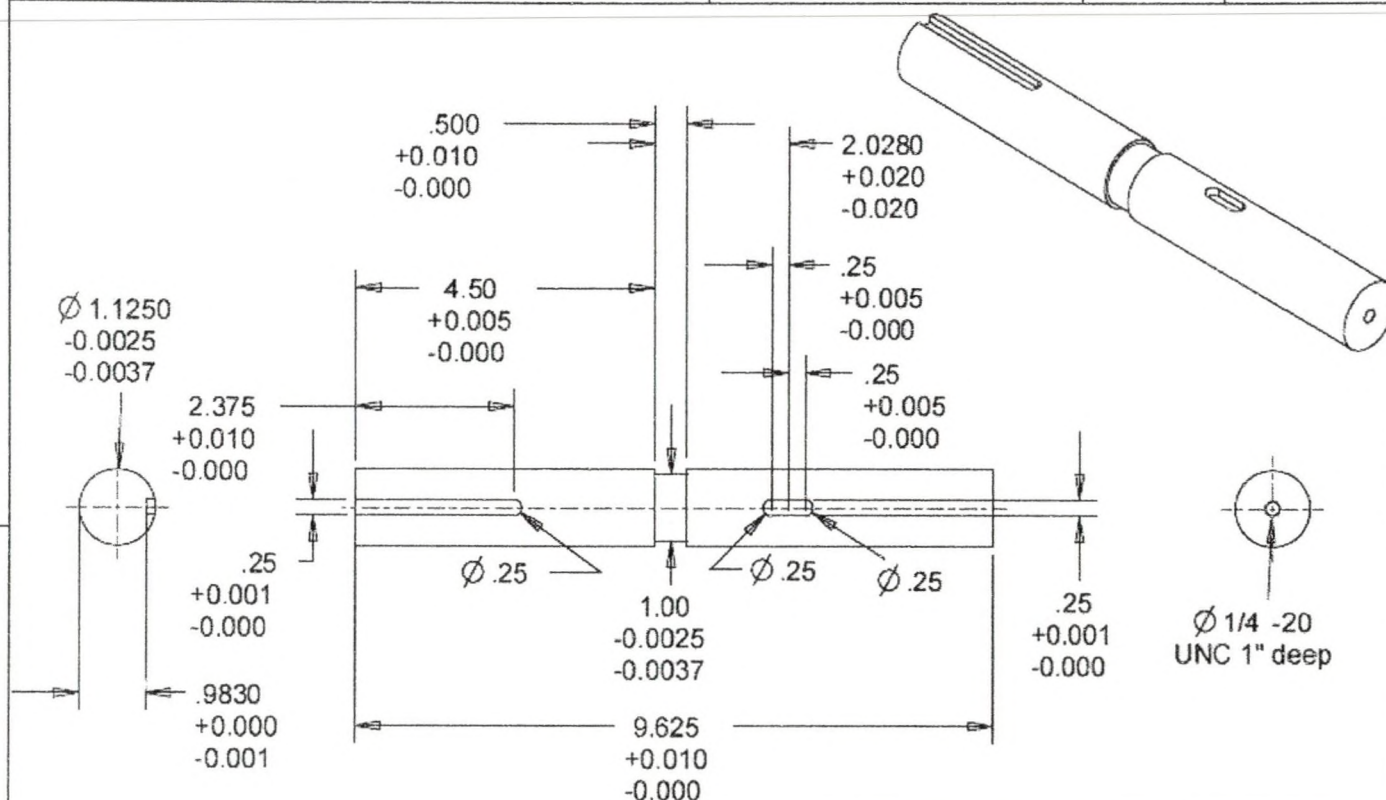


Unit No. Shaft Diam.	Dimensions in mm										Load Rating (Lbs.)	
	D	Bi	Bo	r	n	m	G	W	ds	(UNF-Thread)	Dynamic	Static
	UNF-Thread	UNF-Thread	UNF-Thread	UNF-Thread	UNF-Thread	UNF-Thread	UNF-Thread	UNF-Thread	UNF-Thread		UNF-Thread	UNF-Thread
FHSR01-8 FHSR01-12mm	1/2 12mm											
FHSR02-9 FHSR02-10 FHSR02-15mm	9/16 5/8 15mm	1.5749 40.000	0.886 22.50	0.512 13.00	0.031 0.80	0.2559 6.500	0.630 16.00	0.197 5.00	0.960 24.60	1/4-28x3/16 M6xP1.0	2150	880
FHSR03-11 FHSR03-17mm	11/16 17mm											
FHSR04-12 FHSR04-17 FHSR04-20mm	3/4 13/16 20mm	1.6514 47.000	0.984 25.00	0.591 15.00	0.059 1.50	0.2953 7.500	0.689 17.50	0.177 4.50	1.130 28.70	1/4-28x1/4 M6xP1.0	2900	1410
FHSR05-12 FHSR05-13 FHSR05-14 FHSR05-15 FHSR05-18 FHSR05-25mm	3/4 13/16 7/8 15/16 1 1/8 25mm											
		2.0472 52.000	1.063 27.00	0.591 15.00	0.039 1.00	0.2953 7.500	0.788 20.00	0.197 5.00	1.327 33.70	1/4-28x1/4 M6xP1.0	3150	1610
FHSR09-17 FHSR09-18 FHSR09-19 FHSR09-20 FHSR09-30mm	1 1/16 1 1/8 1 3/16 1 1/4 30mm											
		2.4410 62.000	1.181 30.00	0.708 18.00	0.059 1.50	0.3543 9.000	0.827 21.00	0.285 7.24	1.557 39.50	5/16-24x5/16 M6xP1.0	4370	2320

Part Number: FHSR206-18 (1 1/8 shaft diameter)

Bottom Roller Shaft for S-RCF Tester (Heat Treated the Same as the Rollers)

SHEET 1 OF 1 SRCF-5000PD-01M

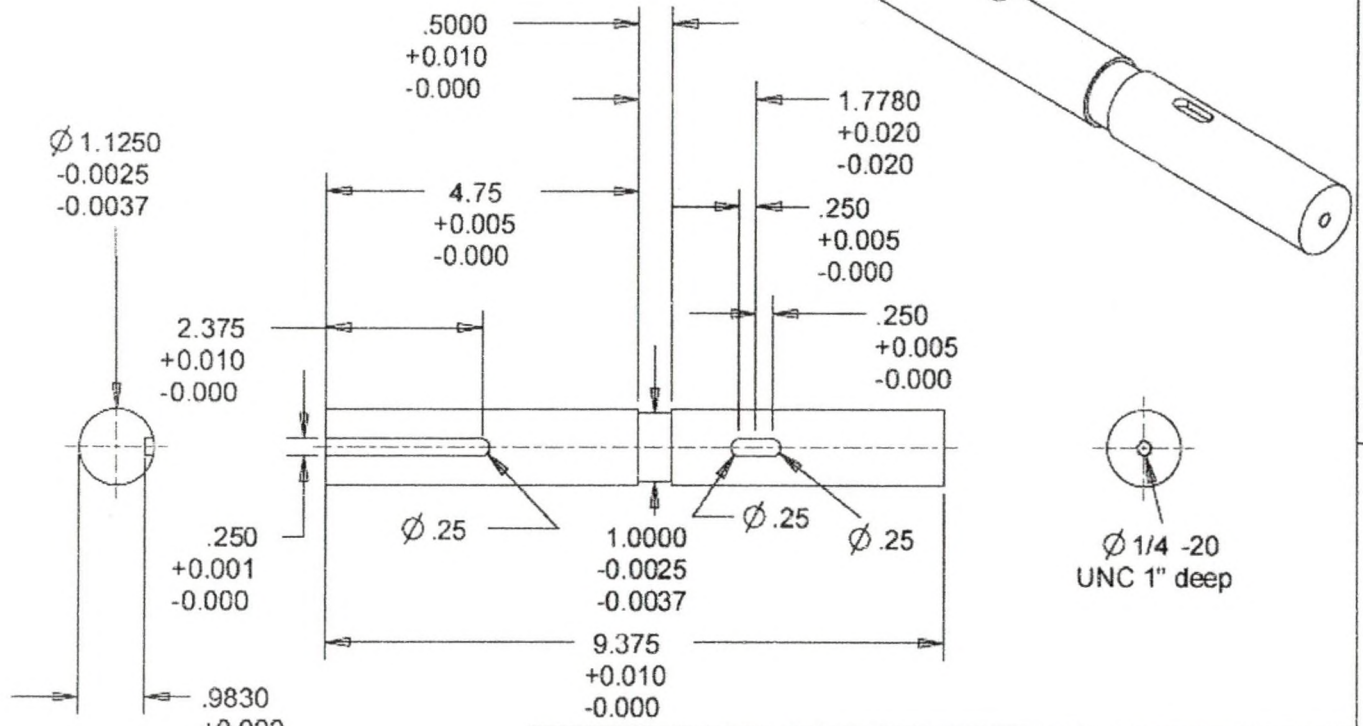


This information is solely the property of the University of North Dakota's Engineering Surface Center.		SCHOOL OF ENGINEERING AND MINES UNIVERSITY OF NORTH DAKOTA	
DATE ISSUED	27-Nov-05	SRCF-5000P-01M	
DESIGN BY	Penta X	SIZE	A
CHECK BY	Penta X	COURSE SECTION	RCF-5000PD-01M
		SCALE	0.500
		MATERIAL	AISI 8620
			SHEET 1 OF 1



Top Roller Shaft for S-RCF Tester (Heat Treated the Same as the Rollers)

SHEET 1 OF 1 SRCF-5000PD-10M



This information is solely the property of the University of North Dakota's Engineering Surface Center.		SCHOOL OF ENGINEERING AND MINES UNIVERSITY OF NORTH DAKOTA	
DATE ISSUED	27-Nov-06	SRCF-5000P-10M	
DRAWN BY	Penta X	SIZE	A
CHKD BY	Penta X	COURSE SECTION	RCF-5000PD-10M
PROJECTION ANGLE		SCALE	0.500
		MATERIAL	AISI 8620
		SHEET 1 OF 1	

BIBLIOGRAPHY

- [1] Stephens, R.I., Fatemi, A., Stephens, R.R., & Fuchs, H.O. (2001). *Metal Fatigue in Engineering* 2nd Edition. New York, NY: John Wiley & Sons Inc.
- [2] ASTM Subcommittee E08.02. (2000). *Standard Terminology Relating to Fatigue and Fracture*. (Vol. 03.01, pp.1034). Testing ASTM Designation E1823, West Conshohocken, PA: ASTM.
- [3] ASM International Handbook Committee. (2002). *ASM Handbook Volume 11: Failure Analysis and Prevention*. Materials Park, OH: ASM International.
- [4] Hoffmann, G., & Jandeska, W. (2007, January/February). Effects on Rolling Contact Fatigue Performance. *GEARTECHNOLOGY*, 42-52.
- [5] Lipp, K., & Hoffman, G. (2003). Design for Rolling Contact Fatigue. *International Journal of Powder Metal*, 39(1), 33-46.
- [6] Kleemola, J., & Aara, A.L. (2006). Development of a High Pressure Twin Disc Test Device for the Simulation of Gear Contact. *Finnish Journal of Tribology*, 25, 8-17.
- [7] Deng, G., Nakanishi, T., & Kato, M. (2002). Surface Temperature Calculation and its Application to Surface Fatigue Strength Evaluation. *Journal of Mechanical Design*, 124, 805-812.
- [8] Kuhnell, B.T. (2004, September/October). Wear in Rolling Element Bearings and Gears – How Age and Contamination Affect Them. *Machinery Lubrication*. Retrieved Mar. 10 2008, from *Machinery Lubrication Magazine*. Online. http://www.machinerylubrication.com/article_detail.asp?articleid=664&relatedbookgroup=Lubrication.
- [9] Lawcock, R. (2006). Rolling Contact Fatigue of Surface Densified Gears. *International Journal of Powder Metallurgy*, 42(1), 17-29.
- [10] Krantz, T.L., Alanou, M.P., Evans, H.P., & Snidle, R.W. (2001). Surface Fatigue Lives of Case-Carburized Gears with an Improved Surface Finish. *Journal of Tribology*, 123, 709-716.
- [11] Krantz, T., Cooper, C., Townsend, D., & Hansen, B. (2004). Increased Surface Fatigue Lives of Spur Gears by Application of a Coating. *Journal of Mechanical Design*, 126, 1047-1054.

- [12] Niskanen, P., Manesh, A., & Morgan, R. (2003). Reducing Wear with Superfinish Technology. *The AMPTIAC Quarterly*, 7(1), 3-9.
- [13] Hoffman, G. & Rice, J.A. (2005). Initiation and Propagation of Cracks in Wrought and Sintered Steels during Rolling Contact Fatigue. *Advances in Powder Metallurgy & Particulate Materials*, 3(3), Part 10 176-200.
- [14] Beardmore, R. (2007). Coefficient of Rolling Friction. Retrieved Mar. 14 2008, from RoyMech Index Page. Online. http://www.roytech.co.uk/Useful_Tables/Tribology/co_of_friect.htm.
- [15] (n.d.). Tie Rod Air Cylinders. Retrieved Mar. 21 2008, from McMaster-Carr Catalog. Online. <http://www.mcmaster.com>.
- [16] (n.d.). Heavy-Duty Mechanically Operated Air Valves. Retrieved Mar. 22 208, from MSC Industrial Supply Company Catalog. Online. <http://www.screwshop.com/PDF/2005/3957.pdf>.
- [17] (n.d.). Air Filter/Regulator/Lubricators (FRLs). Retrieved Mar. 21 2008, from McMaster-Carr Catalog. Online. <http://www.mcmaster.com>.
- [18] (n.d.). Solid State Pressure Transducer. Retrieved Mar. 21 2008, from Omega Catalog. Online. www.omega.com/pptst/PX209_PX219.html.
- [19] Baldev, R., Jayakumar, T., & Thavasimuthu, M. (2002). *Practical Non-Destructive Testing* 2nd Edition. Cambridge, England: Woodhead Publishing Limited.
- [20] Larson, B.F. (n.d.). Introduction to Eddy Current Testing. Retrieved Mar. 20 2008, from NDT Resource Center. Online. http://www.ndt-ed.org/EducationResources/CommunityCollege/EddyCurrents/cc_ec_index.htm
- [21] Harkins, W. (1999). NASA-STD-5007: LLIS-0760 Eddy Current Testing of Aerospace Materials. Retrieved Mar. 21 2008, from NASA Technical Standards Program. Online. <http://www.nasa.gov/offices/oce/llis/0760.html>.
- [22] Cartz, L. (1995). *Nondestructive Testing: Radiography, Ultrasonics, Liquid Penetrant, Magnetic Particle, Eddy Current*. Materials Park, OH: ASM International.
- [23] Foerster Instruments Incorporated. (2003.). *Defectomat: Eddy Current Testing Equipmment*. Retrieved Mar. 20 2008, from Foerster Instruments Incorporated. Online. <http://www.foerstergroup.com/NDT/defectomat.html>.
- [24] (n.d.). Pipe Plug Thermistor Probes. Retrieved Mar 21 2008, from Omega Catalog. Online. <http://www.omega.com/pptst/THX-400-NPT.html>.

- [25] Hoffmann, G., & Jandeska, W. (2007, March/April). Effects on Rolling Contact Fatigue Performance – Part II. *GEARTECHNOLOGY*, 42-51.
- [26] Asi, O. (2006). Fatigue Failure of a Helical Gear in a Gearbox. *Engineering Failure Analysis*, 13, 1116-1125.
- [27] CES Selector Version 4.7.0. Copyright© Granta Design Limited.
- [28] Advisory Circular. (2001). Acceptable Methods, Techniques, and Practices – Aircraft Inspection and Repair. U.S. Department of Transportation and Federal Aviation Administration, AC 43.13-1B, Chapter 5 1-7.